The Dissertation Committee for Jing Li Certifies that this is the approved version of the following dissertation:

Dialkynylimidazoles as Irreversible MAPK Inhibitors, Kinase Docking Site Probes, and Anti-cancer Agents

Committee:

Sean M. Kerwin, Supervisor

Kevin N. Dalby

Christian P. Whitman

Jennifer S. Brodbelt

Walter L. Fast

Dialkynylimidazoles as Irreversible MAPK Inhibitors, Kinase Docking Site Probes, and Anti-cancer Agents

by

Jing Li, B.A.; B.S.

Dissertation

Presented to the Faculty of the Graduate School of

The University of Texas at Austin

in Partial Fulfillment

of the Requirements

for the Degree of

Doctor of Philosophy

The University of Texas at Austin

August 2011

Dedication

To mom and dad for their unconditional love and support

Acknowledgements

For the past five years, it has been a fortunate and rewarding experience to work with an excellent mentor, Professor Kerwin. I would like to thank him for his enormous patience and constant guidance and encouragement, both through this dissertation research and in many other ways. His incredible knowledge, and strong passion and dedication to research, have truly inspired me to advance my career in science. Over the years, I have learned that, as a scientist, I should always think critically, pay attention to experimental details, and never ignore failed results. I would also like to thank Professor Dalby for the wonderful opportunity to collaborate with his graduate student, Tamer Kaoud, who is my great colleague and friend as well. Thanks to Professor Dalby, I expanded my knowledge in protein biology and kinetics. During our regular scientific discussions, he always gave me helpful suggestions and made me think more carefully and deeply about the questions I want to address. Moreover, I would like to acknowledge my committee members Professors Whitman, Fast and Brodbelt for their critique about my research projects throughout the years and support in my future endeavors. Additionally, I have valued my time with all the past and current Kerwin and Dalby group members, and many friends. Their companionship has brought laughter into my journey to the doctoral degree and made the whole experience more enjoyable and memorable.

I would not have got so far without the continuing support from my dear mom and dad. They have always encouraged me to pursue my dreams and set an example of how to be a good and loving person. I appreciate the time they have spent with me through many ups and downs. Some days are not so bright, but they are always there to

cheer me up, and never let me lose confidence in myself. Lastly, I would like to thank my grandparents who sparked my interest in science at a young age. Their inspiration will always stay with me.

Dialkynylimidazoles as Irreversible MAPK Inhibitors, Kinase Docking Site Probes, and Anti-cancer Agents

Jing Li, Ph.D.

The University of Texas at Austin, 2011

Supervisor: Sean Michael Kerwin

This dissertation research was aimed at investigating an interesting class of 1,2-dialkynylimidazoles as: 1. irreversible p38 MAP kinase α-isoform (p38α) inhibitors; 2. p38α docking site probes; 3. anti-cancer agents.

Based on the mild, thermal rearrangement of 1,2-dialkynylimidazoles to reactive carbene or diradical intermediates, a series of 1,2-dialkynylimidazoles was designed as potential irreversible p38α inhibitors. The synthesis of these dialkynylimidazoles and their kinase inhibition activity were reported. Interestingly, one of the 1-ethynyl-substituted dialkynylimidazoles is a potent (IC_{50} = 200 nM) and selective inhibitor of p38α. Additionally, this compound covalently modifies p38α as determined by ESI-MS after 12 h incubation at 37 °C. The unique kinase inhibition, covalent kinase adduct formation, and minimal CYP450 2D6 inhibition by this compound demonstrate that dialkynylimidazoles are a new, promising class of p38α inhibitors.

Blocking docking interactions between kinase network partners is a promising alternative approach for selectively inhibiting kinases. The second project involves the identification of a new class of small molecules, covalent p38α MAP kinase docking site probes. We proposed that the mechanism may involve the addition of a thiol to the *N*-ethynyl group. Moreover, we demonstrated that such probes can be used fluorescently to

label p38α both in vitro and in cells via azide-alkyne "Click" chemistry. This serves as the basis of an assay that can be used to identify inhibitors that specifically target the substrate docking site of p38α.

The last project was focused on evaluating a new class of 1,2-dialkynylimidazoles as anti-cancer agents. One 1,2-dialkynylimidazole analog was found to be cytotoxic against a range of human cancer lines and to induce apoptosis in the human non-small cell lung cancer cell line A549. In order to elucidate the relationship between the structural basis and role of the thermal generation of diradical or carbene intermediates, a series of dialkynylimidazoles and related *N*-alkynylimidazoles was prepared and their cytotoxicity was determined against A549 cell line. Although the experimentally determined activation energy is in excellent agreement with that predicated from the DFT calculation, there is no correlation between the rate of Bergman cyclization and cytotoxicity to A549 cells. An alternative mechanism was proposed involving the unexpected selective thiol addition to the *N*-ethynyl group of certain 1,2-dialkynylimidazoles.

Table of Contents

List of Tables

List of Figures

List of Schemes

Chapter 1: Introduction

1.1. PROTEIN KINASES AS DRUG TARGETS

Protein kinases are key regulators in signal transduction pathways. The human genome encodes approximately 518 protein kinases, which share a conserved catalytic domain but which are different in how catalysis is regulated (*1*). Deregulation of kinase activity has been implicated in a number of diseases, ranging from cancer and inflammation to diabetes, and neurological and metabolic disorders. Thus, protein kinases are considered as a promising drug class for the treatment of these diseases (*1, 2*). To date, nearly 30 distinct kinase targets have been developed to the level of Phase I clinical trial, and 11 kinase inhibitors have been approved by the US Food and Drug Administration for cancer treatment (*3*).

The pharmaceutical industry became interested in protein kinases after the discovery of staurosporine, which is an antifungal agent produced by bacteria of the genus *Streptomyces*. Staurosporine was found to be a nanomolar inhibitor of protein kinase C (Figure 1.1) (*4*). Subsequently, several companies began making derivatives of this bisindolyl maleimide. However, these derivatives later were shown to lack specificity, inhibiting several other protein kinases (*5, 6*).

A landmark event occurred in May 2001 when Imatinib (Gleevec™) was approved for clinical use. Gleevec was the first approved small molecule drug for cancer therapy, targeting the Abelson tyrosine kinase (ABL) (Figure 1.1). ABL becomes fused to the oncogenic breakpoint cluster region (BCR) protein as a result of chromosome rearrangement in nearly all types of chronic myeloid leukeamia (CML). The success of Gleevec has generated a great amount of interest in identifying aberrantly regulated signaling pathways and developing novel small molecules targeting the protein kinases (*7, 8*).

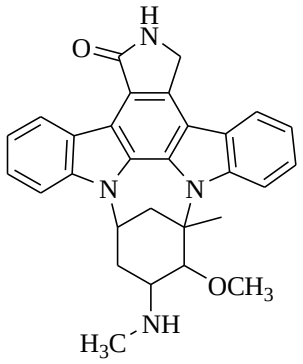

Staurosporine

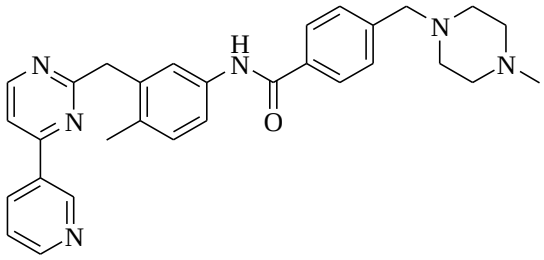

Gleevec

Figure 1.1. Structures of two representative protein kinase inhibitors.

1.2. MITOGEN ACTIVATED PROTEIN KINASE SIGNALING

Mitogen-activated protein kinases (MAPK) are important components of signaling cascades, which convert extracellular stimuli into intracellular responses. All eukaryotic cells possess multiple MAPK pathways that regulate diverse cellular activities, such as motility, survival, apoptosis and differentiation. So far, seven groups of MAPKs have been characterized in mammals. Conventional MAPKs are composed of extracellular signal-regulated kinases 1/2 (ERK1/2), c-Jun amino-terminal kinases 1/2/3 (JNK1/2/3), p38 isoforms (α, β, γ, and δ), and ERK5. Atypical MAPKs comprise ERK 3/4, ERK7, and Nemo-like kinase (NLK) (*9-11*).

MAPKs can be activated by a variety of stimuli: ERK1/2 are activated by growth factors including platelet-derived growth factor (PDGF), epidermal growth factor (EGF), nerve growth factor (NGF) (*12*), insulin (*13*), and to a lesser extent by ligands for heterotrimeric G protein-coupled receptors (GPCR), cytokines, osmotic stress and microtubule disorganization (*14*). JNKs and p38 MAPKs are activated in response to stress stimuli including osmotic shock, ionizing radiation, ischemia and cytokine stimulation (*15*). Each conventional MAPK cascade is composed of three evolutionarily conserved kinases: a MAPKK kinase (MAPKKK), MAPK kinase (MAPKK), and a MAPK. Similar to many other protein kinases, the activation/phosphorylation of MAPKs occurs on a flexible loop, termed the phosphorylation loop or activation loop. Upon activation, MAPKs adopt conformational changes that relieve steric blocking and stabilize the activation loop in order to facilitate substrate binding and enhance the catalytic activity of MAPKs (*16*). In response to extracellular stimuli, MAPKKKs are activated through phosphorylation as a result of their interaction with a small GTP-binding protein of the Ras/Rho family (*17, 18*). MAPKKK phosphorylation leads to activation of a MAPKK, which, in turn, stimulates MAPK activity through dual phosphorylation on Thr and Tyr residues (Thr-X-Tyr). Subsequently, MAPKs phosphorylate their downstream substrates, such as phospholipases, transcription factors and cytoskeletal proteins, as well as several protein kinases, termed MAPK-activated protein kinases (MKs) (*19*).

The activation mechanism of atypical MAPKs still remains elusive. These kinases are not organized into a conventional set of three-tiered kinase cascades. The Thr-X-Tyr motif is absent in ERK3/4 and NLK; instead, a Gly or Glu residue replaces the Tyr. ERK7 appears to autophosphorylate on the Thr-Glu-Tyr motif. However, once activated, both conventional and atypical kinases are Pro-directed kinases, namely phosphorylating substrates on Ser or Thr followed by a Pro residue (*20*).

1.3. P38 MAPK

p38 MAPK belongs to the class of serine-threonine MAP kinases. To date, four isoforms have been identified (α, β, γ, and δ), and they have been shown to be highly homologous and widely expressed in various tissues (*21*). p38α MAPK was first identified as a protein that was rapidly phosphorylated on Tyr residue in response to lipopolysaccharide (LPS) stimulation (*22*), and p38α was a target of pyridinylimidazole drugs that inhibited the production of pro-inflammatory cytokines (*23*). Of the four isoforms, p38α is ubiquitously expressed and has been extensively studied. The other isoforms seem to be expressed in a more tissue specific manner; for example, p38β is predominately expressed in the brain, p38γ in skeletal muscle, and p38δ in endocrine glands (*24*).

In response to a variety of physical and chemical stresses, for instance, oxidative stress, UV irradiation, hypoxia, ischemia, and cytokines including interleukin-1 (IL-1) and tumor necrosis factor alpha (TNFα), p38 kinases are phosphorylated on a conserved Thr-Gly-Tyr (TGY) motif by three dual-specificity MAPKKs (MKKs). MKK3 and MKK6 are highly specific for p38, as they do not activate ERK1/2 or JNK. MKK6 can phosphorylate all four p38 MAPK isoforms, however, MKK3 preferentially phosphorylates α, γ, and δ (*25, 26*). Two mechanisms may account for the specificity in p38 activation: 1. the selective formation of functional complexes between MKK3/6 and different p38 isoforms; 2. the selective recognition of the activation loop of p38 isoforms by MKK3/6 (*27*). Additionally, p38α can be phosphorylated by MKK4, an activator of the JNK cascade (*28, 29*).

Besides the canonical p38 MAPK-activation pathway described above, p38α (and probably p38β) can be activated by several non-canonical mechanisms. An alternative activation mechanism involves phosphorylation of p38α on Tyr323 by the T-cell receptor-proximal tyrosine kinases and $p56^{lck}$, leading to p38α autophosphorylation on the activation loop and consequently increasing p38α kinase activity towards substrates (*30*). The second reported alternative pathway of p38α activation involves TAK1-binding protein 1 (TAB1), which binds selectively to the p38α isoform and induces p38α autophosphorylation (*31, 32*). The last non-

canonical p38 MAPK-activation pathway has been proposed to operate upon down-regulation of the protein phosphatase Cdc7. This pathway induces an abortive S-phase leading to p38α–mediated apoptosis in HeLa cells (*33*).

p38 MAPKs have been detected in both the nucleus and cytoplasm of quiescent cells. However, upon cell stimulation, the cellular localization of p38 is controversial. Some evidence indicates that p38 translocates to the nucleus from the cytoplasm (*34*), whereas other evidence shows that activated p38 is present in the cytosol (*35*). The difference in pools of p38 may explain the discrepancy, as p38 may be located in different subcellular compartments and bound to different partners (*16*).

The p38 MAPK signaling cascade plays an important role in normal immune and inflammatory responses. p38 MAPK activation lead to increased pro-inflammatory cytokine production by modulating transcription factors, such as NF-κB (*16, 36*), or at the mRNA level, by modulating cytokine mRNA stability and translation through regulating MNK1(*37*) and MK2/3 (*38*). Furthermore, p38 MAPKs also play roles in cell proliferation and survival. Some studies show that p38α has a pro-survival function, and others report that p38α activity is associated with the induction of apoptosis by cellular stresses (*24*).

1.4. P38α MAPK INHIBITORS

Since the initial discovery of p38α MAPK in the early 1990s, there has been a great interest in identifying small molecules that target this kinase for the treatment of various inflammatory diseases (*39*). More than 234 patents regarding p38 MAPK inhibitors have been published since 1996, and approximately 20 inhibitors have entered clinical trials (*40*). However, the development of many p38 MAPK inhibitors has been hindered due to poor toxicity profiles such as liver toxicity, cardiotoxicity, lightheadedness, CNS toxicity, skin irritation and infection (*41*). The vast majority of p38 MAPK inhibitors has targeted the highly conserved ATP binding pocket. A small number of inhibitors have been shown to interact with other binding sites.

1.4.1. ATP-competitive and DFG-out allosteric p38α MAPK inhibitors

Following the discovery of the pyridinylimidazole class of p38α MAPK inhibitors, exemplified by SB-203580, multiple pharmaceutical companies, e.g. Merck, Roche, Vertex, Aventis and Amgen, explored substituent modification as well as imidazole and/or pyridine ring replacement (*42, 43*). These efforts resulted in a number of p38α inhibitors that either maintained or improved potency (Figure 1.2). Many of these inhibitors have a similar binding mode to the p38α active site as the original SB-203580 inhibitor (Figure 1.3). Two key interactions between p38α and inhibitors have been observed from X-ray co-crystal structures, including a hydrogen bond interaction with the hinge region Met109-NH and a lipophilic interaction of the inhibitor with hydrophobic pocket I that is not accessed by ATP. A non-conserved residue, the so-called gatekeeper, controls the access to hydrophobic pocket I. This residue is relatively small in p38α (Thr106) whereas 75 % of all kinases have bulky residues in this position. Thus, kinases with large gatekeeper residues are usually insensitive to pyridinylimidazoles and related p38 inhibitors. Most of these inhibitors are highly potent in vitro with IC_{50} values in the low nanomolar and sub-nanomolar range. However, the drawback of this class is that these compounds also interact with cytochrome P450 enzymes which are associated with liver toxicity (*42*). Many efforts have been made to reduce cytochrome interaction,

however, inhibitors with reduced cytochrome inhibition are also less potent kinase inhibitors (*44*).

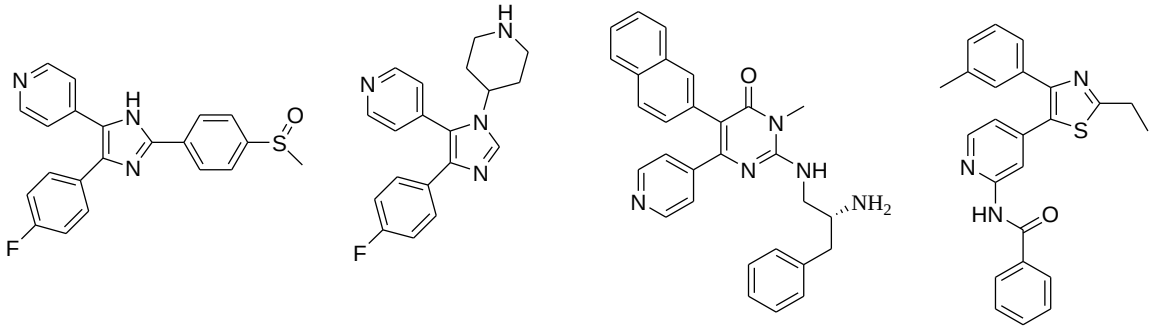

Figure 1.2. Pyridinylimidazole and pyridinylimidazole-like p38α MAPK inhibitors.

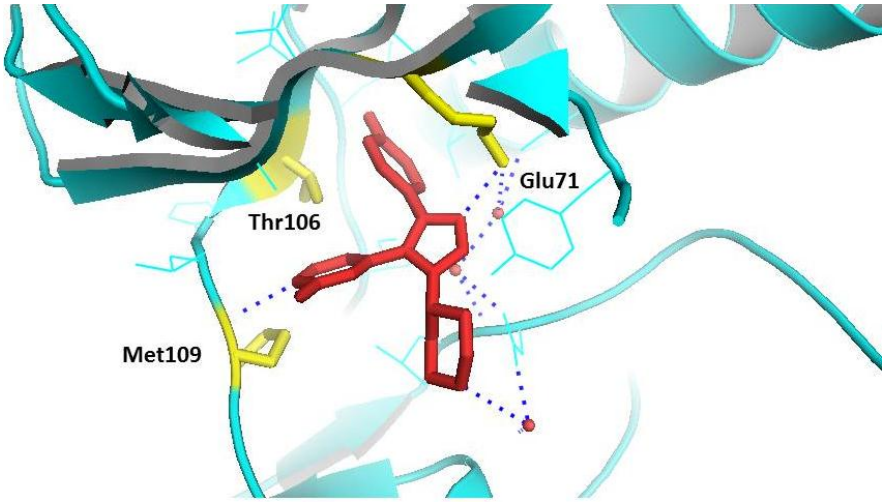

Figure 1.3. Crystal structure of p38α in complex with SB 220025 (1BL7).

The *N*,*N*'-diaryl urea class of inhibitors was independently discovered at Bayer, Boehringer Ingelheim and Vertex (*45-47*). The most representative example is BIRB 796. BIRB 796 binds to a novel allosteric site, which is spatially distinct from the ATP binding site, causing a large conformational change. This compound has a reported K_d of 0.05 nM for inactive p38α and inhibits the phosphorylation of p38α in the picomolar range (Figure 1.4). According to the crystal structure of BIRB 796 with human p38α, the tert-butyl group is placed in the DFG pocket

and the naphthalenyl group is positioned in hydrophobic pocket I. Three hydrogen bonds are formed, between one urea NH and Glu71, carbonyl-O and the amide NH of Asp168, and morpholine-O and the linker residue Met109 (Figure 1.5). This compound advanced to phase II/III clinical trials for the treatment of autoimmune disorders. Unfortunately, due to non-selective inhibition, there is no further clinical development for this compound (*42*).

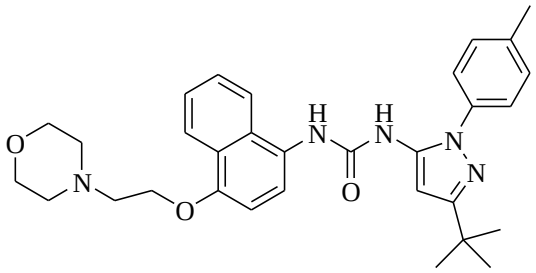

BIRB 796

Figure 1.4. DFG-out p38α MAPK inhibitor.

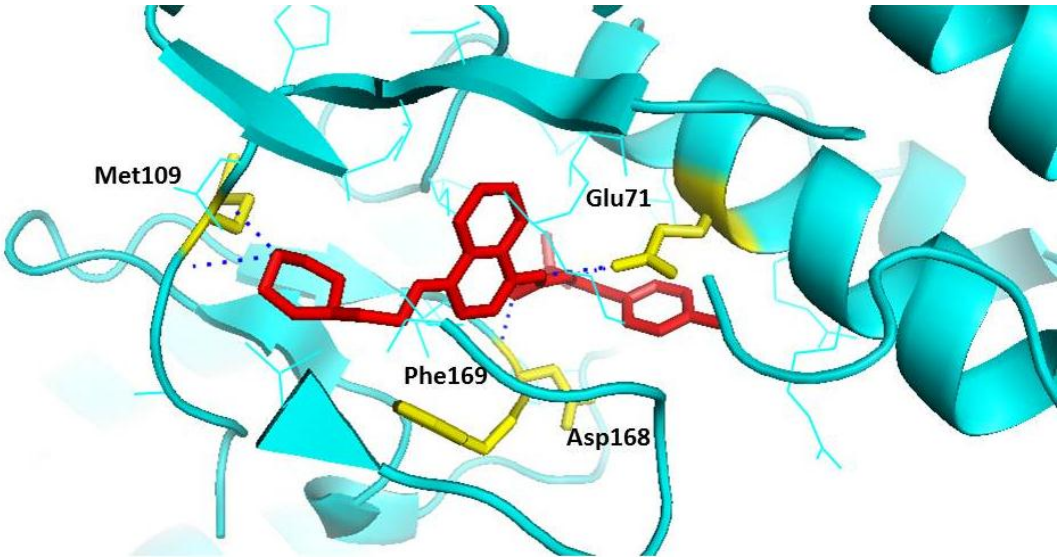

Figure 1.5. Crystal structure of p38α in complex with BIRB 796 (1KV2).

Bicyclic 6,6-heterocycles and related structures are an alternative structural class of p38α inhibitors. The first compound from this class was developed by Vertex and has a high selectively profile (*48, 49*) (Figure 1.6). To date, no crystal structure of this compound in

complex with p38α is available. Co-crystal structures of other analogs developed by Merck have been solved. So it has been proposed that the pyrimidopyridazinone ring of Vertx compound may also bind to p38α by forming two hydrogen bonds to Met109-NH and Gly110-NH (Figure 1.7). The peptide flip in the hinge region of p38α may account for the high selectivity of this compound. Vertex compound progressed to phase IIb clinical trials. However, development was discontinued because of CNS toxicity in preclinical evaluations (*40*).

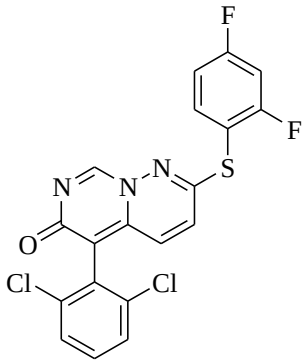

VX 745

Figure 1.6. p38α MAP kinase inhibitor VX 745.

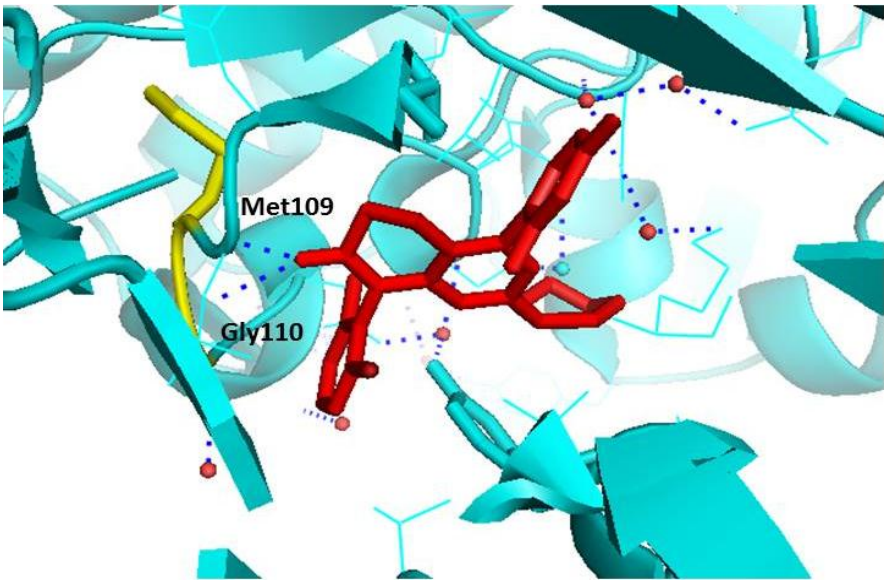

Figure 1.7. Crystal structure of p38α in complex with quinazolinone (1OVE).

The last structural class is linear binders: diarylketones and indole amides (Figure 1.8). Ketopyrzole was identified in a high throughput screening assay from Roche (*48*). Based on the crystal structure, the carbonyl-O forms a hydrogen bond to Met109, and the pyrzole rings forms two hydrogen bonds to His107-O and Thr106. The 4-fluorophenyl ring is placed in hydrophobic pocket I (Figure 1.9) (*42*). This compound shows high selectivity and efficacy. It was selected as a clinical candidate for the treatment of rheumatoid arthritis (*40*).

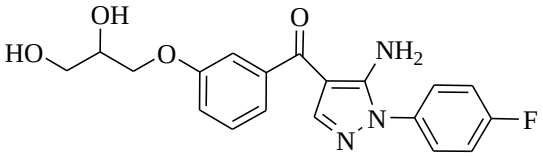

RO 3201195

Figure 1.8. Linear binder RO 3201195.

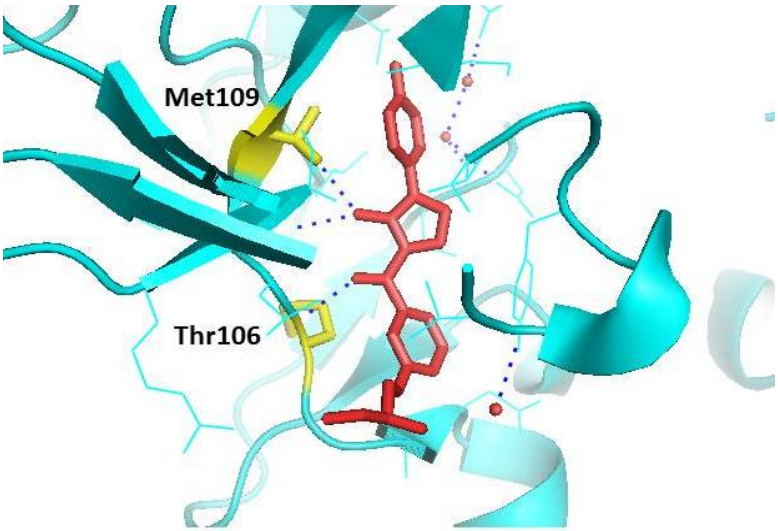

Figure 1.9. Crystal structure of p38α in complex with RO 3201195 (2GFS).

1.4.2. Non-ATP competitive p38α MAPK inhibitors

In 2004, a substrate selective and non-ATP competitive MAPK p38α inhibitor was discovered (Figure 1.10). This small molecule inhibited the phosphorylation of MK2a with a K_i

of 330 nM, and inhibited the phosphorylation of ATF2 with a K_i of more than 20 μM. Isothermal titration calorimetry analysis indicated the inhibitor did not compete with ATP for p38α, and surface plasmon resonance study showed that this inhibitor was not able to interrupt the binding of p38α to MK2a. Furthermore, a deuterium exchange mass spectrometry (DXMS) study suggested that this compound binds in the vicinity of the p38 MAPK active site, resulting in perturbations to ATP binding site and docking groove residues (*49*).

Recently, Comess *et al.* reported the identification and characterization of several non-ATP competitive p38α MAPK inhibitors through an affinity-based lead discovery campaign (Figure 1.10). The co-crystal structures showed that the inhibitor binds to a novel allosteric binding site located at the C-terminal lobe of p38α MAPK. This inhibitor directly inhibits p38α with an IC_{50} of 1.2 μM and exhibits no activity against other p38 isoforms β, γ, δ (*50*).

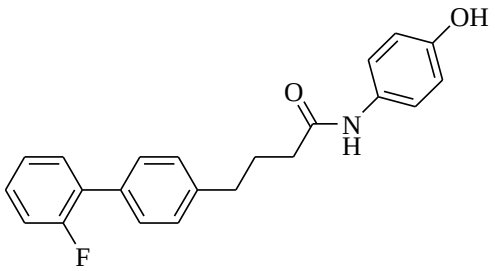

CMPD1

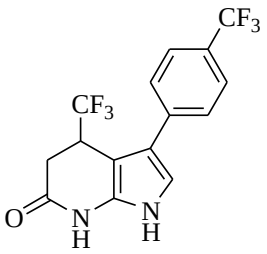

p38 Allosteric Inhibitor

Figure 1.10. Non-ATP competitive inhibitors.

1.5. COVALENT KINASE INHIBITORS

The majority of known kinase inhibitors are ATP-competitive. The main challenge in kinase inhibitor discovery has been poor selectivity and the high intracellular concentration of the endogenous competitive substrate, ATP. An alternative strategy is to develop highly targeted covalent, irreversible inhibitors to overcome these challenges. Over the last decade, many efforts have been made towards covalent kinase inhibitors. Covalent inhibitors have shown exceptional potency in overcoming cellular ATP competition and selectivity that is currently faced by reversible kinase inhibitors (*51*).

For example, the most well-characterized, selective irreversible inhibitors of epidermal growth factor receptor (EGFR), such as HKI-272 (*52*) and CL-387785 (*53*) and PD 168393 (*54*) were developed to target a relatively rare cysteine residue located at the lip of the ATP binding site (Figure 1.11). These molecules were rationally designed by appending an electrophile to the EGFR-selective 4-anilinoquinazoline and 4-anilinoquinoline-3-carbonitrile scaffolds, which undergo Michael addition reaction with the thiol present in the cysteine residue (Cys773). As a result, these inhibitors irreversibly block the binding of ATP to the kinase, rendering the kinase inactive. These compounds also show low reactivity with DTT in enzyme assays and glutathione in cellular assays, suggesting that their reactivity towards non-specific thiols are low (*51*). So far, five such EGFR kinase inhibitors are being investigated in lung cancer clinical trials (*55-57*). Additionally, irreversible inhibitors have also been shown to target several other kinases such as vascular endothelial growth factor receptor 2 (VEGFR2) (*58*), the Tec family kinase BTK (*59*) and RSK (*60*).

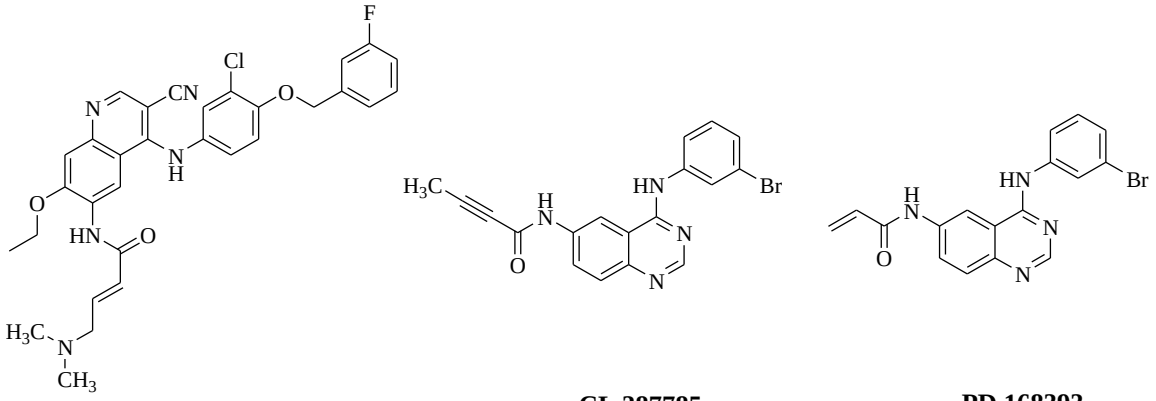

HKI 272 **CL 387785** **PD 168393**

Figure 1.11. Examples of EGFR covalent inhibitors.

1.6. DOCKING INTERACTIONS IN MAPK CASCADE

MAPKs recognize their substrates and regulators through docking interaction, and the docking interactions may account for the MAPK pathway efficiency and specificity (*61, 62*). At least two types of docking interactions between MAPKs and their substrates, activators and phosphatases have been identified. In both docking interactions, short motifs are found within substrates with a complementary pocket or groove on the kinase (*11*).

The first docking motif is called the D domain (D site, δ domain, DEJL domain), which consists of a cluster of basic residues, a short spacer and a hydrophobic patch (Lys/Arg-Lys/Arg-Xaa2-6-ϕ-X-ϕ, where ϕ is a hydrophobic residue, such as Leu, Iso, or Val) (*63*). The interactions between MAPK and D domains have been characterized by mutagenesis, hydrogen exchange-mass spectrometry, and X-ray crystallography. The D domain motif was first identified in c-Jun involved in MAPK docking (*64, 65*). Subsequently, sequences related to the D domain were also found in other transcription factors, including the MAPK-regulated bZIP, ETS, and MAD, and many MAPK regulatory proteins, including upstream activating kinases (MAPKKs), phosphatases (PTP-SL, STEP, and MKPs), and scaffold proteins (KSR) across different species (*27, 64*). The D-recruitment site (DRS) on MAP kinase is composed of acidic patch in the C-terminal known as the CD (Common Docking) domain (*66*) and hydrophobic docking groove(*67, 68*) (or referred to as "ED) (*63*).

The second MAPK docking domain is known as the DEF domain (Docking site for ERK, FXFP, F site or DEF site). The DEF domain consists of the Phe-Xaa-Phe-Pro sequence, where Xaa is any amino acid and one of the Phe residues can also be a Tyr (*69-71*). The DEF domain has been identified in a number of ERK1/2 substrates, located between 6 and 20 amino acids C terminal to the phosphoacceptor site. DEF domains are required for efficiently binding to ERK1/2 and subsequent phosphorylation (*72, 73*). Additionally, the DEF domain in the transcription factor SAP-1 has been reported to contribute to efficient phosphorylation by p38α (*74*).

Chang and Goldsmith reported crystallographic studies of p38α in complex with docking site peptides derived from substrate MEF2A and activating enzyme MKK3b. Both peptides bind to the site in the C-terminal domain of the kinase. Binding to this site induces conformational changes in the active site as well as structural disorder in the phosphorylation loop (*68*). Additionally, Bardwell demonstrated that all MAPKK D domain binding site bind better to their cognate MAPKs compared to non-cognate MAPKs. For instance, the MKK3 D domain peptide inhibits p38α with an IC_{50} of <10 nM, and this peptide does not inhibit JNK1 or JNK2 (*75*).

The hydrophobic docking groove in the DRS appears to be a great potential drug site target as it has a significant hydrophobic site (*76, 77*). The hydrophobic docking grooves vary significantly among p38α, ERK2 and JNK's. Interestingly, cysteine residues are present in the hydrophobic docking groove. P38α has two cysteine residues, Cys119 and C162, facing the pocket. ERK2 and JNK have one cysteine, Cys159 and Cys163, respectively. It has been suggested that covalent inhibitors could be developed directed towards cysteine (*77*).

1.7. ENEDIYNE AND BERGMAN CYCLIZATION

The enediyne structural moiety, containing two acetylenic groups conjugated to a double bond [(Z)-3-ene-1,5-diyne], has been identified in several naturally occurring anticancer antibiotics (*78, 79*). The naturally occurring enediynes can be grouped into two classes based on the ring size of the enediyne core structure: the 9-membered ring enediyne and the 10-membered ring enediyne. Almost all the 9-membered ring enediynes with the exception of N199A2 are produced as chromophore-protein complexes, exemplified by neocarzinostatin (NCS), C-1027, kedarcidin and maduropeptin. In contrast, 10-membered ring enediynes are produced as isolated chromophores, exemplified by calicheamicin γ_1^I (*80*), esperamicin A_1 (*81*), dynemicin A (*82*), uncialamycin (*83*), namenamicin (*84*), and shishijimicin (Figure 1.13) (*85*). Some of these naturally occurring enediynes are able to kill cancer cells *in vitro* at concentrations as low as 10^{-12}M (*86*), and that has aroused interest in studying the mechanism of action of these agents, and which came from the studies by Bergman.

In 1972, Robert Bergman and coworkers reported the Bergman cyclization involving the thermal rearranging of enediynes to reactive *p*-benzyne diradicals which then abstracts two hydrogens from solvent to form benzene (Figure 1.12) (*87*). It has been proposed that the generation of benzenoid diradicals from naturally occurring enediynes abstract hydrogen atoms from the deoxyribose sugar backbone of DNA, causing DNA strand scission.

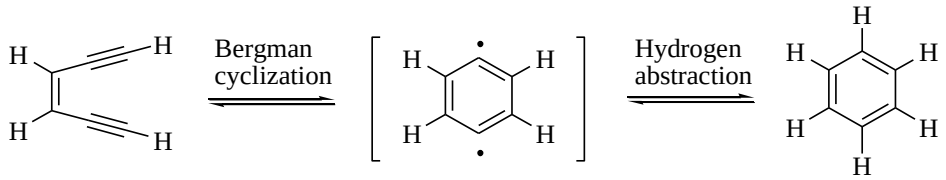

Figure 1.12. Bergman cyclization.

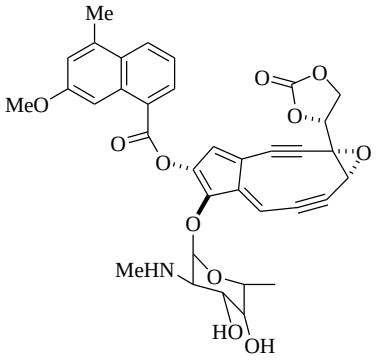

NSC-chromophore

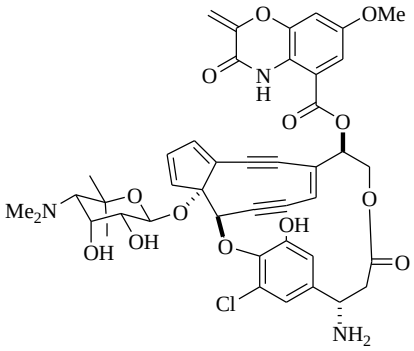

C-1027 (lidamycin)

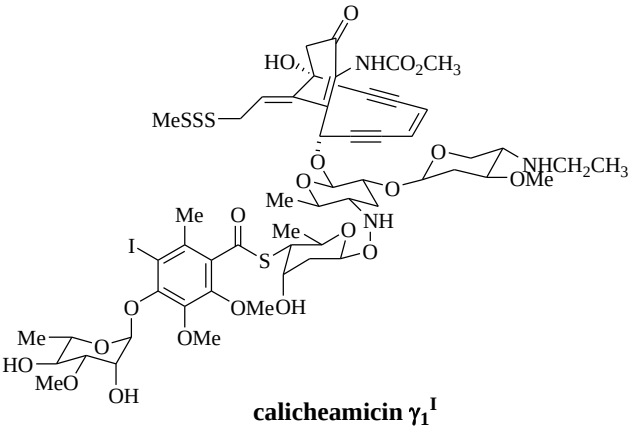

calicheamicin γ_1^I

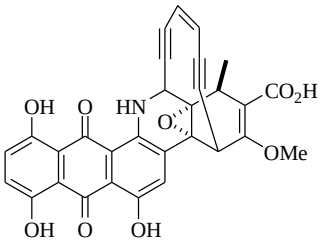

dynemicin A

Figure 1.13. Examples of naturally occurring enediyne antibiotics.

In the case of calicheamicin, it is stable to diradical-generating Bergman cyclization until activated via nucleophilic attack. Activation involves an intramolecular Michael addition to the cyclohexenone core followed by a bioreduction of the trisulfide to a thiolate anion. The resulting rehybridization of the bridgehead carbon from sp^2 to sp^3 triggers the Bergman cyclization, generating *p*-benzyne diradicals (Figure 1.14) (*88*).

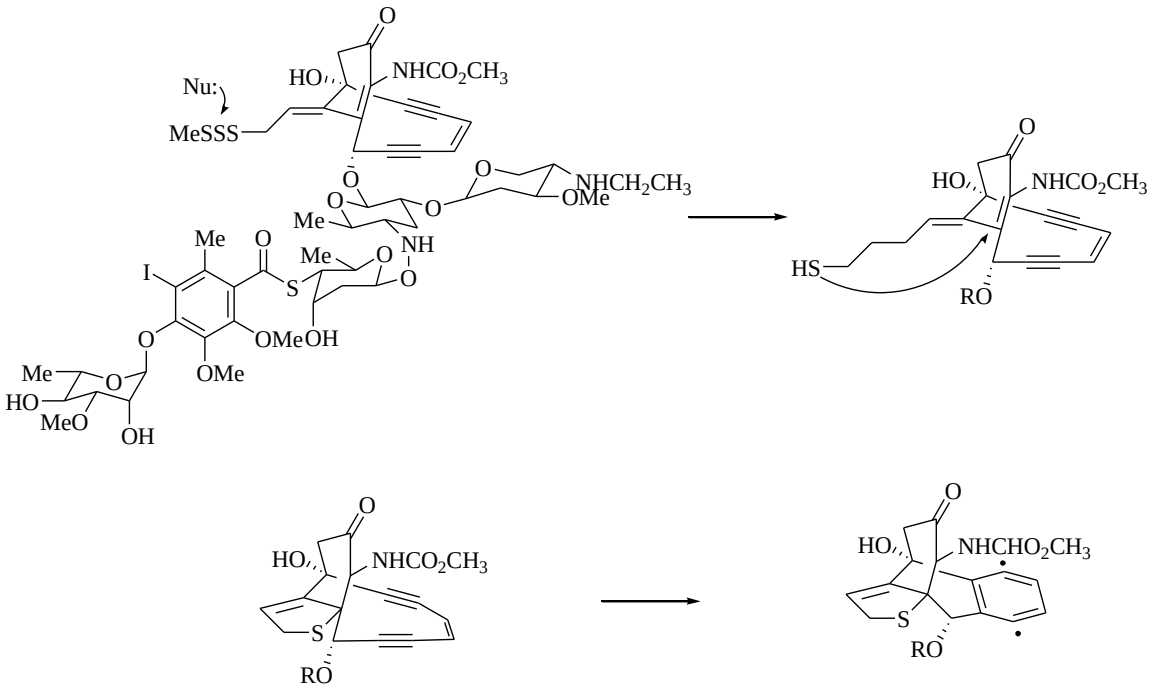

Figure 1.14. Bioactivation of calicheamicin.

In the case of dynemicin A, the triggering mechanism involves the reduction of anthraquinone to hydroquinone and the following rearrangement to open the epoxide. The ring opening brings the two alkynyl group into close proximity allowing cycloaromatization (Figure 1.15) (*89-91*).

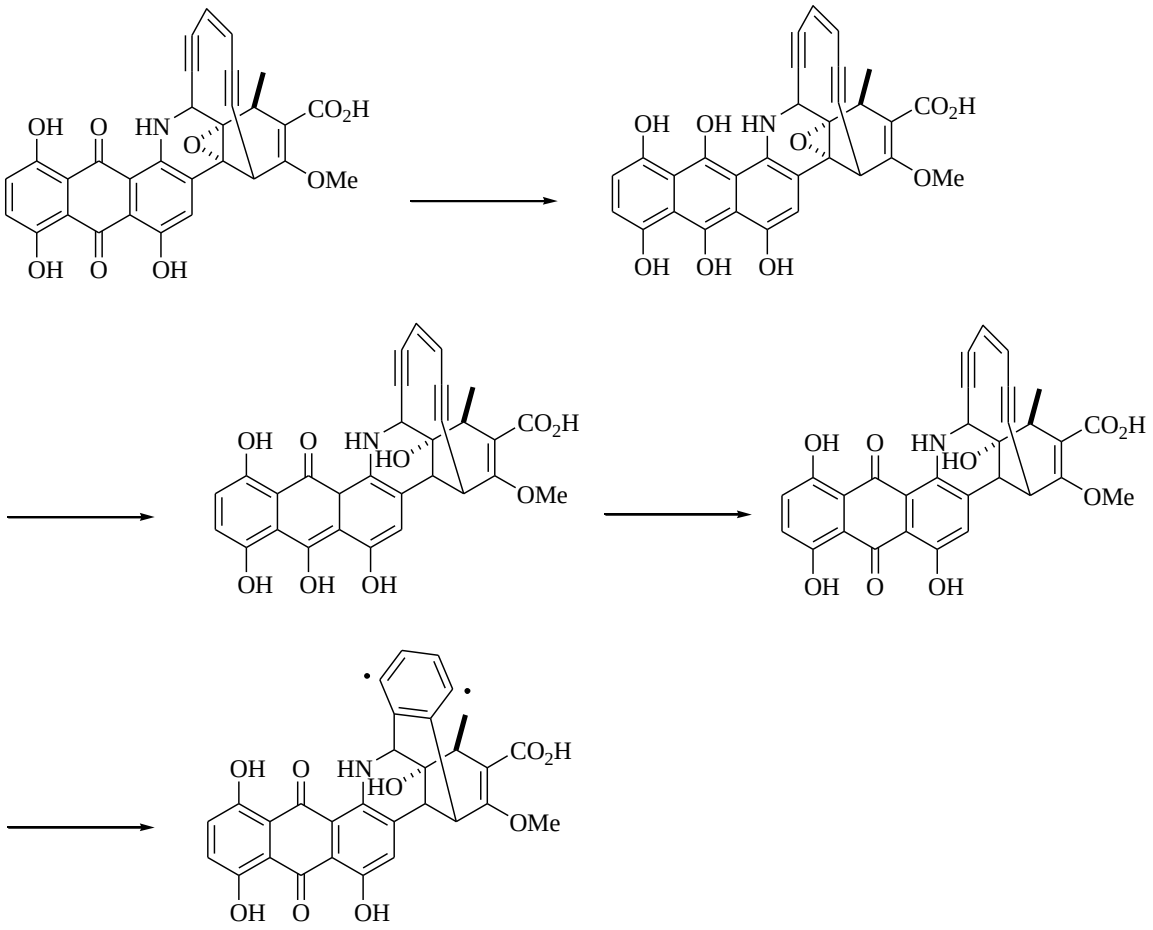

Figure 1.15. Bioactivation of dynemicin A.

Activation of neocarzinostatin involves with nucleoephilic attack by a thiol group, such as glutathione, followed by epoxide ring opening to generate an eneyne cumulene, which then cycloarmatizes to form a diradical species (Figure 1.16) (*92-94*).

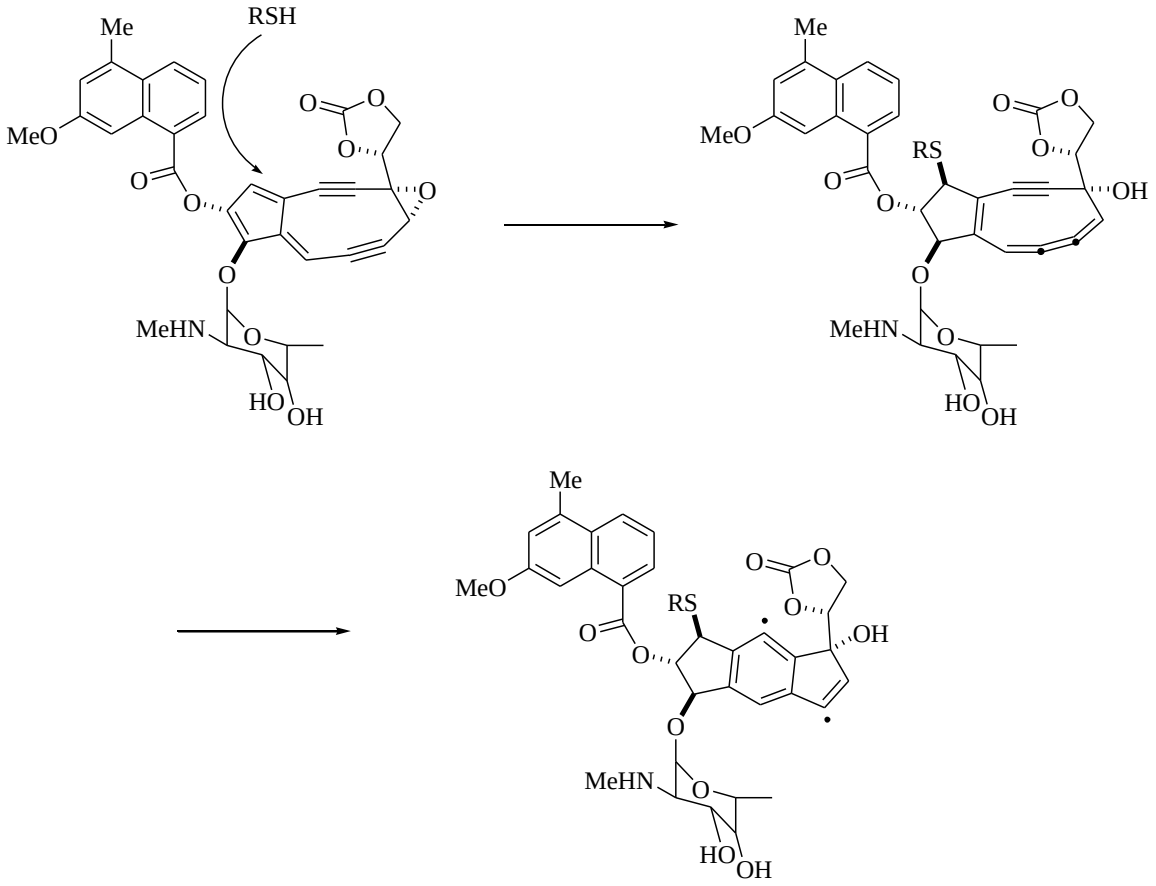

Figure 1.16. Bioactivation of neocarzinostatin.

1.8. AZA-ENEDIYNE AND AZA-BERGMAN CYCLIZATION

In 2007, David and Kerwin reported the first synthesis of a new class of enediynes, 3-aza-enediynes (C,*N*-dialkynyl imines), and their thermal facile rearrangement to β-alkynylacrylonitriles, structurally related to the Bergman rearrangement of (Z)-hexenediynes (Figure 1.17) (*95*). The replacement of a sp^2 carbon with a sp^2 nitrogen may accelerate the Bergman cyclization by disturbing π-delocalization and decreasing the degree of repulsion of the in-plane π-orbitals in the transition state. The diradical intermediate, 2,5-didehydropyridine could not be trapped. Instead, (Z)-β-alkynylacrylonitrile, derived from the retro-aza-Bergman rearrangement, was exclusively isolated (*95*). Chen and co-workers reported the detection of a small amount of pyridine products by GC/MS in the thermolysis of the aza-enediyne under acidic conditions (*96*). The overall conversion of **1** to **3** is highly exothermic. Computational studies suggested that the barrier for the aza-Bergman cyclization is lower than the barrier for the Bergman cyclization (*96*), and the barrier for the retro-aza-Bergman cyclization is also low with the formation of more stable nitrile (*97*).

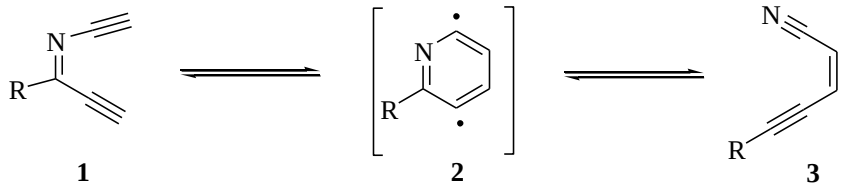

Figure 1.17. aza-Bergman cyclization.

Subsequently, Feng and co-workers in the Kerwin goup continued to study a series of 6-unsubstituted and 6-triisopropylsilyl substituted 1-phenyl-4-aryl-3-aza-hexe-3-ene-1,4-diynes. Both enediynes undergo retro-aza-Bergman rearrangement to generate β-alkynylacrylonitriles products (*98*). These and related aza-enediynes have been explored as potential DNA-cleaving anticancer agents with improved selectivity compared to the enediynes (*95, 96, 98, 99*). Numerous computational studies have been carried out so that aza-enediynes can be designed to

undergo a pH-dependent switch in reactivity mediated by changes in the kinetic stability and reactivity of the diradical upon nitrogen atom protonation (*97, 100, 101*).

Additionally, Nadipuram and co-workers in the Kerwin group reported the synthesis of 1,2-dialkynylimidazles, as a class of aza-enediynes, as well as their thermal cyclization and rearrangements (DAIms) (Scheme 1.18). Mild thermolysis of DAIms in the presence of chlorinated solvents or HCl leads to the isolation of imidazo[1,2-α]pyridine (ImPy) products, which may result from the trapping of an initially-formed diradical intermediate via aza-Bergman cyclization (*102, 103*). Thermolysis under neutral conditions in non-halogenated solvents affords products derived from trapping cyclopentapyrazine (CyPP) carbene intermediates by H-atom abstraction, C–H bond insertion, and alkene addition reactions (*104-106*). The CyPP carbene is proposed to be derived from an intermediate cyclic cumulene that results from the collapse of the diradical (*104*).

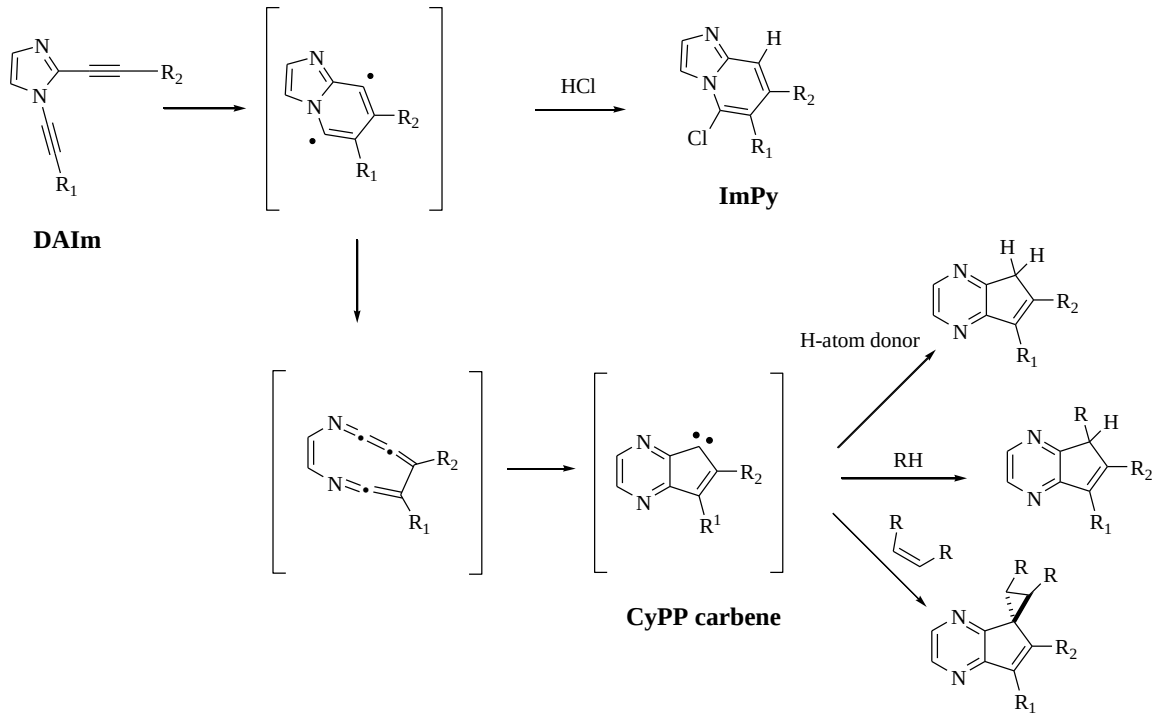

Figure 1.18. Thermal cyclization and rearrangement of 1,2-dialkynylimidazoles.

1.9. REFERENCES

1. Noble, M. E. M., Endicott, J. A., and Johnson, L. N. (2004) Protein kinase inhibitors: Insights into drug design from structure, *Science 303*, 1800-1805.
2. Cohen, P. (2002) Protein kinases - the major drug targets of the twenty-first century?, *Nat Rev Drug Discov 1*, 309-315.
3. Zhang, J., Yang, P. L., and Gray, N. S. (2009) Targeting cancer with small molecule kinase inhibitors, *Nat Rev Cancer 9*, 28-39.
4. Tamaoki, T., Nomoto, H., Takahashi, I., Kato, Y., Morimoto, M., and Tomita, F. (1986) Staurosporine, a potent inhibitor of phospholipid/Ca++dependent protein kinase, *Biochem Biophys Res Commun 135*, 397-402.
5. Davies, S. P., Reddy, H., Caivano, M., and Cohen, P. (2000) Specificity and mechanism of action of some commonly used protein kinase inhibitors, *Biochem J 351*, 95-105.
6. Alessi, D. R. (1997) The protein kinase C inhibitors Ro 318220 and GF 109203X are equally potent inhibitors of MAPKAP kinase-1 beta (Rsk-2) and p70 S6 kinase, *Febs Lett 402*, 121-123.
7. Hunter, T. (2007) Treatment for chronic myelogenous leukemia: the long road to imatinib, *J Clin Invest 117*, 2036-2043.
8. Brognard, J., and Hunter, T. (2011) Protein kinase signaling networks in cancer, *Curr Opin Genetics Dev 21*, 4-11.
9. Chen, Z., Gibson, T. B., Robinson, F., Silvestro, L., Pearson, G., Xu, B., Wright, A., Vanderbilt, C., and Cobb, M. H. (2001) MAP kinases, *Chem Rev 101*, 2449-2476.
10. Kyriakis, J. M., and Avruch, J. (2001) Mammalian mitogen-activated protein kinase signal transduction pathways activated by stress and inflammation, *Physiol Rev 81*, 807-869.
11. Cargnello, M., and Roux, P. P. (2011) Activation and Function of the MAPKs and Their Substrates, the MAPK-Activated Protein Kinases, *Microbiol Mol Biol R 75*, 50-83.
12. Lewis, T. S., Shapiro, P. S., and Ahn, G. G. (1998) Signal transduction through MAP kinase cascades, *Adv. Cancer Res 74*, 49-139.
13. Boulton, T. G., Yancopoulos, G. D., Gregory, J. S., Slaughter, C., Moomaw, C., Hsu, J., and Cobb, M. H. (1990) An insulin-stimulated protein kinase similar to yeast kinases involved in cell cycle control, *Science 249*, 64-67.
14. Raman, M., Chen, W., and Cobb, M. H. (2007) Differential regulation and properties of MAPKs, *Oncogene 26*, 3100-3112.
15. Pearson, G., Robinson, F., Gibson, T. B., Xu, B. E., Karandikar, M., Berman, K., and Cobb, M. H. (2001) Mitogen-activated protein (MAP) kinase pathways: Regulation and physiological functions, *Endocrine Reviews 22*, 153-183.

16. Cuadrado, A., and Nebreda, A. R. (2010) Mechanisms and functions of p38 MAPK signalling, *Biochem J 429*, 403-417.

17. Dan, I., Watanabe, N. M., and A., K. (2001) The Ste20 group kinases as regulators of MAP kinase cascades, *Trends Cell Biol 11*, 220-230.

18. Kolch, W. (2000) Meaningful relationships: the regulation of the Ras/Raf/MEK/ERK pathway by protein interactions, *Biochem J 351 Pt 2*, 289-305.

19. Roux, P. P., and Blenis, J. (2004) ERK and p38 MAPK-activated protein kinases: a family of protein kinases with diverse biological functions, *Microbiol Mol Biol Rev 68*, 320-344.

20. Coulombe, P., and Meloche, S. (2007) Atypical mitogen-activated protein kinases: structure, regulation and functions, *Biochim Biophys Acta 1773*, 1376-1387.

21. Ono, K., and Han, J. (2000) The p38 signal transduction pathway: activation and function, *Cell Signal 12*, 1-13.

22. Han, J., Lee, J. D., Bibbs, L., and Ulevitch, R. J. (1994) A Map Kinase Targeted by Endotoxin and Hyperosmolarity in Mammalian-Cells, *Science 265*, 808-811.

23. Lee, J. C., Laydon, J. T., McDonnell, P. C., Gallagher, T. F., Kumar, S., Green, D., McNulty, D., Blumenthal, M. J., Heys, J. R., Landvatter, S. W., and et al. (1994) A protein kinase involved in the regulation of inflammatory cytokine biosynthesis, *Nature 372*, 739-746.

24. Cuenda, A., and Rousseau, S. (2007) p38 MAP-kinases pathway regulation, function and role in human diseases, *Biochim Biophys Acta 1773*, 1358-1375.

25. Enslen, H., Raingeaud, J., and Davis, R. J. (1998) Selective activation of p38 mitogen-activated protein (MAP) kinase isoforms by the MAP kinase kinases MKK3 and MKK6, *J Biol Chem 273*, 1741-1748.

26. Alonso, G., Ambrosino, C., Jones, M., and Nebreda, A. R. (2000) Differential activation of p38 mitogen-activated protein kinase isoforms depending on signal strength, *J Biol Chem 275*, 40641-40648.

27. Enslen, H., Brancho, D. M., and Davis, R. J. (2000) Molecular determinants that mediate selective activation of p38 MAP kinase isoforms, *Embo J 19*, 1301-1311.

28. Doza, Y. N., Cuenda, A., Thomas, G. M., Cohen, P., and Nebreda, A. R. (1995) Activation of the MAP kinase homologue RK requires the phosphorylation of Thr-180 and Tyr-182 and both residues are phosphorylated in chemically stressed KB cells, *Febs Lett 364*, 223-228.

29. Brancho, D., Tanaka, N., Jaeschke, A., Ventura, J. J., Kelkar, N., Tanaka, Y., Kyuuma, M., Takeshita, T., Flavell, R. A., and Davis, R. J. (2003) Mechanism of p38 MAP kinase activation in vivo, *Genes Dev 17*, 1969-1978.

30. Salvador, J. M., Mittelstadt, P. R., Guszczynski, T., Copeland, T. D., Yamaguchi, H., Appella, E., Fornace, A. J., Jr., and Ashwell, J. D. (2005) Alternative p38 activation pathway mediated by T cell receptor-proximal tyrosine kinases, *Nat Immunol 6*, 390-395.

31. Ge, B., Gram, H., Di Padova, F., Huang, B., New, L., Ulevitch, R. J., Luo, Y., and Han, J. (2002) MAPKK-independent activation of p38alpha mediated by TAB1-dependent autophosphorylation of p38alpha, *Science 295*, 1291-1294.

32. Zhou, H., Zheng, M., Chen, J., Xie, C., Kolatkar, A. R., Zarubin, T., Ye, Z., Akella, R., Lin, S., Goldsmith, E. J., and Han, J. (2006) Determinants that control the specific interactions between TAB1 and p38alpha, *Mol Cell Biol 26*, 3824-3834.

33. Im, J. S., and Lee, J. K. (2008) ATR-dependent activation of p38 MAP kinase is responsible for apoptotic cell death in cells depleted of Cdc7, *J Biol Chem 283*, 25171-25177.

34. Raingeaud, J., Gupta, S., Rogers, J. S., Dickens, M., Han, J., Ulevitch, R. J., and Davis, R. J. (1995) Pro-inflammatory cytokines and environmental stress cause p38 mitogen-activated protein kinase activation by dual phosphorylation on tyrosine and threonine, *J Biol Chem 270*, 7420-7426.

35. Ben-Levy, R., Hooper, S., Wilson, R., Paterson, H. F., and Marshall, C. J. (1998) Nuclear export of the stress-activated protein kinase p38 mediated by its substrate MAPKAP kinase-2, *Curr Biol 8*, 1049-1057.

36. Karin, M. (2006) Nuclear factor-kappaB in cancer development and progression, *Nature 441*, 431-436.

37. Buxade, M., Parra-Palau, J. L., and Proud, C. G. (2008) The Mnks: MAP kinase-interacting kinases (MAP kinase signal-integrating kinases), *Front Biosci 13*, 5359-5373.

38. Ronkina, N., Kotlyarov, A., and Gaestel, M. (2008) MK2 and MK3--a pair of isoenzymes?, *Front Biosci 13*, 5511-5521.

39. Kumar, S., Boehm, J., and Lee, J. C. (2003) p38 MAP kinases: key signalling molecules as therapeutic targets for inflammatory diseases, *Nat Rev Drug Discov 2*, 717-726.

40. Karcher, S. C., and Laufer, S. A. (2009) Successful structure-based design of recent p38 MAP kinase inhibitors, *Curr Top Med Chem 9*, 655-676.

41. Goldstein, D. M., and Gabriel, T. (2005) Pathway to the clinic: inhibition of P38 MAP kinase. A review of ten chemotypes selected for development, *Curr Top Med Chem 5*, 1017-1029.

42. Lee, M. R., and Dominguez, C. (2005) MAP kinase p38 inhibitors: clinical results and an intimate look at their interactions with p38alpha protein, *Curr Med Chem 12*, 2979-2994.

43. Wrobleski, S. T., and Doweyko, A. M. (2005) Structural comparison of p38 inhibitor-protein complexes: a review of recent p38 inhibitors having unique binding interactions, *Curr Top Med Chem 5*, 1005-1016.

44. Laufer, S. A., Zimmermann, W., and Ruff, K. J. (2004) Tetrasubstituted imidazole inhibitors of cytokine release: probing substituents in the N-1 position, *J Med Chem 47*, 6311-6325.

45. Dumas, J., Sibley, R., Riedl, B., Monahan, M. K., Lee, W., Lowinger, T. B., Redman, A. M., Johnson, J. S., Kingery-Wood, J., Scott, W. J., Smith, R. A., Bobko, M., Schoenleber, R., Ranges, G. E., Housley, T. J., Bhargava, A., Wilhelm, S. M., and Shrikhande, A.

(2000) Discovery of a new class of p38 kinase inhibitors, *Bioorg Med Chem Lett 10*, 2047-2050.

46. Salituro, F. G., Germann, U. A., Wilson, K. P., Bemis, G. W., Fox, T., and Su, M. S. (1999) Inhibitors of p38 MAP kinase: therapeutic intervention in cytokine-mediated diseases, *Curr Med Chem 6*, 807-823.

47. Regan, J., Breitfelder, S., Cirillo, P., Gilmore, T., Graham, A. G., Hickey, E., Klaus, B., Madwed, J., Moriak, M., Moss, N., Pargellis, C., Pav, S., Proto, A., Swinamer, A., Tong, L., and Torcellini, C. (2002) Pyrazole urea-based inhibitors of p38 MAP kinase: from lead compound to clinical candidate, *J Med Chem 45*, 2994-3008.

48. Goldstein, D. M., Alfredson, T., Bertrand, J., Browner, M. F., Clifford, K., Dalrymple, S. A., Dunn, J., Freire-Moar, J., Harris, S., Labadie, S. S., La Fargue, J., Lapierre, J. M., Larrabee, S., Li, F., Papp, E., McWeeney, D., Ramesha, C., Roberts, R., Rotstein, D., San Pablo, B., Sjogren, E. B., So, O. Y., Talamas, F. X., Tao, W., Trejo, A., Villasenor, A., Welch, M., Welch, T., Weller, P., Whiteley, P. E., Young, K., and Zipfel, S. (2006) Discovery of S-[5-amino-1-(4-fluorophenyl)-1H-pyrazol-4-yl]-[3-(2,3-dihydroxypropoxy)ph enyl]methanone (RO3201195), an orally bioavailable and highly selective inhibitor of p38 MAP kinase, *J Med Chem 49*, 1562-1575.

49. Davidson, W., Frego, L., Peet, G. W., Kroe, R. R., Labadia, M. E., Lukas, S. M., Snow, R. J., Jakes, S., Grygon, C. A., Pargellis, C., and Werneburg, B. G. (2004) Discovery and characterization of a substrate selective p38alpha inhibitor, *Biochemistry 43*, 11658-11671.

50. Comess, K. M., Sun, C., Abad-Zapatero, C., Goedken, E. R., Gum, R. J., Borhani, D. W., Argiriadi, M., Groebe, D. R., Jia, Y., Clampit, J. E., Haasch, D. L., Smith, H. T., Wang, S., Song, D., Coen, M. L., Cloutier, T. E., Tang, H., Cheng, X., Quinn, C., Liu, B., Xin, Z., Liu, G., Fry, E. H., Stoll, V., Ng, T. I., Banach, D., Marcotte, D., Burns, D. J., Calderwood, D. J., and Hajduk, P. J. (2011) Discovery and characterization of non-ATP site inhibitors of the mitogen activated protein (MAP) kinases, *ACS Chem Biol 6*, 234-244.

51. Singh, J., Petter, R. C., and Kluge, A. F. (2010) Targeted covalent drugs of the kinase family, *Curr Opin Chem Biol 14*, 475-480.

52. Rabindran, S. K., Discafani, C. M., Rosfjord, E. C., Baxter, M., Floyd, M. B., Golas, J., Hallett, W. A., Johnson, B. D., Nilakantan, R., Overbeek, E., Reich, M. F., Shen, R., Shi, X. Q., Tsou, H. R., Wang, Y. F., and Wissner, A. (2004) Antitumor activity of HKI-272, an orally active, irreversible inhibitor of the HER-2 tyrosine kinase, *Cancer Res 64*, 3958-3965.

53. Kobayashi, S., Ji, H. B., Yuza, Y., Meyerson, M., Wong, K. K., Tenen, D. G., and Halmos, B. (2005) An alternative inhibitor overcomes resistance caused by a mutation of the epidermal growth factor receptor, *Cancer Res 65*, 7096-7101.

54. Fry, D. W., Bridges, A. J., Denny, W. A., Doherty, A., Greis, K. D., Hicks, J. L., Hook, K. E., Keller, P. R., Leopold, W. R., Loo, J. A., McNamara, D. J., Nelson, J. M., Sherwood, V., Smaill, J. B., Trumpp-Kallmeyer, S., and Dobrusin, E. M. (1998) Specific, irreversible inactivation of the epidermal growth factor receptor and erbB2, by a new class of tyrosine kinase inhibitor, *Proc Natl Acad Sci U S A 95*, 12022-12027.

55. Kwak, E. L., Sordella, R., Bell, D. W., Godin-Heymann, N., Okimoto, R. A., Brannigan, B. W., Harris, P. L., Driscoll, D. R., Fidias, P., Lynch, T. J., Rabindran, S. K., McGinnis, J. P., Wissner, A., Sharma, S. V., Isselbacher, K. J., Settleman, J., and Haber, D. A. (2005) Irreversible inhibitors of the EGF receptor may circumvent acquired resistance to gefitinib, *Proc Natl Acad Sci U S A 102*, 7665-7670.

56. Heymach, J. V., Nilsson, M., Blumenschein, G., Papadimitrakopoulou, V., and Herbst, R. (2006) Epidermal growth factor receptor inhibitors in development for the treatment of non-small cell lung cancer, *Clin Cancer Res 12*, 4441s-4445s.

57. Felip, E., Santarpia, M., and Rosell, R. (2007) Emerging drugs for non-small-cell lung cancer, *Expert Opin Emerg Drugs 12*, 449-460.

58. Wissner, A., Fraser, H. L., Ingalls, C. L., Dushin, R. G., Floyd, M. B., Cheung, K., Nittoli, T., Ravi, M. R., Tan, X., and Loganzo, F. (2007) Dual irreversible kinase inhibitors: quinazoline-based inhibitors incorporating two independent reactive centers with each targeting different cysteine residues in the kinase domains of EGFR and VEGFR-2, *Bioorg Med Chem 15*, 3635-3648.

59. Pan, Z., Scheerens, H., Li, S. J., Schultz, B. E., Sprengeler, P. A., Burrill, L. C., Mendonca, R. V., Sweeney, M. D., Scott, K. C., Grothaus, P. G., Jeffery, D. A., Spoerke, J. M., Honigberg, L. A., Young, P. R., Dalrymple, S. A., and Palmer, J. T. (2007) Discovery of selective irreversible inhibitors for Bruton's tyrosine kinase, *ChemMedChem 2*, 58-61.

60. Cohen, M. S., Hadjivassiliou, H., and Taunton, J. (2007) A clickable inhibitor reveals context-dependent autoactivation of p90 RSK, *Nat Chem Biol 3*, 156-160.

61. Bardwell, L. (2006) Mechanisms of MAPK signalling specificity, *Biochemical Society Transactions 34*, 837-841.

62. Smith, J. A., Poteet-Smith, C. E., Malarkey, K., and Sturgill, T. W. (1999) Identification of an extracellular signal-regulated kinase (ERK) docking site in ribosomal S6 kinase, a sequence critical for activation by ERK in vivo, *J Biol Chem 274*, 2893-2898.

63. Tanoue, T., and Nishida, E. (2003) Molecular recognitions in the MAP kinase cascades, *Cell Signal 15*, 455-462.

64. Sharrocks, A. D., Yang, S. H., and Galanis, A. (2000) Docking domains and substrate-specificity determination for MAP kinases, *Trends Biochem Sci 25*, 448-453.

65. Tanoue, T., Adachi, M., Moriguchi, T., and Nishida, E. (2000) A conserved docking motif in MAP kinases common to substrates, activators and regulators, *Nat Cell Biol 2*, 110-116.

66. Bardwell, A. J., Flatauer, L. J., Matsukuma, K., Thorner, J., and Bardwell, L. (2001) A conserved docking site in MEKs mediates high-affinity binding to MAP kinases and cooperates with a scaffold protein to enhance signal transmission, *J Biol Chem 276*, 10374-10386.

67. Gum, R. J., and Young, P. R. (1999) Identification of two distinct regions of p38 MAPK required for substrate binding and phosphorylation, *Biochem Biophys Res Commun 266*, 284-289.

68. Chang, C. I., Xu, B. E., Akella, R., Cobb, M. H., and Goldsmith, E. J. (2002) Crystal structures of MAP kinase p38 complexed to the docking sites on its nuclear substrate MEF2A and activator MKK3b, *Molecular Cell 9*, 1241-1249.

69. Fantz, D. A., Jacobs, D., Glossip, D., and Kornfeld, K. (2001) Docking sites on substrate proteins direct extracellular signal-regulated kinase to phosphorylate specific residues, *J Biol Chem 276*, 27256-27265.

70. Jacobs, D., Beitel, G. J., Clark, S. G., Horvitz, H. R., and Kornfeld, K. (1998) Gain-of-function mutations in the Caenorhabditis elegans lin-1 ETS gene identify a C-terminal regulatory domain phosphorylated by ERK MAP kinase, *Genetics 149*, 1809-1822.

71. Murphy, L. O., Smith, S., Chen, R. H., Fingar, D. C., and Blenis, J. (2002) Molecular interpretation of ERK signal duration by immediate early gene products, *Nat Cell Biol 4*, 556-564.

72. Lee, T., Hoofnagle, A. N., Kabuyama, Y., Stroud, J., Min, X., Goldsmith, E. J., Chen, L., Resing, K. A., and Ahn, N. G. (2004) Docking motif interactions in MAP kinases revealed by hydrogen exchange mass spectrometry, *Mol Cell 14*, 43-55.

73. Sheridan, D. L., Kong, Y., Parker, S. A., Dalby, K. N., and Turk, B. E. (2008) Substrate discrimination among mitogen-activated protein kinases through distinct docking sequence motifs, *J Biol Chem 283*, 19511-19520.

74. Galanis, A., Yang, S. H., and Sharrocks, A. D. (2001) Selective targeting of MAPKs to the ETS domain transcription factor SAP-1, *J Biol Chem 276*, 965-973.

75. Bardwell, A. J., Frankson, E., and Bardwell, L. (2009) Selectivity of docking sites in MAPK kinases, *J Biol Chem 284*, 13165-13173.

76. Zhou, T. J., Sun, L. G., Humphreys, J., and Goldsmith, E. J. (2006) Docking interactions induce exposure of activation loop in the MAP kinase ERK2, *Structure 14*, 1011-1019.

77. Akella, R., Moon, T. M., and Goldsmith, E. J. (2008) Unique MAP Kinase binding sites, *Biochim Biophys Acta 1784*, 48-55.

78. Smith, A. L., and Nicolaou, K. C. (1996) The enediyne antibiotics, *J Med Chem 39*, 2103-2117.

79. Van Lanen, S. G., and Shen, B. (2008) Biosynthesis of enediyne antitumor antibiotics, *Curr Top Med Chem 8*, 448-459.

80. Lee, M. D., Manning, J. K., Williams, D. R., Kuck, N. A., Testa, R. T., and Borders, D. B. (1989) Calicheamicins, a Novel Family of Antitumor Antibiotics .3. Isolation, Purification and Characterization of Calicheamicin-Beta-1br, Calicheamicin-Gamma-1br, Calicheamicin-Alpha-2i, Calicheamicin-Alpha-3i, Calicheamicin-Beta-1i, Calicheamicin-Gamma-1i and Calicheamicin-Delta-1i, *J Antibiot 42*, 1070-1087.

81. Golik, J., Dubay, G., Groenewold, G., Kawaguchi, H., Konishi, M., Krishnan, B., Ohkuma, H., Saitoh, K., and Doyle, T. W. (1987) Esperamicins, a Novel Class of Potent Antitumor Antibiotics .3. Structures of Esperamicins-A1, Esperamicin-A2, and Esperamicin-A1b, *J Am Chem Soc 109*, 3462-3464.

82. Konishi, M., Ohkuma, H., Matsumoto, K., Tsuno, T., Kamei, H., Miyaki, T., Oki, T., Kawaguchi, H., Vanduyne, G. D., and Clardy, J. (1989) Dynemicin a, a Novel Antibiotic with the Anthraquinone and 1,5-Diyn-3-Ene Subunit, *J Antibiot 42*, 1449-1452.

83. Davies, J., Wang, H., Taylor, T., Warabi, K., Huang, X. H., and Andersen, R. J. (2005) Uncialamycin, a new enediyne antibiotic, *Org Lett 7*, 5233-5236.

84. McDonald, L. A., Capson, T. L., Krishnamurthy, G., Ding, W. D., Ellestad, G. A., Bernan, V. S., MAiese, W. M., Lassota, P., Discafani, C., Kramer, R. A., and Ireland, C. M. (1996) Namenamicin, a new enediyne antitumor antibiotic from the marine ascidian Polysyncraton lithostrotum, *J Am Chem Soc 118*, 10898-10899.

85. Oku, N., Matsunaga, S., and Fusetani, N. (2003) Shishijimicins A-C, novel enediyne antitumor antibiotics from the ascidian Didemnum proliferum, *J Am Chem Soc 125*, 2044-2045.

86. Nicolaou, K. C., Dai, W. M., Tsay, S. C., Estevez, V. A., and Wrasidlo, W. (1992) Designed enediynes: a new class of DNA-cleaving molecules with potent and selective anticancer activity, *Science 256*, 1172-1178.

87. Jones, R. R., and Bergman, R. G. (1972) Para Benzyne - Generation as an Intermediate in a Thermal Isomerization Reaction and Trapping Evidence for 1,4-Benzenediyl Structure, *J Am Chem Soc 94*, 660-&.

88. Magnus, P., Fortt, S., Pitterna, T., and Snyder, J. P. (1990) Synthetic and Mechanistic Studies on Esperamicin-A1 and Calicheamicin-Gamma-1 - Molecular Strain Rather Than Pi-Bond Proximity Determines the Cycloaromatization Rates of Bicyclo[7.3.1] Enediynes, *J Am Chem Soc 112*, 4986-4987.

89. Sugiura, Y., Arakawa, T., Uesugi, M., Shiraki, T., Ohkuma, H., and Konishi, M. (1991) Reductive and nucleophilic activation products of dynemicin A with methyl thioglycolate. A rational mechanism for DNA cleavage of the thiol-activated dynemicin A, *Biochemistry 30*, 2989-2992.

90. Semmelhack, M. F., and Gallagher, J. C., D. . (1990) *Tetrahedron Lett 31*, 1521-1522.

91. Snyder, J. P., and Tipsword, G. E. (1990) Proposal for blending classical and biradical mechanisms in antitumor antibiotics: dynemicin A, *J Am Chem Soc 112*, 4040-4042.

92. Myers, A. G. (1987) *Tetrahedron Lett 28*, 4493-4496.

93. Myers, A. G., Harrington, P. M., and Kwon, B. (1992) *J Am Chem Soc 114*, 1086-1087.

94. Myers, A. G., Cohen, S. B., and Kwon, B. (1994) *J Am Chem Soc 116*, 1670-1682.

95. David, W., and SM., K. (1997) Synthesis and thermal rearrangement of C,N-dialkynyl imines: A potential Aza-Bergman route to 2,5-didehydropyridine, *J Am Chem Soc 119*, 1464-1465.

96. Hoffner, J., Schottelius, M. J., Feichtinger, D., and Chen, P. (1998) Chemistry of the 2,5-didehydropyridine biradical: Computational, kinetic, and trapping studies toward drug design, *J Am Chem Soc 120*, 376-385.

97. Cramer, C. J. (1998) Bergman, aza-bergman, and protonated aza-bergman cyclizations and intermediate 2,5-arynes: Chemistry and challenge to computation, *J Am Chem Soc 120*, 6261-6269.

98. Feng, L., Kumar, D., and Kerwin, S. M. (2003) An extremely facile aza-Bergman rearrangement of sterically unencumbered acyclic 3-aza-3-ene-1,5-diynes, *J Org Chem 68*, 2234-2242.

99. Feng, L., Zhang, A., and Kerwin, S. M. (2006) Enediynes from aza-enediynes: C,N-dialkynyl imines undergo both aza-Bergman rearrangement and conversion to enediynes and fumaronitriles, *Org Lett 8*, 1983-1986.

100. Feng, L., and Kerwin, S. M. (2003) *Tetrahedron Lett 44*, 3463.

101. Yang, W. Y., Breiner, B., Kovalenko, S., Ben, C., Singh, M., LeGrand, S. N., Sang, Q. X. A., Strouse, G. F., Copeland, J. A., and Alabugin, I. V. (2009) *J Am Chem Soc 131*, 11458-11470.

102. Khandekar, S. S., Feng, B., Yi, T., Chen, S., Laping, N., and Bramson, N. (2005) A liquid chromatography/mass spectrometry-based method for the selection of ATP competitive kinase inhibitors, *J Biomol Screen 10*, 447-455.

103. Barluenga, S., Dakas, P. Y., Boulifa, M., Moulin, E., and Winssinger, N. (2008) Resorcylic acid lactones: A pluripotent scaffold with therapeutic potential, *Cr Chim 11*, 1306-1317.

104. Nadipuram, A. K., and Kerwin, S. M. (2006) Thermal cyclization of 1,2-dialkynylimidazoles to imidazo[1,2-a]pyridines, *Tetrahedron 62*, 3798-3808.

105. Nadipuram, A. K., David, W. M., Kumar, D., and Kerwin, S. M. (2002) Synthesis and thermolysis of heterocyclic 3-aza-3-ene-1,5-diynes(1), *Org Lett 4*, 4543-4546.

106. Kerwin, S. M., and Nadipuram, A. (2004) 5H-cyclopentapyrazines from 1,2-dialkynylimidazoles, *Synlett*, 1404-1408.

Chapter 2

Synthesis and biological evaluation of p38α kinase-targeting dialkynylimidazoles

2.1. INTRODUCTION

A number of p38α inhibitors have been synthesized and characterized (*1*). Although these compounds show good inhibition of p38α, many also inhibit other protein kinases with similar or greater potency (*2*). There has been a growing interest in irreversible inhibitors of protein kinases (*3, 4*), and a number of these drugs are in clinical trials (*5*). Advantages of irreversible kinase inhibition include increased selectivity (*6*), duration (*7-9*), and therapeutic utility, especially against kinases that are resistant to competitive, ATP-binding pocket-targeting drugs (*10*). Additionally, irreversible inhibitors and related selective, covalent kinase modifying small molecules are of interest as probes for chemical genetics studies (*11*). While certain natural products and ATP analogs irreversibly inhibit kinases (*12, 13*), none are selective towards p38α. Thus, there is a need to develop selective and irreversible inhibitors that target p38α.

2.2. DESIGN AND SYNTHESIS OF P38α KINASE-TARGETING 1,2-DIALKYNYLIMIDAZOLES

The novel thermal cyclization and rearrangement of 1,2-dialkynylimidazoles (DAIms) have been reported as described in Chapter 1. Non-covalent association between DAIms and a kinase may facilitate the rate-determining aza-Bergman cyclization. The formation of reactive diradical and carbene intermediates under mild conditions from DAIms has led us to propose that DAIms can be designed to undergo kinase binding-induced cyclization and covalent inactivation of specific kinase targets. Specifically, the structural similarity between DAIms and the known p38α inhibitors such as SB-203580 (*14*) and RWJ-67657 (*15*) (Figure 2.1) has inspired the design and inhibition studies of p38α-targeting DAIms described here.

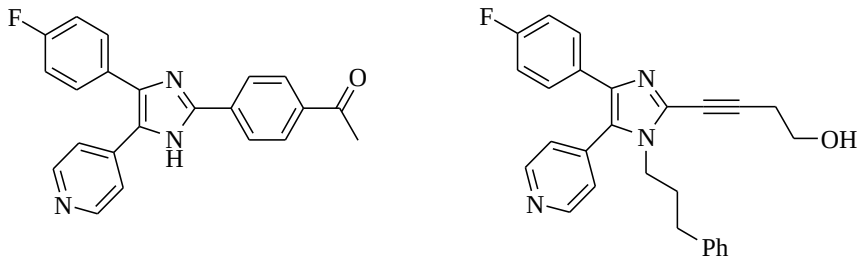

SB-203580 **RWJ-67657**

Figure 2.1. Examples of 4,5-diarylimidazole p38 inhibitors.

An initial route to kinase-targeting dialkynylimidazoles is shown in Scheme 2.1 The known 4 (5)-(4-fluorophenyl)-5(4)-(4-pyridyl)imidazole **1** (*16*) was protected with trityl group. Interestingly, this reaction only afforded one regioisomer, which was assigned as the 5-(4-fluorophenyl)-4-(4-pyridyl)imidazole **2** based on COSY and NOESY NMR. Compound **2** was deprotonated with *n*-BuLi at 0 °C, and quenched with I_2 to give the 2-iodo-imidazole **3**, which was deprotected in aqueous TFA to afford **4**. Coupling of the lithium anion of imidazole **4**, formed by deprotonation with LHMDS, with phenyl(phenylethynyl)-iodonium tosylate (*17*) afforded a 15 % yield of a 1:1 mixture of the regioisomeric *N*-alkynyl-2-iodoimidazoles **5** and **6**. The separated regioisomers were subjected to Sonogashra coupling with various terminal acetylene partners to provide the regioisomeric dialkynylimidazoles **7** and **8**. The regiochemical assignments within this series were made based on the X-ray crystal structure of **7b** shown in Figure 2.2.

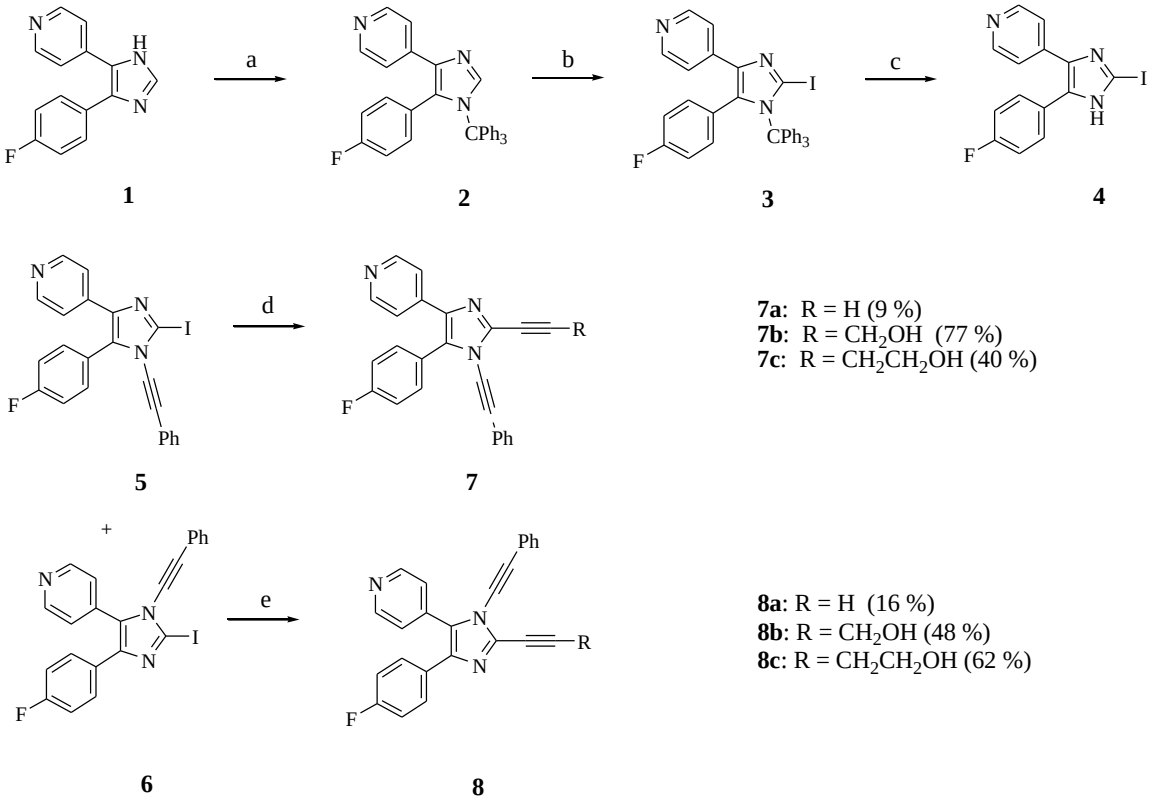

Scheme 2.1. Synthesis of dialkynylimidazoles. Reagents and conditions: (a) Et_3N, Ph_3CCl, CH_2Cl_2 (58 %); (b) i) *n*-BuLi, ii) I_2, THF, 0 °C (60 %); (c) TFA, H_2O (83 %); (d) LHMDS, $PhI^+CCPhTsO^-$ (15 %, 1: 1 **5**/**6**); (e) RCCH, $Pd(PPh_3)_4$, CuI, Et_3N.

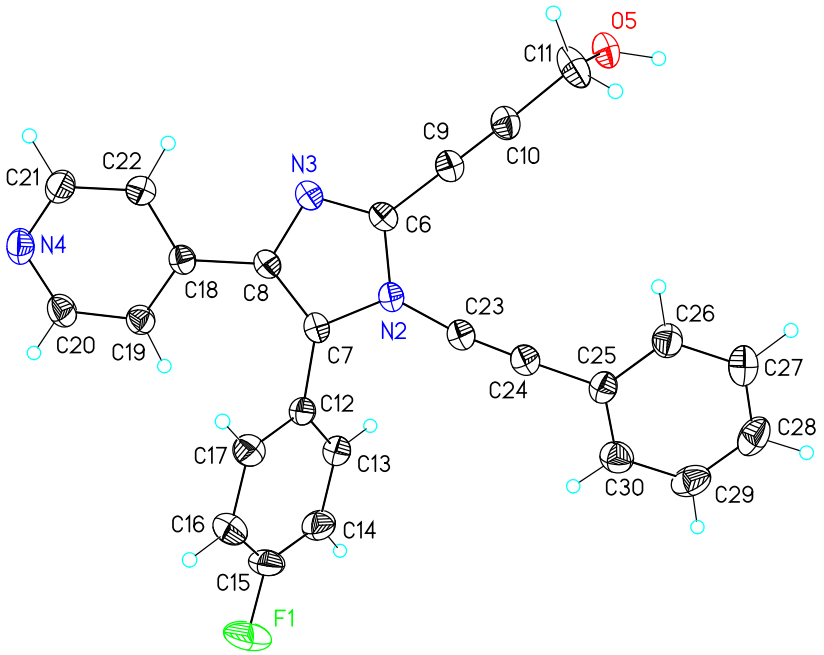

Figure 2.2. X-ray crystal structure of dialkynylimidazole **7b**.

Although providing access to select kinase-targeting dialkynylimidazoles, the synthetic route shown in Scheme 2.1 suffers from a number of limitations associated with the alkynyliodonium coupling reaction. Only the phenylethynyl and TMS-ethynyl iodonium reagents could be employed in this coupling (*18*), and even in these cases, the yields are poor and mixtures of regioisomers are produced. We recently reported a copper-catalyzed *N*-alkynylation of imidazole with bromoalkyne (Scheme 2.2). An improved synthetic route to these dialkynylimidazoles employing this coupling reaction was devised (Scheme 2.3). Treating 4-fluorophenylimidazole **9** (*19*) with TIPS-protected bromo-acetylene in the presence of catalytic CuI and 2-acetyl-cyclohexanone as ligand affords a 9:1 mixture of regioisomeric alkynylimidazoles **10b** and **10a**, respectively, in 79 % yield (*18*). Iodination of the 2-position of **10b** affords the 2-iodoimidazole **11**, which undergoes Sonogashira coupling with *O*-TIPS protected homopropargyl alcohol to give the dialkynylimidazole **12** in 73 % yield (*20*). Deprotonation of **12** with *n*-BuLi followed by

iodine quench affords the 5-iodoimidazole **13** in 74 % yield. A final Suzuki-Miyaura coupling of the 5-iodo imidazole **13** with pyridine-4-boronic acid followed by TBAF deprotection gives the dialkynyl-imidazole **14**. Mild thermolysis of **14** at 80° C under acidic conditions in the presence of chloride afforded **15**, the product of HCl addition to the diradical, in 50 % yield.

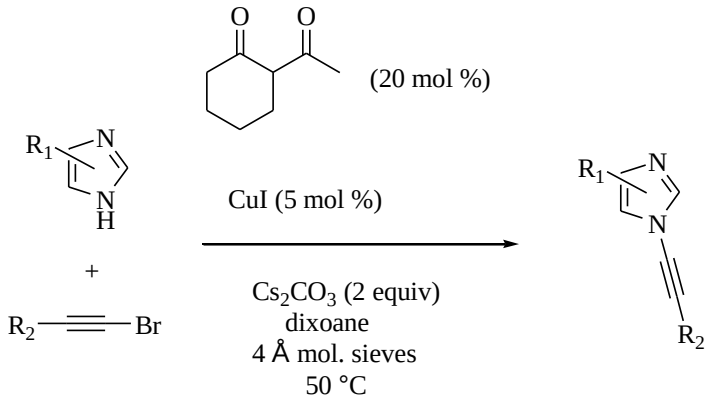

Scheme 2.2. Coupling reactions of bromoalkynes with imidazoles mediated by copper salts.

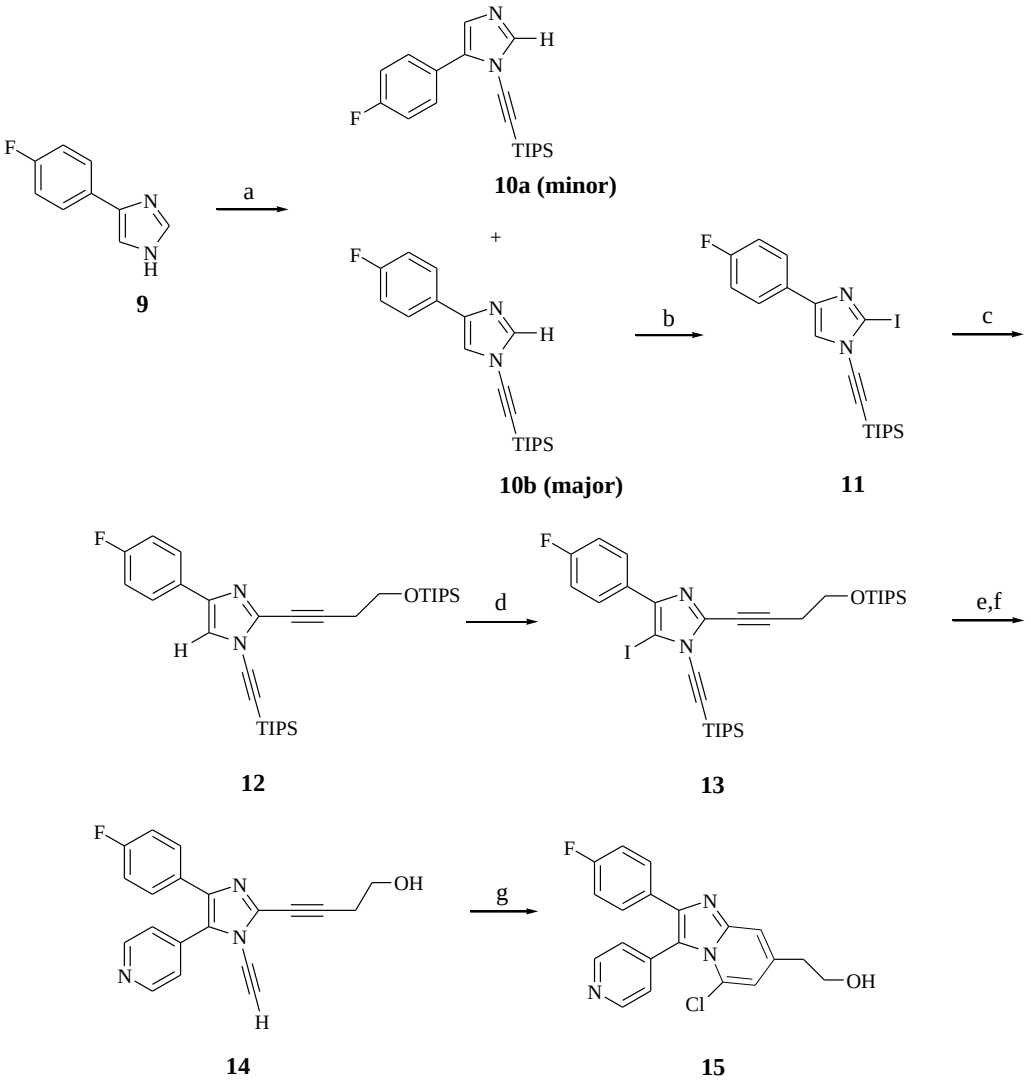

Scheme 2.3. Synthesis of dialkynylimidazoles. Reagents and conditions: (a) BrCCTIPS, CuI, AcC, Cs_2CO_3, dioxane, 50 °C overnight followed by reflux for 4 h (79 %, 1:9 **10a**/**10b**); (b) i) *n*-BuLi, ii) I_2, THF, -78 °C (91 %); (c) $TIPSOCH_2CH_2CCH$, $Pd(PPh_3)_4$, CuI, Et_3N (73 %); (d) i) *n*-BuLi, ii) I_2, THF, -78 °C (74 %); (e) pyridine 4-boronic acid, $Pd(PPh_3)_4$, K_2CO_3 (41 %); (f) TBAF, THF, -78 °C (89 %); (g) Me_4NCl, TfOH, DMF, 80 °C, 5 days (50 %).

2.3. P38α INHIBITION STUDIES OF 1,2-DIALKYNYLIMIDAZOLES

All kinase inhibition studies were performed by Invitrogen using the Z'-Lyte™ assay at [ATP] = $K_{m[app]}$ and protein substrate concentration of 20 μM. These 1,2-dialkynylimidazoles were assayed against p38α MAPK at a fixed time-point of 60 min (Table 2.1). Compounds **7a–c** and **8a–c** display modest inhibition at 10 μM concentration. In this series there is little difference in activity between the 1-alkynyl-5-fluorophenyl regioisomers **7a–c** and the 1-alkynyl-5-pyridylisomers **8a–c**, in contrast to reported 1-substituted pyridylimidazole p38α inhibitors (*21*). Interestingly, the 1-ethynylsubstituted analog **14** is a potent inhibitor of p38α. Compound **14** completely inhibits p38α at 10 μM (Table 2.1), and has an IC_{50} for p38α of 200 nM. The inhibition due to **14** in these assays is primary due to non-covalent inhibition. Pre-incubation of the kinase with **14** for 60 min prior to the addition of ATP did not change the IC_{50} value. In comparison, the IC_{50} of **14** against p38β (5.4 μM) is >25-fold higher. Dialkyny-limidazole **14** was also assayed at concentration of 20 μM against a panel of 53 additional human kinases (Table 2.2). Only one kinase, (MAPK4/HGK) was strongly inhibited (> 90 % inhibition at 20 μM, IC_{50} = 4.2 μM), while six additional kinases were moderately inhibited (between 50–90 % inhibition). The cyclized **15** also inhibited p38α (IC_{50} = 370 nM).

Compound	p38α % inhibition (@ 10 μM)[a]
7a	19
8a	28
7b	63
8b	83
7c	53
8c	75
14	100

[a]Tests were carried out in duplicates.

Table 2.1. In vitro activity of 1,2-dialkynylimidazoles against p38α.

Kinase	% inhibition[a]	Kinase	% inhibition[a]
ABL1	15	MAP4K4 (HGK)	92
ACVR1B (ALK4)	72	MAPK1 (ERK2)	6
AKT1 (PKBα)	29	MAPK12 (p38γ)	14
AMPK A1/B1/G1	-11	MAPK13 (p38δ)	12
AURKA (Aurora A)	7	MAPK8 (JNK1)	21
BTK	9	MAPK9 (JNK2)	88
CDK1/cyclin B	3	MAPKAPK2	3
CHEK1 (CHK1)	5	MARK2	14
CSNK1G2 (CK1 γ2)	36	MET (cMet)	11
CSNK2A1 (CK2α 1)	3	NEK1	11
DYRK3	8	NTRK1 (TRKA)	1
EGFR (ErbB1)	84	PAK4	8
EPHA2	23	PDGFRB (PDGFRβ)	10
ERBB2 (HER2)	41	PHKG2	-15
FGFR1	8	PIM1	3
FLT3	17	PLK1	7
FRAP1 (mTOR)	6	PRKACA (PKA)	50
GSK3B (GSK3β)	44	PRKCB1 (PKCβ I)	80
IGF1R	-1	RAF1 (cRAF)	82
IKBKB (IKKβ)	5	RET	21
INSR	7	ROCK1	15
IRAK4	1	RPS6KA3 (RSK2)	0
JAK3	4	RPS6KB1 (p70S6K)	7
KDR (VEGFR2)	36	SRC	27
KIT	5	SYK	3
LCK	48	TEK (Tie2)	5
MAP2K1 (MEK1)	10		

[a] Average of two separate trials.

Table 2.2. Kinase specificity of compound **14** (20 μM) against a panel of 53 kinases.

2.4. COVALENT ADDUCTION OF P38α BY 1,2-DIALKYNYLIMIDAZOLES

To examine whether 1,2-dialkynylimidazoles covalently modify p38α, **14** (100 μM) was incubated with non-phosphoryated p38α (5 μM) at 37 °C in 50 mM HEPES, 10 mM $MgCl_2$, 2 mM DTT, 1 mM EGTA, pH 7.5 for 12 h, followed by extensive dialysis, and the sample was analyzed by ESI-MS. A new peak in the mass spectrum at m/z = 41896, which corresponds to addition of a single molecule of **14** (MW = 331) to p38α, was observed (~25 % adduct) (Figure 2.3). Under identical conditions but with 1 mM DTT present, the adduct was the predominant species observed (Figure 2.4). On the contrary, in the presence of 4 mM DTT, the adduct formation is much reduced.

a.

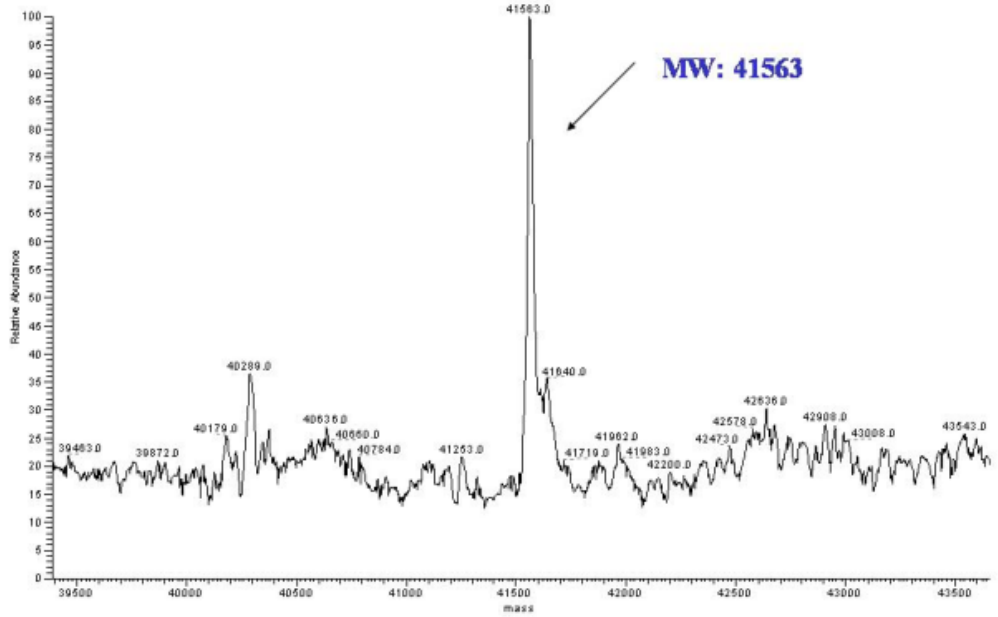

b.

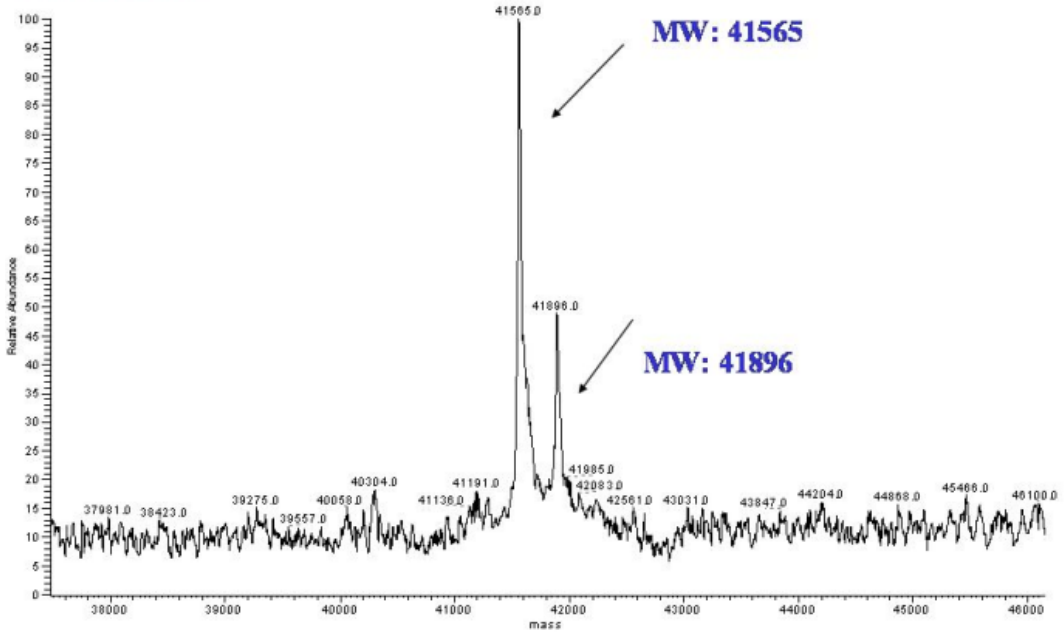

Figure 2.3. ESI-MS spectra of p38α and modified p38α by compound **14**. (a) Unphosphorylated p38α incubated for 12 h at 37 °C; (b) Unphosphorylated p38α incubated with dialkynylimidazole **14** for 12 h at 37 °C, followed by extensive dialysis.

p38α with 1 mM DTT:

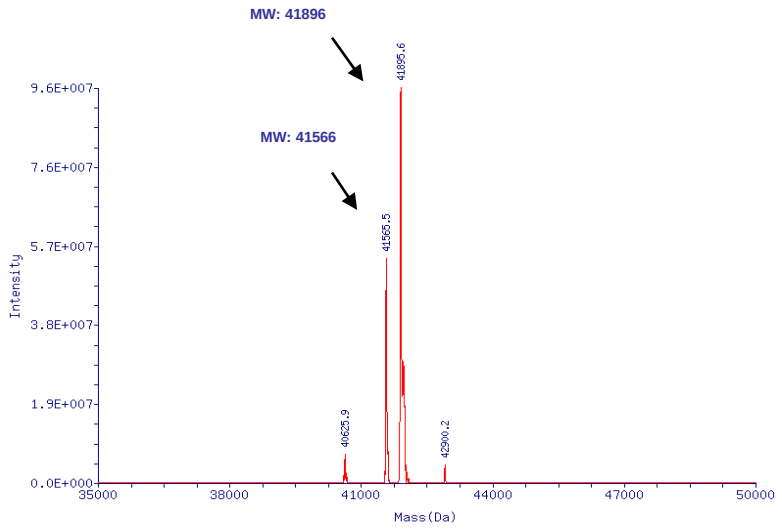

p38α with 4 mM DTT:

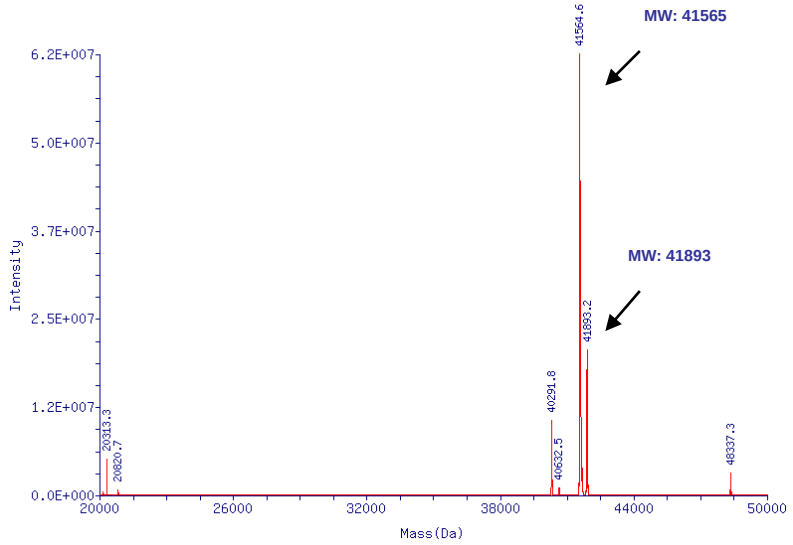

Figure 2.4. ESI-MS spectra of modified p38α by compound **14** in the presence of DTT. Unphosphorylated p38α was incubated with **14** in the presence of 1 mM or 4 mM DTT for 12 h at 37 °C.

2.5. HEPATOTOXICITY STUDIES OF 1,2-DIALKYNYLIMIDAZOLES

A common concern for pyridinylimidazole MAPK inhibitors such as RWJ 67657 and SB-203580 is their inhibition of cytochrome P450 (CYP450) enzymes, which may be linked to hepatotoxicity (*22*). Interestingly, the dialkynylimidazole **14** displays a much lower level of inhibition of CYP450 2D6 (4 % inhibition at 10 μM) compared to SB-203580 (78 % inhibition at 10 μM).

Compound	% inhibition (CYP450, 2D6)	% inhibition (CYP450, 2C19)
KeAZB-339	4	93
SB-203580	78	97

Table 2.3. Inhibition study of CYPP450 isoforms.

2.6. CONCLUSION

In summary, novel p38α-targeting dialkynylimidazoles were designed, synthesized and evaluated. Although 1-phenethynyl-substituted dialkynylimidazoles **7a–c** and **8a–c** are only modest inhibitors of p38α, the 1-ethynyl-substituted dialkynylimidazole **14** is a potent and selective inhibitor. Commensurate with the increased facility of rearrangement of 1-ethynylsubstituted dialkynylimidazols relative to 1-phenethynyl analogues, compound **14** forms a covalent adduct with p38α (*23*). However, the conditions for p38α adduct formation (12 h at 37 °C) are much milder than those required for cyclization/trapping of **14** to afford 15 (5 days at 80 °C), indicating that the kinase may facilitate the cyclization of **14**. Further studies on the site and mechanism of this covalent modification of p38α by 1-ethynyl-substituted dialkynylimidazoles are on-going. The unique kinase inhibition, covalent kinase adduct formation, and minimal CYP450 2D6 inhibition by compound **14** demonstrate that dialkynylimidazoles are a new, promising class of p38α inhibitors.

2.7. EXPERIMENTAL SECTION

General: All reactions were carried out under argon in oven-dried glassware with magnetic stirring. Unless otherwise noted, all commercial chemicals were used without further purification. Tetrahydrofuran (THF), 1,4-dioxane, and diethyl ether (Et_2O) was distilled from sodium/benzophenone prior to use. Dichloromethane (CH_2Cl_2) and triethylamine (Et_3N) was distilled from CaH_2 prior to use. CuI was purified by recrystallization. Unless otherwise noted, organic extracts were dried with Na_2SO_4, filtered through a fritted glass funnel, and concentrated with a rotary evaporator (20-30 mmHg). Flash chromatography was performed with silica gel (230-400 mesh) using the mobile phase indicated. Melting points (open capillary) are uncorrected. Unless otherwise noted, ^1H and ^{13}C NMR spectra were determined in DMSO or $CDCl_3$ on a spectrometer operating at 400 and 100 MHz, respectively, and are reported in ppm using solvent as internal standards (7.26 ppm for ^1H and 77.0 ppm for ^{13}C). Unless otherwise noted, all mass spectra were obtained in the positive mode by chemical ionization using methane as the ionizing gas.

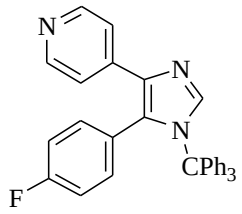

4-(4-pyridyl)-5-(4-fluorophenyl)-1-trityl-1*H*-imidazole (2):

A 250 mL three-necked round bottom flask was charged with 4(5)-(4-fluorophenyl)-5(4)-(4-pyriyl)imidazole (0.87 g, 3.64 mmol). To the flask was added anhydrous CH_2Cl_2 (29 mL) followed by drop-wise addition of a solution of Et_3N (1.01 mL, 7.27 mmol) and triphenylmethyl chloride (1.22 g, 4.36 mmol). After the reaction mixture was stirred for 12 h, to the reaction flask CH_2Cl_2 (50 ml) and water (50 ml) were added. The resulting mixture was extracted with CH_2Cl_2 three times. The combined extracts were washed three times with brine, dried, concentrated and subjected to flash chromatography (100 % EtOAc) to afford 4-(4-pyridyl)-5-(4-fluorophenyl)-1-trityl-1*H*-imidazole (1.0 g, 58 % yield) as a white solid: mp 191-192 ºC; ^{1}H NMR ($CDCl_3$) δ 8.30 (dd, 2 H, J = 1.6, 3.2 Hz), 7.78 (s, 1H), 7.26-7.23 (m, 9H), 7.13-7.11 (m, 6H), 7.09 (dd, 2H, J = 1.6, 3.2 Hz), 6.55-6.50 (m, 2H), 6.45-6.41 (m, 2H); ^{13}C NMR ($CDCl_3$) δ: 162.3 (d, J = 248.5 Hz), 149.8 (2C), 142.1 (3C), 141.5 (2C), 139.4, 138.9, 134.0 (d, 2C, J = 8.9 Hz), 131.4, 130.6 (6C), 128.2 (3C), 128.1 (6C), 127.0 (d, J = 3.7 Hz), 120.9, 115.1 (d, 2C, J = 21.6 Hz), 76.1; MS *m/z*: HRMS (ESI) calcd for $C_{33}H_{25}N_3F$ (M^+) 482.2033, found 482.2027.

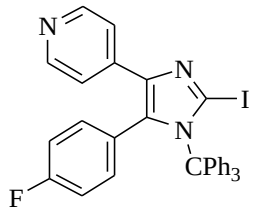

4-(4-pyridyl)-5-(4-fluorophenyl)-1-trityl-2-iodo-1*H*-imidazole (3):

A 50 mL three-necked round bottom flask was charged with **2** (212.3 mg, 0.44 mmol) and dry THF (5.5 ml). To the flask was added *n*-BuLi (0.256 mL, 2.06 M in hexane, 0.53 mmol) at 0 ºC. The solution, which gradually turned red, was stirred at room temperature for 15 min. The solution was then cooled to 0 ºC, and I_2 (89.4 mg, 0.35 mmol) was added to the reaction flask. The reaction mixture was stirred for 10 min at room temperature, and H_2O (5.5 ml) was poured into the reaction mixture. The solution was concentrated, extracted with CH_2Cl_2, dried and subjected to flash chromatography (50:50 EtOAc/hexane) to afford 4-(4-pyridyl)-5-(4-fluorophenyl)-1-trityl-2-iodo-1*H*-imidazole (160 mg, 60 % yield) as a white solid: mp = 145-146 ºC; ^{1}H NMR ($CDCl_3$) δ: 8.28 (dd, 2H, *J* = 1.6, 3.0 Hz), 7.23-7.09 (m, 15 H), 6.99 (dd, 2H, *J* = 1.6, 3.0 Hz), 6.68-6.59 (m, 4H); ^{13}C NMR ($CDCl_3$) δ: 161.9 (d, *J* = 247.7 Hz), 149.3 (2C), 141.6 (2C), 140.9 (3C), 140.2, 135.7, 132.8 (d, 2C, *J* = 8.2 Hz), 131.4 (6C), 128.0, 127.9 (3C), 127.5 (6C), 120.9, 115.4 (d, 2C, *J* = 21.5 Hz), 94.6, 79.1; MS *m/z*: HRMS (ESI) calcd for $C_{33}H_{24}N_3FI$ (M^+) 608.1007, found 608.0993.

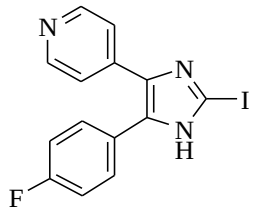

4-(4-pyridyl)-5-(4-fluorophenyl)-2-iodo-imidazole (4):

A 50 mL three-necked round bottom flask was charged with **3** (300 mg, 0.5 mmol) and THF (7 ml). To the flask were added TFA (1.0 equiv) and H_2O (2.0 equiv). After the reaction mixture was stirred for 4 h, to the reaction flask was added saturated aqueous $NaHCO_3$ (5 ml). The reaction mixture was extracted with CH_2Cl_2 several times. The combined extracts were dried, concentrated and subjected to flash chromatography (100 % EtOAc) to afford 4-(4-pyridyl)-5-(4-fluorophenyl)-2-iodo-imidazole (152 mg, 83 % yield) as a yellow solid: mp = 148.5-149.8 ºC; ^{1}H NMR (DMSO-*d6* + TFA) δ: 8.68 (d, 2H, *J* = 6.6 Hz), 7.88 (d, 2H, *J* = 6.6 Hz), 7.60-7.57 (m, 2H), 7.39-7.35 (m, 2H); MS *m/z*: HRMS (CI) calcd for $C_{14}H_{10}N_3FI$ (M^+) 365.9904, found 365.9901.

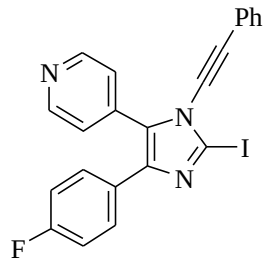

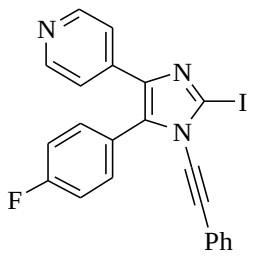

4-(4-flurophenyl)-5-(4-pyridyl)-2-iodo-1-(phenylethynyl)-1*H*-imidazole (5) and 4-(4-pyridyl)-5-(4-fluorophenyl)-2-iodo-1-(phenylethynyl)-1*H*-imidazole (6):

To a solution of **4** (185.4 mg, 0.51 mmol) in dry THF (4 ml) at 0 ºC was added LHMDS (0.51 ml, 1 M in hexanes). After stirring at 0 ºC for 30 min, the solution was transferred via cannula to a solution of phenyl(phenylethynyl)-iodinium tosylate (369.3 mg, 0.78 mmol) in CH_2Cl_2 (4 ml). After stirring at room temperature for 2 h, to the reaction flask was added H_2O (10 ml), the aqueous layer was extracted with CH_2Cl_2 three times and the combined organic layers were dried and evaporated. The residue was purified by flash chromatography (50:50 EtOAc/hexane) to afford **5** (17 mg, 7 % yield) as a yellow solid: mp 157.5-161.7 ºC; ^{13}C NMR ($CDCl_3$) δ: 163.7 (d, J = 250.0 Hz), 149.5 (2C), 140.3, 138.0, 135.0, 132.2 (d, 2C, J = 8.9 Hz), 131.3 (2C), 129.3, 128.5 (2C), 124.0, 120.9 (2C), 120.5, 116.4 (d, 2C, J = 21.6 Hz), 95.1, 78.1, 77.2; MS (*m/z*): HRMS (CI) calcd for $C_{22}H_{14}N_3FI$ (M^+) 466.0217, found 466.0216, and **6** (20 mg, 8 % yield) as a yellow solid: mp 181.0-184.8 ºC; ^{1}H NMR ($CDCl_3$) δ: 8.50 (br, 2H), 7.62-7.51 (m, 2H), 7.41 (d, 2H, *J* = 6 Hz), 7.36-7.32 (m, 5H), 7.24-7.20 (m, 2H); ^{13}C NMR ($CDCl_3$) δ: 163.6 (d, *J* = 250.0 Hz), 149.9 (2C), 139.9, 138.2, 134.8, 132.2 (d, 2C, *J* = 8.2 Hz), 131.3 (2C), 129.3, 128.5 (2C), 124.0 (d, *J* = 2.9 Hz), 120.8 (2C), 120.5, 116.3 (d, 2C, *J* = 21.6 Hz), 95.0, 78.0, 77.2; MS *m/z*: HRMS (CI) calcd for $C_{22}H_{14}N_3FI$ (M^+) 466.0217, found 466.0212.

General procedure for the preparation of 1,2-dialkynylimidazoles:

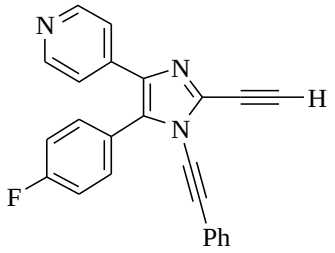

5-(4-fluorophenyl)-4-(4-pyridyl)-1-(phenylethynyl)-2-ethynyl-1*H*-imidazole (7a):

To a solution of **6** (45 mg, 0.097 mmol) in Et_3N (1.2 ml) was added the terminal alkyne (0.12 mmol), $Pd(PPh_3)_4$ (5.6 mg, 0.005 mmol) and CuI (1.9 mg, 0.01 mmol). The reaction mixture was stirred at room temperature until **5** was completely consumed. The reaction mixture was filtered. The filtrate was evaporated, and the residue was purified by flash chromatography (0-25 % EtOAc/hexane) to afford the silylated dialkynylimidazole (6 mg, 0.01 mmol). To this material in THF (2 ml) at -78 °C was added TBAF (0.015 ml of 1 M solution in THF, 0.015 mmol), and the reaction mixture was stirred at -78 °C until completion. The reaction mixture was quenched with water (2 ml) and extracted with CH_2Cl_2 three times. The organic layers were combined, dried over Na_2SO_4 and the solvent was evaporated under reduce pressure. The residue was purified by flash chromatography (0-25 % EtOAc/hexane) to afford 5-(4-fluorophenyl)-4-(4-pyridyl)-1-(phenylethynyl)-2-ethynyl-1*H*-imidazole 3 mg (yield 9 %) **7a** as a yellow solid: mp = 171.1-173.5 ºC; ^{1}H NMR ($CDCl_3$) δ: 8.53 (br, 2H), 7.55-7.50 (m, 2H), 7.46 (br, 2H), 7.38-7.33 (m, 5H), 7.25-7.19 (m, 2H), 3.53 (s, 1H); MS *m/z*: HRMS (CI) calcd for $C_{24}H_{15}N_3F$ (M^+) 364.1250, found 364.1252.

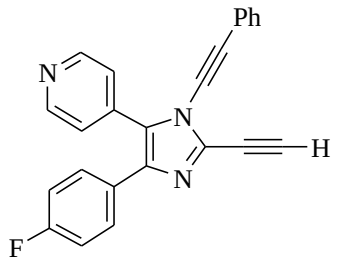

4-(4-fluorophenyl)-5-(4-pyridyl)-1-(phenylethynyl)-2-ethynyl-1*H*-imidazole (8a):

Following the general procedure described, **8a** (16 % yield) was obtained as a yellow solid: mp 138.4-141.4 °C (dec); ^{1}H (CDCl$_3$) δ: 8.72 (d, 2H, *J* = 4.0 Hz), 7.53-7.46 (m, 4H), 7.43-7.33 (m, 3H), 7.04-6.98 (m, 2H), 3.54 (s, 1H); MS *m/z*: HRMS (CI) calcd for $C_{24}H_{15}N_3F$ (M^+) 364.1250, found 364.1250.

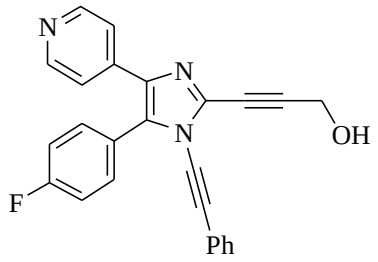

5-(4-fluorophenyl)-4-(4-pyridyl)-1-(phenylethynyl)-2-(prop-2-yn-1-ol)-1*H*-imidazole (7b): Following the general procedure described, **7b** (77 % yield) was obtained as a yellow solid: mp 181-185 °C (dec); ^{1}H ($CDCl_3$) δ: 8.50 (d, 2H, J = 3.0 Hz), 7.53-7.50 (m, 2H), 7.44 (d, 2H, J = 3.0 Hz), 7.50-7.34 (m, 5H), 7.24-7.19 (m, 2H); 4.61 (s, 2H); MS *m/z*: HRMS (CI) calcd for $C_{25}H_{17}N_3OF$ (M^+) 394.1356, found 394.1354.

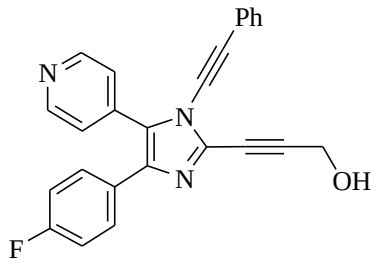

4-(4-fluorophenyl)-5-(4-pyridyl)-1-(phenylethynyl)-2-(prop-2-yn-1-ol)-1*H*-imidazole (8b): Following the general procedure described, **8b** (48 % yield) was obtained as a yellow solid: mp: 181-184 °C; ^{1}H ($CDCl_3$) δ: 8.71 (dd, 2H, *J* = 1.6 Hz, 3.2 Hz), 7.51-7.44 (m, 4H), 7.41-7.33 (m, 5H), 7.02-6.98 (m, 2H), 4.61 (s, 2H); ^{13}C NMR ($CDCl_3$) δ: 162.7 (d, *J* = 247.7 Hz), 150.3 (2C), 139.1, 136.2, 135.1, 131.4 (2C), 129.6 (d, 2C, *J* = 8.2 Hz), 129.3, 128.6 (2C), 128.1 (d, *J* = 3.0 Hz), 127.0, 124.0, 120.5 (2C), 115.7 (d, 2C, *J* = 21.6 Hz), 94.6, 77.4, 76.0, 73.6, 51.2; MS *m/z*: HRMS (CI) calcd for $C_{25}H_{17}N_3OF$ (M^+) 394.1358, found 394.1350.

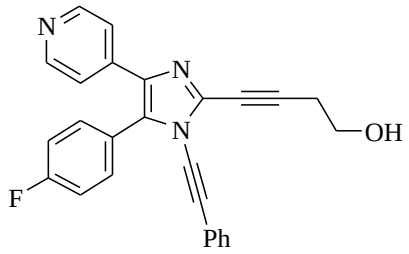

5-(4-fluorophenyl)-4-(4-pyridyl)-1-(phenylethynyl)-2-(but-3-yn-1-ol)-1*H*-imidazole (7c): Following the general procedure described, **7c** (40 % yield) was obtained as a yellow solid: mp 163-165 °C; ^{1}H ($CDCl_3$) δ: 8.49 (dd, 2H, *J* = 1.6 Hz, 3.2 Hz), 7.52-7.49 (m, 2H), 7.43 (dd, 2H, *J* = 1.6 Hz, 3.2 Hz), 7.36-7.33 (m, 5H), 7.23-7.19 (m, 2H), 3.90 (t, 2H, *J* = 6.4 Hz), 2.83 (t, 2H, *J* = 6.4 Hz); ^{13}C NMR ($CDCl_3$) δ: 163.6 (d, *J* = 249.9 Hz), 149.9 (2C), 140.2, 135.0, 134.9, 132.2 (d, 2C, *J* = 8.2 Hz), 131.3, 131.3, 129.2 (2C), 128.6 (2C), 123.9, 121.1 (2C), 120.7, 116.3 (d, 2C, *J* = 21.6 Hz), 94.0, 77.2, 76.2, 70.9, 60.5, 24.0; MS *m/z*: HRMS (CI) calcd for $C_{26}H_{19}N_3OF$ (M^+) 408.1512, found 394.1506.

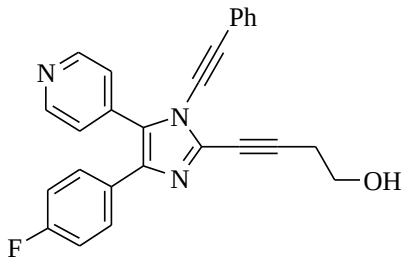

4-(4-fluorophenyl)-5-(4-pyridyl)-1-(phenylethynyl)-2-(but-3-yn-1-ol)-1*H*-imidazole (8c): Following the general procedure described, **8c** (40 % yield) was obtained as a yellow solid: mp: 163.3-165.5 °C; ^{1}H ($CDCl_3$) δ: 8.71 (br, 2H), 7.51-7.47 (m, 2H), 7.45 (d, 2H, *J* = 5.2 Hz), 7.40-7.35 (m, 5H), 7.02-6.98 (m, 2H), 3.89 (t, 2H, *J* = 6.2 Hz), 2.83 (t, 2H, *J* = 6.2 Hz); MS *m/z*: HRMS (CI) calcd for $C_{26}H_{19}N_3OF$ (M^+) 408.1512, found 394.1505.

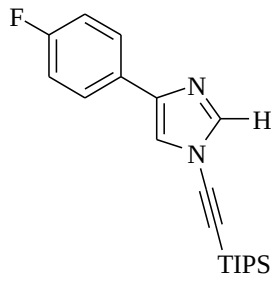

4-(4-fluorophenyl)-1-(2-triisopropylsilanylethynyl)-1H-imidazole 10b: A reaction flask under argon was charged with Cs_2CO_3 (652 mg, 2 mmol), CuI (10 mg, 0.05 mmol), and 4-fluorophenyl-imidazole (*20*) (162 mg, 1 mmol) and backfilled with argon. Dry 1,4-dioxane (2 mL) was added followed by the bromophenylacetylene (0.237 mL, 2 mmol), the 2-acetylcyclohexanone (0.026 mL, 0.2 mmol), and 4 Å molecular sieves (75-115 mg). The mixture was heated to 50 °C in an oil bath for 14 h and then heated to reflux for 4 h. The reaction mixture was cooled to room temperature, quenched with 5 mL of a saturated NH_4Cl solution, and extracted with CH_2Cl_2 (3× 20 mL). The combined organic layers were evaporated and (flash chromatography; 0–10 % EtOAc/hexane), 246 mg of **15a** (72 %) was obtained as an orange solid: mp = 29.5–30.7 °C; ^{1}H NMR δ 7.76 (1H, d, *J* = 1.2 Hz), 7.75-7.70 (2H, m), 7.32 (1H, d, *J* = 1.2 Hz), 7.08-7.03 (2H, m), 1.14-1.12 (21H, m); ^{13}C NMR δ 162.3 (d, *J* = 245.5 Hz), 140.8, 140.3, 128.9 (d, *J* = 2.9 Hz), 126.8 (2C, d, *J* = 8.2 Hz), 116.5, 115.5 (2C, d, *J* = 21.6 Hz), 91.5, 70.1, 18.5 (6C), 11.1 (3C); IR (KBr) 3145, 2945, 2893, 2866, 2195, 2164, 1564, 1501, 1463, 1397, 1232, 1156, 1028, 996 cm-1; MS (m/z): HRMS calc for $C_{20}H_{28}FN_2Si$ (M^+) 343.2006, found 343.2003.

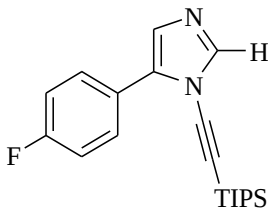

5-(4-fluorophenyl)-1-(2-triisopropylsilanylethynyl)-1H-imidazole 10a:

Also isolated from the chromatography referred to above was 23 mg of **10a** (7 %) obtained as a yellow liquid: ^{1}H NMR δ 7.83 (1H, s, br), 7.65-7.61 (2H, m), 7.12-7.06 (3H, m), 1.14-1.01 (21H, m); IR (neat) 3082, 2945, 2866, 2194, 2159, 1600, 1564, 1504, 1468, 1384, 1291, 1236, 1196, 1161, 1102, 1015cm-1; MS (m/z): HRMS calc for $C_{20}H_{28}FN_2Si$ (M^+) 343.2006, found 343.2004.

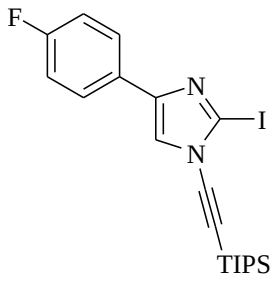

4-(4-fluorophenyl)-2-iodo-1-((triisopropylsilyl)ethynyl)-1*H*-imidazole (11): To a solution of **10b** (216 mg, 0.63 mmol) in THF (5.5 ml) was added *n*-BuLi (0.30 ml of 2.5 M solution in hexane, 0.75 mmol). The reaction mixture was stirred for 3 h at -78 °C. To the reaction flask was added I_2 (160 mg, 0.63 mmol). After stirring for 1 h at -78 °C, the reaction mixture was quenched with saturated $Na_2S_2O_3$ solution and the temperature was cooled to room temperature. The reaction mixture was extracted with CH_2Cl_2 several times. The combined organic layers were dried over Na_2SO_4 and the solvent was evaporated under reduce pressure. The residue was purified by flash chromatography (0-5 % EtOAc/hexane) to afford 4-(4-fluorophenyl)-2-iodo-1-((triisopropylsilyl)ethynyl)-1*H*-imidazole (267 mg, 91 % yield) as a yellow oil **11**: ^{1}H NMR ($CDCl_3$) δ: 7.72-7.68 (m, 2H), 7.45 (s, 1H), 7.08-7.04 (m, 2H), 1.18-1.13 (m, 21H); ^{13}C NMR ($CDCl_3$) δ: 162.5 (d, J = 245.5 Hz), 143.9, 128.1 (d, J = 3.0 Hz), 126.8 (d, 2C, J = 8.2 Hz), 120.1, 115.6 (d, 2C, J = 21.6 Hz), 94.6, 91.5, 75.0, 18.6 (6C), 11.2 (3C); MS *m/z*: HRMS (CI) calcd for $C_{20}H_{27}N_2FSiI$ (M^+) 469.0972, found 469.0969.

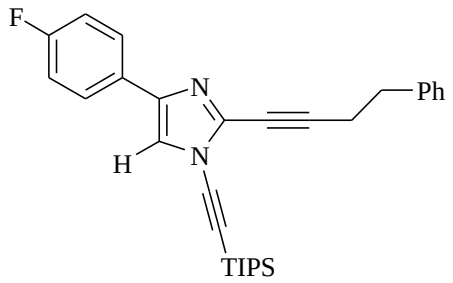

4-(4-fluorophenyl)-1-((triisopropylsilyl)ethynyl)-2-(4-(triisopropylsilyloxy)but-1-ynyl)-1*H*-imidazole (12): To a solution of **11** (0.82 g, 1.45 mmol) in Et_3N (20 ml) was added triisopropyl(pent-3-ynyloxy)silane (0.36 ml, 0.12 mmol), $Pd(PPh_3)_4$ (84 mg, 0.073 mmol) and CuI (29 mg, 0.152 mmol). The reaction mixture was stirred at room temperature until **5** was completely consumed. The reaction mixture was filtered. The filtrate was evaporated, and the residue was purified by flash chromatography (0-5 % EtOAc/hexane) to afford 4-(4-fluorophenyl)-1-((triisopropylsilyl)ethynyl)-2-(4-(triisopropylsilyloxy)but-1-ynyl)-1*H*-imidazole (0.60 g, 73 % yield) as a yellow oil: ^{1}H NMR ($CHCl_3$) δ 7.75-7.71 (m, 2H), 7.28 (s, 1H), 7.07-7.03 (m, 2H), 3.91 (t, 2H, *J* = 8.0 Hz), 2.71 (t, 2H, *J* = 8.0 Hz), 1.18-1.07 (m, 42 H); ^{13}C NMR ($CHCl_3$): δ 162.4 (d, *J* = 245.5 Hz), 140.3, 135.6, 128.4 (d, *J* = 3.0 Hz), 126.9 (d, 2C, *J* = 8.2 Hz), 116.5, 115.5 (d, 2C, *J* = 21.6 Hz), 92.6, 90.9, 72.8, 70.4, 61.5, 23.7, 18.5 (6C), 17.8 (6C), 11.8 (3C), 11.1 (3C); MS *m/z*: HRMS (CI) calcd for $C_{33}H_{51}N_2OSi_2IF$ (M^+) 567.3602, found 567.3597.

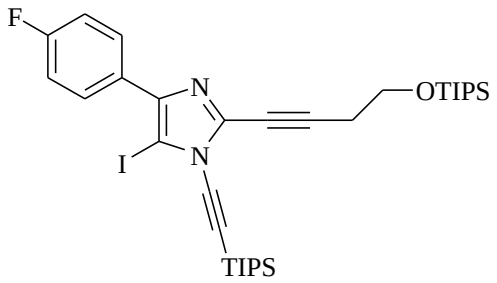

4-(4-fluorophenyl)-5-iodo-1-((triisopropylsilyl)ethynyl)-2-(4(triisopropylsilyloxy)but-1-ynyl)-1*H*-imidazole (13): To a solution of **12** (35 mg, 0.062 mmol) in THF (0.9 ml) was added *n*-BuLi (0.025 ml of 2.5 M solution in hexane, 0.0625 mmol). The reaction mixture was stirred for 30 min at -78 °C. To the reaction flask was added I_2 (16 mg, 0.062 mmol). After stirring for 10 min at -78 °C, the reaction mixture was quenched with saturated $Na_2S_2O_3$ solution and the temperature was cooled to room temperature. The reaction mixture was extracted with CH_2Cl_2 several times. The combined organic layers were dried over Na_2SO_4 and the solvent was evaporated under reduce pressure. The residue was purified by flash chromatography (0-1 % EtOAc/hexane) to afford 4-(4-fluorophenyl)-5-iodo-1-((triisopropylsilyl)ethynyl)-2-(4-(triisopropylsilyloxy)but-1-ynyl)-1*H*-imidazole (32 mg, 74 % yield) as an orange oil **13**: ^{1}H NMR ($CDCl_3$) δ: 7.96-7.92 (m, 2H), 7.12-7.08 (m, 2H), 3.90 (t, 2H, *J* = 7.8 Hz), 2.73 (t, 2H, *J* = 7.8 Hz). ^{13}C NMR ($CHCl_3$) δ 162.6 (d, *J* = 247.0 Hz), 143.3, 137.2, 129.1 (d, 2C, *J* = 8.1 Hz), 128.4, 115.2 (d, 2C, 21.6 Hz), 94.1, 90.3, 77.8, 70.5, 70.4, 61.5, 23.8, 18.6 (6C), 18.0 (6C), 11.9 (3C), 11.2 (3C); MS *m/z*: HRMS (CI) calcd for $C_{33}H_{51}N_2OSi_2IF$ (M^+) 693.2569, found 693.2572.

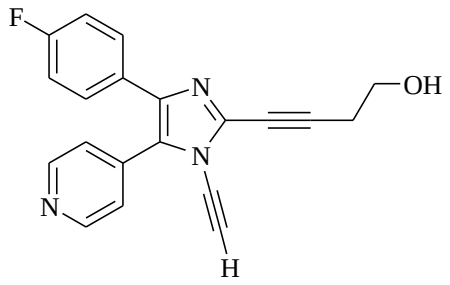

4-(4-fluorophenyl)-5-(4-pyridyl)-1-(ethynyl)-2-(but-3-yn-1-ol)-1H-imidazole (14):

A mixture of **13** (89 mg, 0.13 mmol), 4-pyridine-boronic acid (19.3 mg, 0.16 mmol), $Pd(PPh_3)_4$ (15 mg ,0.013 mmol), toluene (2.1 ml), methanol (0.16 ml) and 2M potassium carbonate (0.16 ml) was refluxed for 4 days under argon. After the reaction mixture was cooled to room temperature, the mixture was filtered. The filtrate was evaporated, and the residue was purified by flash chromatography (0-10 % EtOAc/hexane) to afford the silylated dialkynylimidazole (34 mg, 41 % yield). To this material in THF (1.3 ml) at -78 °C was added TBAF (0.05 ml of 1 M solution in THF, 0.05 mmol), and the reaction mixture was stirred at -78 °C until completion. The reaction mixture was quenched with water (2 ml) and extracted with CH_2Cl_2 three times. The organic layers were combined, dried over Na_2SO_4 and the solvent was evaporated under reduce pressure. The residue was purified by flash chromatography (50-100 % EtOAc/hexane) to obtain 4-(4-fluorophenyl)-5-(4-pyridyl)-1-(ethynyl)-2-(but-3-yn-1-ol)-1H-imidazole (16 mg, 89 % yield) as a light yellow solid: mp 120.8-123.8 °C (dec); ^{1}H NMR ($CHCl_3$) δ 8.50 (d, 2H, J = 5.4 Hz), 7.42-7.39 (m, 2H), 7.35 (d, 2H, J = 5.4 Hz), 6.98-6.94 (m, 2H), 3.88 (t, 2H, J = 6.4 Hz), 3.24 (s, 1H), 2.79 (t, 2H, J = 6.4 Hz); ^{13}C NMR ($CHCl_3$) δ 162.6 (d, J = 247.0 Hz), 150.3 (2C), 138.2, 136.1, 136.0, 129.5 (d, 2C, J = 8.2 Hz), 128.0 (d, J = 3.7 Hz), 126.6, 123.9 (2C), 116.6 (d, 2C, J = 21.5 Hz), 94.8, 70.4, 69.6, 65.5, 60.3, 23.9; MS m/z: HRMS (CI) calcd for $C_{20}H_{15}N_3OF$ (M^+) 332.1196, found 332.1194. Anal. Calcd for $C_{20}H_{15}N_3OF$: C, 72.50; H, 4.26; N, 12.68. Found: C, 72.11; H, 4.19; N, 12.45.

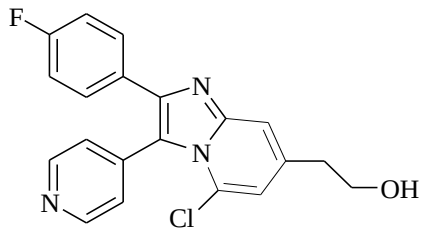

2-(4-Fluorophenyl)-3(4-pyridinyl)-5-chloro-7-ethanol-imidazo[1,2-α]-pyridine (**15**): To a solution of **14** (18 mg, 0.054 mmol) in dry DMF (1.74 ml) was added tetramethylammonium chloride (5.89 mg, 0.054 mmol) and TFA (4.16 µl, 0.054 mmol). The mixture was stirred at 80 ºC for 5 days. The solvent was removed and the residue was purified by flash chromatography (100 % EtOAc) to afford 2-(4-fluorophenyl)-3(4-pyridinyl)-5-chloro-7-ethanol-imidazo[1,2-α]-pyridine (10 mg, 50 % yield) as a yellow solid: mp 180.8 -181.5 ºC; ^{1}H NMR ($CDCl_3$) δ 8.70 (br, 2 H), 7.52 (s, 1H), 7.41-7.38 (m, 4H), 6.97-6.92 (m, 2H), 6.78 (d, 1H, *J* = 0.8 Hz), 3.95 (t, 2H, *J* = 6.2 Hz), 2.91 (t, 2H, *J* = 6.2 Hz); ^{13}C NMR ($CDCl_3$) δ: 162.6 (d, 2C, *J* = 247.0 Hz), 149.3, 147.0, 143.7, 140.0, 138.0, 130.1 (d, 2C, *J* = 8.2 Hz), 129.1 (d, 2C, *J* = 3.7 Hz), 127.5, 126.4, 119.0, 116.4, 115.4 (d, 2C, *J* = 20.8 Hz), 115.3, 62.1, 38.1; MS m/z: HRMS (CI) calcd for $C_{20}H_{16}N_3OFCl$ (M+) 368.0965, found 368.0966.

Covalent adduction of p38 by 14:

The reaction consists of 5 μM p38-alpha, 100 μM **14** in 50 mM HEPES, pH 7.5, 1 mM EGTA, various concentrations DTT (1 mM, 2 mM, 4 mM), 10 mM $MgCl_2$. After 12 h incubation, the reaction mixture was dialyzed in 1 Liter of 25 mM HEPES, pH 7.5, 1 mM DTT, 50 mM KCl, 0.1 mM EDTA, 0.1 mM EGTA, 10 % (v/v) glycerol. After 12 h dialysis, the protein was concentrated and subjected to ESI mass spectrometry.

2.8. REFERENCES

1. Pettus, L. H., and Wurz, R. P. (2008) Small molecule p38 MAP kinase inhibitors for the treatment of inflammatory diseases: novel structures and developments during 2006-2008, *Curr Top Med Chem 8*, 1452-1467.
2. Bain, J., Plater, L., Elliott, M., Shpiro, N., Hastie, C. J., McLauchlan, H., Klevernic, I., Arthur, J. S., Alessi, D. R., and Cohen, P. (2007) The selectivity of protein kinase inhibitors: a further update, *Biochem J 408*, 297-315.
3. Denny, W. A. (2002) Irreversible inhibitors of the erbB family of protein tyrosine kinases, *Pharmacol Ther 93*, 253-261.
4. Rastelli, G., Rosenfeld, R., Reid, R., and Santi, D. V. (2008) Molecular modeling and crystal structure of ERK2-hypothemycin complexes, *J Struct Biol 164*, 18-23.
5. Mukherji, D., and Spicer, J. (2009) Second-generation epidermal growth factor tyrosine kinase inhibitors in non-small cell lung cancer, *Expert Opin Investig Drugs 18*, 293-301.
6. Cohen, M. S., Zhang, C., Shokat, K. M., and Taunton, J. (2005) Structural bioinformatics-based design of selective, irreversible kinase inhibitors, *Science 308*, 1318-1321.
7. Tsou, H. R., Overbeek-Klumpers, E. G., Hallett, W. A., Reich, M. F., Floyd, M. B., Johnson, B. D., Michalak, R. S., Nilakantan, R., Discafani, C., Golas, J., Rabindran, S. K., Shen, R., Shi, X., Wang, Y. F., Upeslacis, J., and Wissner, A. (2005) Optimization of 6,7-disubstituted-4-(arylamino)quinoline-3-carbonitriles as orally active, irreversible inhibitors of human epidermal growth factor receptor-2 kinase activity, *J Med Chem 48*, 1107-1131.
8. Tummino, P. J., and Copeland, R. A. (2008) Residence time of receptor-ligand complexes and its effect on biological function, *Biochemistry 47*, 5481-5492.
9. Smith, A. J., Zhang, X., Leach, A. G., and Houk, K. N. (2009) Beyond picomolar affinities: quantitative aspects of noncovalent and covalent binding of drugs to proteins, *J Med Chem 52*, 225-233.
10. Michalczyk, A., Kluter, S., Rode, H. B., Simard, J. R., Grutter, C., Rabiller, M., and Rauh, D. (2008) Structural insights into how irreversible inhibitors can overcome drug resistance in EGFR, *Bioorgan Med Chem 16*, 3482-3488.
11. Blair, J. A., Rauh, D., Kung, C., Yun, C. H., Fan, Q. W., Rode, H., Zhang, C., Eck, M. J., Weiss, W. A., and Shokat, K. M. (2007) Structure-guided development of affinity probes for tyrosine kinases using chemical genetics, *Nat Chem Biol 3*, 229-238.
12. Khandekar, S. S., Feng, B. B., Yi, T., Chen, S., Laping, N., and Bramson, N. (2005) A liquid chromatography/mass spectrometry-based method for the selection of ATP competitive kinase inhibitors, *J Biomol Screen 10*, 447-455.
13. Barluenga, S., Dakas, P. Y., Boulifa, M., Moulin, E., and Winssinger, N. (2008) Resorcylic acid lactones: A pluripotent scaffold with therapeutic potential, *Cr Chim 11*, 1306-1317.

14. Gallagher, T. F., Fierthompson, S. M., Garigipati, R. S., Sorenson, M. E., Smietana, J. M., Lee, D., Bender, P. E., Lee, J. C., Laydon, J. T., Griswold, D. E., Chabotfletcher, M. C., Breton, J. J., and Adams, J. L. (1995) 2,4,5-Triarylimidazole Inhibitors of Il-1 Biosynthesis, *Bioorgan Med Chem Lett 5*, 1171-1176.

15. Wadsworth, S. A., Cavender, D. E., Beers, S. A., Lalan, P., Schafer, P. H., Malloy, E. A., Wu, W., Fahmy, B., Olini, G. C., Davis, J. E., Pellegrino-Gensey, J. L., Wachter, M. P., and Siekierka, J. J. (1999) RWJ 67657, a potent, orally active inhibitor of p38 mitogen-activated protein kinase, *J Pharmacol Exp Ther 291*, 680-687.

16. Boehm, J. C., Smietana, J. M., Sorenson, M. E., Garigipati, R. S., Gallagher, T. F., Sheldrake, P. L., Bradbeer, J., Badger, A. M., Laydon, J. T., Lee, J. C., Hillegass, L. M., Griswold, D. E., Breton, J. J., Chabot-Fletcher, M. C., and Adams, J. L. (1996) 1-substituted 4-aryl-5-pyridinylimidazoles: a new class of cytokine suppressive drugs with low 5-lipoxygenase and cyclooxygenase inhibitory potency, *J Med Chem 39*, 3929-3937.

17. Koser, G. F., Rebrovic, L., and Wettach, R. H. (1981) Functionalization of Alkenes and Alkynes with [Hydroxy(Tosyloxy)Iodo]Benzene - Bis(Tosyloxy)Alkanes, Vinylaryliodonium Tosylates, and Alkynylaryliodonium Tosylates, *J Org Chem 46*, 4324-4326.

18. Laroche, C., Li, J., Freyer, M. W., and Kerwin, S. M. (2008) Coupling reactions of bromoalkynes with imidazoles mediated by copper salts: Synthesis of novel N-alkynylimidazoles, *J Org Chem 73*, 6462-6465.

19. Ho, K. K., Auld, D. S., Bohnstedt, A. C., Conti, P., Dokter, W., Erickson, S., Feng, D., Inglese, J., Kingsbury, C., Kultgen, S. G., Liu, R. Q., Masterson, C. M., Ohlmeyer, M., Rong, Y., Rooseboom, M., Roughton, A., Samama, P., Smit, M. J., Son, E., van der Louw, J., Vogel, G., Webb, M., Wijkmans, J., and You, M. (2006) Imidazolylpyrimidine based CXCR2 chemokine receptor antagonists, *Bioorg Med Chem Lett 16*, 2724-2728.

20. Lynch, W.E., Kurtz, D. M., Wang, S., Scott, R. A. (1994) Strcutrual and functional models for the dicopper site in hemocyanin. Dioxygen binding by copper complexes of tris(1-R-4-R'-imidazolyl-κ*N*)phosphines.

Chapter 3

Targeting kinase docking sites: a fluorescence-based assay for p38α inhibitors targeting a substrate binding site

3.1. INTRODUCTION

The mitogen-activated protein kinases (MAPKs) are serine/theronine kinases that serve as important mediators of inflammatory cytokines including tumor necrosis factor alpha (TNFα) and interleukin-1 beta (1L-1β) (*1, 2*). The vast majority of MAPK inhibitors reported to date target the highly conserved ATP binding sites of these enzymes. However, using the ATP binding site as a drug target has several limitations. For example, the ATP binding site is highly conserved among kinases. Thus, it is challenging to discover highly selective small molecules. Moreover, intracellular ATP is typically present at a concentration of 1mM, leading to a discrepancy between IC_{50} values measured by biochemical versus cellular assays (*3, 4*). In addition to ATP-competitive inhibitors, a few small molecules have been found to exploit a new hydrophobic pocket, which is adjacent to the ATP binding site. The hydrophobic pocket is created by the activation loop which contains the conserved DFG motif. Upon binding to these inhibitors, the DFG motif undergoes a conformational change, which causes the residue Phe169 to move from a buried conformation (DFG-in) to a solvent exposed conformation (DFG-out) (*5*).

Recently, there has been a growing interest in developing drug candidates against more variable substrate docking sites. At least two types of docking interactions between MAPKs and their substrates, activators and phosphatases have been identified (*6*). In both docking interactions, short motifs are found within substrates: the D domain (D site, δ domain, DEJL domain) and the DEF domain (Docking site for ERK, FXFP, F site or DEF site); a complementary pocket or groove is found on the kinase. In particular, the interactions between

MAPK and D domains have been characterized by mutagenesis, hydrogen exchange-mass spectrometry, and X-ray crystallography (*7, 8*). The D domain consists of a cluster of basic residues, a short spacer and a hydrophobic patch (Lys/Arg-Lys/Arg-Xaa2-6-ϕ-X-ϕ, where ϕ is a hydrophobic residue, such as Leu, Iso, or Val) (*9*). The complementary D-recruitment site (DRS) on MAP kinase is composed of acidic patch in the C-terminal known as the CD (Common Docking) domain (*10*) and hydrophobic docking groove (*11, 12*) (or referred to as "ED) (*9*).

MAPK substrate specificity has been shown to be mediated through docking interactions involving substrate docking motifs that interact with kinase docking sites (*7, 13-15*). Blocking docking interactions between kinase network partners is a promising alternative approach for selectively inhibiting kinase (and/or phosphatase) signaling. First, this approach can overcome the limitations of targeting ATP-binding sites. Second, since protein kinases achieve high biological specificity by recognizing their targets through docking interactions, disrupting this interaction can result in specific individual kinase inhibition. Additionally, many protein phosphatases also bind to substrates and regulators in the same manner (*16*). It has been reported that small molecule inhibitors that target calcineurin phosphatase activity showed success by disrupting docking interactions (*17*).

In the past decade, many efforts have been made to design specific docking peptide inhibitors (*18*). For instance, cell-permeable docking peptides were shown to selectively modulate MAPK and PP1 activity in vivo (*19-21*). Recently, Bardwell *et al.* reported that MKK D-sites have a greater preference for binding to their cognate MAPKs than to non-cognate MAPKs with a 10-fold difference. In their study, D-site peptide derived from MKK3 is a highly selective and potent inhibitor of p38α (*22*). Although docking peptide inhibitors offer high specificity, and often low concentration of peptide inhibitors are required to compete with peptide or protein substrates, they also encounter common problems including metabolic instability and inability to cross cell membranes (*23*). So far, small molecules that target the substrate binding site of MAPKs have remained largely unexplored. An approach to docking-

based drug design is to use high-throughput experimental and computational structure-based screens (*16*).

Here we report the identification of dialkynylimidazoles as a new class of small molecule, covalent p38α MAP kinase docking site probes. We propose that a mechanism involving the nucleophilic addition of a docking site cysteine thiol to the *N*-ethynyl group of the probe. We further demonstrate that such probes can be used to fluorescently label p38α both in vitro and in cells via azide-alkyne "Click" chemistry. This serves as the basis of an assay that can be used to identify inhibitors that specifically target a substrate docking site of p38α.

3.2. COVALENT ADDUCTION OF P38α BY *N*-ALKYNYLIMIDAZOLE

In our prior work, we showed that the 1,2-dialkynylimidazole **1** forms a covalent adduct with p38α at 37 °C (25 % abundance) (*24*). In a study of related *N*-alkynylimidazoles, we discovered that *N*-alkynylimidazole **2** also covalently modifies p38α (Figure 3.1). First, *N*-alkynylimidazole **2** was prepared from previously reported 4-(4-fluorophenyl)-5-(4-pyridyl)-1-(2-triisopropylsilanyl)imidazole (*25*), followed by silyl deprotection with TBAF in THF. Next, non-phosphorylated p38α (5 μM) was incubated with **2** (100 μM) at room temperature in 50 mM HEPES, 10 mM $MgCl_2$, 2 mM DTT, 1 mM EGTA, pH 7.5 for 12 h, followed by extensive dialysis, and the sample was analyzed by ESI-MS (Figure 3.2). A new peak in the mass spectrum at m/z = 41824, which corresponds to addition of a single molecule of **2** (MW = 263 Da) to p38α, was observed (100 % abundance).

In order to identify the site of adduction, the sample was digested with chymotrypsin and further analyzed by MALDI-MS/MS. The MASCOT generated chymotrypsin digest coverage based on MS values showed 88 % coverage of the protein in the untreated sample (p38α alone), with peptides 36-59, 130-132, 208-216, 271-274 unobserved. For the treated digest (modified p38α by compound **2**), the coverage was 83 %, with peptides 36-59, 105-132, 208-216 unobserved. The major difference in coverage was the absence of peptide 105-129 in the treated sample. Comparative MALDI analysis and de novo sequencing identified the modification site. In the untreated sample, the peptide 104-129 is seen at 2952.476, with sequence confirmed by MS/MS. This peptide is absent from the treated sample. However, a new peptide is observed at 3215.553 (Figure 3.3). De novo sequencing identified the peptide as residues 104-129 with modification of Cys119 by a mass addition of 263 Da (Figure 3.4). The modification at Cys119 was observed in five additional peptide sequences for peptides only in the treated sample. They were observed with same modification of 263 Da, and at lower signal intensity with modification of 261 Da: residues 115-119 at 965.435/967.450, 110-119 at 1435.6/1437.660, 115-129 at 2048.960/2050.976, 111-129 at 2464.155, and 110-129 at 2519.171/2521.178. However, none of these peptides were observed in the untreated sample. The MS of the treated protein

chymotrypsin digest does not contain peptide 104-129 in an unlabeled form, only the labeled peptide, implying that this site is modified stoichiometrically. Thus, it is unlikely that any other site on the protein is modified. As a control, a common cysteine alkylating agent, iodoacetamide, was incubated with p38α under the same conditions except that TCEP was used as a reducing agent. New peaks corresponding to multiple additions of iodoacetamide were observed by ESI-MS (Figure 3.5).

After we determined the site of modification by compound **2**, we studied the X-ray crystal structure of p38α. Cys119 residue is located in the D-recruitment site (DRS) facing the pocket (Figure 3.6) (*26*). This groove appears to be a potential druggable site. First, it has a significant hydrophobic pocket that favors small molecule interaction. Second, this groove also contains polar residues, and polar groups in the binding site were shown to play an important role in the recognition of drug-like molecules (*27*). Furthermore, this pocket is not conserved within MAPK family (*28, 29*). Wang *et al* reported that four amino acids in the p38α surface groove may determine substrate specificity: Asn114, Cys119, Lys121 and Gly219 (*26*). More importantly, targeting this site with small molecules will potentially result in disruption of protein-protein interaction, thereby inhibiting kinase activity. Additionally, we were also intrigued by the result that the *N*-alkynylimidazole **2** selectively modifies Cys119, despite the presence of three other Cys residues in its primary sequence. Interestingly, Cys162, one of the three Cys residues, is highly exposed at the protein surface (*26*). Thus, this unique modification of Cys119 led to further mechanistic study and development of p38α docking site probes.

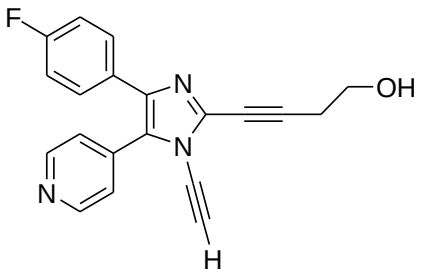

1

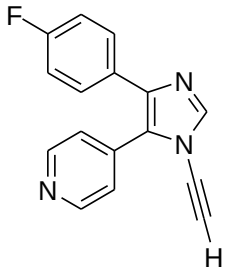

2

Figure 3.1. Structures of 1,2-dialkynylimidazole and *N*-alkynylimidazole.

a.

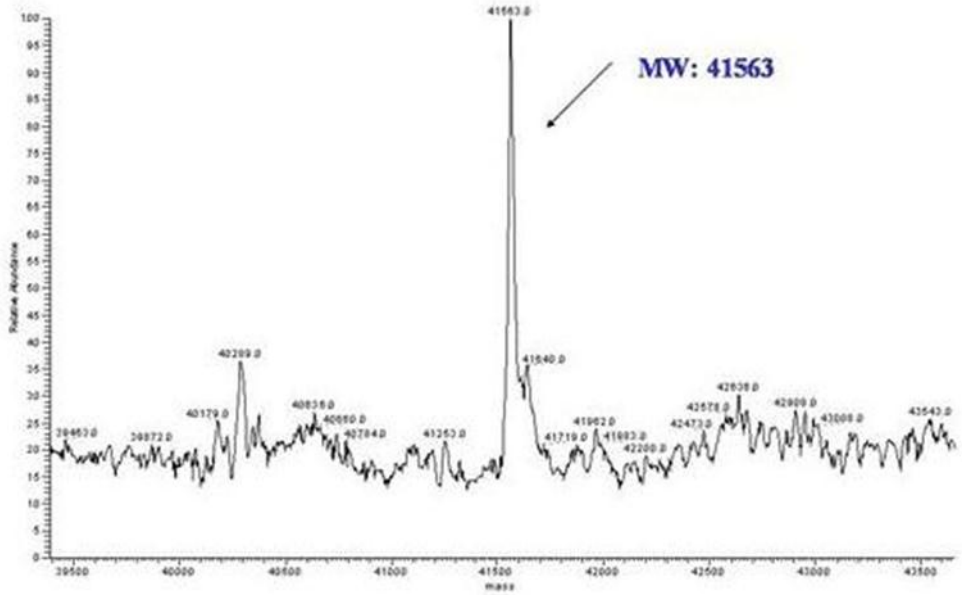

b.

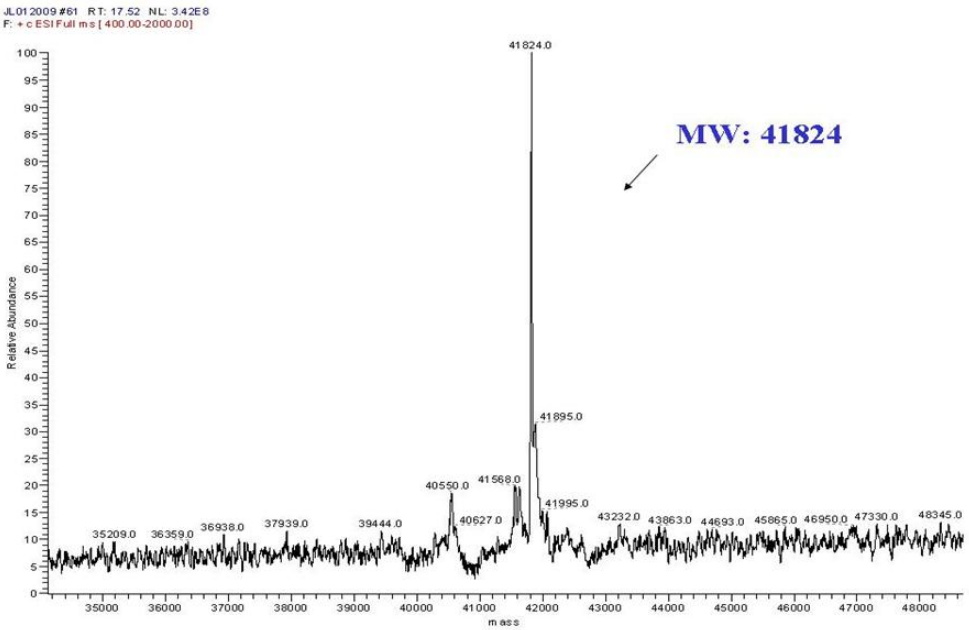

Figure 3.2. ESI-MS spectra of p38α and modified p38α by compound **2**. (a) Unphosphorylated p38α was incubated for 12 h at 25 °C; (b) Unphosphorylated p38α incubated with *N*-alkynylimidazole **2** for 12 h at 25 °C, followed by extensive dialysis.

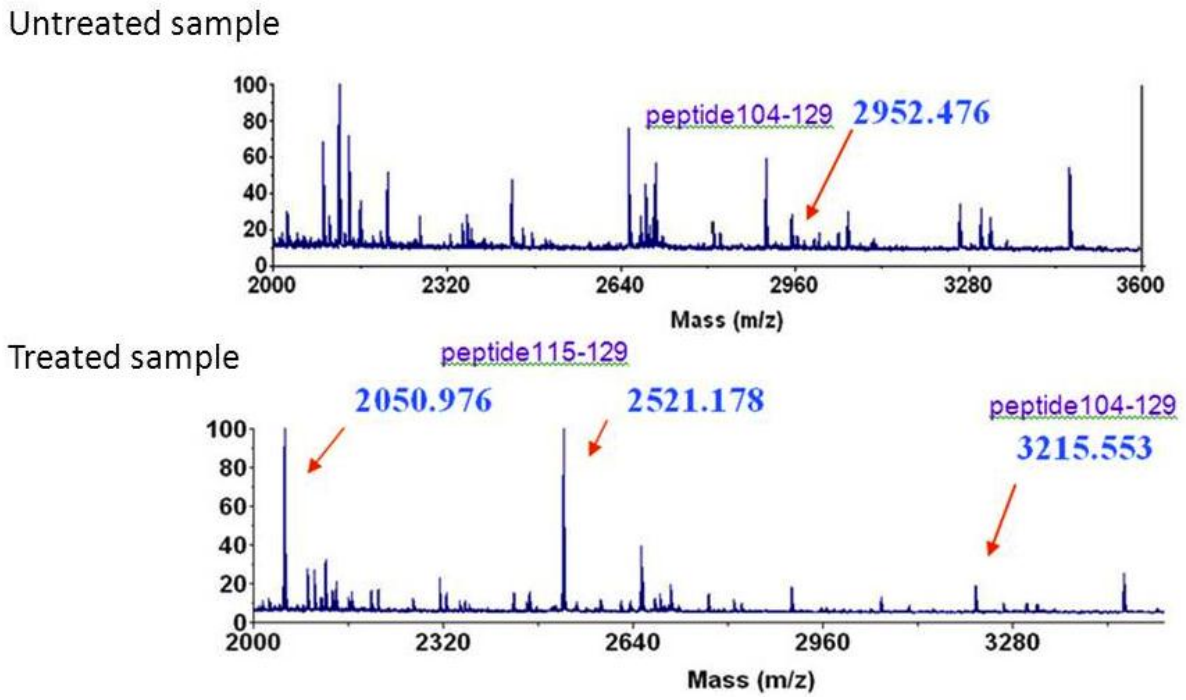

Figure 3.3. MALDI-MS spectra of p38α treated with *N*-alkynylimidazole **2** and untreated p38α after digestion with chymotrypsin.

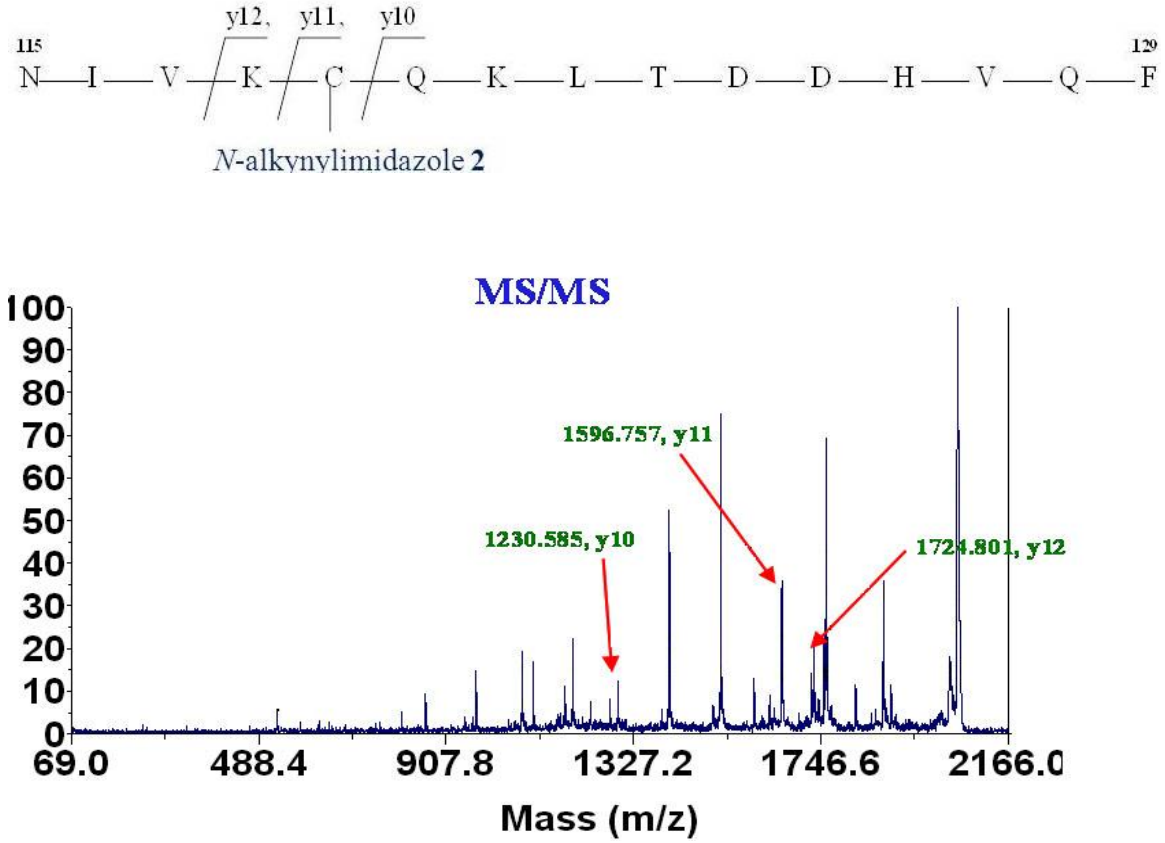

Figure 3.4. MALDI-MS/MS spectrum of *N*-alkynylimidazole **2** adducted p38α after digestion with chymotrypsin.

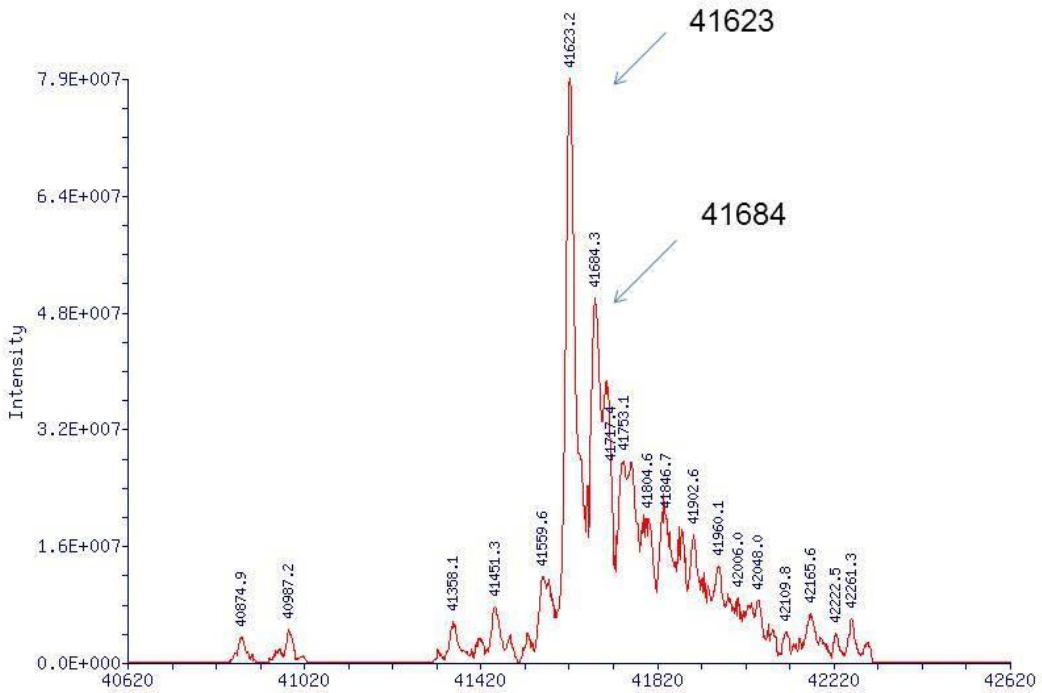

Figure 3.5. ESI-MS spectrum of unphosphorylated p38α incubated with iodoacetamide for 12 h at 25 °C.

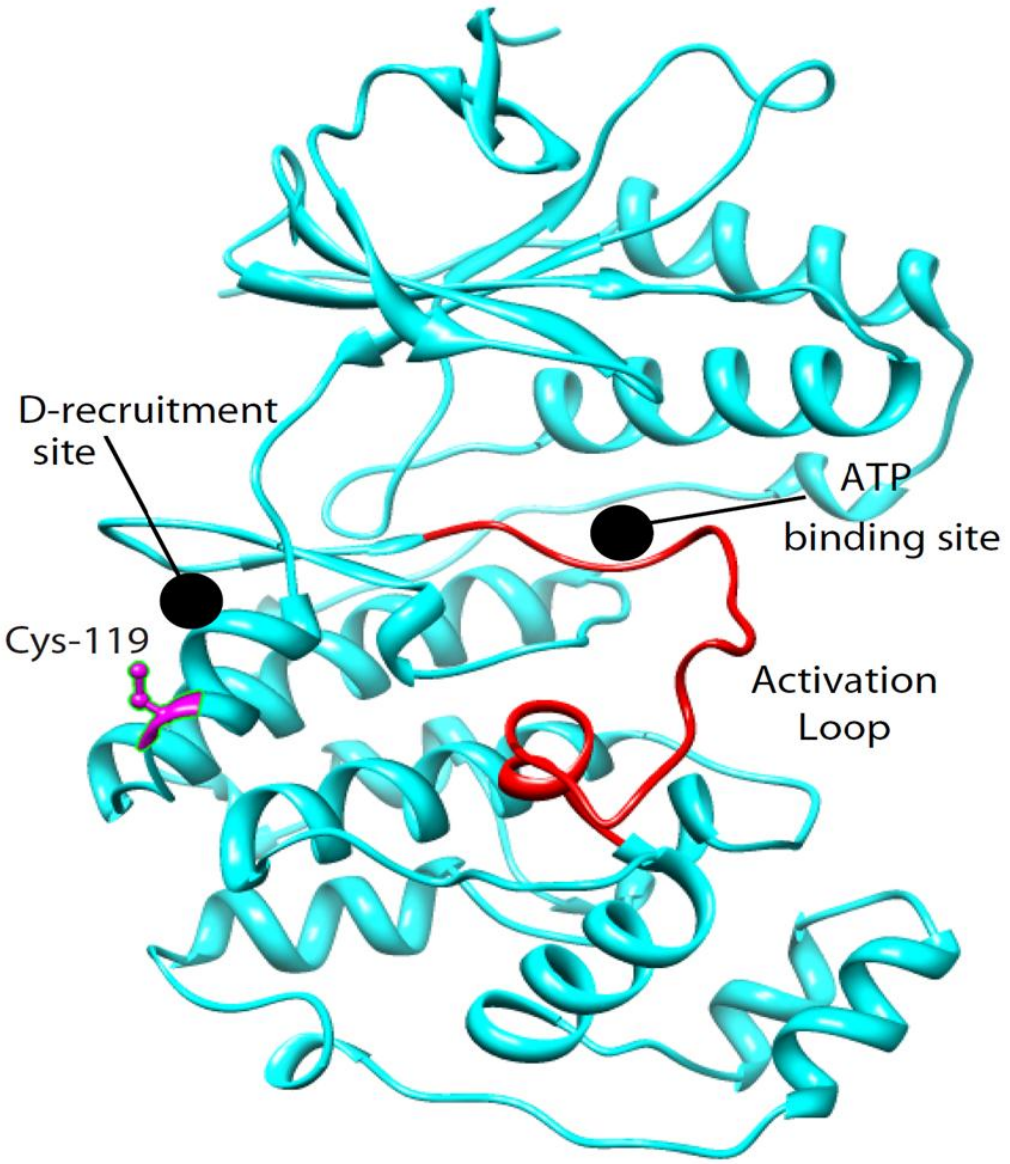

Figure 3.6. Crystal structure of p38α (1P38).

3.3. DETERMINATION OF KINETIC PARAMETERS OF MODIFIED P38α BY COMPOUND 2

We showed that compound **2** covalently modifies Cys119 in the D-recruitment site of p38α. To investigate whether this modification would affect p38α kinetic properties, we performed in vitro kinase assays to evaluate the ability of the modified p38α to phosphorylate two different protein substrates, activating transcription 2 (ATF2) and mitogen-activated protein kinase-activated protein kinase 2 (MK2), and one peptide substrate (Ste7 peptide).

Substrate	p38α		Modified p38α	
	K_m (μM)	k_{cat} (sec^{-1})	K_m (μM)	k_{cat} (sec^{-1})
ATF2	2.22 ± 0.64	1.5 ± 0.06	3.74 ± 0.74	1.075 ± 0.02
MK2	6.65 ± 2	1.3 ± 0.12	1.12 ± 0.21	0.563 ± 0.02
Ste7-peptide Substrate	47.82 ± 22.05	5.4 ± 1.11	28.77 ± 8.71	3.4 ± 0.37

Table 3.1. Kinetic constants for phosphorylation of different substrates by p38α and modified p38α.

Table 3.1 shows the kinetic parameters K_m and k_{cat} obtained by measuring the initial velocity data at different concentrations of each tested substrate and fixed concentration of ATP. Modification of p38α by compound **2** at Cys119 affected both the binding affinity of p38α to ATF2 and the ability of p38α to phosphorylate ATF2, as K_m increased from 2.22 to 3.74 μM and k_{cat} decreased from 1.5 to 1 s^{-1} (Figure 3.7). The specificity constant k_{cat}/K_m is decreased by 2-3 fold (from 0.67 to 0.26 $\mu M^{-1}s^{-1}$), suggesting that modification at Cys119 by compound **2** might affect the docking of ATF2 to p38α.

In contrast, modification of Cys119 by compound **2** showed an increase in the specificity constant k_{cat}/ K_m when MK2 was used as a substrate of p38α (from 0.19 to 0.5 $\mu M^{-1}s^{-1}$) (Figure 3.8). The specificity constant k_{cat}/K_m was not affected when Ste7 peptide was used as a substrate (~0.1 $\mu M^{-1}s^{-1}$ for both p38α and modified p38α) (Figure 3.9). Ste7 peptide substrate

(FQRKTLQRRLKGLNLNL-AHX-TGPL*S*PGPF, where AHX is a linker) has a specific D-site to the MAP kinases (described in Lee et al, *Submitted to Biochemistry*). This suggests that MK2 and Ste7 peptide have different modes of binding to p38α compared to ATF2.

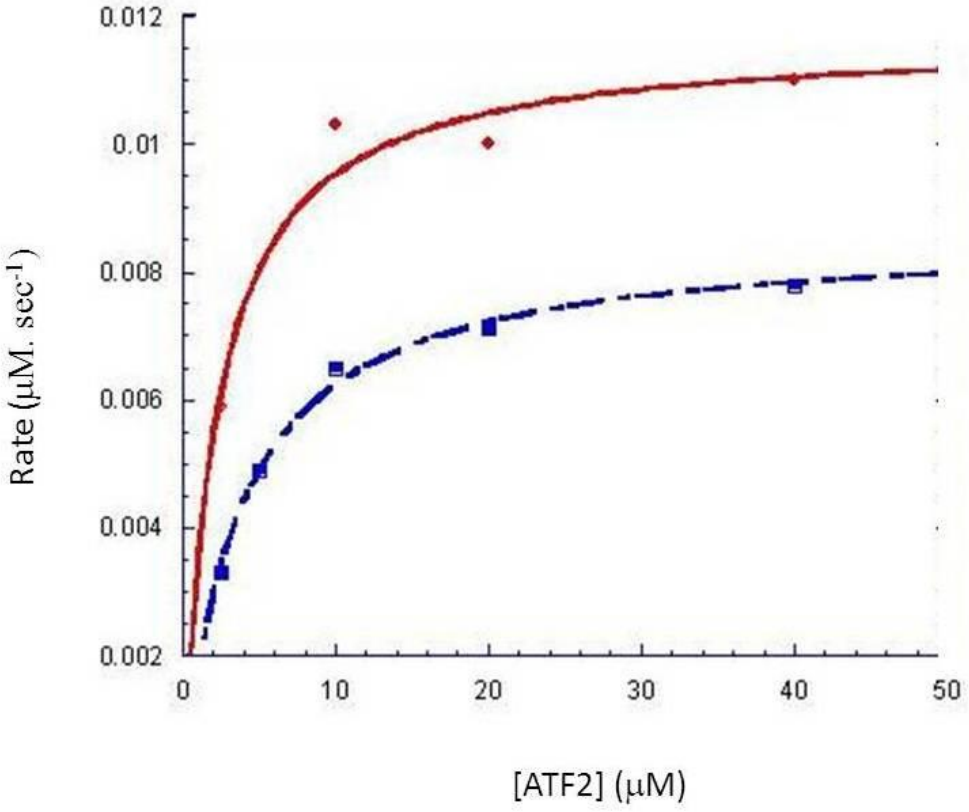

Figure 3.7. Analysis of the kinase activity of the modified p38α with ATF2 substrate. Phosphorylation of the protein substrate ATF2 (2.5-40 μM) by 8 nM activated p38α (red solid line) or 8 nM activated modified p38α by compound **2** (blue dashed line) in the presence of 0.5 mM ATP and 10 mM $MgCl_2$. The data were fitted to Michaelis–Menten equation.

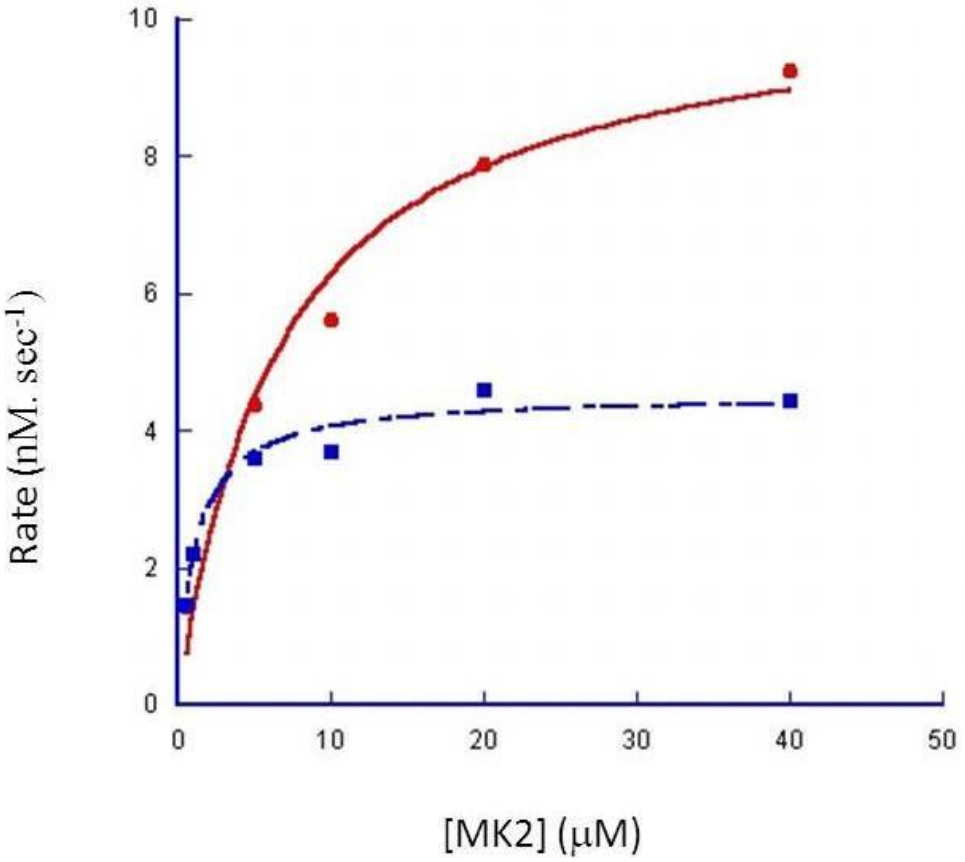

Figure 3.8. Analysis of the kinase activity of the modified p38α with MK2 substrate. Phosphorylation of the protein substrate MK2 (0.5-40 μM) by 10 nM activated p38α (red solid line) or 10 nM activated modified p38α with compound **2** (blue dashed line) in the presence of 0.5 mM ATP and 10 mM $MgCl_2$. The data were fitted to Michaelis–Menten equation.

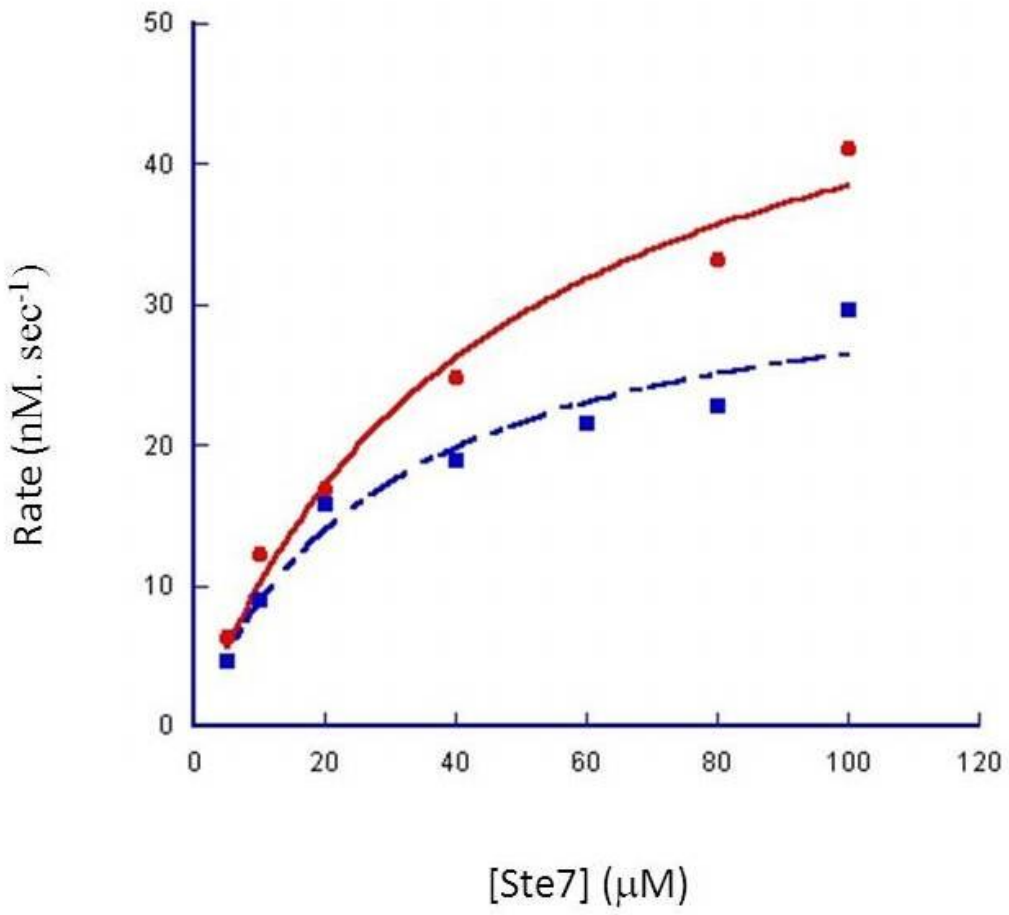

Figure 3.9. Analysis of the kinase activity of the modified p38α with Ste7 peptide substrate. Phosphorylation of the Ste7-peptide substrate (5-100 μM) by 10 nM activated p38α (red solid line) or 10 nM activated modified p38α with compound **2** (blue dashed line) in the presence of 0.5 mM ATP and 10 mM $MgCl_2$. The data were fitted to Michaelis–Menten equation.

3.4. DESIGN AND SYNTHESIS OF COVALENT P38α DOCKING SITE PROBE

We propose that the reaction mechanism involves nucleophilic addition of the cysteine thiol to the *N*-ethynyl group. To model the thioenol ether formation in the protein modification, *N*-alkynylimidazole derivatives **3, 4, 5** were treated with thiophenol in THF at room temperature (Scheme 3.1). Based on NOESY NMR, the isolated thiol enol ether adduction products **6, 7, 8** were assigned the (Z) configuration.

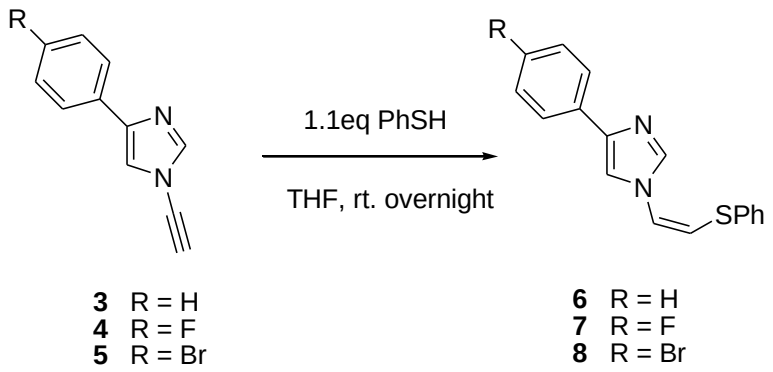

Scheme 3.1. Synthesis of (Z)-thioenol ether.

To the best of our knowledge, no small molecule class has been identified to selectively modify Cys119 residue in p38α. Such compounds would be useful in serving as docking site probes for biochemical and cellular studies. Recently, we reported a mechanism for cytotoxicity involving the selective thiol addition to the *N*-ethynyl group of certain 1,2-dialkynylimidazoles (Scheme 3.2) (*30*). Based on the unexpected electrophilic nature of the *N*-ethynyl group, dialkynylimidazole **11** was developed as a covalent p38α docking site probe. After the addition of docking site cysteine thiol to the *N*-ethynyl group, the second alkyne introduced at the 2 position of the imidazole is available for further functionalization, such as azide-alkyne "Click" chemistry. Dialkynylimidazole **11** was synthesized using our previously published synthetic route (*31*). Iodination of **9** gave 1-alkynyl-2-iodo-4-(4-fluorphenyl)-imidazole **10,** which was then coupled to triisopropylsilyl acetylene under standard Sonogashira coupling condition,

followed by desilylation (Scheme 3.3). As shown in Figure 3.10, after incubation of **11** with p38α at 25 °C, we carried out a Cu(I) catalyzed 1,3-dipolar cycloaddition with an azide-labeled fluorescent dye. Then the reaction mixture was subjected to denaturing gel electrophoresis and analyzed by in-gel fluorescence scanning.

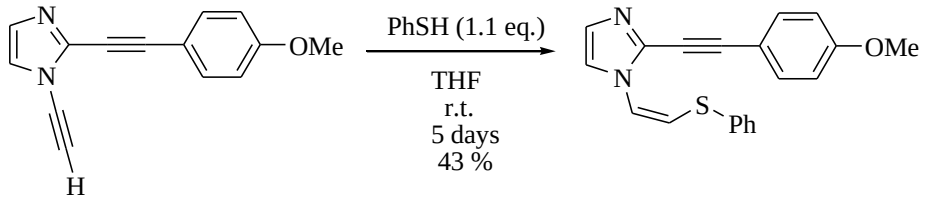

Scheme 3.2. Synthesis of (Z)-thioenol ether.

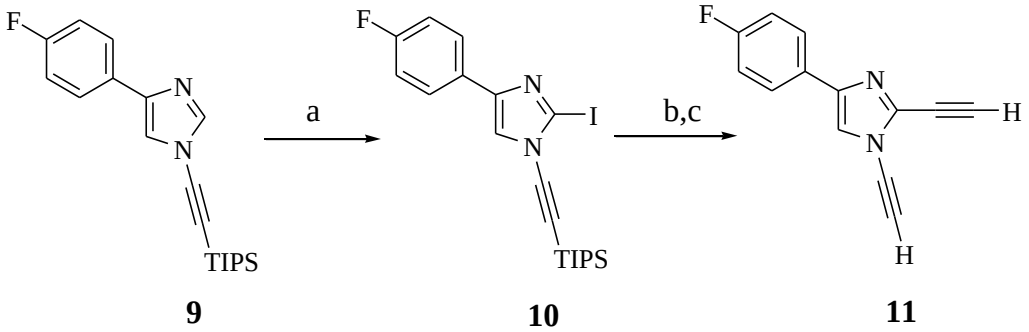

Scheme 3.3. Synthesis of dialkynylimidazole. Reagents and conditions: (a) (i) *n*-BuLi; (ii) I_2, THF, -78 °C (90 %); (b) (i) TMSCCH, $Pd(PPh_3)_4$, CuI, Et_3N; (ii) TBAF, THF, -78 °C (82 %).

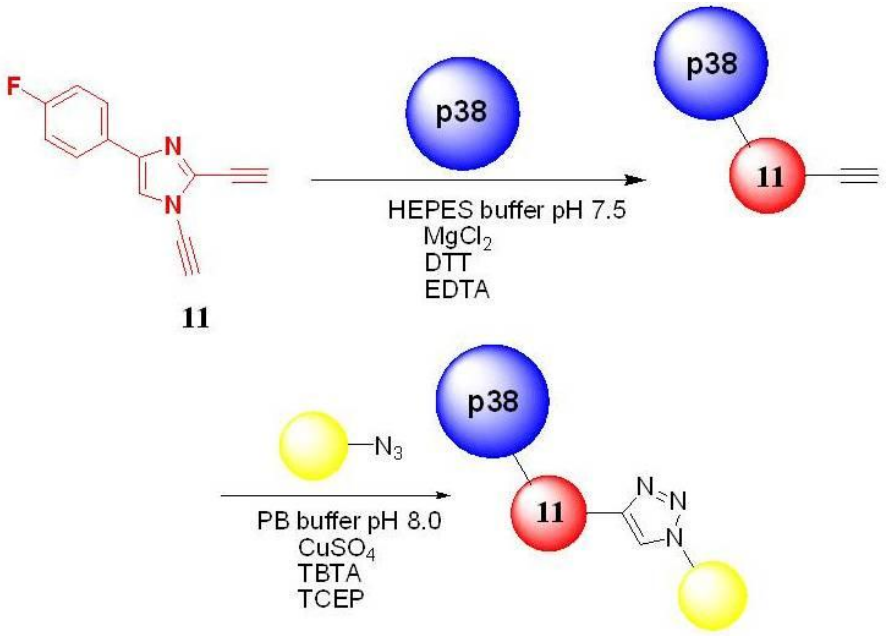

Figure 3.10. In vitro and in cell probe for p38α.

3.5. IN VITRO AND IN CELL LABELING OF P38α

p38α (5 μM) was incubated with **11** (100 μM) in 50 mM HEPES, pH 7.5, 1 mM EGTA, 2 mM DTT, 10 mM $MgCl_2$ for 16 h at 25°C. After incubation, the Cu (I) catalyzed 1,3 dipolar cycloaddition reaction was carried out as follows: 25 μg p38α in 50 mM phosphate buffer (50 μl total volume) was incubated with 0.5 μl $CuSO_4$ (50 mM), 0.5 μl tris(2-carboxyethyl)phosphine (TCEP, 50 mM) and 1.65 μl tris[(1-benzyl-1H-1,2,3-triaol-4-yl)methyl]amine (TBTA, 1.5 mM) at 25 °C for 16 h. Then the "Click" reaction was quenched with addition of 2x SDS loading buffer and heat inactivated at 95 °C for 10 min. The samples were analyzed by 10 % SDS PAGE. The gel was scanned and the data were analyzed. As shown in Figure 3.8, a strong fluorescent band with a loading of 0.4 μg of the protein was detected in Lane 3. As two controls, p38α alone or treatment of p38α with the "Click" reaction reagents (Alexa594-azide, $CuSO_4$, TBTA and TCEP) showed no fluorescent bands with a loading of 2 μg of the protein in Lanes 1 and 2 (Figure 3.11). The approximate detection limit for the adducted p38α was determined to be 1 ng.

In addition, we also studied the kinetics of the "Click" chemistry reaction. After incubation of p38α with **11** for 16 h at 25 °C, the "Click" chemistry was carried out: 5 μg p38α in 50 mM phosphate buffer (50 μl total volume) was incubated with 0.5 μl $CuSO_4$ (50 mM), 0.5 μl tris(2-carboxyethyl)phosphine (TCEP, 50 mM) and 1.65 μl tris[(1-benzyl-1H-1,2,3-triaol-4-yl)methyl]amine (TBTA, 1.5 mM), 0.5 μl GSH (0.5 mM) at 25 °C. Aliquots of the solution were then removed at various time points from 0.5 h to 24 h (Figure 3.12), followed by SDS-PAGE analysis. The gel was scanned and the data was fit to $P = P_{max}(1-e^{-k_{obs}t})$, and the k_{obs} and the half-life were estimated to be 0.117 $h^{-1}$and 5.9 h, respectively, following pseudo first-order kinetics (Figure 3.13).

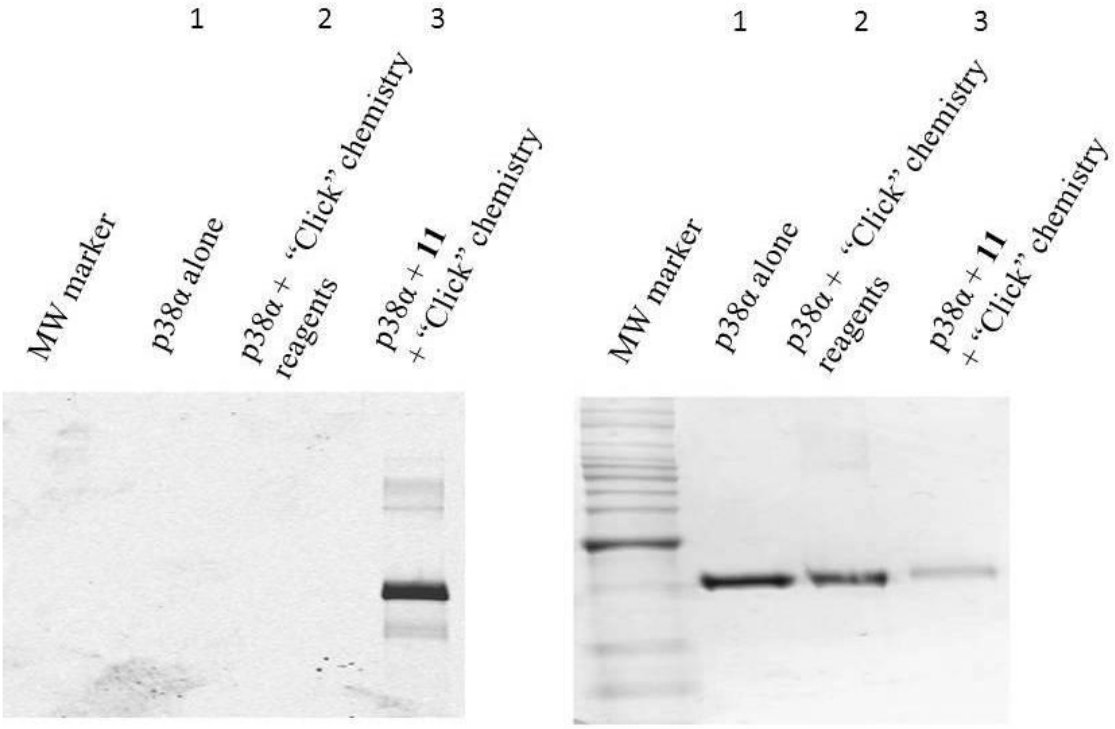

Figure 3.11. In vitro labeling of p38α. p38α was incubated with **11** followed by "Click" chemistry. Left gel: As two controls, p38α was either incubated alone or with the "Click" chemistry reagents: Alexa594-azide, $CuSO_4$, TBTA and TCEP. Right gel: SDS-PAGE gel was stained with Commassie Blue.

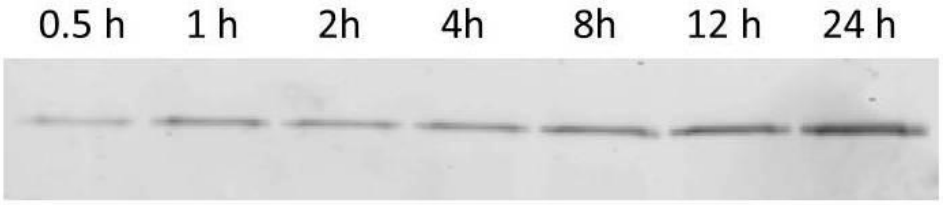

Figure 3.12. Time-course study of the "Click" chemistry reaction. p38α was incubated with **11** for 16 h at °C**.** Aliquots were removed at various time points during the "Click" chemistry.

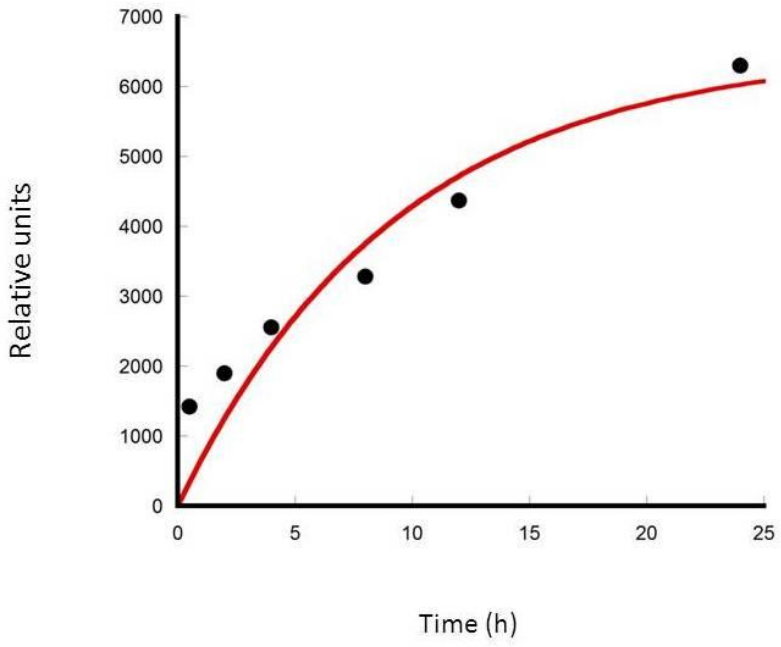

Figure 3.13. Determination of the half-life of the "Click" chemistry.

We next investigated the ability of this probe to detect p38α in cells. By transient transfection, p38α bearing an N-terminal FlAG-tag was expressed in HEK 293T cells. We treated the cells with **11** in DMSO (final concentrations: 1 μM, 5 μM, 50 μM) and incubated the cells at 37 °C for 4 h. Subsequently, the cells were pooled, washed with cold PBS pH 7.4, and harvested. Cell pellets were lysed in lysis buffer containing protease inhibitors. After lysis, the cell lysate were centrifuged. Supernatant was then collected and incubated with ANTI-FLAG M2 affinity gel overnight at 4 °C. The resin was centrifuged and washed with TBS three times. FlAG-p38α was eluted by a competition with FLAG peptide. The resulting supernatant was incubated with Alexa594-azide and catalysts for the cycloaddition reaction, followed by SDS-PAGE analysis. Addition of various concentrations of **11** to the cells resulted in an increase in fluorescence in a dose-dependent manner as shown in Lanes 2, 3 and 4. As a negative control, treatment of the cells with DMSO did not show fluorescence band. As a positive control, treatment of the cell lysate with **11** in vitro followed by immunoprecipitation and "Click" chemistry also gave a fluorescent band (Figure 3.14).

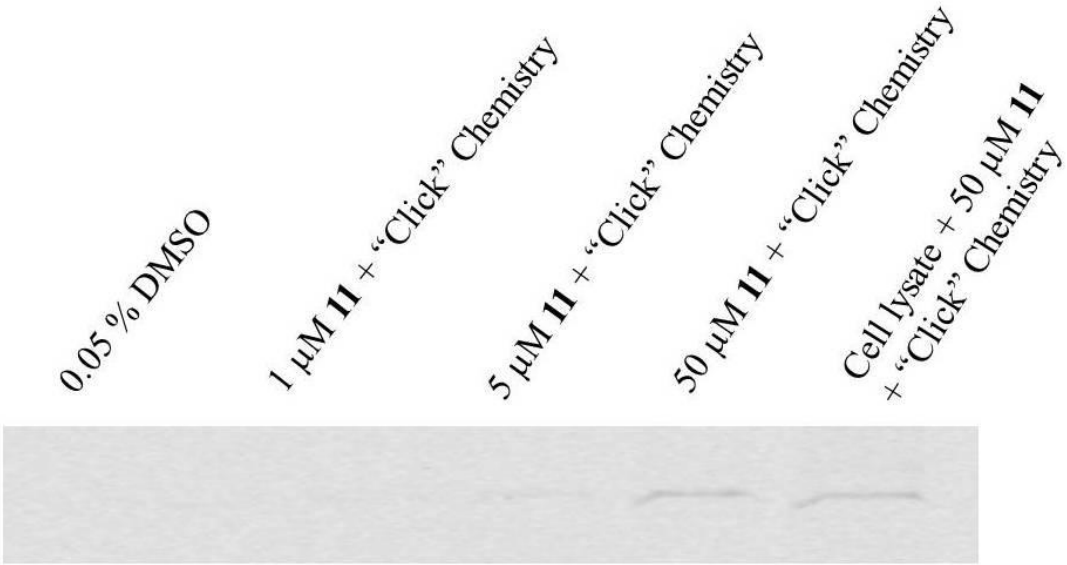

Figure 3.14. In cell labeling of p38α by **11**. After transient transfection of p38α, HEK293T cells were treated with 1 μM, 5 μM, 50 μM **11,** and 0.05 % DMSO followed by immunoprecipitation and "Click" chemistry. Cell lysate was also treated with 50 μM **11** followed by "Click" chemistry.

3.6. SELECTIVITY OF 11 TOWARDS ENDOGENOUS P38α

We have demonstrated that our probe can fluorescently label recombinant p38α in vitro and overexpressed p38α in cells. To test the reactivity of **11** with p38α, we next added recombinant p38α to THP-1 cell lysate (THP-1 cell lysate: p38α = 10: 1 by mass), and carried out an incubation with compound **11** for 16 h at 25 °C followed by the "Click" chemistry. As a result, our compound **11** showed selectivity towards p38α as shown in Lane 2. As a negative control, THP-1 cell lysate was incubated with compound **11** followed by the "Click" chemistry (Lane 1). As a positive control, p38α was incubated with **11** followed by the "Click" chemistry (Lane 3) (Figure 3.15).

In order to test the selectivity of **11** towards endogenous p38α, we incubated THP-1 (100 μg) cell lysate with compound **11** (0.5 mM) for 24 h at 25 °C followed by the "Click" chemistry (Lane 4). As negative controls, THP-1 cell lysate was incubated alone (Lane 1); THP-1 cell lysate was incubated with compound **11** only without the following "Click" chemistry (Lane 2); THP-1 cell lysate was incubated with the "Click" reaction reagents (Alexa594-azide, $CuSO_4$, TBTA and TCEP) (Lane 3). No fluorescent bands were detected in these three lanes. As a positive control, p38α was incubated with **11** followed by the "Click" chemistry, resulting in a fluorescent band (Lane 5). As shown in lane 4, multiple proteins were labeled by **11** in the cell lysate, suggesting that **11** is not selective towards endogenous p38α (Figure 3.16).

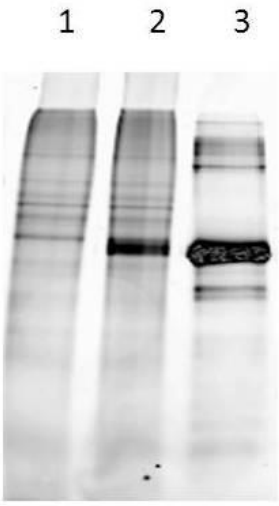

Lane 1: THP-1 cell lysate + **11** + "Click" chemistry

Lane 2: THP-1 cell lysate/ p38α (10:1) + **11** + "Click" chemistry

Lane 3: p38α + **11** + "Click" chemistry

Figure 3.15. Selectivity study of **11** in THP-1 cell lysate with recombinant p38α. THP-1 (40 μg) cell lysate or cell lysate/p38α mixture (40 μg) was incubated with **11** (0.2 mM) for 16 h at 25 °C followed by "Click" chemistry.

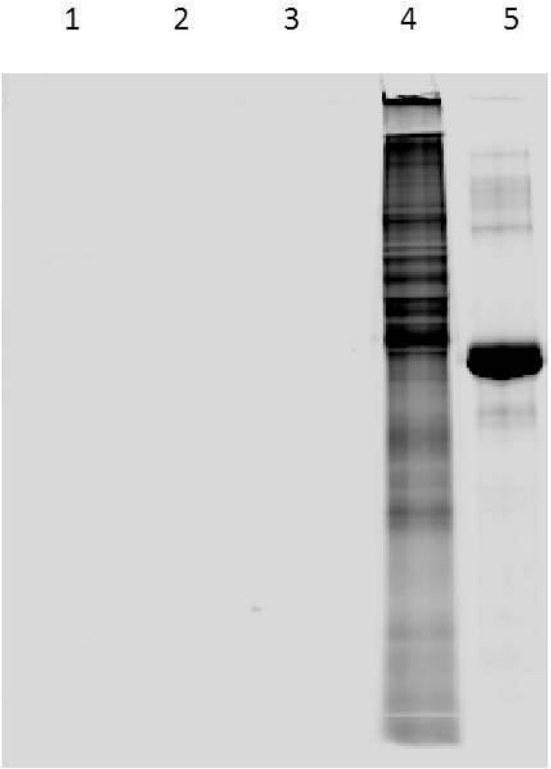

Lane 1: THP-1 cell lysate
Lane 2: THP-1 cell lysate + **11**
Lane 3: THP-1 cell lysate + "Click" chemistry reagents
Lane 4: THP-1 cell lysate + **11** + "Click" chemistry
Lane 5: p38 α + **11** + "Click" chemistry

Figure 3.16. Selectivity study of **11** in THP-1 cell lysate. THP-1 (100 μg) cell lysate was incubated with **11** (0.5 mM) for 24 h at 25 °C followed by the "Click" chemistry.

3.7. MKK3 D-SITE PEPTIDE CAN DIMINISH THE INTERACTION BETWEEN 11 AND P38α

Recently, the selectivity of the MKK3 D-site peptide among MAPKs has been evaluated: the results indicate that the peptide is a remarkably potent inhibitor of p38α (IC_{50} <10 nM), and this peptide does not inhibit JNK1 or JNK2 (*22*). To ascertain if our probe **11** targets the DRS, the following study was carried out to determine whether MKK3 peptide could affect the interaction between **11** and the DRS. We pre-incubated p38α with either MKK3 peptide or compound **2** for 16 h at 25 °C followed by incubation with **11** for an additional 16 h and "Click" chemistry. In comparison to the control (incubation of p38α with **11** alone), a reduction in fluorescence intensity (23 normalized %) was detected in Lane 2 (Figure 3.17). This suggests the MKK3 peptide is able to diminish the interaction between **11** and the DRS in p38α. In Lane 3, 44 % relative fluorescence was detected. It is possible that Cys119 in p38α did not completely react with compound **2** during the pre-incubation. In addition, **11** and the MKK3 peptide were added simultaneously to p38α followed by "Click" chemistry. As a control, we used Ste7 peptide, which has a lower affinity for p38α (described in Lee et al, *Submitted to Biochemistry*). Interestingly, our data showed that the MKK3 peptide competes against **11** for binding to p38α, resulting in 84 % inhibition of adduct in lane 1 (Figure 3.18). Additionally, 28 % inhibition of adduct was detected when p38α was incubated with Ste7 peptide and **11** in Lane 2 (Figure 3.18). Altogether, the above results demonstrate that **11** targets the DRS and the MKK3 peptide can reduce the interaction between **11** and p38α (Figure 3.19).

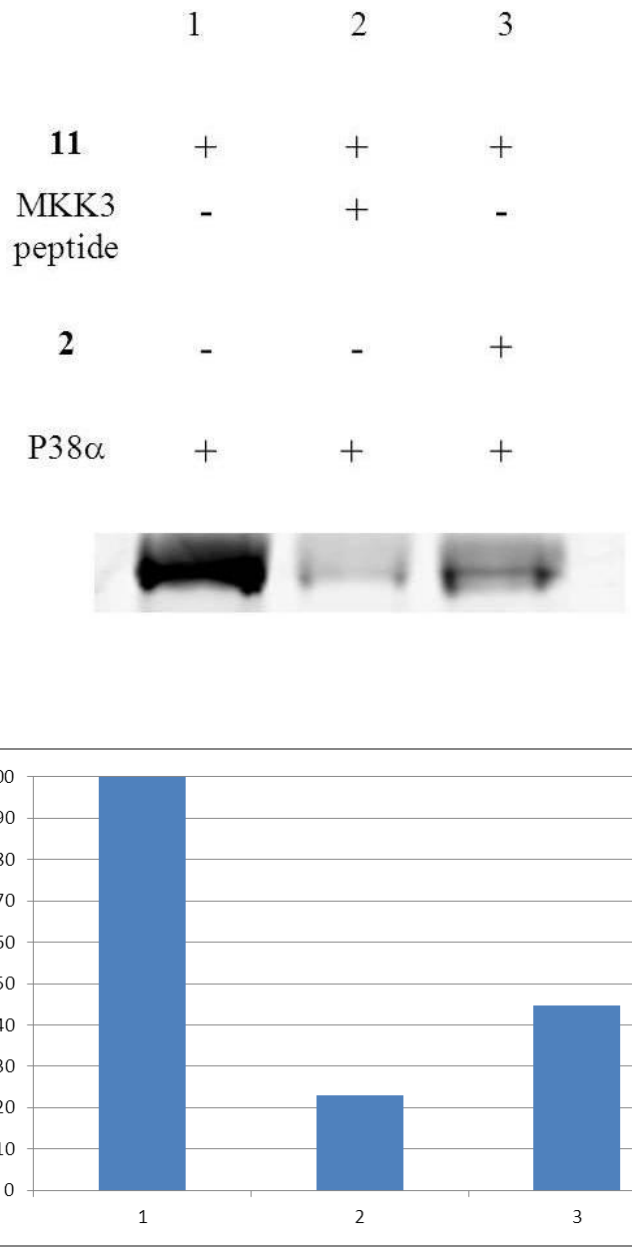

Figure 3.17. Competition assay between MKK3 peptide and compound **11**. MKK 3 peptide (Lane 2) or **2** (Lane 3) was pre-incubated with p38α for 16 h at 25 °C followed by addition of **11** and incubation for another 16 h and "Click" chemistry.

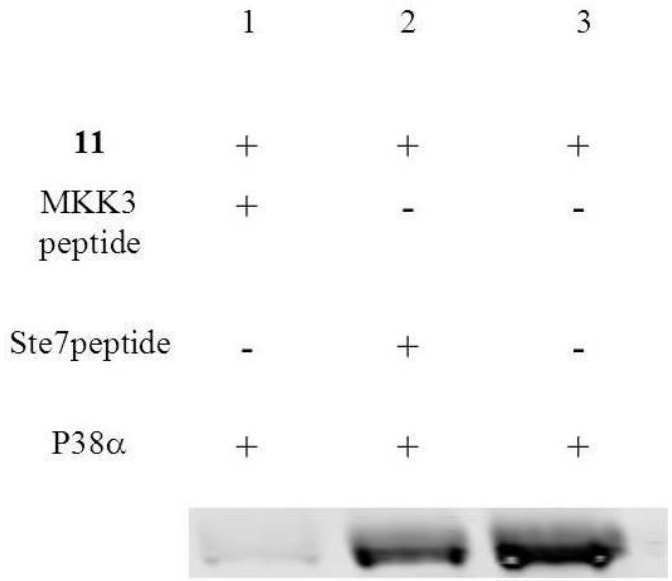

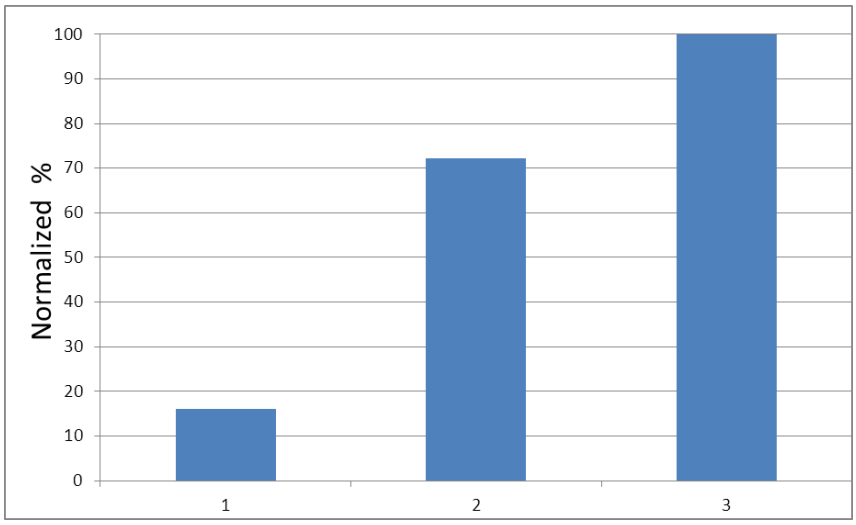

Figure 3.18. Competition assay between MKK3 peptide and compound **11**. MKK3 peptide (Lane 1) or Ste7 peptide (Lane 2) was incubated with p38α and **11** together for 16 h at 25 °C followed by "Click" chemistry.

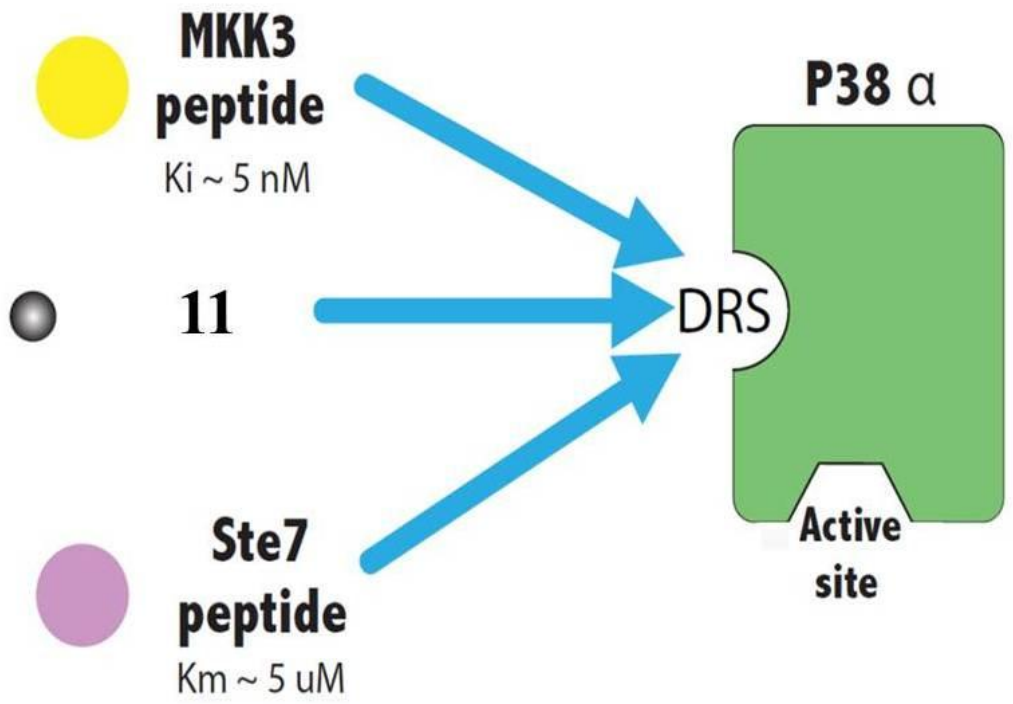

Figure 3.19. MKK3 peptide and Ste7 peptide bind to the D-recruitment site (DRS). 1,2-dialkynylimidazole **11** labels Cys119 in the DRS of p38α.

3.8. COMPETITION ASSAY BETWEEN 11 AND TEST COMPOUNDS

Encouraged by our previous results, we carried out the subsequent studies to test the possibility of further developing this fluorescent-based assay for screening new DRS inhibitors. We first carried out a competition assay by adding *N*-alkynylimidazole analogs **3, 4, 5, 12** (100 μM each) along with **11** (100 μM) to p38α (5 μM). The incubation was performed at 25 °C for 16 h followed by the "Click" chemistry. Clearly, analog **12** in Lane 5 competes with **11** for binding to Cys119 in the docking site of p38α, as the fluorescence intensity is much reduced compared to the control in Lane 1. Analog **11** is a water soluble *N*-alkynylimidazole whereas other analogs are hydrophobic. Therefore, we suspect that hydrophilicity may play a role in the observed competition.

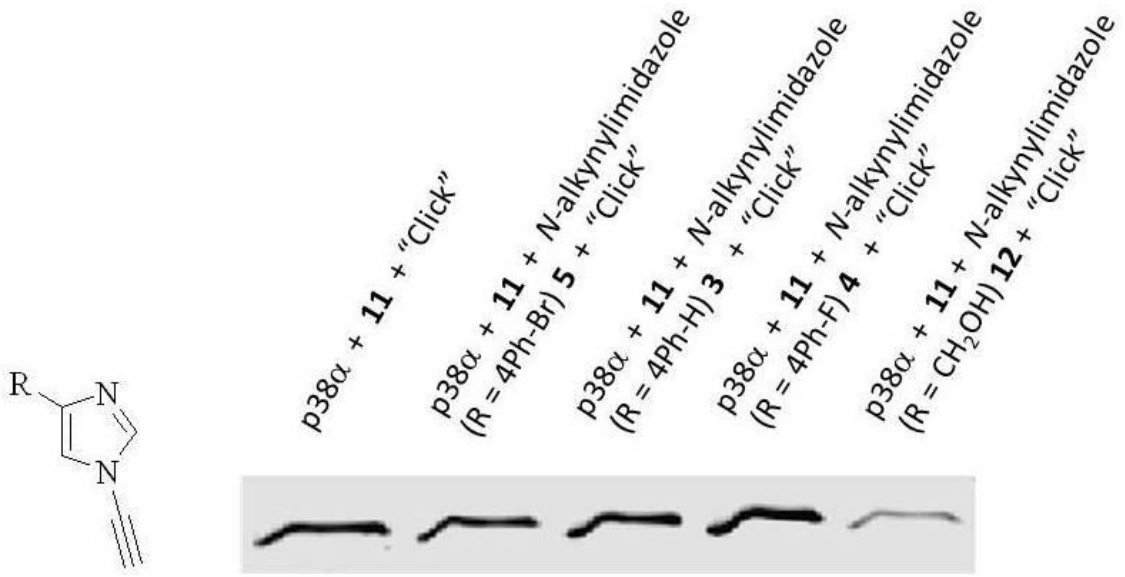

Figure 3.20. Competition assay between **11** and *N*-alkynylimidazole analogs. p38α was incubated with **11** and *N*-alkynylimidazole analogs for 16 h at 25 °C followed by "Click" chemistry.

In addition to *N*-alkynylimidazole analogs, we also carried out a competition assay between caffeic acid phenethyl ester (CAPE) and **11**. The structure of CAPE is shown below. Similarly, the competition experiment was performed by incubating p38α (5 μM) with CAPE (100 μM) and **11** (100 μM) at 25 °C for 16 h followed by the "Click" chemistry (Lane 2). As a positive control, p38α was incubated with **11** followed by the "Click" chemistry (Lane 1). Interestingly, CAPE reduces the interaction between **11** and p38α. It is possible that the mechanism involves nucleophilic addition of the cysteine thiol to the Michael receptor of CAPE. Based on the above competition studies, we can potentially use this fluorescence based assay to identify small molecules that react more quickly than **11** with Cys119. Additionally, further mechanistic study of CAPE on p38α remains to be investigated.

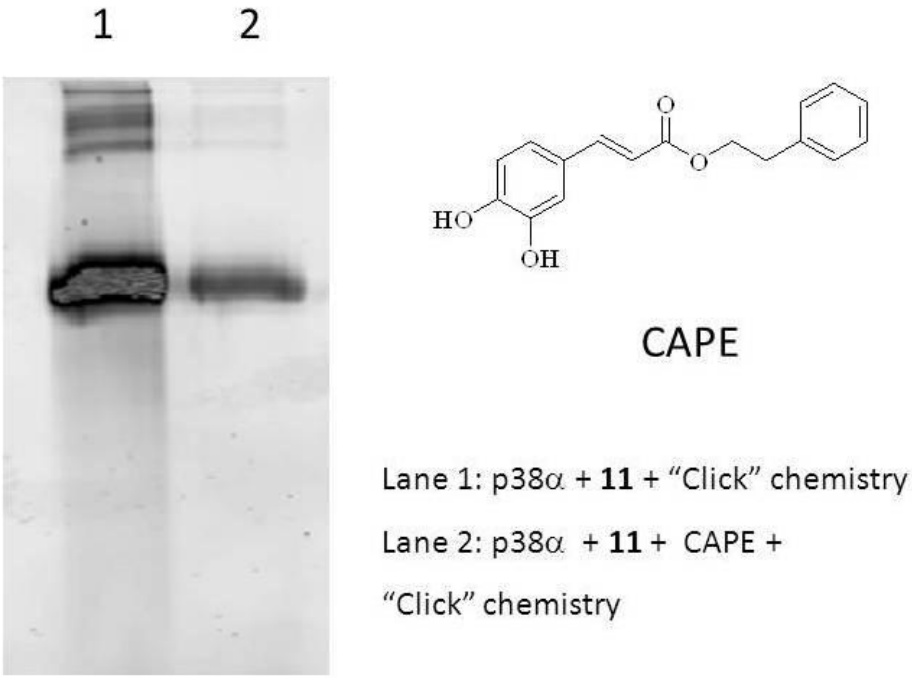

Figure 3.21. Competition assay between **11** and CAPE. p38α was incubated with **11** and CAPE for 16 h at 25 °C followed by "Click" chemistry.

3.9. Determination of the half-life of p38α adduction by 11

In order to optimize the incubation time for this fluorescence-based assay, we first determined the half-life for this covalent adduction. Compound **11** (25 μM) was incubated with p38α (5 μM), and aliquots were removed at various time points followed by "Click" chemistry and SDS-PAGE analysis. The fluorescent gel was scanned and quantified using Image J software. The data was fit to $P = P_{max}(1-e^{-k_{obs}t})$, and the k_{obs} and the half-life of this covalent adduction was estimated to be 0.11 h^{-1} and 6 h, respectively, following pseudo first-order kinetics. Assuming that the pseudo-first order rate constant for the adduct formation is linearly dependent on the excess concentration of compound **11**, and the observed increase in the fluorescence level after the "Click" chemistry reaction is a direct result of compound **11** irreversibly binding to p38α (k_{off} = zero). We can extract a second-order rate constant for compound **11** binding to p38α: $k_{on} = 0.0045\ \mu M^{-1}h^{-1}$ (Figure 3.22).

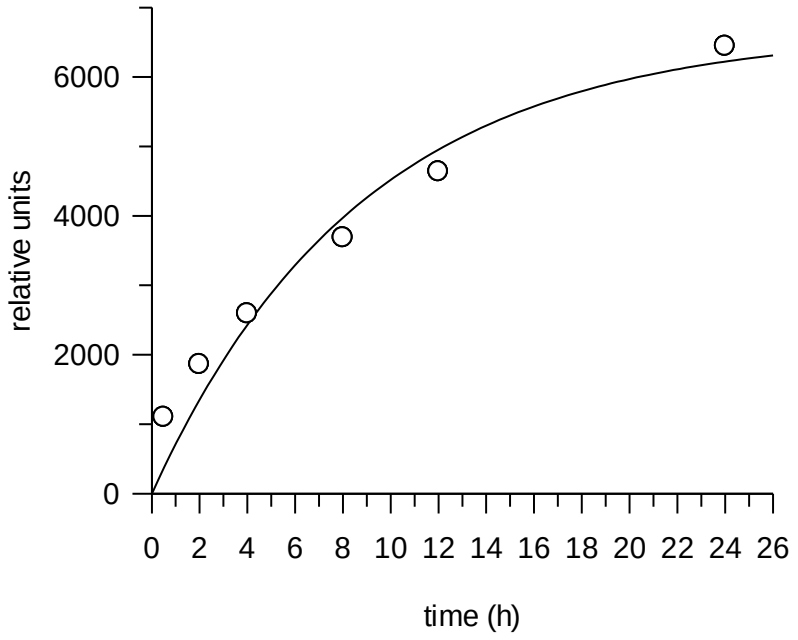

Figure 3.22. Determination of the half-life of the covalent adduction reaction. Compound **11** was incubated with p38α, and aliquots were removed as different time points followed by "Click" chemistry.

3.10. CONCLUSION AND FUTURE DIRECTION

The research discussed here provides a potential alternative for developing new and selective inhibitors that target the substrate binding site. Here we present a novel class of small molecules as docking site probes for p38α. We showed that *N*-alkynylimidazole **2** selectively labels Cys119 in the D-recruitment site of p38α. We also demonstrated that 1,2-dialkynylimidazole **11** can fluorescently label p38α in vitro and in cells, and the interaction between **11** and p38α can be diminished by the p38α-cognate MKK3 peptide. However, several limitations also arise from this fluorescence-based assay. For instance, our probe is not selective towards endogenous p38α. Therefore, further development of a kinase/substrate specific probe is required. Moreover, the reaction time of the covalent chemistry is long. It would not be ideal for a high-throughput screening assay. Furthermore, this fluorescence-based approach must be optimized so that the wash steps would be minimized for a screening assay.

To design a more kinase/substrate specific probe for p38α, one way is to couple a dialkynylimidazole analog with a highly selective D-site peptide (i.e. MKK3 peptide) (Figure 3.23). The D-site peptide will guide the probe to the docking site of p38α, where the covalent modification occurs. A high-throughput screening assay can be developed using this covalent peptide. This approach not only allows us to discover selective D-site inhibitors but also has an advantage of ruling out false hits that target the ATP binding pocket. Additionally, we can apply the same strategy to other kinases that contains cysteine residues in the unique binding site. For example, both ERK2 and JNK have one cysteine in the D-recruitment site, Cys159 and Cys163, respectively (*29*).

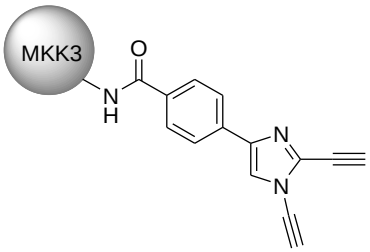

Figure 3.23. Dialkynylimidazole-coupled MKK3 peptide.

In the meantime, a structural optimization of compound **11** can be carried out. We showed that compound **12** is able to compete with **11** for binding to Cys119. Further functionalization at the 4 or 5 position of the imidazole is required to identify a better analog that quickly reacts with Cys119. Then we can perform competition studies described previously in the chapter to evaluate the reactivity of dialkynylimidazole candidates.

In general, fluorescence assays that do not require wash steps are much preferred. One way to minimize wash steps is to label p38α with a second fluorophore near Cys119. Instead of measuring the fluorescence of Alexa 594 in our current fluorescence-based assay, we can detect a FRET signal between the new fluorophore (near Cys119) and the fluorophore (from "Click" chemistry). For example, we can use the tetracysteine-biarsenical system to fluorescently label p38α. The biarsenical labeling reagents FlAsh-EDT2 and ReAsH-EDT2 bind to recombinant p38α containing the tetracysteine (TC) motif Cys-Cys-Pro-Gly-Cys-Cys bind to. Upon binding, the labeling reagents become fluorescent. By this way, we can avoid the step for washing out free fluorophore after the "Click" chemistry step (*32*). Overall, this approach can shorten the overall assay time and provide more accuracy in data analysis.

3.11. EXPERIMENTAL SECTION

General: All reactions were carried out under argon in oven-dried glassware with magnetic stirring. Unless otherwise noted, all materials were obtained from commercial suppliers and were used without further purification. CuI was purified by recrystallization and Cs_2CO_3 was heated several times with a heat gun in the reaction flask under vacuum prior to use. THF, 1,4-dioxane were distilled from sodium/benzophenone prior to use. Unless otherwise noted, organic extracts were dried with Na_2SO_4, filtered through a fritted glass funnel, and concentrated with a rotary evaporator (20–30 mmHg). R_f values are reported for analytical thin-layer chromatography (TLC) performed on 0.25 mm silica gel 60-F plates with UV light or $KMnO_4$ visualization. Flash chromatography was performed with silica gel (230–400 mesh) using the mobile phase indicated. Melting points (open capillary) are uncorrected. Unless otherwise noted, ^1H and ^{13}C NMR spectra were determined in $CDCl_3$ on a spectrometer operating at 400 and 100 MHz, respectively, and are reported in ppm using solvent as internal standard (7.26 ppm for ^1H and 77.0 ppm for ^{13}C). All mass spectra were obtained in the positive mode by chemical ionization using methane as the ionizing gas.

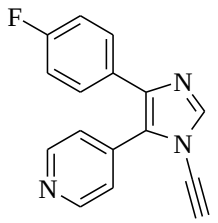

4-(4-fluorophenyl)-5-(4-pyridyl)-1-ethynyl-1*H*-imidazole (2):

To 4-(4-fluorophenyl)-5-(4-pyridyl)-1-(2-triisopropylsilanyl)-1*H*-imidazole (5 mg, 0.01 mmol) in THF (2 ml) at -78 °C was added TBAF (0.015 ml of 1 M solution in THF, 0.012 mmol), and the reaction mixture was stirred at -78 °C until completion. The reaction mixture was quenched with water (2 ml) and extracted with CH_2Cl_2 three times. The organic layers were combined, dried over Na_2SO_4 and the solvent was evaporated under reduce pressure. The residue was purified by flash chromatography (0-50 % EtOAc/hexane) to afford 4-(4-fluorophenyl)-5-(4-pyridyl)-1-ethynyl-1*H*-imidazole **2** (3 mg, yield 96 %) as a light yellow solid: mp = 123.0-124.0 ºC; ^{1}H NMR ($CDCl_3$) δ: 8.69 (br, 2H), 7.94 (s, 1H), 7.48-7.39 (m, 2H), 7.40-7.39 (m, 2H), 7.02-6.98 (m, 2H); MS *m/z*: HRMS (CI) calcd for $C_{16}H_{11}N_3FN_3$ (M^+) 264.0937, found 264.0932.

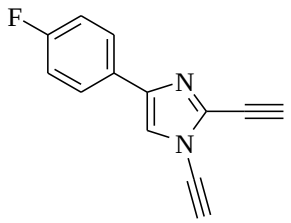

4-(4-fluorophenyl)-1-(ethynyl)-2-(ethynyl)-1*H*-imidazole (11):

To a solution of 4-(4-fluorophenyl)-2-iodo-1-((triisopropylsilyl)ethynyl)-1*H*-imidazole (145 mg, 0.30 mmol) in Et_3N (4 ml) was added ethynyltrimethylsilane (0.05 ml, 0.36 mmol), $Pd(PPh_3)_4$ (17 mg, 0.015 mmol) and CuI (5.7 mg, 0.03 mmol). The reaction mixture was stirred at room temperature until the starting material was completely consumed. The reaction mixture was filtered. The filtrate was evaporated, and the residue was purified by flash chromatography (0-2 % EtOAc/hexane) to afford 4-(4-fluorophenyl)-1-(2-triisopropylsilylethynyl)-2-(2-trimethylsilylethynyl)-1*H*-imidazole (Quantitative yield). To this material (18 mg, 0.045 mmol) in THF (1.4 ml) at -78 °C was added TBAF (0.09 ml of 1 M solution in THF, 0.09 mmol), and the reaction mixture was stirred at -78 °C until completion. The reaction mixture was quenched with water (2 ml) and extracted with CH_2Cl_2 three times. The organic layers were combined, dried over Na_2SO_4 and the solvent was evaporated under reduce pressure. The residue was purified by flash chromatography (0-20 % EtOAc/hexane) to afford 4-(phenyl)-1-(ethynyl)-2-(ethynyl)-1*H*-imidazole **11** (8 mg, 82 % yield) as an off-white solid: mp 89.7-91.5 °C; ^{1}H NMR (400 MHz, $CDCl_3$) δ 7.75-7.72 (2H, m), 7.34 (1H, s), 7.10-7.06 (2H, m), 3.44 (1H, s), 3.24 (1H, s); ^{13}C NMR (100 MHz, $CDCl_3$) δ 162.6 (d, J = 246 Hz), 141.2, 134.4, 128.1 (d, J = 2.9 Hz), 127.1 (2C, d, J = 8.2 Hz), 117.2, 115.7 (2C, d, J = 21.6 Hz), 82.7, 71.5, 70.4, 62.3; MS *m/z*: HRMS (CI) calc for $C_{13}H_8N_2F$ ($M+H^+$) 211.0672, found 211.0668.

General procedure for the preparation of (Z)-thioenol ether:

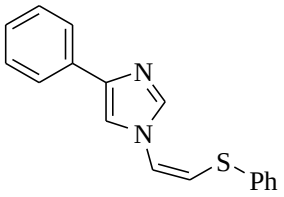

(Z)-4-phenyl-1-(2-(phenylthio)vinyl)-1*H*-imidazole (6):

To a solution of 4-phenyl-1-ethynyl-1*H*-imidazole (15 mg, 0.09 mmol) in THF (2 ml) was added thiophenol (0.1mmol, 0.01 ml). The reaction mixture was stirred at room temperature overnight. The reaction mixture was concentrated, and the residue was purified by flash chromatography (10-30 % EtOAc/hexane) to afford **6** as a yellow solid (20 mg, 81 % yield): mp: 125.5-128.1 $^{\circ}$C; ^{1}H NMR (400 MHz, $CDCl_3$) δ 7.77-7.76 (2H, m), 7.75 (1H, s), 7.67 (1H, s), 7.40- 3.38 (2H, m), 7.35-7.26 (4H, m), 7.24-7.19 (2H, m), 6.81 (1H, d, *J* = 8.4 Hz), 6.04 (1H, d, *J* = 8.4 Hz); ^{13}C NMR (100 MHz, $CDCl_3$) δ 142.4, 137.7, 134.2, 133.5, 130.1 (2C), 129.4 (2C), 128.6 (2C), 127.8, 127.1, 125.0 (2C), 121.2, 115.1, 114.1; MS *m/z*: HRMS (CI) calc for $C_{17}H_{15}N_2S$ (M^+) 279.0956, found 279.0952.

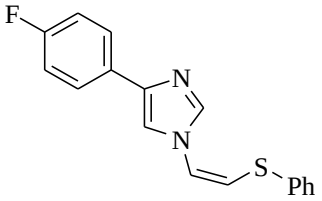

(Z)-4-(4-fluorophenyl)-1-(2-(phenylthio)vinyl)-1*H*-imidazole (7):

Following the general procedure described: **7** (61 % yield) was obtained as a light orange solid: mp 110.5-111.9 °C; ^{1}H NMR (400 MHz, $CDCl_3$) δ 7.82 (1H, d, *J* = 1.2 Hz), 7.80-7.77 (2H, m), 7.67 (1H, d, J = 1.2 Hz), 7.46-7.43 (2H, m), 7.39-7.30 (3H, m), 7.11-7.06 (2H, m), 6.87 (1H, d, *J* = 8.4 Hz), 6.11 (1H, d, *J* = 8.4 Hz); ^{13}C NMR (100 MHz, $CDCl_3$) δ 162.1 (d, *J* = 244.1 Hz), 141.5, 137.7. 134.1, 130.0 (2C), 129.7 (d, *J* = 3.0 Hz), 129.4 (2C), 127.8, 126.6 (2C, d, *J* = 8.1 Hz), 121.1, 115.6, 115.3 (2C, d, J = 12.6 Hz), 113.7; MS *m/z*: HRMS (CI) calc for $C_{17}H_{14}N_2FS$ (M^+) 297.0862, found 297.0866.

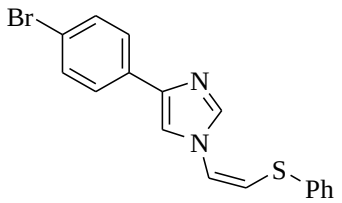

(Z)-4-(4-bromophenyl)-1-(2-(phenylthio)vinyl)-1*H*-imidazole (8):

Following the general procedure described: **8** (95 % yield) was obtained as an off-white solid: mp 154.3-154.7 °C; ^{1}H NMR (400 MHz, $CDCl_3$) δ 7.83, 7.72-7.68 (3H, m), 7.53-7.50 (2H, m), 7.47-7.44 (2H, m), 7.40-7.32 (3H, m); ^{13}C NMR (100 MHz, $CDCl_3$) δ 141.4, 137.8, 134.1, 132.5, 131.7 (2C), 130.1 (2C), 129.4 (2C), 127.8, 126.6 (2C), 121.0, 120.8, 115.6, 114.3 ; MS *m/z*: HRMS (CI) calc for $C_{17}H_{14}N_2Br\,S$ (M^+) 357.0061, found 357.0059.

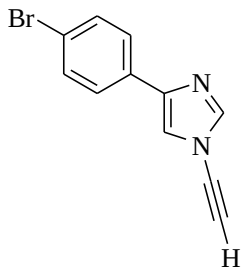

1-ethynyl-4-(4-bromophenyl)-1*H*-imidazole (5):

A reaction flask under argon was charged with Cs_2CO_3 (3.25 g, 10 mmol), CuI (60 mg, 0.25 mmol), and 4-bromophenyl-imidazole (1.1g, 5 mmol) and backfilled with argon. Dry 1,4-dioxane (10 mL) was added followed by bromotriisopropylacetylene (0.237 mL, 10 mmol), 2-acetylcyclohexanone (0.125 mL, 1 mmol). The mixture was heated to 50 °C in an oil bath for 14 h and then heated to reflux for 4 h. The reaction mixture was cooled to room temperature, quenched with 10 mL of a saturated NH_4Cl solution, and extracted with CH_2Cl_2 (3× 20 mL). The combined organic layers were evaporated and (flash chromatography; 0–5% EtOAc/hexane), 55 mg of **4-(4-bromophenyl)-1-((triisopropylsilyl)ethynyl)-1*H*-imidazole** (67 % yield) was obtained as an off-white solid: mp 54.6-55.1 °C; ^{1}H NMR (400 MHz, $CDCl_3$) δ 7.77 (1H, d, J = 1.2 Hz), 7.65-7.63 (2H, m), 7.52-7.50 (2H, m), 7.39 (1H, d, J = 1.2 Hz), 1.14-1.12 (21H, m); ^{13}C NMR (100 MHz, $CDCl_3$) δ 140.6, 140.5, 131.8 (2C), 131.7, 126.7 (2C), 121.3, 117.1, 91.4, 70.5, 18.5 (6C), 11.1 (3C); MS *m/z*: HRMS (CI) calc for $C_{20}H_{27}N_2SiBr$ (M^+) 402.1127, found 402.1129. To this material (59 mg, 0.15 mmol) in THF (3.2 ml) at -78 °C was added TBAF (0.15 ml of 1 M solution in THF, 0.15 mmol), and the reaction mixture was stirred at -78 °C until completion. The reaction mixture was quenched with water (4 ml) and extracted with CH_2Cl_2 three times. The organic layers were combined, dried over Na_2SO_4 and the solvent was evaporated under reduce pressure. The residue was purified by flash chromatography (0-20 % EtOAc/hexane) to afford 34 mg **5** as an off-white solid (95 % yield): ^{1}H NMR (400 MHz,

$CDCl_3$) δ 7.79 (1H, s), 7.63-7.60 (2H, m), 7.51-7.48 (2H, m), 7.36 (1H, s); ^{13}C NMR (100 MHz, $CDCl_3$) δ 140.8, 140.5, 131.8 (2C), 131.4, 126.8 (2C), 121.5, 116.8, 71.3, 59.7; MS *m/z*: HRMS (CI) calc for $C_{11}H_7N_2Br$ (M^+) 247.9775, found 247.9772.

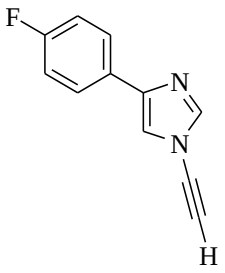

4-(4-fluorophenyl)-1-ethynyl-1*H*-imidazole (4):

Following the same procedure described: **4** was obtained as a beige solid (79 % yield): ^{1}H NMR (400 MHz, $CDCl_3$) δ 7.79 (1H, s), 7.75-7.70 (2H, m), 7.33 (1H, s), 7.11-7.05 (2H, m); ^{13}C NMR (100 MHz, $CDCl_3$) δ162.4 (d, *J* = 245.5 Hz), 141.1, 140.4 (2C), 128.71 (d, *J* = 3 Hz), 127.0, 126.9 (2C, d, *J* = 8.2 Hz), 116.2 (2C), 115.6 (2C, d, *J* = 21.6 Hz), 71.4, 59.5; MS *m/z*: HRMS (CI) calc for $C_{11}H_7N_2F$ ($M+H^+$) 186.0593, found 186.0593.

Identification of site modification on p38α by *N*-alkynylimidazole 2:

The reaction consists of 5 μM p38α, 100 μM **2** in 50 mM HEPES, pH 7.5, 1 mM EGTA, 2 mM DTT, 10 mM $MgCl_2$. After 12 h incubation at 25 °C , the reaction mixture was dialyzed in 1 Liter of 25 mM HEPES, pH 7.5, 1 mM DTT, 50 mM KCl, 0.1 mM EDTA, 0.1 mM EGTA, 10 % (v/v) glycerol. After 12 h dialysis at 4 °C, the protein was concentrated and subjected to ESI mass spectrometry.

The *N*-alkynylimidazole **2** adducted p38α was digested with chymotrypsin (chymotrypsin: peptide = 1: 20 w/w) in 100 mM Tris-HCl containing 20 mM $CaCl_2$, pH 7.8 at 30 °C for 12 h. The digested sample was subjected to MALDI mass spectrometry.

In vitro labeling of p38α by 11:

The reaction consists of 5 μM p38α, 100 μM **2** in 50 mM HEPES, pH 7.5, 1 mM EGTA, 2 mM DTT, 10 mM $MgCl_2$. After 16 h incubation at 25 °C, the Cu (I) catalyzed 1,3 dipolar cycloaddition reaction was carried out as follows: 25 μg p38α in 50 mM Phosphate Buffer was incubated with 0.5 μl $CuSO_4$ (50 mM), 0.5 μl tris(2-carboxyethyl)phosphine (TCEP, 50 mM) and 1.65 μl tris[(1-benzyl-1H-1,2,3-triaol-4-yl)methyl]amine (TBTA, 1.5 mM) at 25 °C for 16 h. Then the "click" reaction was quenched with addition of 2x SDS loading buffer and heat inactivated at 95 °C for 10 min. The samples were analyzed by 10 % SDS PAGE. The gel was scanned by Typhoon Trio from GE heathcare and the data were analyzed by Image J software.

In cell labeling of p38α:

HEK 293T cells (5 x 10^5 cells) were seeded on a 6 well polystyrene plate in DMEM supplemented with 10 % FBS (Invitrogen) and 1 % L-glutamine. Cells were grown to 90-95 % confluency in an atmosphere of 5 % CO_2, pCDNA3 Flag p38α (Addgene) was transfected into HEK 293T cells using polyethyleneimine (PEI). After 48 h incubation, old medium was removed. Compound **11** was added in new growth medium. The cells were incubated at 37 °C for 4 h. After the treatment, cells were pooled, spinned down at 1200 rpm and washed twice with cold PBS pH 7.4. Cell pellets were lysed in lysis buffer containing protease inhibitors (Thermo Scientific). The resulting solution was incubated at 4 °C for 30 min. The cell lysates were centrifuged at 14,000 rpm at 4 °C for 10 min. Supernatant was collected and incubated with ANTI-FLAG M2 affinity gel overnight at 4 °C. The resin was centrifuged and washed with TBS three times. Flag-p38α was eluted by a competition with FLAG peptide. The Cu (I) catalyzed 1,3 dipolar cycloaddition reaction was carried out following the procedures described above.

Steady-state kinetics

p38 MAPKα assays were conducted at 27 °C in assay buffer A1 (20 mm Hepes, 2 mm dithiothreitol, 100 mm KCl, 0.1 mm EDTA, 0.1 mm EGTA, 10 $\mu g \cdot mL^{-1}$ bovine serum albumin, pH 7.6) containing 8–10 nm activated p38 MAPKα and 10 mm $MgCl_2$ in a final volume of 100 μL. The concentrations of substrates ranged as follows: ATF2 (1-115) or MK2 (Δ40 MK2) or Ste7 (0.5–100 μM), ATP (0.5 mM, 1000 $c.p.m.pmol^{-1}$). The reaction mixture was incubated for 5 min before the addition of ATP. Aliquots (10 μL) were taken at set time points and applied to a 2 x 2 cm P81 cellulose papers, which were allowed to air-dry, washed with 50 mm phosphoric acid (5 x 10 min), then in acetone (1 x 10 min) and dried. The incorporation of radioactivity was determined by counting in 1.5 mL CytoScint on a Packard 1500 scintillation counter at a σ-value of 2. Protein concentrations were determined at 280 nm using the following molar extinction coefficients: $\varepsilon = 52\ 501\ M^{-1} \cdot cm^{-1}$ (p38 MAPKα), ATP concentration was determined at 259 nm using $52\ 501\ M^{-1} \cdot cm$. The initial velocities were fitted using KaleidaGraph 4.0.

3.12. REFERENCES

1. Chen, Z., Gibson, T. B., Robinson, F., Silvestro, L., Pearson, G., Xu, B., Wright, A., Vanderbilt, C., and Cobb, M. H. (2001) MAP kinases, *Chem Rev 101*, 2449-2476.
2. Johnson, G. L., and Lapadat, R. (2002) Mitogen-activated protein kinase pathways mediated by ERK, JNK, and p38 protein kinases, *Science 298*, 1911-1912.
3. Kirkland, L. O., and McInnes, C. (2009) Non-ATP competitive protein kinase inhibitors as anti-tumor therapeutics, *Biochem Pharmacol 77*, 1561-1571.
4. Garuti, L., Roberti, M., and Bottegoni, G. (2010) Non-ATP competitive protein kinase inhibitors, *Curr Med Chem 17*, 2804-2821.
5. Kufareva, I., and Abagyan, R. (2008) Type-II kinase inhibitor docking, screening, and profiling using modified structures of active kinase states, *J Med Chem 51*, 7921-7932.
6. Cargnello, M., and Roux, P. P. (2011) Activation and Function of the MAPKs and Their Substrates, the MAPK-Activated Protein Kinases, *Microbiol Mol Biol R 75*, 50-83.
7. Sharrocks, A. D., Yang, S. H., and Galanis, A. (2000) Docking domains and substrate-specificity determination for MAP kinases, *Trends Biochem Sci 25*, 448-453.
8. Tanoue, T., Adachi, M., Moriguchi, T., and Nishida, E. (2000) A conserved docking motif in MAP kinases common to substrates, activators and regulators, *Nat Cell Biol 2*, 110-116.
9. Tanoue, T., and Nishida, E. (2003) Molecular recognitions in the MAP kinase cascades, *Cell Signal 15*, 455-462.
10. Bardwell, A. J., Flatauer, L. J., Matsukuma, K., Thorner, J., and Bardwell, L. (2001) A conserved docking site in MEKs mediates high-affinity binding to MAP kinases and cooperates with a scaffold protein to enhance signal transmission, *J Biol Chem 276*, 10374-10386.
11. Gum, R. J., and Young, P. R. (1999) Identification of two distinct regions of p38 MAPK required for substrate binding and phosphorylation, *Biochem Biophys Res Commun 266*, 284-289.
12. Chang, C. I., Xu, B. E., Akella, R., Cobb, M. H., and Goldsmith, E. J. (2002) Crystal structures of MAP kinase p38 complexed to the docking sites on its nuclear substrate MEF2A and activator MKK3b, *Molecular Cell 9*, 1241-1249.
13. Smith, J. A., Poteet-Smith, C. E., Malarkey, K., and Sturgill, T. W. (1999) Identification of an extracellular signal-regulated kinase (ERK) docking site in ribosomal S6 kinase, a sequence critical for activation by ERK in vivo, *J Biol Chem 274*, 2893-2898.
14. Jacobs, D., Glossip, D., Xing, H., Muslin, A. J., and Kornfeld, K. (1999) Multiple docking sites on substrate proteins form a modular system that mediates recognition by ERK MAP kinase, *Genes Dev 13*, 163-175.
15. Bardwell, L. (2006) Mechanisms of MAPK signalling specificity, *Biochemical Society Transactions 34*, 837-841.

16. Remenyi, A., Good, M. C., and Lim, W. A. (2006) Docking interactions in protein kinase and phosphatase networks, *Curr Opin Struct Biol 16*, 676-685.

17. Roehrl, M. H., Kang, S., Aramburu, J., Wagner, G., Rao, A., and Hogan, P. G. (2004) Selective inhibition of calcineurin-NFAT signaling by blocking protein-protein interaction with small organic molecules, *Proc Natl Acad Sci U S A 101*, 7554-7559.

18. Eldar-Finkelman, H., and Eisenstein, M. (2009) Peptide inhibitors targeting protein kinases, *Curr Pharm Des 15*, 2463-2470.

19. Borsello, T., Clarke, P. G., Hirt, L., Vercelli, A., Repici, M., Schorderet, D. F., Bogousslavsky, J., and Bonny, C. (2003) A peptide inhibitor of c-Jun N-terminal kinase protects against excitotoxicity and cerebral ischemia, *Nat Med 9*, 1180-1186.

20. Kelemen, B. R., Hsiao, K., and Goueli, S. A. (2002) Selective in vivo inhibition of mitogen-activated protein kinase activation using cell-permeable peptides, *J Biol Chem 277*, 8741-8748.

21. Guergnon, J., Dessauge, F., Dominguez , V., Viallet, J., Bonnefoy, S., Yuste, V., Mercereau-Puijalon, O., Cayla, X., Rebollo, A., and Susin, S. (2006) Use of penetrating peptides interacting with PP1/PP2A proteins as a general approach for a drug phosphatase technology, *Mol Pharmacol 69*, 1115.

22. Bardwell, A. J., Frankson, E., and Bardwell, L. (2009) Selectivity of docking sites in MAPK kinases, *J Biol Chem 284*, 13165-13173.

23. Bogoyevitch, M. A. (2005) Therapeutic promise of JNK ATP-noncompetitive inhibitors, *Trends Mol Med 11*, 232-239.

24. Li, J., Kaoud, T. S., Laroche, C., Dalby, K. N., and Kerwin, S. M. (2009) Synthesis and biological evaluation of p38 alpha kinase-targeting dialkynylimidazoles, *Bioorgan Med Chem Lett 19*, 6293-6297.

25. Laroche, C., Li, J., Freyer, M. W., and Kerwin, S. M. (2008) Coupling reactions of bromoalkynes with imidazoles mediated by copper salts: Synthesis of novel N-alkynylimidazoles, *J Org Chem 73*, 6462-6465.

26. Wang, Z. L., Harkins, P. C., Ulevitch, R. J., Han, J. H., Cobb, M. H., and Goldsmith, E. J. (1997) The structure of mitogen-activated protein kinase p38 at 2.1-angstrom resolution, *P Natl Acad Sci USA 94*, 2327-2332.

27. Schmidtke, P., and Barril, X. (2010) Understanding and predicting druggability. A high-throughput method for detection of drug binding sites, *J Med Chem 53*, 5858-5867.

28. Zhou, T. J., Sun, L. G., Humphreys, J., and Goldsmith, E. J. (2006) Docking interactions induce exposure of activation loop in the MAP kinase ERK2, *Structure 14*, 1011-1019.

29. Akella, R., Moon, T. M., and Goldsmith, E. J. (2008) Unique MAP Kinase binding sites, *Biochim Biophys Acta 1784*, 48-55.

30. Laroche, C., Li, J., and Kerwin, S. M. (2011) Cytotoxic 1,2-dialkynylimidazole-based aza-enediynes: aza-Bergman rearrangement rates do not predict cytotoxcitiy *J Med Chem 54*, 5059-5069.

31. Laroche, C., Li, J., Gonzales, C., David, W. M., and Kerwin, S. M. (2010) Cyclization kinetics and biological evaluation of an anticancer 1,2-dialkynylimidazole, *Org Biomol Chem 8*, 1535-1539.

32. Lin, M., and Wang, L. (2008) Selective labeling of proteins with chemical probes in living cells, *Physiology 23*, 131-141.

Chapter 4

Biological evaluation of 1,2-dialkynylimidazole as anti-cancer agents: aza-Bergman rearrangement do not predict cytotoxicity

4.1. INTRODUCTION

The extreme cancer cell cytotoxicity of natural enediyne compounds such as calcheamincin γ_1 (*1*), esperamicin A1 (*2*) or dynemicin A (*3*) involves DNA cleavage via diradical intermediates arising from cyclization of enediyne core (*4*). In order to address the selectivity issues associated with natural products, a wide variety of enediyne analogs have been prepared and examined for DNA cleavage and cancer cell cytotoxicity activities (*5-8*). In this respect, computational chemistry has substantially aided in the design of enediynes that undergo diradical-generating Bergman cyclization under physiological conditions (*9-13*).

Recently, several enediynes have been described that do not undergo Bergman cyclization under physiological conditions, but which still display interesting cancer cell cytotoxicity (*14-16*). These enediynes induce G2/M cell cycle arrest by targeting microtubule formation (*14*), although other targets such as topoisomerase I and MAPK pathways have also been proposed (*15, 16*).

1,2-Dialkynylimidazoles have been investigated as a class of aza-enediynes (Figure 1) (*17-20*), which are considered potential DNA-cleaving anticancer agents with improved selectivity in comparison with the enediynes. We reported the novel thermolysis and rearrangement of 1,2-dialkynylimidazoles as described in Chapter 1. Here we address the unique and potent cancer cell cytotoxicity of the 1,2-dialkynylimidazole **1a** (Figure 4.1). In order to better understand the structural basis and role of the thermal generation of diradical and/or carbene intermediates in the cytotoxicity demonstrated by **1a**, we have prepared a series of dialkynylimidazoles and related imidazoles and determined their cytotoxicity against A549 human non-small cell lung cancer cells. The aza-Bergman cyclization kinetics of selected

dialkynylimidazoles was also studied experimentally and by DFT calculations. Interestingly, although some of these dialkynylimidazoels are very cytotoxic to A549 cells, the degree of cytotoxicity is unrelated to the kinetics of aza-Bergman cyclization. Furthermore, we find evidence that the 1-ethynylimidazole moiety contributes to the cytotoxicity of these compounds, possibly as a result of the unexpected reactivity of this functionality with thiols.

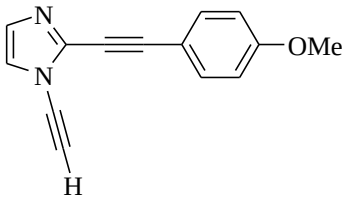

Figure 4.1. Structure of 1,2-dialkynylimidazole **1a**.

4.2. SYNTHESIS OF 1,2-DIALKYNYLIMIDAZOLES AND *N*-ALKYNYLIMIDAZOLES

The 1,2-dialkynylimidazoles **1a-p** were prepared with Dr. Christophe Laroche from previously reported 1-alkynyl-2-idoimiiidazoles **4a-g**, which were coupled to a variety of terminal alkynes under standard Sonogashira coupling conditions followed by silyl deprotection with TBAF in THF if necessary (Table 4.1).

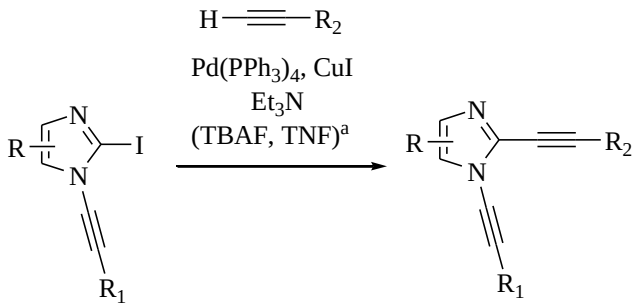

Starting Iodoimidzole	R =	R_1 =	R_2 =	Product (Yield)
4a[b]	H	H	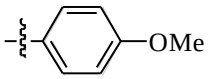	**1a** (75 %)[b]
4b[c]	H	H	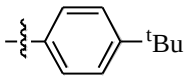	**1b** (75 %)
4b[c]	H	H	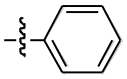	**1c** (69 %)[c]
4b[c]	H	H	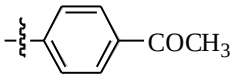	**1d** (73 %)
4b[c]	H	H	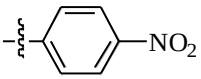	**1e** (71 %)

4b[c]	H	H	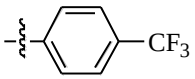	**1f** (69 %)[h]
4b[c]	H	H	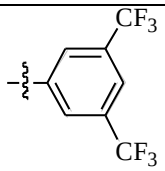	**1g** (68 %)
4b[c]	H	H	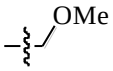	**1h** (70 %)[c]
4c[d]	H	Ph	H	**1i** (63 %)[d]
4d[e]	H	CH_2OH	CH_2OH	**1j** (71 %)
4e[f]	Ph	H	H	**1k** (79 %)[d]
4e[f]	Ph	H	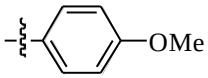	**1l** (78 %)[d]
4f[g]	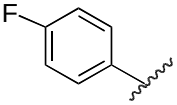	H	H	**1m** (82 %)
4f[g]	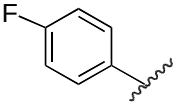	H	CH_2CH_2OH	**1n** (35 %)
4g[f]		H	H	**1o** (75 %)
4g[f]		H	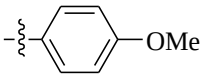	**1p** (92 %)

Table 4.1. Synthesis of Dialkynylimidazoles **1a-p**.

[a]An optional deprotection of silyl groups was carried out, except in the case of reactions of **4c**. [b]In **4a** R = TIPS; see ref 27. [c]In **4b** R = TMS; see ref 19.[d] See ref 20 . [e]In **4c** R = $CH_2OTBDMS$; see ref 20. [f]In **4e,g,** R = TIPS; see ref 20. [g]see ref 19. [h]see ref 18.

Related alkynylimidazoles **5a** and **5b** were prepared as previously described (*21*). Deprotection of the silylalkynylimidazole **6a** afforded the ethynylimidazole **6b**. The 1-methylimidazole **7** was prepared from 1-tert-butoxycarbonyl-2-iodoimidazole by Sonogashira coupling, deprotection, and methylation (Scheme 4.1). Treating the dialkynylimidazole **1a** with thiophenol in THF at room temperature for 5 days afforded the addition product **8** as a single diastereomer that was assigned the (Z)-configuration based on ^{1}H NMR coupling constants (8.4 Hz) for the alkenyl protons.

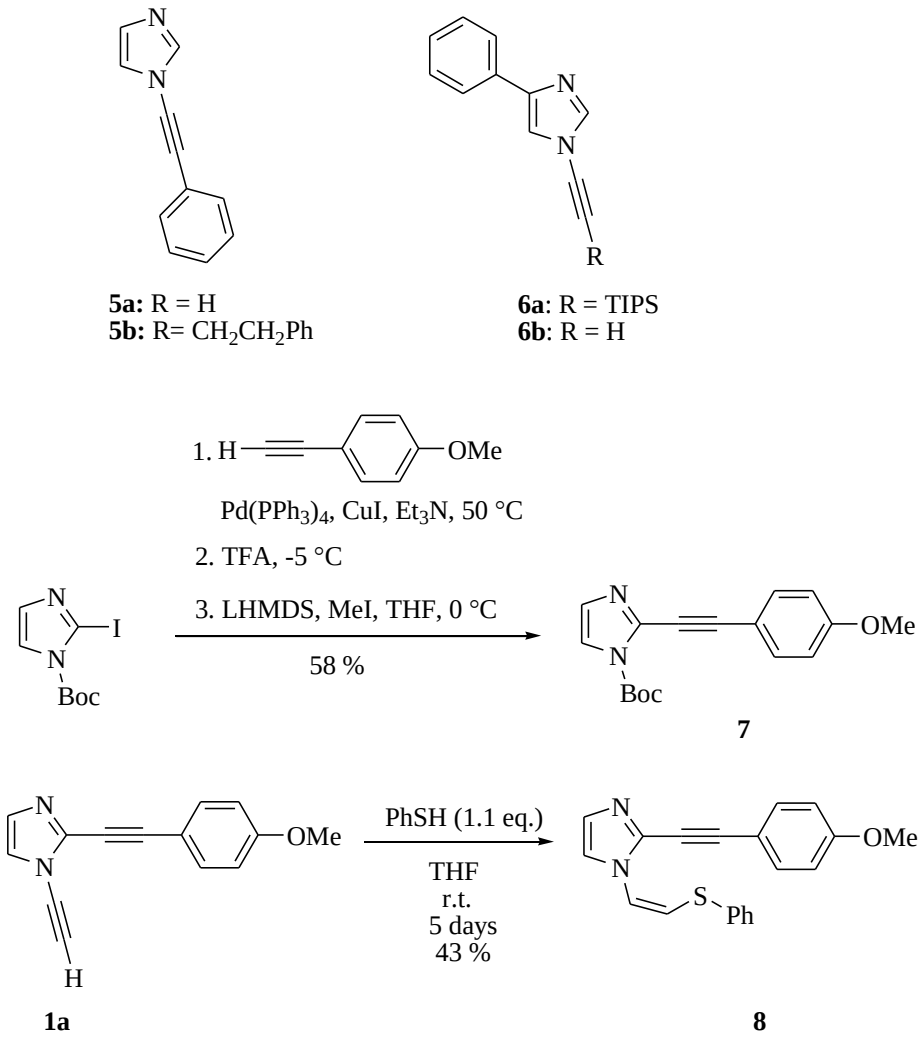

Scheme 4.1. Synthesis of related alkynylimidazoles.

4.3. APOPTOSIS ASSAY OF 1,2-DIALKYNYLIMIDAZOLE

The cytotoxicity (*22*) of 1,2-dialkynylimidazole **1a** has been evaluated by the National Cancer Institute against 60 cancer cell lines. Compound **1a** showed inhibition activity against a range of cell lines with GI_{50} values from 10^{-8} to 10^{-6} M and a mean GI_{50} of 3 μM. Although a COMPARE analysis (*23*) showed that these is no similarities between **1a** and standard anticancer drugs (correlation co-efficient < 0.5), within the set of compounds selected by the NCI for *in vivo* testing, the activity of **1a** correlated most strongly (P = 0.727 to 0.602) to a series of quinoxaline 1,4-dioxides. These specific quinoxaline 1,4-dioxides have been shown to produce hydroxyl radicals and cleave DNA under aerobic conditions through redox cycling involving the NADPH/cytochrome P450 reductase system (*24*). Under anaerobic conditions, the one-electron reduction of quinoxaline 1,4-dioxides is accompanied by radical fragmentation to afford stoichiometric hydroxyl radicals (*25*).

In order to gain more insight into the mechanism of action of the dialkynylimidazole **1a**, studies were conducted in the human non-small cell lung cancer cell line A549 (*26*), which is a well characterized standard human alveolar epithelial cell line. A549 cells were incubated with various concentration of **1a** and the extent of apoptosis was determined by flow cytometry (Figure 4.2).

After treating A549 cells with 5 μM of compound **1a** for 24 h, the proportion of apoptotic cells increased to 63 %, 25-times higher than the proportion of apoptotic cells in the absence of **1a**. Even at concentrations as low as 1.25 μM, compound **1a** caused a significant increase in the proportion of apoptotic cells (*27*).

The spectrum of anticancer activity of **3** analyzed by COMPARE correlates with the known DNA cleaving quinoxaline 1,4-dioxides. Agents of a wide variety of mechanistic actions, including DNA-damaging agents, are able to induce apoptosis in A549 cells (*28-30*).

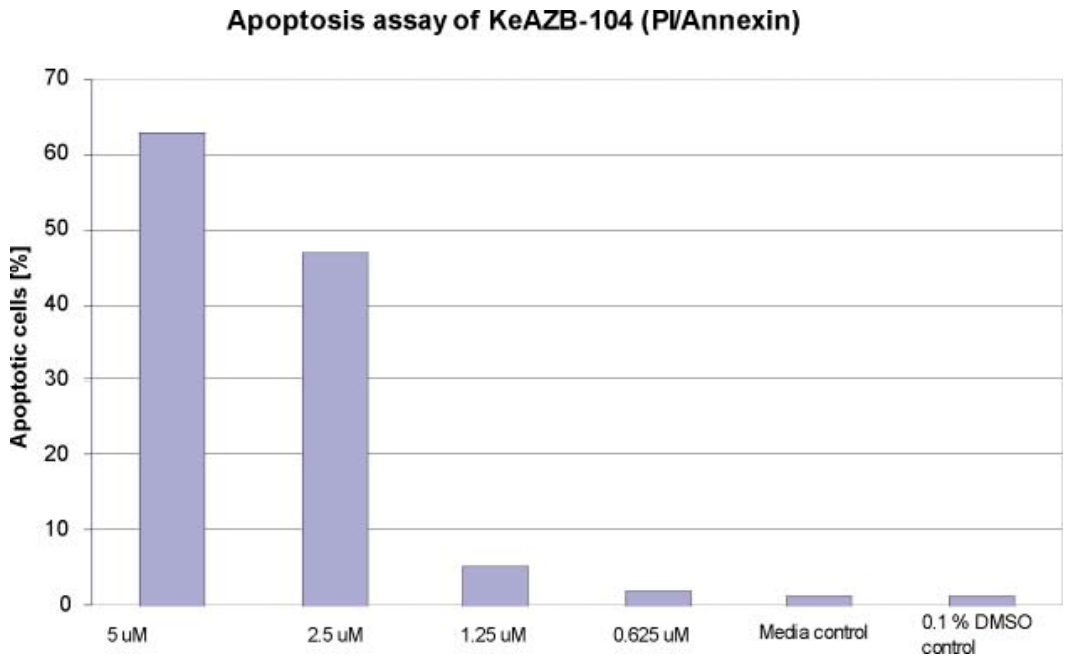

Figure 4.2. Apoptosis of A549 cancer cells in the presence of **1a**.

4.4. CYTOTOXICITY STUDIES OF 1,2-DIALKYNYLIMIDAZOLES AND RELATED *N*-ALKYNYLIMIDAZOLES

As describe above, compound **1a** showed cytotoxic against a range of human cancer cells and induced apoptosis in the human non-small cell lung cancer cell line A549. In order to investigate the effect of 1,2-alkynylimidazole structure on biological activity, the cytotoxicity of the 1,2-dialkynyimidazoles **1a-k** were determined using the AlamarBlue assay against the A549 cell line (*31*) (Table 4.2).

Within the 1,2-dialkynylimidazole series **1a-g**, the cytotoxicity against A549 cells ranges from moderate (IC_{50} ~ 5-6 μM) for **1c,f** to high (IC_{50} = 0.12–0.5 μM) for **1a,d,e**. Both electron-withdrawing (e.g., **1e**) and electron-donating (e.g., **1a**) substituents on the phenyl ring within this series provide highly cytotoxic analogs; however, this is not uniformly the case (e.g., 1f). The 4-substituted analog **1k** is marginally more cytotoxic than the 1- and 2-substuted analogs **1i** and **1c**; however, **1k** is 10-fold less cytotoxic than **1a**.

The aza-Bergman rearrangement of these 1,2-dialkynyliidazoles has been investigated theoretically at the B3LYP/6-31G(d,p) level and experimentally by measuring the kinetics of rearrangement in 1,4-cyclohexadiene by Dr. Christophe Laroche. There is a good correlation between the theoretical and experimental results. However, the cytotoxicity results contrast with the DFT calculations and experimental half-lives for Bergman cyclization. The most cytotoxic analog in this series, the nitrophenyl substituted compound **1e**, has the longest half-life and highest predicted E_a for Bergman cyclization. In contrast, the compound predicted to undergo Bergman cyclization most readily, **1k**, is only moderately cytotoxic. Despite nearly identical half-lives from Bergman cyclization, compounds **1a** and **1b** have IC_{50} values that differ by a factor of five.

The contrast between the predicted facility with which these 1,2-dialkynylimidazoles undergo Bergman cyclization and their cytotoxicity against cancer cells led to a more expansive exploration of the structural basis for cytotoxicity of **1b** (Table 4.3). Within a wider structural range of 1,2-dialkynylimidazoles **1h-p**, there is little variation in cytotoxicity. Hydroxymethyl

(**1j**) methoxymethyl (**1h**) and hydroxyethyl (**1n**) substitutents on the 2-alkynyl group are all well tolerated. Variation of the 4-phenyl substituent of **1k** (e.g., **1m**) or benzannulation (e.g., **1o**) are similarly well tolerated. In addition, within the 4-substituted and benzannulated series, there is little effect in going from a 2-ethynyl substituent (**1m,1o**) to the 2-*p*-methoxyphenethynyl substitutent (**1n,1p**). These results led to a more careful examination of the effect of the 1-alkynyl substituent. Both 2-unsubstituted (**5a**) and 2-substituted (**5b**) 1-phenylethynylimidazoles are only weakly cytotoxic, as is the 1-methyl-2-alkynylimidazole **7.** However, the 1-ethynylimidazole **6b** displays cytotoxicity on par with that of the 1,2-dialkynylimidazoles **1h-p**. As these results implicate the 1-ethynyl group in the cytotoxicity of the 1,2-dialkynylimidazole **1a**, selective modification of this group in **1a** was explored. Interestingly, thiophenol selectively adds to the 1-ethynyl group of **1a** to afford predominantly the (*Z*)-thioenol ether **8** (Scheme 4.1). This modification of the 1-ethynyl group leads to greatly reduced cytotoxicity; the IC_{50} for **8** is 20-fold higher than that of **1a**.

Compound	IC_{50} (μM)[a]	$t_{1/2}$ (h)[b]	E_a (kcal/mol)[c]
1a	0.5 ± 0.2	17 ± 2	29.7[d]
1b	2.5 ± 0.9	16 ± 1	29.7
1c	6 ± 3	*nd*[e]	29.9
1d	0.5 ± 0.1	*nd*	*nd*
1e	0.12 ± 0.02	32 ± 1	30.5
1f	6 ± 4	*nd*	*nd*
1g	2.5 ± 0.9	*nd*	*nd*
1i	5.0 ± 0.3	*nd*	28.9
1k	2.5 ± 0.9	*nd*	25.8

Table 4.2. Comparison of Cytotoxicity, Cyclization Rates, and DFT-Predicted Cyclization Energy of Activation for a series of 1,2-dialkynylimidazoles.

a. A549 cells 72 h.

b. First-order half-life for disappearance of dialkynylimidazole at 110 °C in neat 1,4-cyclohexadiene.

c. Predicted energy of activation ($E_a = \Delta H^{\ddagger} + RT$) for the Bergman-type cyclization at 37 °C from B3LYP/6-31G(d,p) DFT calculations.

d. Experimental E_a at 110 °C is 30.0 kcal/mol, see ref 27.

e. Not determined.

Compound	IC_{50} (μM)
1h	1.0 ± 0.6
1j	1.9 ± 0.7
1l	2.0 ± 1.0
1m	2.6 ± 1.4
1n	2.5 ± 1.0
1o	2.0 ± 1.1
1p	2.9 ± 1.4
5a	9.2 ± 4.5
5b	>15
6b	1.1 ± 0.9
7	>15
8	10.1 ± 2.8

Table 4.3. Cytotoxicity of 1,2-dialkynylimidazoles and related 1- or 2-alkynimidazoles.

4.5. DNA AND PROTEIN CLEAVAGE STUDIES

In order to address the possible role of DNA or protein cleavage activity as a basis for the observed cytotoxicity of 1,2-dialkynylimidazoles, selected compounds were assayed for their ability to effect the cleavage of supercoiled plasmid DNA or BSA. Compounds **1a,e,m** at 100 μM concentrations were incubated with supercoiled ΦX174 plasmid DNA (50 μM base pair) in 50 mM Tris buffer, pH 7.0, at 37 °C for 16 h (Figure 4.3). The resulting DNA products were separated by agarose gel electrophoresis and visualized by ethidium bromide staining. None of these compounds afforded products (relaxed circular or linear duplex) of DNA cleavage.

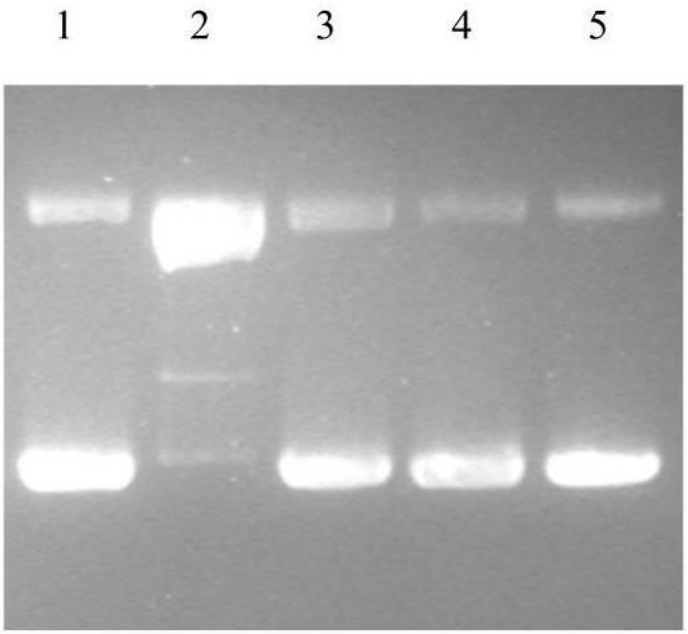

Figure 4.3. Supercoiled DNA cleavage assay. Supercoiled ΦX174 plasmid DNA phage DNA (50 μM base pairs) was incubated alone (lane 1), with 100 μM 1-propargyl-2-(2-(4-methoxyphenyl)ethynyl)pyridinium triflate,(*32*) or with 1,2-dialkynylimidazoles 1m (lane 3), 1e (lane 4), or 1a (lane 5) in 50 mM Tris buffer at pH 7 and 13 % (v/v) DMSO for 16 h at 37 °C and analyzed by gel electrophoresis (1 % agarose, ethidium bromide stain). Only lane 2 shows products of DNA cleavae (94 %).

Compound **1m** (500 μM) was incubated with 25 μM BSA in 50 mM Tris buffer, pH 7 at either 25 °C or 37 °C for 16 h. No higher-mobility bands corresponding to protein cleavage products were observed (Figure 4.4).

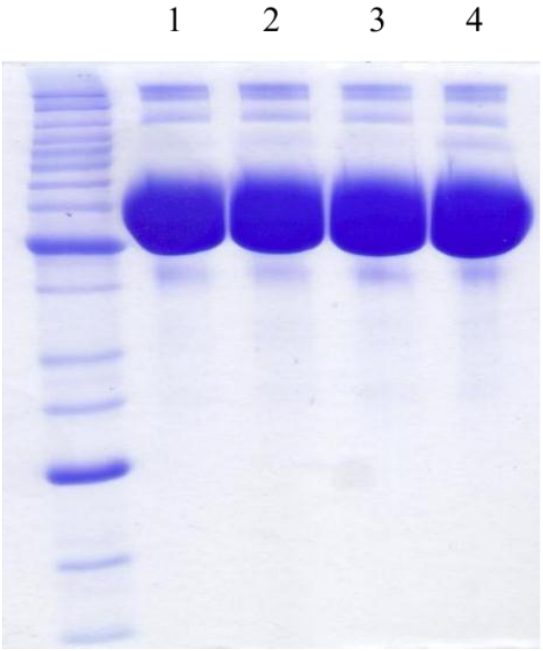

Figure 4.4. Protein cleavage assay. BSA (25 μM) was incubated alone (lane 1, at 25 °C, lane 3, at 37 °C) in 50 mM Tris buffer at pH 7 or with compound **1m** (0.5 mM) (lane 2, at 25 °C, lane 4, at 37 °C) for 16 h at 25 °C or 37 °C and analyzed by 10 % SDS-PAGE. No protein cleavage was detected in lanes 2 or 4 by SDS-PAGE.

4.6. CONCLUSION

In summary, despite the ability of these 1,2-dialkynylimidazoles to undergo Bergman rearrangement to diradical/carbene intermediates under relatively mild conditions, there is no correlation between the rate of Bergman cyclization and cytotoxicity to A459 cells. Even 1,2-diethynylimidazoles such as **1k** that are predicted to undergo cyclization at physiological temperatures are not as cytotoxic as 1,2-dialkynylimidazoles such as **1a** that do not undergo any appreciable cyclization at this temperature. The *p*-nitrophenyl aubstituted 1,2-dialkynylimidazole **1e**, which undergoes cyclization at about one-half the rate of **1a** is four-fold more cytotoxic than **1a**.

There is no evidence that the cytotoxicity of these 1,2-dialkynylimidazoles is due to DNA cleavage or non-specific protein cleavage. Unlike other cytotoxic aza-enediynes that cleave supercoiled DNA at micromolar concentration via a hydrogen atom abstraction from the deoxyribose backbone, dialkynylimidazole **1a,e,m** do not cleave supercoiled DNA, even at 100 μM concentrations. Certain enediynes analogs have been shown to cleave a variety of proteins, and hydrogen abstraction from proteins is a mechanism for self-resistance to naturally occurring enediynes. However, there is no effect of 1,2-dialkynylimidazole **1m** on BSA, even at concentrations over 100-times higher than the IC_{50} for this compound.

These observations rule out a role for an unfacilitated Bergman cyclization in the cytotoxicity of these 1,2-dialkynylimidazoles. However, it is likely that 1,2-dialkynylimidazole with Bergman cyclization barriers even lower than **1k** can be designed by encompassing the dialkynes in 9- or 10-membered rings, and these may function as cytotoxic agents via spontaneous Bergman cyclization. Alternatively, 1,2-dialkynylimidazoles could be designed to undergo cyclization more rapidly when bound to DNA or proteins, leading to the production of diradical or carbene intermediates capable of modifying these binding partners. It is possible that this sort of facilitated cyclization gives rise to the enhanced cytotoxicity of certain 1,2-dialkynylimdiazoles examine here such as **1a**,**d**, and **e**. Finally, just as certain acyclic enediynes have been shown to display potent anticancer effects independent of their Bergman cyclization

potential, the enhanced cytotoxicity of the 1,2-dialkynylimidazoles examined here may not involve aza-Bergman cyclization at all.

An alternative or additional mechanism for the cytotoxicity of these 1,2-dialkynylimidazoles has been revealed from the study of structurally related alkynylimidazoles presented here. Although not as cytotoxic as the 1,2-dialkynylimidazoles **1a**,**d**, and **e**, the *N*-ethynylimidazole **6b** is at least as cytotoxic as the other 1,2-dialkynylimidazoles examined. Interestingly, the *N*-ethynyl group of the 1,2-dialkynylimidazole **1a** was found to react selectively with thiophenol, and this addition abrogates the cytotoxicity of this compound. This unexpected electrophilic nature of the imidazole *N*-ethynyl group bears further study, as it stands in contrast with the established role of related *N*-alkynyl heterocycles and *N*-alkynylamides as electron-rich, nucleophilic species. In light of this reactivity and the lack of DNA cleavage ability, the 1,2-dialkynylimidazoles and 1-alkynylimidazoles may have more in common with other heterocyclic, thiol-reactive anticancer agents than the enediyne natural products or recently reported DNA-cleaving cytotoxic lysine-acetylene conjugates. Interestingly, certain 1,2-dialkynylimidazoles such as 1a and 1e are notably more cytotoxic against A549 cells than thiol-reactive heterocycles currently in clinical trials. Thus, the potential of N-ethynylimidazoles to react with biological thiols deserves further investigation, and studies exploring this possibility are ongoing.

4.7. EXPERIMENTAL SECTION

General: All reactions were carried out under argon in oven-dried glassware with magnetic stirring. Unless otherwise noted, all materials were obtained from commercial suppliers and were used without further purification. THF was distilled from sodium/benzophenone prior to use. Flash chromatography was performed with EM Reagent silica gel (230–400 mesh) using the mobile phase indicated. Melting points (open capillary) are uncorrected. Unless otherwise noted, ^{1}H and ^{13}C NMR spectra were determined in $CDCl_3$ on a spectrometer operating at 400 and 100 MHz, respectively, and are reported in ppm using solvent as internal standard (7.26 ppm for ^{1}H and 77.0 ppm for ^{13}C in $CDCl_3$). Mass spectra were obtained in the positive mode either by chemical ionization using methane as the ionizing gas or by electrospray ionization. The purity of all test compounds was determined to by >95% by HPLC.

Typical procedure for the synthesis of 1,2-dialkynylimidazoles:

1-ethynyl-2-(2-(4-methoxyphenyl)-ethynyl)-1*H*-benzimidazole (**1p**): To a solution of 2-iodo-1-(2-triisopropylsilylethynyl)-1*H*-benzimidazole 4g (212 mg, 0.5 mmol) in Et_3N (10 mL) under argon was added 4-ethynylanisole (0.075 mL, 0.55 mmol), $Pd(PPh_3)_4$ (30 mg, 0.026 mmol) and CuI (10 mg, 0.05 mmol). The reaction mixture was stirred at 50 °C until complete consumption of 4 g. The solvent was removed under reduce pressure and the residue was purified by flash chromatography (0-5 % EtOAc/hexane) to afford 210 mg (98 %) of the TIPS-protected compound as a yellow crystalline solid. To this material in THF (10 mL) at -78 °C was added TBAF (0.5 mL of 1 M solution in THF, 0.5 mmol) and the mixture was stirred at -78 °C until completion. The reaction mixture was quenched at -78 °C with 10 mL of water and extracted with CH_2Cl_2 (3×25 mL). The organic layers were combined, dried over Na_2SO_4 and the solvent was evaporated under reduced pressure. The residue was purified by flash chromatography (0-20 % EtOAc/hexane) to afford 122 mg (92 %) of compound **1p** as a white solid: mp 140.1-141.3 °C; ^{1}HNMR(400MHz, $CDCl_3$) δ 7.75 (d, *J* = 7.4 Hz, 1H), 7.58 (d, *J* = 7.4 Hz, 1H), 7.50 (d, *J* = 8.8 Hz, 2H), 7.37 (p, *J* = 7.6 Hz, 2H), 6.89 (d, *J* = 8.8 Hz, 2H), 3.81 (s, 3H), 3.46 (s, 1H). ^{13}C NMR (100 MHz, $CDCl_3$) δ 160.9, 141.7, 138.8, 134.6, 134.0, 125.2, 124.6, 120.4, 114.2, 112.5, 110.7, 96.6, 79.9, 69.7, 64.4, 55.3. MS *m/z*: HRMS calc for $C_{18}H_{13}N_2O$ (M^+) 273.1028, found 273.1028. Anal. Calcd. for $C_{18}H_{12}N_2O$: C,79.39; H, 4.44; N, 10.20. Found: C, 79.35; H, 4.27; N, 10.18.

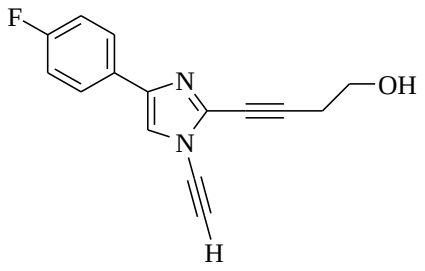

4-(4-Fluorophenyl)-1-ethynyl-2-ethynyl-1H-imidazole (1m):

Following the general procedure described above (flash chromatography; 0-20 % EtOAc/hexane), we obtained 7.8 mg of **1m** (82 % overall yield) as an off-white solid: mp 89.7-91.5 C; ^{1}H NMR (400 MHz, $CDCl_3$) δ 7.75-7.72 (2H, m), 7.34 (1H, s), 7.10-7.06 (2H, m), 3.44 (1H, s), 3.24 (1H, s). ^{13}C NMR (100 MHz, $CDCl_3$) δ 162.6 (d, J = 246 Hz), 141.2, 134.4, 128.1 (d, J = 2.9 Hz), 127.1 (2C, d, J = 8.2 Hz), 117.2, 115.7 (2C, d, J = 21.6 Hz), 82.7, 71.5, 70.4, 62.3; MS *m/z*: HRMS (CI) calc for $C_{13}H_8N_2F$ (M^+) 211.0672; found, 211.0668.

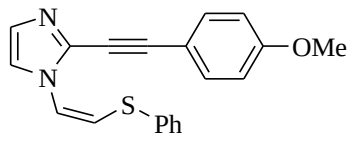

(Z)-2-(4-Methoxyphenyl)ethynyl-1-(2-(phenylthiol)vinyl)-1H-imidazole (8):

To a solution of 1a (20 mg, 0.09 mmol) in THF (2 mL) was added thiophenol (0.1 mmol, 0.01 mL). The reaction mixture was stirred at room temperature for 5 days. The reaction mixture was concentrated, and the residue was purified by flash chromatography (30% EtOAc/hexane) to afford **8** as a brown thick oil (13 mg, 43% yield). 1HNMR(400 MHz, CDCl3) δ 7.71 (1H, s), 7.53-7.50 (2H, m), 7.47-7.44 (2H, m), 7.39-7.35 (2H, m), 7.33-7.29 (1H, m), 7.20 (1H, d, *J* = 8.4 Hz), 6.91-6.88 (2H, m), 6.17 (2H, d, *J* = 8.4 Hz), 3.83 (3H, s).^{13}C NMR (100 MHz, $CDCl_3$) δ 160.4, 134.3, 133.4 (2C), 132.6, 130.1 (2C), 129.4 (2C), 127.7, 121.1, 119.1, 115.5, 114.1 (2C), 113.5, 99.2, 77.2, 55.3; MS *m/z*: HRMS (CI) calc for $C_{20}H_{17}N_2OS$ (M^+) 333.1062; found, 333.1063.

FACS analysis:

A549 Cells (2.0 x 10^5 cells) were plated in a 12-well plate in a final volume of 1 ml/well of F-12K with L-glutamine medium. After 24 h incubation at 37 °C in an atmosphere of 5 % CO2, cells were treated with 1 µl of compound **1a** (5 µM, 2.5 µM, 1.25 µM and 0.625 µM). After 24 h, cells were rinsed with PBS and trypsinized. The cells were pelleted at 400 x g for 4 min, washed with annexin binding buffer (ABB), and pelleted again at 400 x g for 4 min. The media was aspirated and the cells were resuspended in ABB and stained with annexin V-FITC (5 µg/mL) for 8 min at room temperature. Propidium iodide (2 µg/mL) was added to the cell suspension. The cells were analyzed with Beckman Coulter flow cytometer.

Supercoiled plasmid DNA cleavage assay:

The DNA cleavage efficiency was determined by incubation of 3 with solutions of supercoiled ΦX174 plasmid DNA (50 μM base pairs) in 50 mM N,N,N-tris(hydroxymethyl)aminomethane (Tris) buffer at pH 7. The reaction mixtures containing 100 μM test compound, 100 μM 1-propargyl-2-(2-(4-methoxyphenyl)ethynyl)pyridinium triflate1 as positive control, or vehicle (13% (v/v) DMSO) were incubated for 16 h at 37 °C. DNA products were separated by agarose gel electrophoresis [1 × Tris-borate-N,N,N',N'-ethylenediaminetetraacetic acid (EDTA) (TBE) at 90 V for 1 h], stained with ethidium bromide (0.25 μg/mL), and the images were analyzed using a fluorimager with ImageQuant software. The degree of cleavage of Form I DNA was determined using equation 2.

$$\text{Percent cleavage} = \frac{(2X[\text{Form III}]+[\text{Form II}]}{(2X[\text{Form III}]+[\text{Form II}]+[\text{Form I}]} X100 \qquad \text{(eq 1)}$$

The reported, normalized percent cleavage accounts for cleavage in control samples under the reaction conditions employed and this was calculated according to equation 3.

Where Form II refers to relaxed, circular DNA, Form III is linear, duplex DNA. The reported, normalized percent cleavage accounts for cleavage in control samples under the reaction conditions employed and this was calculated according to equation 3.

$$\text{Normalized percent cleavage} = \frac{\%\text{ cleavage (drug)}-\%\text{ cleavage (control)}}{100-\%\text{ cleavage control}} \qquad \text{(eq 2)}$$

Protein Cleavage Assay:

Bovine serum albumin (25 μM, Fisher Bioreagent) was incubated alone or with 0.5 mM of 1,2-dialkynylimidazole **1m** in 50 mM Tris buffer at pH 7 at 25 °C or 37 °C for 16 h. The protein samples were analyzed by 10 % SDS-PAGE and stained with Coomassie Blue.

Alamar Blue Assay:

Cell viability was determined using the AlamarBlue reagent (AbD Serotec). This reagent can be used to easily detect changes in cell proliferation based on the ability of viable cells to cause AlamarBlue to change from its oxidized (non-fluorescent) to a reduced(fluorescent) form. Cell culture cytotoxicity assays were carried out as described by Kumar et al.(*31*) Aliquots of 100 μl cell suspension (1-3x10^3 cells) were placed in microtiter plates in an atmosphere of 5% CO_2 at 37 °C. After 24 h, 100 μL of culture media and 2 μl of the compound in DMSO were added to each well in duplicate, and the plates incubated an additional 24 or 72 h at 37 °C. There was no effect on the growth of cells compared to that of cells in culture media alone at this DMSO concentration. Compounds, along with Mitomycin-C (MP Biomedicals) as a positive control were evaluated at final concentrations ranging from 0.001 to 50 μM. After 72 h incubation, the culture media was removed from each well, and 200 μL of fresh media and 20 μL of AlamarBlue reagent were added, followed by additional 6 h incubation. Cell viability was detected by fluorescence intensity using a Beckman Coulter DTX880 plate reader with excitation at 530 nm and emission at 590 nm. The fluorescence data obtained from the cytotoxicity studies was used to calculate the percent growth according to the following equation:

% Growth = 100*(MeanFtest – Mean Ftime0)/ (MeanFctrl – Mean Ftime0) (eq 3)

Where:

Mean Ftime0 = the averaged measured fluorescence intensities of AlamarBlue reagent at the time just before the exposure of the cells to the test substance.

Mean Ftest = the averaged measured fluorescence intensities of AlamarBlue reagent after 72 h exposure of the cells to the test substance at a particular concentration.

Mean Fcrtl = the averaged measured fluorescence intensities of AlamarBlue reagent after 72 h exposure of the cells to the vehicle without the test substance.

The IC_{50} (50 % Inhibition Concentration) is defined as the test compound concentration where the increase from time0 in the number of mass of treated cells was only 50 % as much as the corresponding increase in the vehicle-control at the end of the experiment. The IC_{50} values of 1,2-dialkynylimidazole and related *N*-alkynylimidazole analogs were determined by non-linear regression using the program Grafit and fitting the data to the following equation:

$y = Min + (Max-Min)/(1+10^{((x-\log IC_{50})*Hill\ slope)})$ (eq 4)

Where:

Min= the minimum response plateau (0 % Growth)

Max= the maximum response plateau (100 % Growth)

y= % Growth at each test compound concentration

4.8. REFERENCES

1. Lee, M. D., Manning, J. K., Williams, D. R., Kuck, N. A., Testa, R. T., and Borders, D. B. (1989) Calicheamicins, a Novel Family of Antitumor Antibiotics .3. Isolation, Purification and Characterization of Calicheamicin-Beta-1br, Calicheamicin-Gamma-1br, Calicheamicin-Alpha-2i, Calicheamicin-Alpha-3i, Calicheamicin-Beta-1i, Calicheamicin-Gamma-1i and Calicheamicin-Delta-1i, *J Antibiot 42*, 1070-1087.
2. Golik, J., Dubay, G., Groenewold, G., Kawaguchi, H., Konishi, M., Krishnan, B., Ohkuma, H., Saitoh, K., and Doyle, T. W. (1987) Esperamicins, a Novel Class of Potent Antitumor Antibiotics. 3. Structures of Esperamicins-A1, Esperamicin-A2, and Esperamicin-A1b, *J Am Chem Soc 109*, 3462-3464.
3. Konishi, M., Ohkuma, H., Matsumoto, K., Tsuno, T., Kamei, H., Miyaki, T., Oki, T., Kawaguchi, H., Vanduyne, G. D., and Clardy, J. (1989) Dynemicin a, a Novel Antibiotic with the Anthraquinone and 1,5-Diyn-3-Ene Subunit, *J Antibiot 42*, 1449-1452.
4. Kerwin, S. M. *in Radical and Radical Ion Reactivity in Nucleic Acid Chemistry, Greenberg, M. (Ed) Wieley: New York*, 389-419.
5. Rawat, D. S., and Zaleski, J. M. (2004) Geometric and electronic control of thermal bergman cyclization, *Synlett*, 393-421.
6. Basak, A., Mandal, S., and Bag, S. S. (2003) Chelation-controlled Bergman cyclization: Synthesis and reactivity of enediynyl ligands, *Chem Rev 103*, 4077-4094.
7. Klein, M., Walenzyk, T., and Konig, B. (2004) Electronic effects on the Bergman cyclisation of enediynes. A review, *Collect Czech Chem C 69*, 945-965.
8. Polukhtine, A., Karpov, G., and Popik, V. V. (2008) Towards photoswitchable enediyne antibiotics: single and two-photon triggering of bergman cyclization, *Curr Top Med Chem 8*, 460-469.
9. Sherer, E. C., Kirschner, K. N., Pickard, F. C., Rein, C., Feldgus, S., and Shields, G. C. (2008) Efficient and Accurate Characterization of the Bergman Cyclization for Several Enediynes Including an Expanded Substructure of Esperamicin A(1), *J Phys Chem B 112*, 16917-16934.
10. Kraka, E., Tuttle, T., and Cremer, D. (2008) Design of a new warhead for the natural enediyne dynemicin A. An increase of biological activity, *J Phys Chem B 112*, 2661-2670.
11. Brzostowska, E. M., Hoffmann, R., and Parish, C. A. (2007) Tuning the bergman cyclization by introduction of metal fragments at various positions of the enediyne. Metalla-Bergman cyclizations, *J Am Chem Soc 129*, 4401-4409.
12. Schreiner, P. R. (1998) Monocyclic enediynes: Relationships between ring sizes, alkyne carbon distances, cyclization barriers, and hydrogen abstraction reactions. Singlet-triplet separations of methyl-substituted p-benzynes, *J Am Chem Soc 120*, 4184-4190.
13. Baroudi, A., Mauldin, J., and Alabugin, I. V. (2010) Conformationally Gated Fragmentations and Rearrangements Promoted by Interception of the Bergman

Cyclization through Intramolecular H-Abstraction: A Possible Mechanism of Auto-Resistance to Natural Enediyne Antibiotics?, *J Am Chem Soc 132*, 967-979.

14. Lo, Y. H., Lin, C. C., Lin, C. F., Lin, Y. T., Duh, T. H., Hong, Y. R., Yang, S. H., Lin, S. R., Yang, S. C., Chang, L. S., and Wu, M. J. (2008) 2-(6-aryl-3(Z)-hexen-1,5-diynyl)anilines as a new class of potent antitubulin agents, *J Med Chem 51*, 2682-2688.

15. Lo, Y. H., Lin, I. L., Lin, C. F., Hsu, C. C., Yang, S. H., Lin, S. R., and Wu, M. J. (2007) Novel acyclic enediynes inhibit Cyclin A and Cdc25C expression and induce apoptosis phenomenon to show potent antitumor proliferation, *Bioorgan Med Chem 15*, 4528-4536.

16. Lin, C. F., Hsieh, P. C., Lu, W. D., Chiu, H. F., and Wu, M. J. (2001) A series of enediynes as novel inhibitors of topoisomerase I, *Bioorgan Med Chem 9*, 1707-1711.

17. Nadipuram, A. K., David, W. M., Kumar, D., and Kerwin, S. M. (2002) Synthesis and thermolysis of heterocyclic 3-aza-3-ene-1,5-diynes(1), *Org Lett 4*, 4543-4546.

18. Kerwin, S. M., and Nadipuram, A. (2004) 5H-cyclopentapyrazines from 1,2-dialkynylimidazoles, *Synlett*, 1404-1408.

19. Nadipuram, A. K., and Kerwin, S. M. (2006) Thermal cyclization of 1,2-dialkynylimidazoles to imidazo[1,2-a]pyridines, *Tetrahedron 62*, 3798-3808.

20. Nadipuram, A. K., and Kerwin, S. M. (2006) Intra- and intermolecular trapping of cyclopentapyrazine carbenes derived from 1,2-dialkynylimidazoles, *Tetrahedron Lett 47*, 353-356.

21. Laroche, C., Li, J., Freyer, M. W., and Kerwin, S. M. (2008) Coupling reactions of bromoalkynes with imidazoles mediated by copper salts: Synthesis of novel N-alkynylimidazoles, *J Org Chem 73*, 6462-6465.

22. Alley, M. C., Scudiero, D. A., Monks, A., Hursey, M. L., Czerwinski, M. J., Fine, D. L., Abbott, B. J., Mayo, J. G., Shoemaker, R. H., and Boyd, M. R. (1988) Feasibility of drug screening with panels of human tumor cell lines using a microculture tetrazolium assay, *Cancer Res 48*, 589-601.

23. Paull, K. D., Shoemaker, R. H., Hodes, L., Monks, A., Scudiero, D. A., Rubinstein, L., Plowman, J., and Boyd, M. R. (1989) Display and analysis of patterns of differential activity of drugs against human tumor cell lines: development of mean graph and COMPARE algorithm, *J Natl Cancer Inst 81*, 1088-1092.

24. Solano, B., Junnotula, V., Marin, A., Villar, R., Burguete, A., Vicente, E., Perez-Silanes, S., Aldana, I., Monge, A., Dutta, S., Sarkar, U., and Gates, K. S. (2007) Synthesis and biological evaluation of new 2-arylcarbonyl-3-trifluoromethylquinoxaline 1,4-di-N-oxide derivatives and their reduced analogues, *J Med Chem 50*, 5485-5492.

25. Ganley, B., Chowdhury, G., Bhansali, J., Daniels, J. S., and Gates, K. S. (2001) Redox-activated, hypoxia-selective DNA cleavage by quinoxaline 1,4-di-N-oxide, *Bioorg Med Chem 9*, 2395-2401.

26. Giard, D. J., Aaronson, S. A., Todaro, G. J., Arnstein, P., Kersey, J. H., Dosik, H., and Parks, W. P. (1973) In vitro cultivation of human tumors: establishment of cell lines derived from a series of solid tumors, *J Natl Cancer Inst 51*, 1417-1423.

27. Laroche, C., Li, J., Gonzales, C., David, W. M., and Kerwin, S. M. (2010) Cyclization kinetics and biological evaluation of an anticancer 1,2-dialkynylimidazole, *Org Biomol Chem 8*, 1535-1539.

28. Erdelyi, K., Bai, P., Kovacs, I., Szabo, E., Mocsar, G., Kakuk, A., Szabo, C., Gergely, P., and Virag, L. (2009) Dual role of poly(ADP-ribose) glycohydrolase in the regulation of cell death in oxidatively stressed A549 cells, *FASEB J 23*, 3553-3563.

29. Zhu, H., and Gooderham, N. J. (2006) Mechanisms of induction of cell cycle arrest and cell death by cryptolepine in human lung adenocarcinoma a549 cells, *Toxicol Sci 91*, 132-139.

30. Ren, J., Agata, N., Chen, D., Li, Y., Yu, W. H., Huang, L., Raina, D., Chen, W., Kharbanda, S., and Kufe, D. (2004) Human MUC1 carcinoma-associated protein confers resistance to genotoxic anticancer agents, *Cancer Cell 5*, 163-175.

31. Kumar, D., Jacob, M. R., Reynolds, M. B., and Kerwin, S. M. (2002) Synthesis and evaluation of anticancer benzoxazoles and benzimidazoles related to UK-1, *Bioorg Med Chem 10*, 3997-4004.

32. Tuesuwan, B., and Kerwin, S. M. (2006) 2-Alkynyl-N-propargyl pyridinium salts: pyridinium-based heterocyclic skipped aza-enediynes that cleave DNA by deoxyribosyl hydrogen-atom abstraction and guanine oxidation, *Biochemistry 45*, 7265-7276.

Appendix A

^{1}H and ^{13}C NMR Spectra

```
Archive directory:
Sample directory:
 expl  Proton
Pulse Sequence: s2pul
      SAMPLE                    SPECIAL
 date    May 18 2007  temp            27.0
 solvent       cdcl3  gain        not used
 file /export/home/~  spin             20
 space/data/kerwin_~  hst           0.008
 HJL051807a_s2pul_N~  pw90         13.900
              1.fid   alfa         6.600
    ACQUISITION              FLAGS
 sw           6410.3  il                n
 at            4.049  in                n
 np            51906  dp                y
 fb             4000  hs               nn
 bs               32      PROCESSING
 ss                2  lb             0.10
 d1            2.000  fn            65536
 nt               64        DISPLAY
 ct               64  sp           -198.8
    TRANSMITTER      wp           4197.5
 tn               H1  rf1          3707.7
 sfrq        399.807  rfp          2894.6
 tof           399.5  rp             51.3
 tpwr             61  lp           -14.6
 pw            4.633        PLOT
     DECOUPLER        wc              250
 dn              C13  sc                0
 dof               0  vs               76
 dm              nnn  th                4
 dmm               c  al  cdc  ph
 dpwr             35
 dmf           25412
```

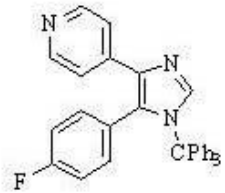

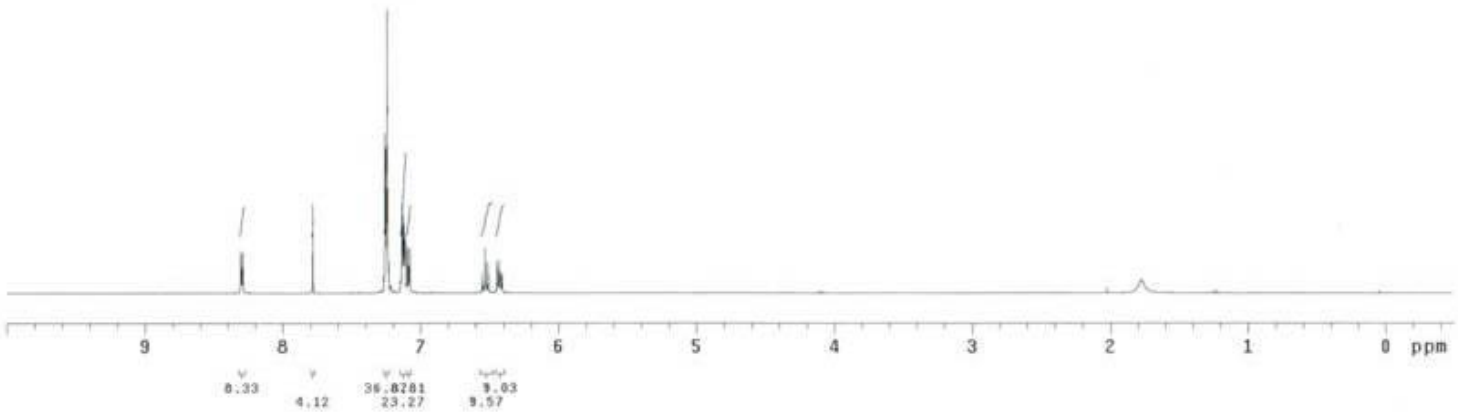

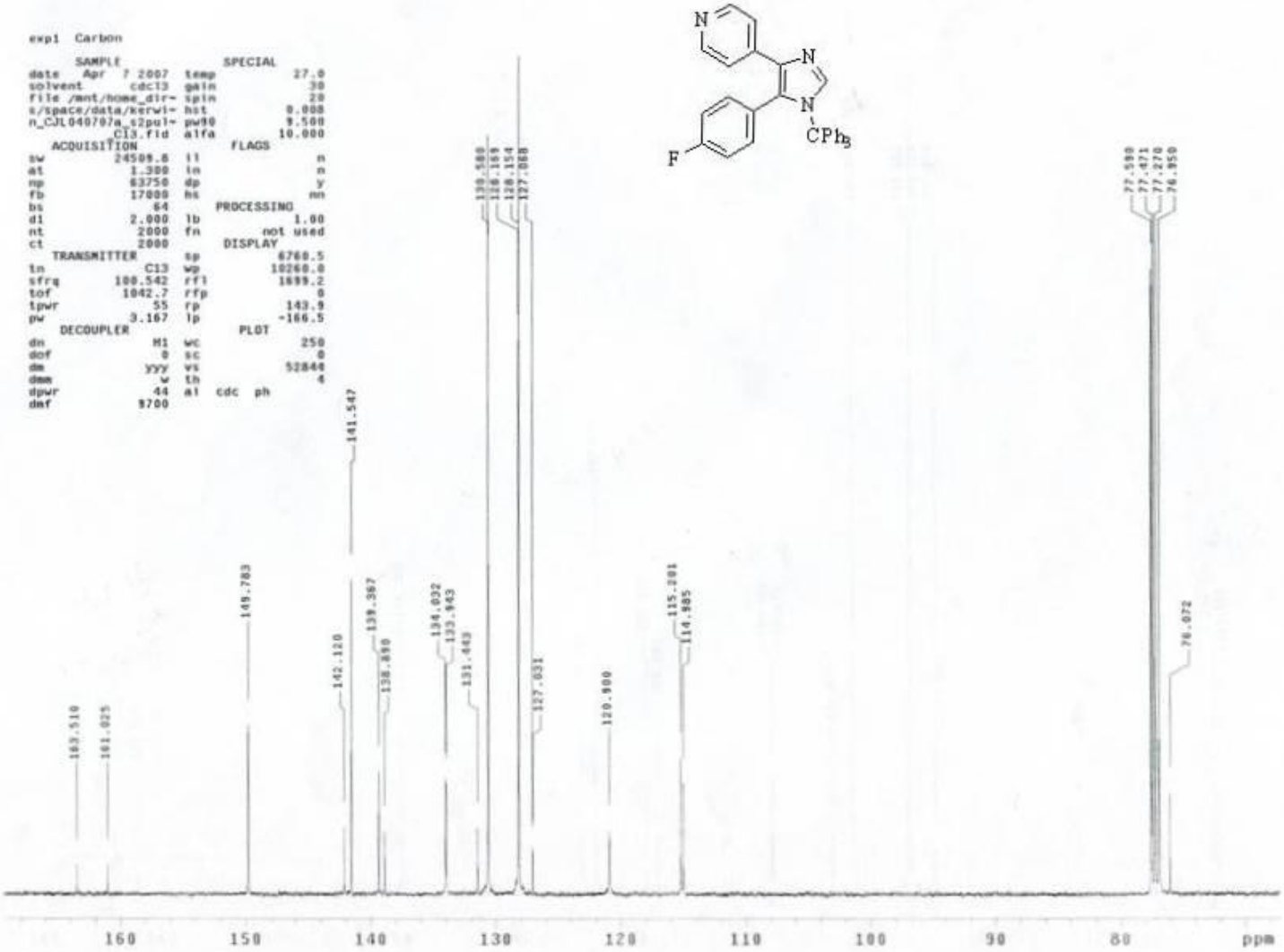
exp1 Carbon
SAMPLE
date Apr 7 2007
solvent cdcl3
file /mnt/home_dir~
s/space/data/kerwi~
n_CJL040707a_s2pul~
C13.fid
ACQUISITION
sw 24509.6
at 1.300
np 63750
fb 17000
bs 64
d1 2.000
nt 2000
ct 2000
TRANSMITTER
tn C13
sfrq 100.542
tof 1042.7
tpwr 55
pw 3.167
DECOUPLER
dn H1
dof 0
dm yyy
dmm w
dpwr 44
dmf 9700
SPECIAL
temp 27.0
gain 30
spin 20
hst 0.008
pw90 9.500
alfa 10.000
FLAGS
il n
in n
dp y
hs nn
PROCESSING
lb 1.00
fn not used
DISPLAY
sp 6760.5
wp 10260.0
rf1 1899.2
rfp 0
rp 143.9
lp -166.5
PLOT
wc 250
sc 0
vs 52844
th 4
al cdc ph
N
N
N
CPh3
F
163.510
161.025
149.783
142.120
141.547
139.367
138.890
134.032
133.943
131.443
130.589
128.189
128.154
127.888
127.031
120.900
115.281
114.985
77.580
77.471
77.270
76.959
76.072
160
150
140
130
120
110
100
90
80
ppm

JL-01-77

exp8 NOESY

SAMPLE		FLAGS	
date	Apr 5 2007	hs	n
solvent	DMSO	vspul	n
sample	undefined	PFGflg	n
ACQUISITION		hsglvl	2000
sw	4629.6	SPECIAL	
at	0.221	temp	27.0
np	2048	gain	40
fb	3000	spin	0
ss	8	F2 PROCESSING	
d1	2.000	gf	0.102
nt	16	gfs	not used
2D ACQUISITION		fn	2048
sw1	4629.6	F1 PROCESSING	
ni	200	gf1	0.040
TRANSMITTER		gfs1	not used
tn	H1	proc1	1p
sfrq	499.352	fn1	2048
tof	114.4	DISPLAY	
tpwr	54	sp	293.6
pw	10.250	wp	4625.1
NOESY		sp1	293.6
mix	0.800	wp1	4625.1
PRESATURATION		rf1	-289.1
satmode	nnnn	rfp	0
satpwr	0	rf11	-289.1
satdly	0	rfp1	0
satfrq	0	PLOT	
DECOUPLER		wc	115.8
dn	H1	sc	10.0
dm	nnn	wc2	115.8
		sc2	0
		vs	702
		th	1
		al ph	

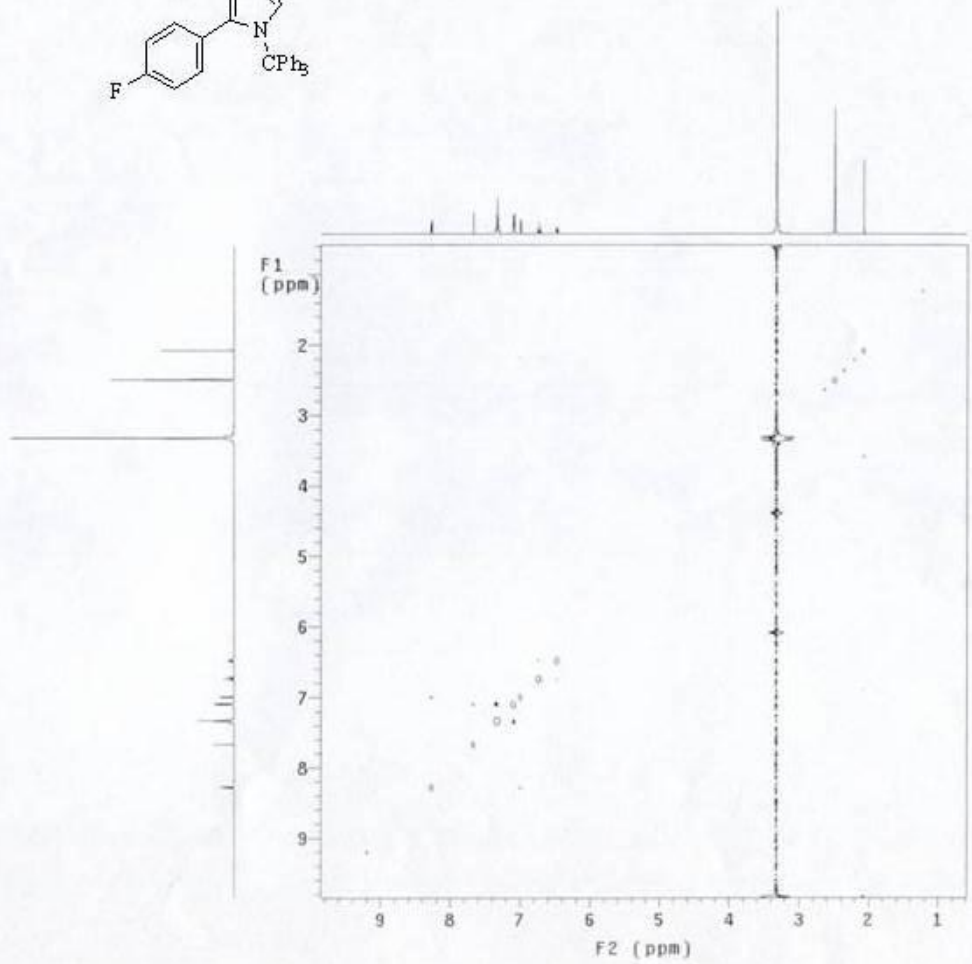

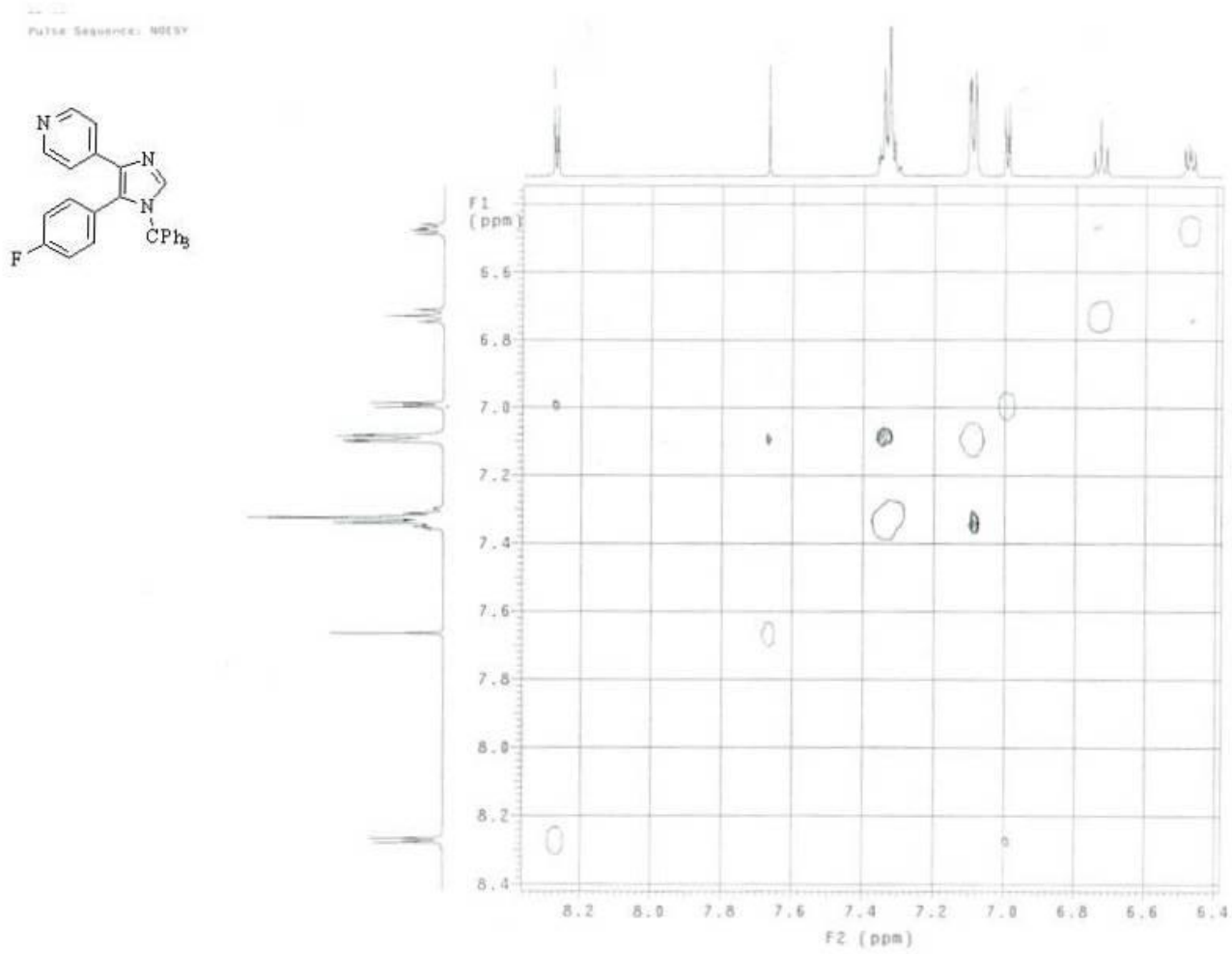
Pulse Sequence: NOESY
N
N
N
CPh3
F
F1 (ppm)
6.6
6.8
7.0
7.2
7.4
7.6
7.8
8.0
8.2
8.4
8.2
8.0
7.8
7.6
7.4
7.2
7.0
6.8
6.6
6.4
F2 (ppm)

JL-01-77

exp3 gCOSY

SAMPLE		FLAGS	
date	Apr 5 2007	hs	nn
solvent	DMSO	sspul	n
sample	undefined	hsglvl	19000
ACQUISITION		SPECIAL	
sw	4629.6	temp	27.0
at	0.221	gain	40
np	2048	spin	0
fb	3000	F2 PROCESSING	
ss	4	sb	-0.111
d1	2.000	sbs	not used
nt	2	fn	2048
2D ACQUISITION		F1 PROCESSING	
sw1	4629.6	sb1	-0.111
ni	512	sbs1	not used
TRANSMITTER		proc1	3p
tn	H1	fn1	2048
sfrq	499.352	DISPLAY	
tof	114.4	sp	293.6
tpwr	54	wp	4625.1
pw	10.250	sp1	293.6
GRADIENTS		wp1	4625.1
gzlvl1	18000	rf1	-289.1
gt1	0.001000	rfp	0
gstab	0.000500	rfl1	-289.1
DECOUPLER		rfp1	0
dn	H1	PLOT	
dm	nnn	wc	115.8
		sc	10.0
		wc2	115.8
		sc2	0
		vs	2177
		th	2
		al cdc av	

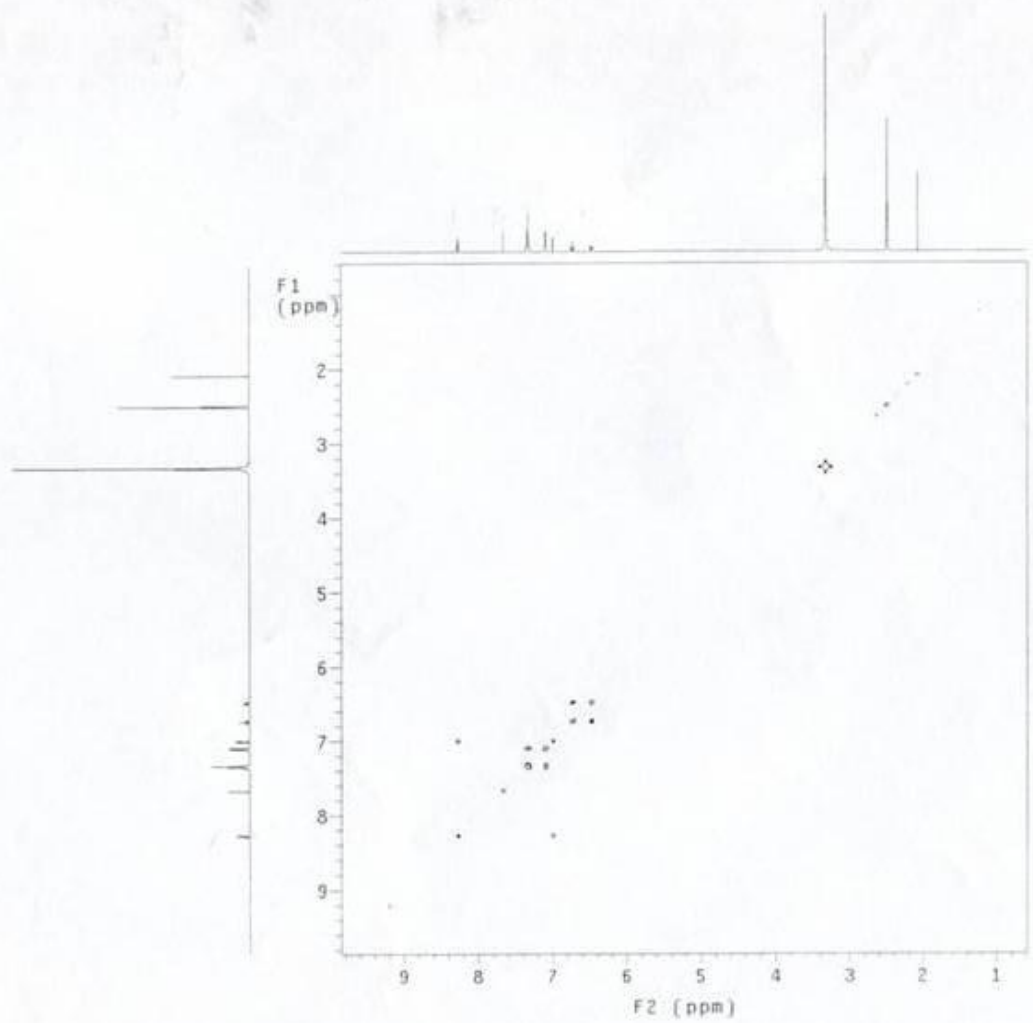

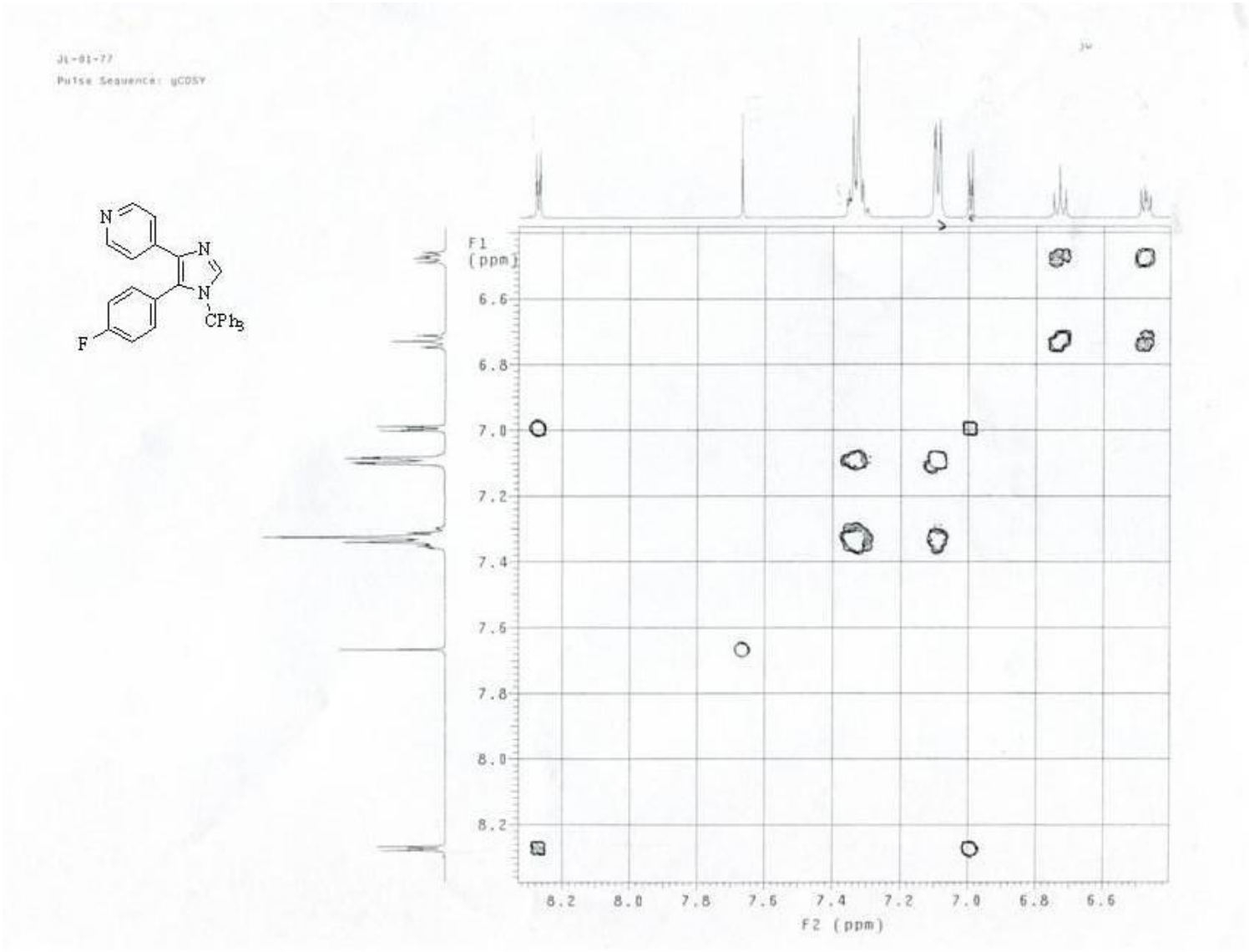
JL-01-77
Pulse Sequence: gCOSY
N
N
N
CPh3
F
F1 (ppm)
6.6
6.8
7.0
7.2
7.4
7.6
7.8
8.0
8.2
8.2
8.0
7.8
7.6
7.4
7.2
7.0
6.8
6.6
F2 (ppm)

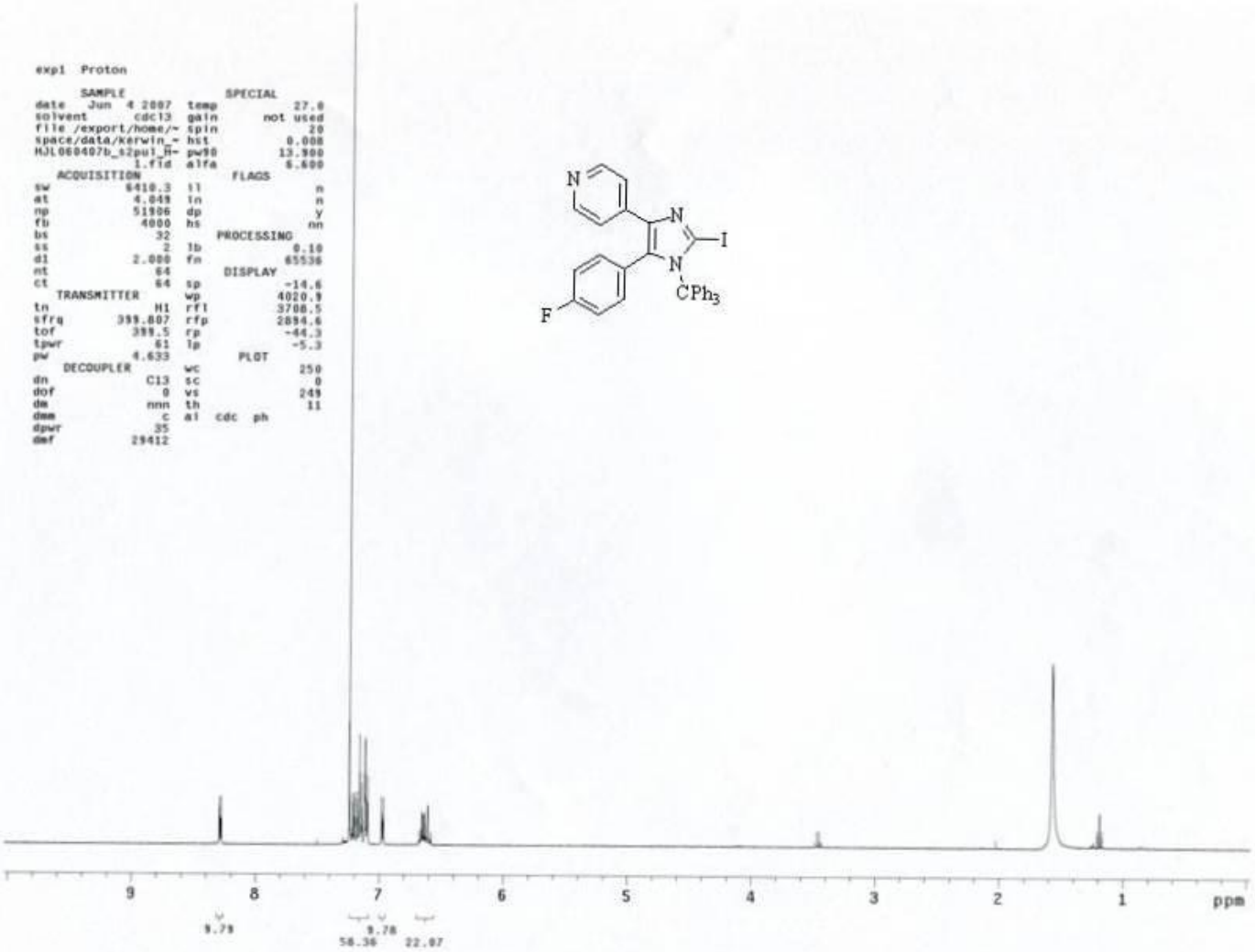
exp1 Proton
SAMPLE
date Jun 4 2007
solvent cdcl3
file /export/home/~
space/data/kerwin_~
HJL060407b_s2pul_H~
1.fid
ACQUISITION
sw 6410.3
at 4.049
np 51906
fb 4000
bs 32
ss 2
d1 2.000
nt 64
ct 64
TRANSMITTER
tn H1
sfrq 399.807
tof 399.5
tpwr 61
pw 4.633
DECOUPLER
dn C13
dof 0
dm nnn
dmm c
dpwr 35
dmf 29412
SPECIAL
temp 27.0
gain not used
spin 20
hst 0.008
pw90 13.900
alfa 6.600
FLAGS
il n
in n
dp y
hs nn
PROCESSING
lb 0.10
fn 65536
DISPLAY
sp -14.6
wp 4020.9
rf1 3708.5
rfp 2894.6
rp -44.3
lp -5.3
PLOT
wc 250
sc 0
vs 249
th 11
al cdc ph
N
N
I
N
CPh3
F
9
8
7
6
5
4
3
2
1
ppm
9.79
9.78
58.36
22.07

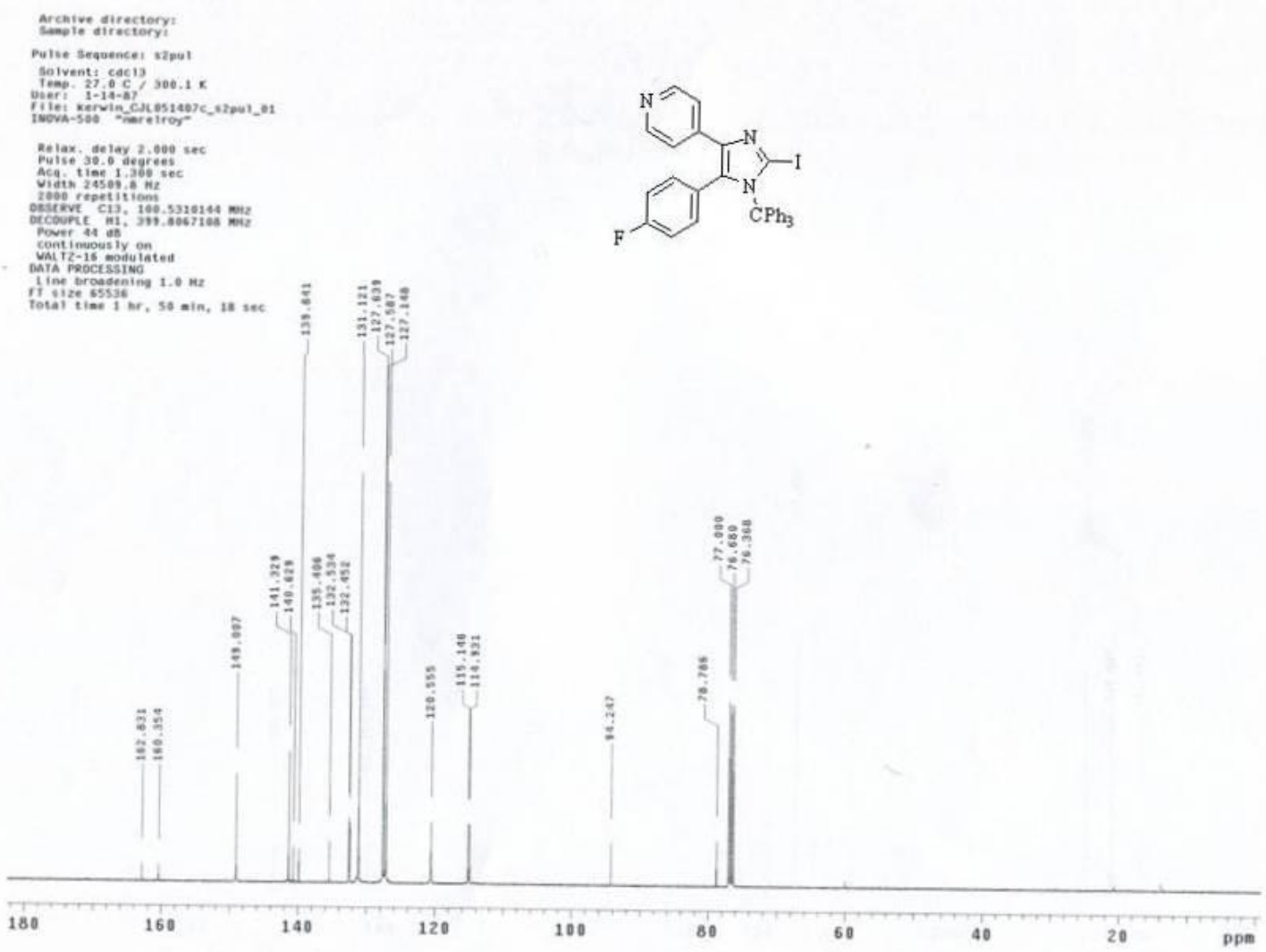
Archive directory:
Sample directory:
Pulse Sequence: s2pul
Solvent: cdcl3
Temp. 27.0 C / 300.1 K
User: 1-14-87
File: kerwin_CJL051407c_s2pul_01
INOVA-500 "nmrelroy"
Relax. delay 2.000 sec
Pulse 30.0 degrees
Acq. time 1.300 sec
Width 24509.8 Hz
2000 repetitions
OBSERVE C13, 100.5310144 MHz
DECOUPLE H1, 399.8067108 MHz
Power 44 dB
continuously on
WALTZ-16 modulated
DATA PROCESSING
Line broadening 1.0 Hz
FT size 65536
Total time 1 hr, 50 min, 18 sec
N
N
I
N
CPh3
F
162.831
160.354
149.007
141.329
140.629
139.841
135.406
132.534
132.452
131.121
127.639
127.507
127.148
120.555
115.148
114.931
94.247
79.786
77.000
76.680
76.360
180
160
140
120
100
80
60
40
20
ppm

exp1 Proton

SAMPLE		SPECIAL	
date	Jun 1 2007	temp	27.0
solvent	dmso	gain	not used
file	/export/home/~	spin	20
space	/data/kerwin_~	hst	0.008
	HJL060107a_s2pul_H~	pw90	13.900
	1.fid	alfa	6.600
ACQUISITION		FLAGS	
sw	4807.7	il	n
at	4.049	in	n
np	38930	dp	y
fb	4000	hs	nn
bs	32	PROCESSING	
ss	2	lb	0.10
d1	2.000	fn	65536
nt	16	DISPLAY	
ct	16	sp	-206.3
TRANSMITTER		wp	4208.0
tn	H1	rf1	1397.5
sfrq	399.809	rfp	995.5
tof	-0.3	rp	-25.1
tpwr	61	lp	-23.5
pw	4.633	PLOT	
DECOUPLER		wc	250
dn	C13	sc	0
dof	0	vs	203
dm	nnn	th	13
dmm	c	al	cdc ph
dpwr	35		
def	29412		

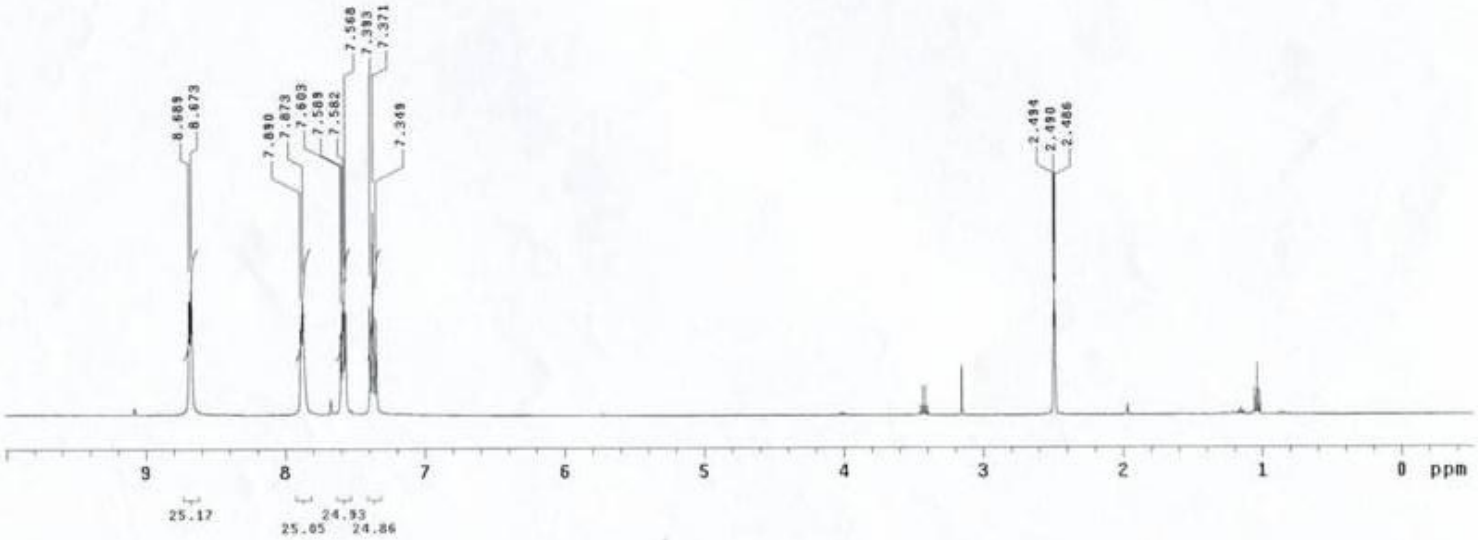

Archive directory:
Sample directory:

Pulse Sequence: s2pul

Solvent: cdcl3
Temp. 27.0 C / 300.1 K
File: kerwin_HJL121307c_s2pul_H1
INOVA-500 "nmrfred"

Relax. delay 2.000 sec
Pulse 30.0 degrees
Acq. time 4.048 sec
Width 6410.3 Hz
32 repetitions
OBSERVE H1, 399.8046911 MHz
DATA PROCESSING
Line broadening 0.1 Hz
FT size 65536
Total time 3 min, 25 sec

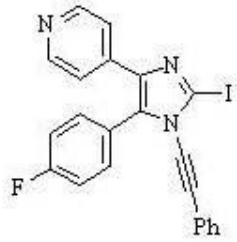

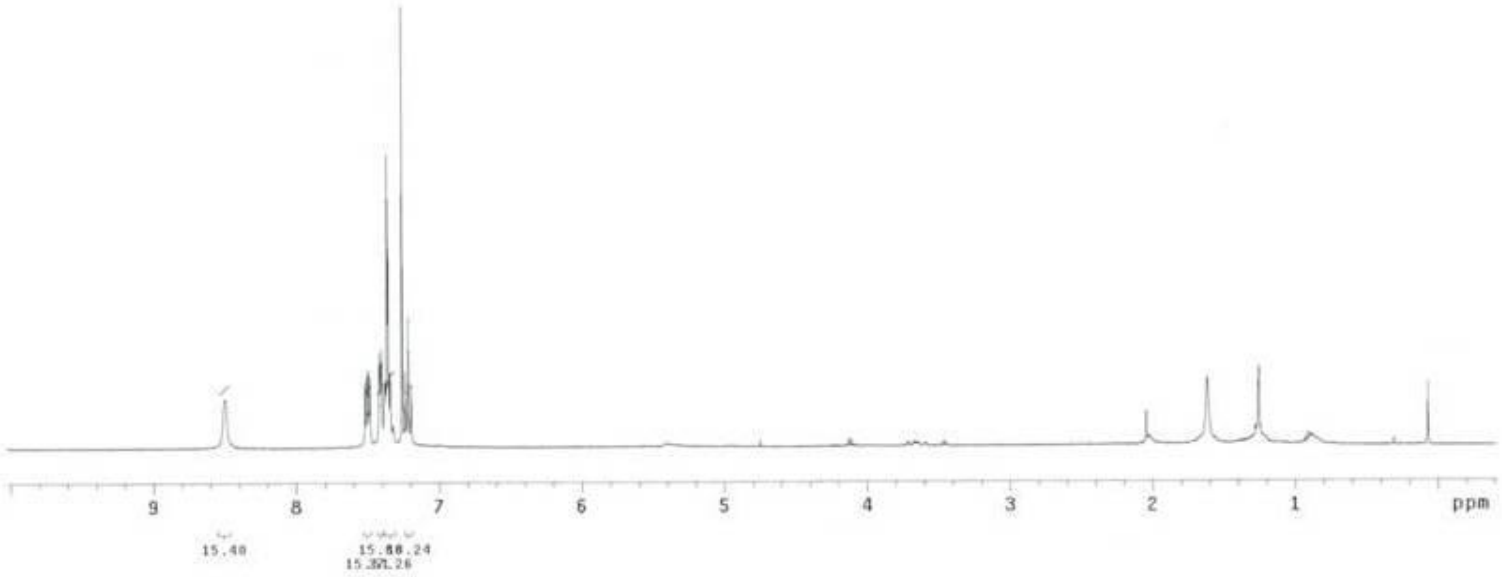

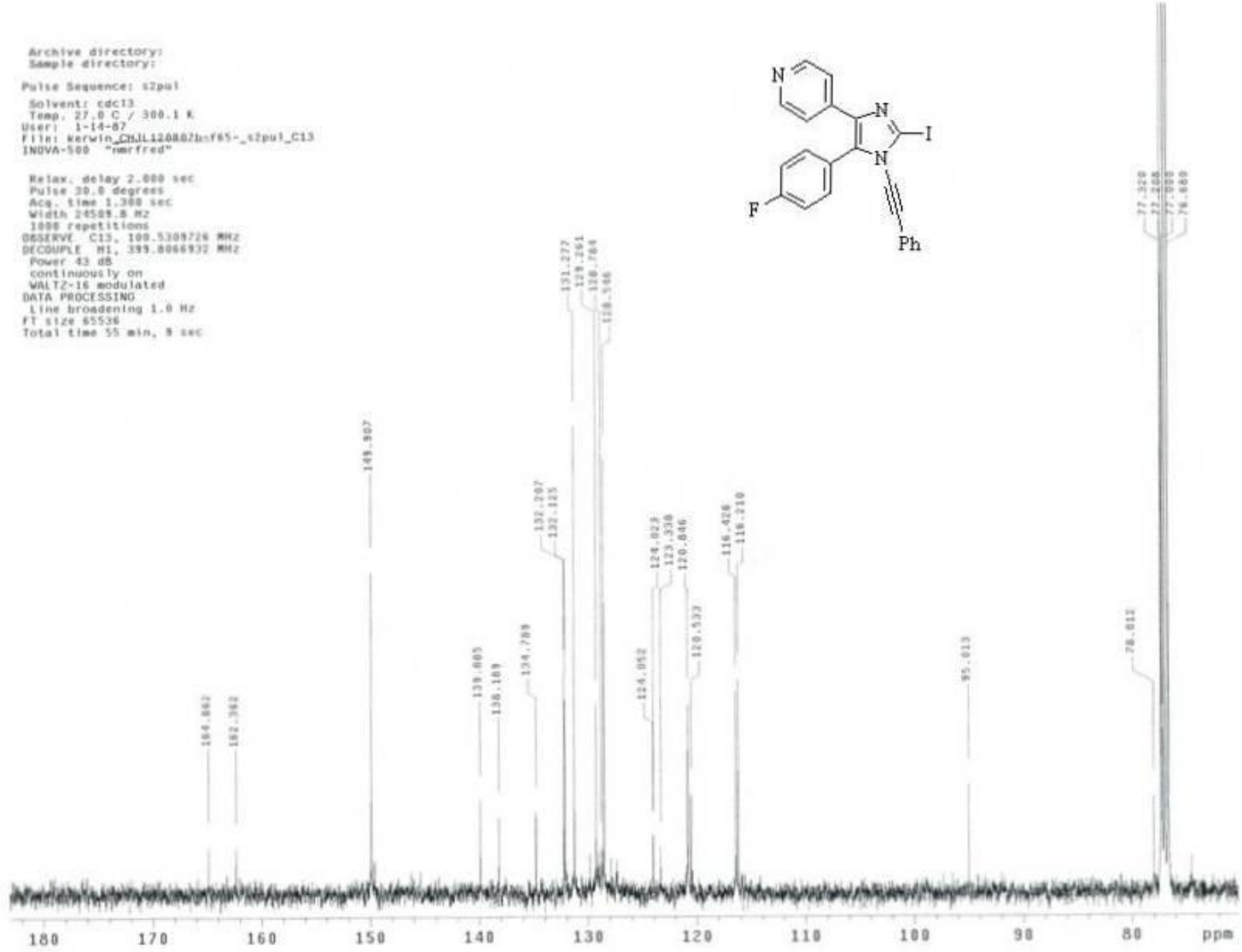
Archive directory:
Sample directory:
Pulse Sequence: s2pul
Solvent: cdcl3
Temp. 27.0 C / 300.1 K
User: 1-14-87
File: kerwin_CHJL120807bsf65-_s2pul_C13
INOVA-500 "nmrfred"
Relax. delay 2.000 sec
Pulse 30.0 degrees
Acq. time 1.300 sec
Width 24509.8 Hz
1000 repetitions
OBSERVE C13, 100.5309726 MHz
DECOUPLE H1, 399.8066932 MHz
Power 43 dB
continuously on
WALTZ-16 modulated
DATA PROCESSING
Line broadening 1.0 Hz
FT size 65536
Total time 55 min, 9 sec
N
N
I
N
F
Ph
164.802
162.362
149.907
139.805
138.169
134.789
132.207
132.125
131.277
129.261
128.784
128.566
124.052
124.023
123.338
120.846
120.533
116.426
116.210
95.013
78.612
77.320
77.208
77.000
76.680
180
170
160
150
140
130
120
110
100
90
80
ppm

Archive directory:
Sample directory:

Pulse Sequence: s2pul

Solvent: cdcl3
Temp. 27.0 C / 300.1 K
File: kerwin_HJL121007a_s2pul_H1
INOVA-500 "nmrfred"

Relax. delay 2.000 sec
Pulse 30.0 degrees
Acq. time 4.049 sec
Width 6410.3 Hz
8 repetitions
OBSERVE H1, 399.8846913 MHz
DATA PROCESSING
Line broadening 0.1 Hz
FT size 65536
Total time 1 min, 0 sec

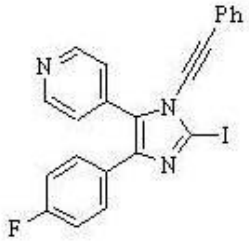

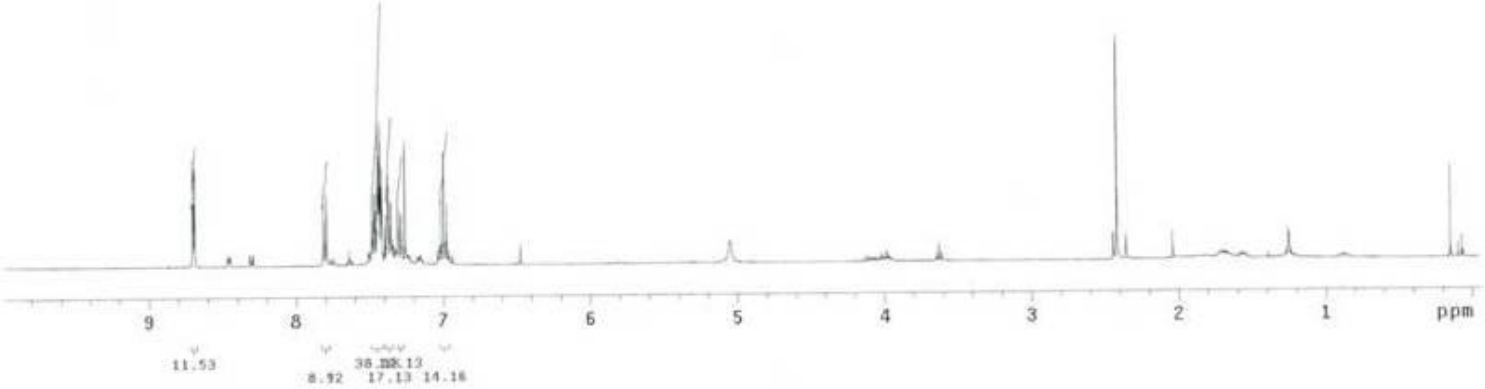

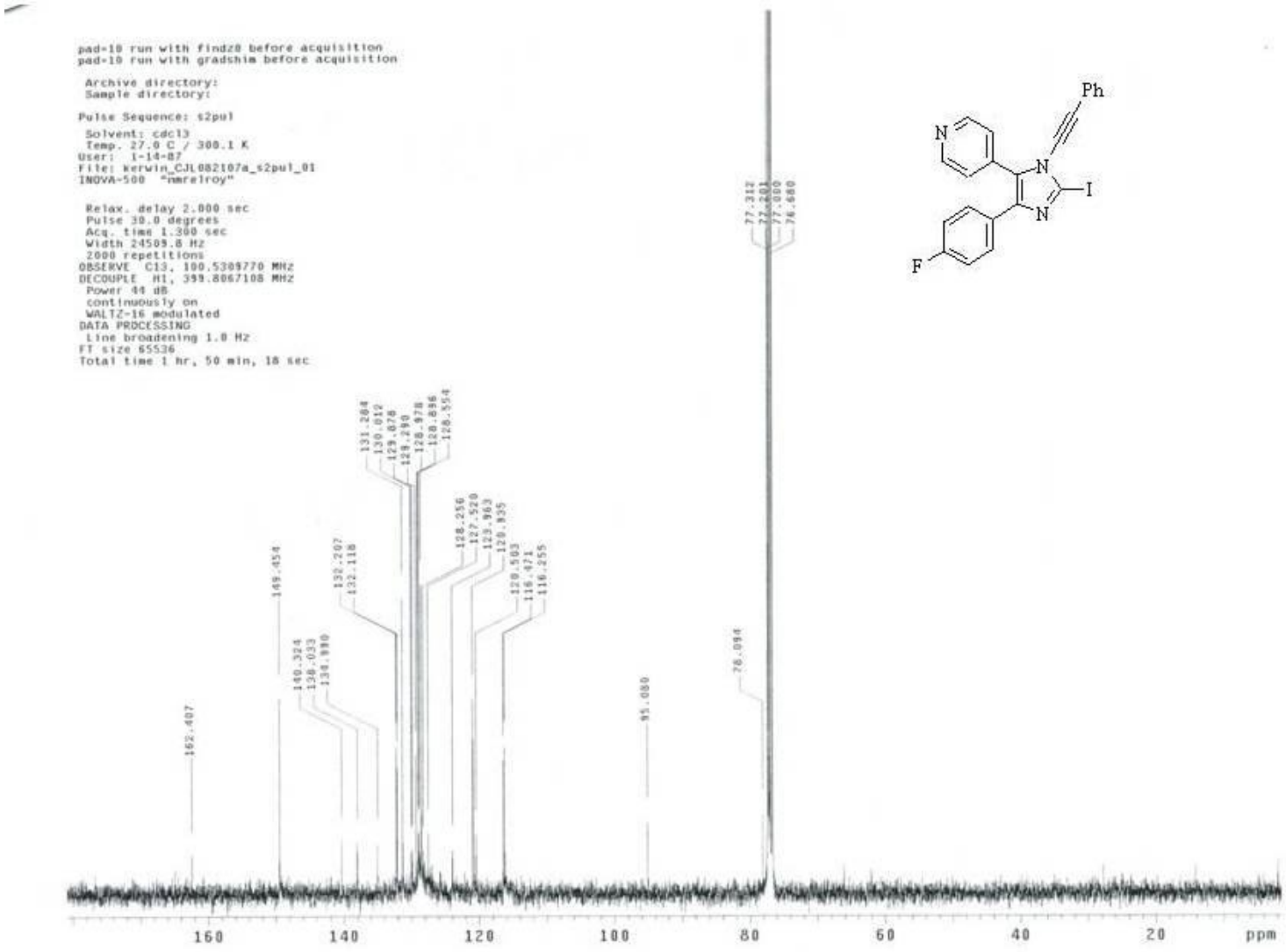
pad=10 run with findz0 before acquisition
pad=10 run with gradshim before acquisition
Archive directory:
Sample directory:
Pulse Sequence: s2pul
Solvent: cdcl3
Temp. 27.0 C / 300.1 K
User: 1-14-87
File: kerwin_CJL082107a_s2pul_01
INOVA-500 "nmrelroy"
Relax. delay 2.000 sec
Pulse 30.0 degrees
Acq. time 1.300 sec
Width 24509.8 Hz
2000 repetitions
OBSERVE C13, 100.5309770 MHz
DECOUPLE H1, 399.8067108 MHz
Power 44 dB
continuously on
WALTZ-16 modulated
DATA PROCESSING
Line broadening 1.0 Hz
FT size 65536
Total time 1 hr, 50 min, 18 sec
162.407
149.454
140.324
138.033
134.880
132.207
132.118
131.284
130.012
129.878
129.290
128.978
128.896
128.554
128.256
127.520
123.963
120.935
120.503
116.471
116.255
95.080
78.094
77.312
77.201
77.000
76.688
Ph
N
N
N
I
F
160
140
120
100
80
60
40
20
ppm

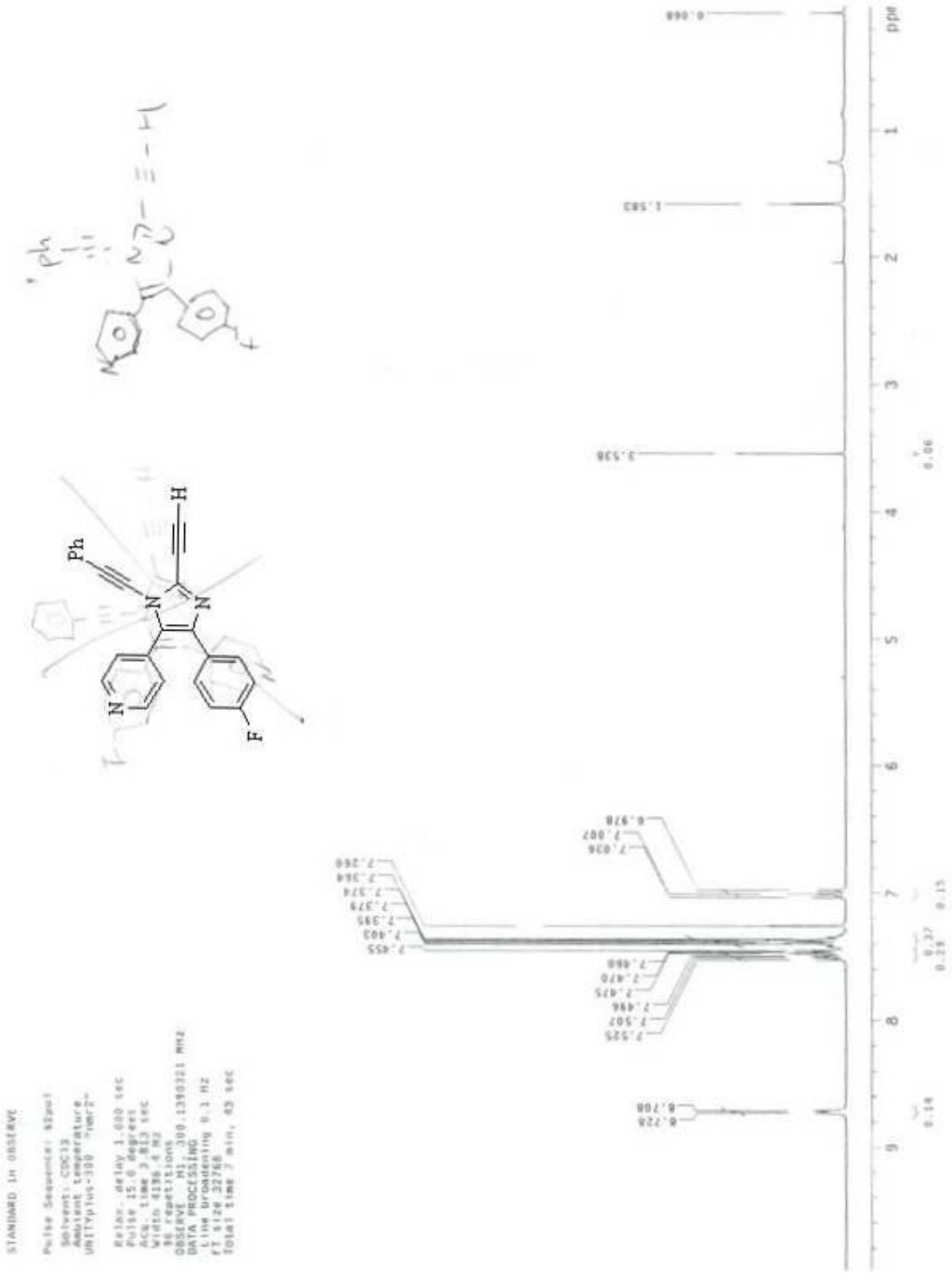
STANDARD 1H OBSERVE
Pulse Sequence: s2pul
Solvent: CDCl3
Ambient temperature
UNITYplus-300 "nmr2"
Relax. delay 1.000 sec
Pulse 15.0 degrees
Acq. time 3.813 sec
Width 4386.4 Hz
96 repetitions
OBSERVE H1, 300.1390321 MHz
DATA PROCESSING
Line Broadening 0.1 Hz
FT size 32768
Total time 7 min, 43 sec
Ph
H
N
N
N
F
ppm

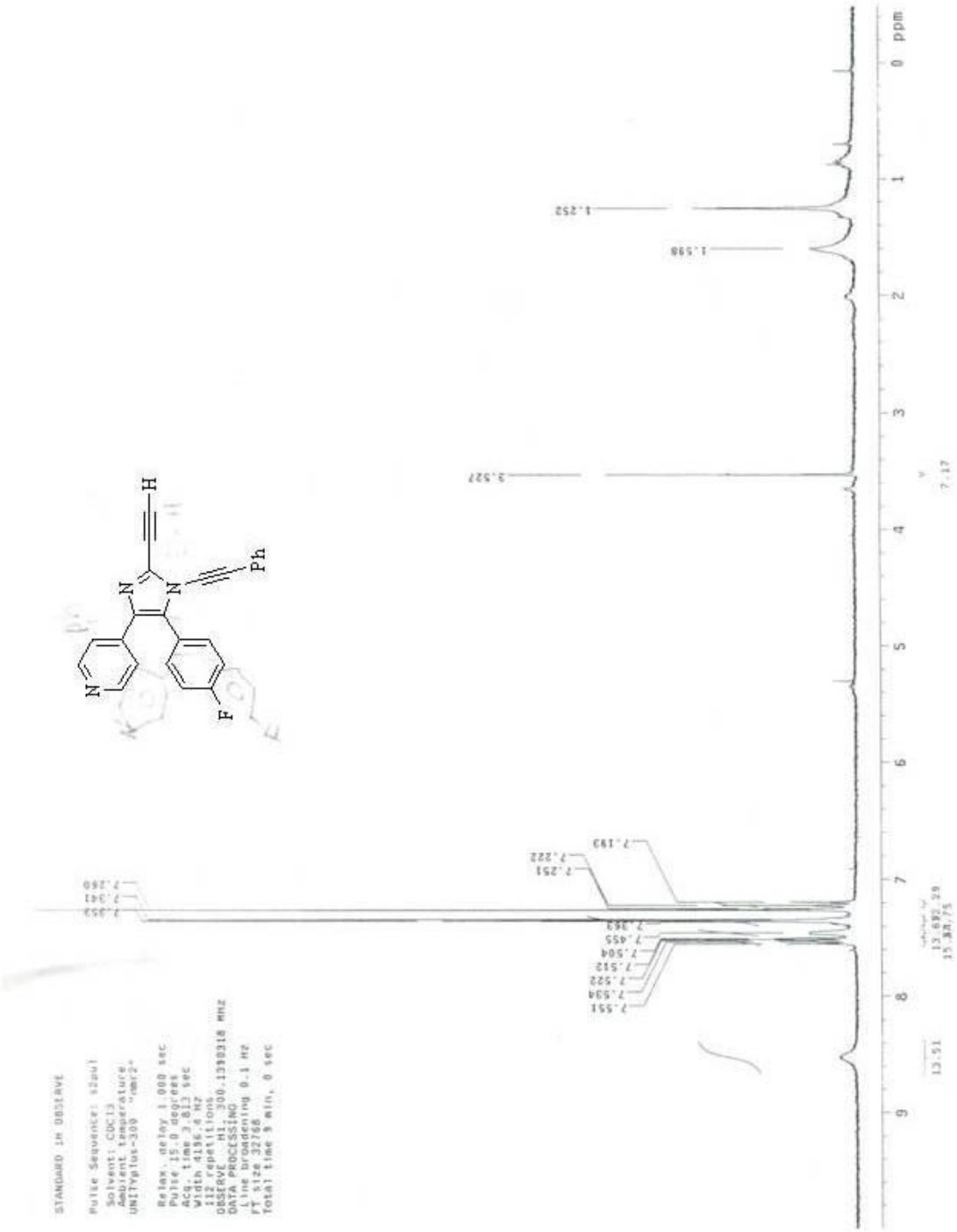
STANDARD IN OBSERVE
Pulse Sequence: s2pul
Solvent: CDCl3
Ambient temperature
UNITyplus-300 "ma02"
Relax. delay 1.000 sec
Pulse 15.0 degrees
Acq. time 3.813 sec
Width 4196.6 Hz
112 repetitions
OBSERVE H1, 300.1390318 MHz
DATA PROCESSING
Line broadening 0.1 Hz
FT size 32768
Total time 9 min, 0 sec
H
Ph
N
N
N
F
7.260
7.261
7.253
7.193
7.251
7.222
7.363
7.455
7.504
7.512
7.522
7.534
7.551
3.527
1.598
1.252
7.17
13.51
ppm

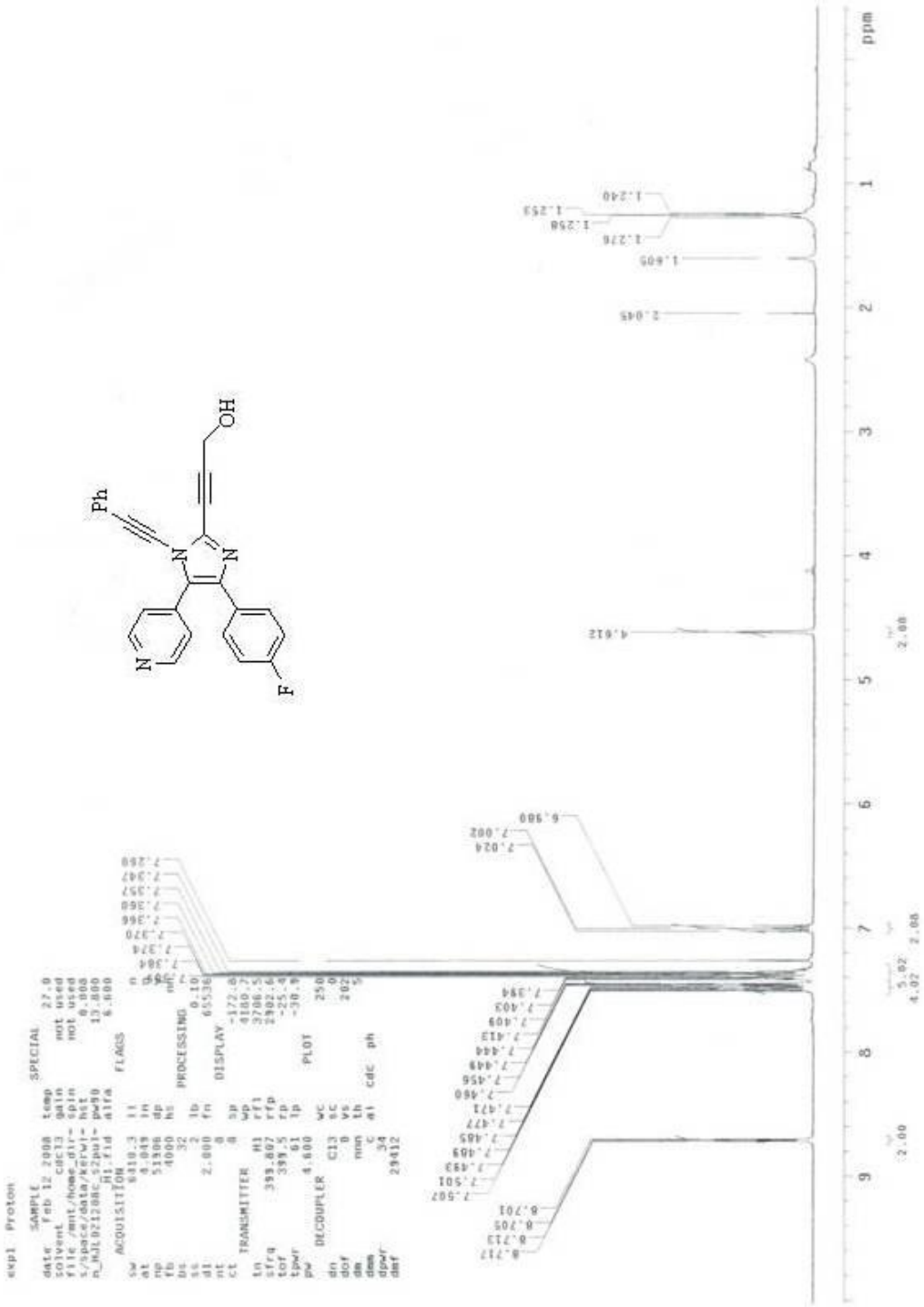
Ph
N
N
N
OH
F
ppm
1.240
1.253
1.258
1.276
1.605
2.045
4.612
6.980
7.024
7.082
7.394
7.403
7.409
7.413
7.444
7.449
7.456
7.460
7.471
7.477
7.485
7.489
7.493
7.501
7.507
6.701
6.705
6.713
6.717

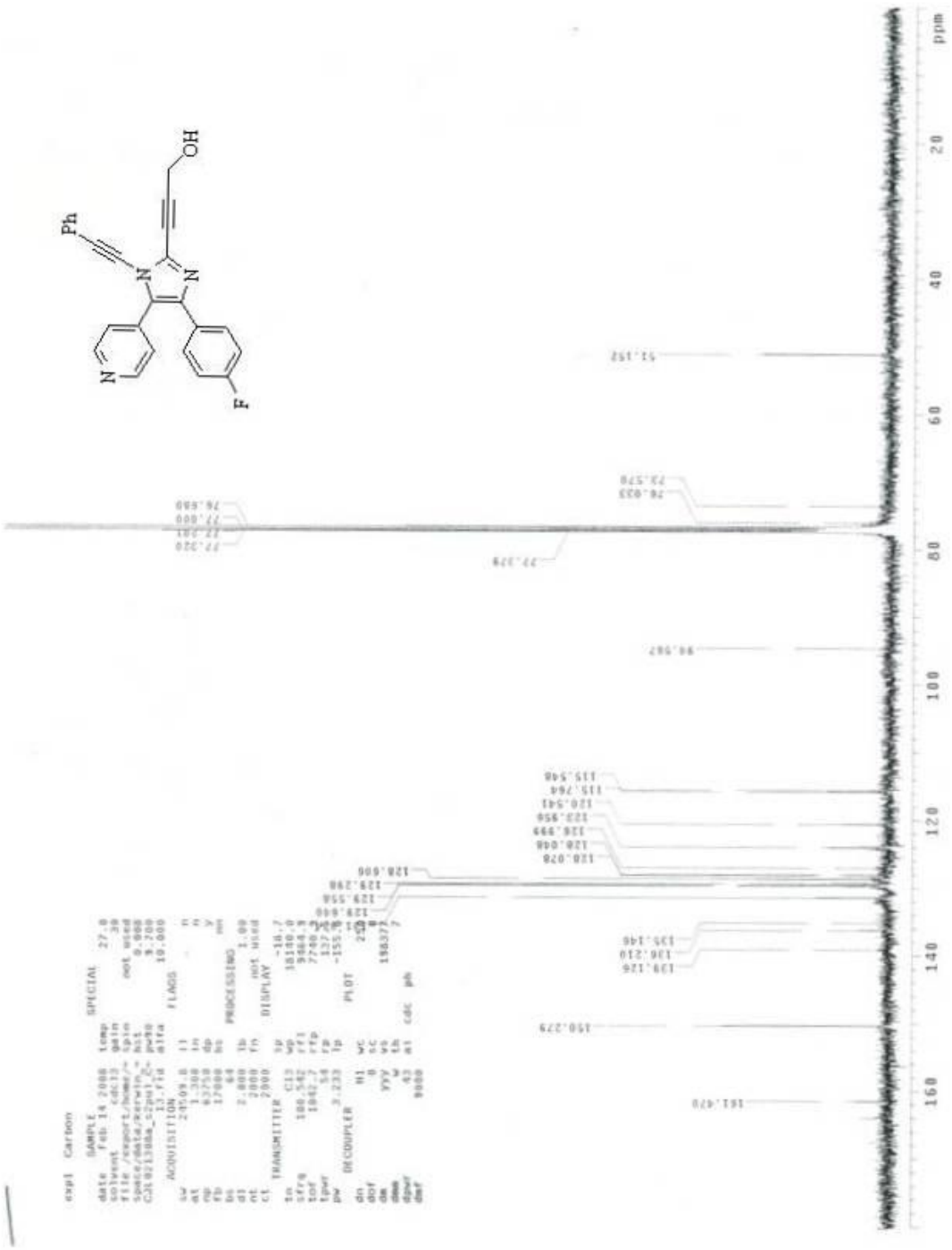
Ph
N
N
N
OH
F
ppm
20
40
60
80
100
120
140
160
51.192
73.579
74.023
76.680
77.000
77.320
77.329
90.587
115.546
115.764
120.941
123.950
126.999
128.048
128.078
128.606
129.290
129.556
129.660
135.146
136.210
139.126
150.279
161.470

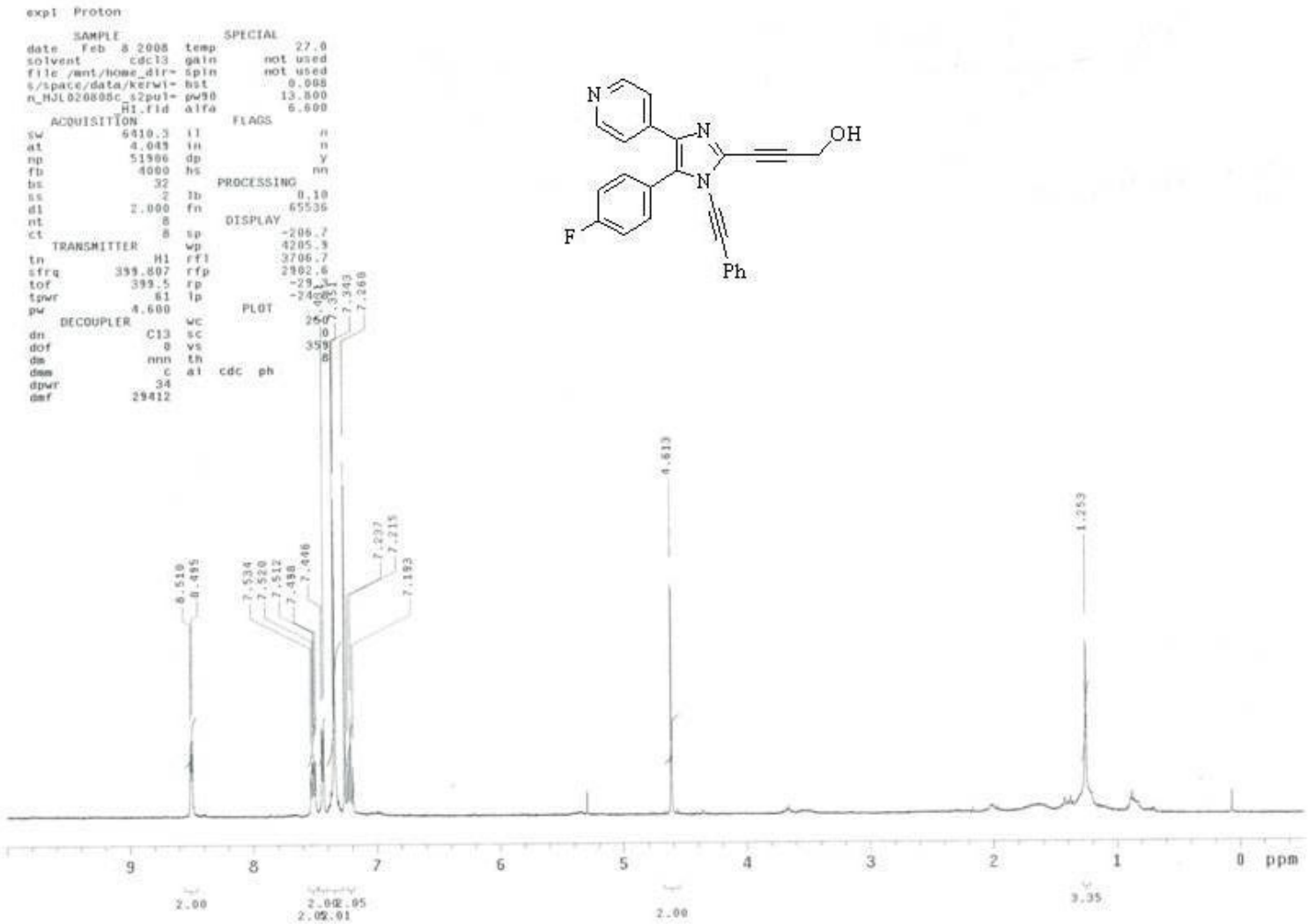
expl Proton
SAMPLE
date Feb 8 2008
solvent cdcl3
file /mnt/home_dir-
s/space/data/kerwi-
n_HJL020808c_s2pul-
H1.fid
ACQUISITION
sw 6410.3
at 4.049
np 51906
fb 4000
bs 32
ss 2
d1 2.000
nt 8
ct 8
TRANSMITTER
tn H1
sfrq 399.807
tof 399.5
tpwr 61
pw 4.600
DECOUPLER
dn C13
dof 0
dm nnn
dmm c
dpwr 34
dmf 29412
SPECIAL
temp 27.0
gain not used
spin not used
hst 0.008
pw90 13.800
alfa 6.600
FLAGS
PROCESSING
lb 0.10
fn 65536
DISPLAY
sp -206.7
wp 4205.9
rf1 3706.7
rfp 2902.6
PLOT
wc 260
sc 0
vs 359
th 8
al cdc ph
N
N
N
OH
F
Ph
8.510
8.495
7.534
7.520
7.512
7.498
7.446
7.237
7.215
7.183
7.343
7.268
4.613
1.253
9
8
7
6
5
4
3
2
1
0 ppm
2.00
2.00
2.05
2.05
2.01
2.00
3.35

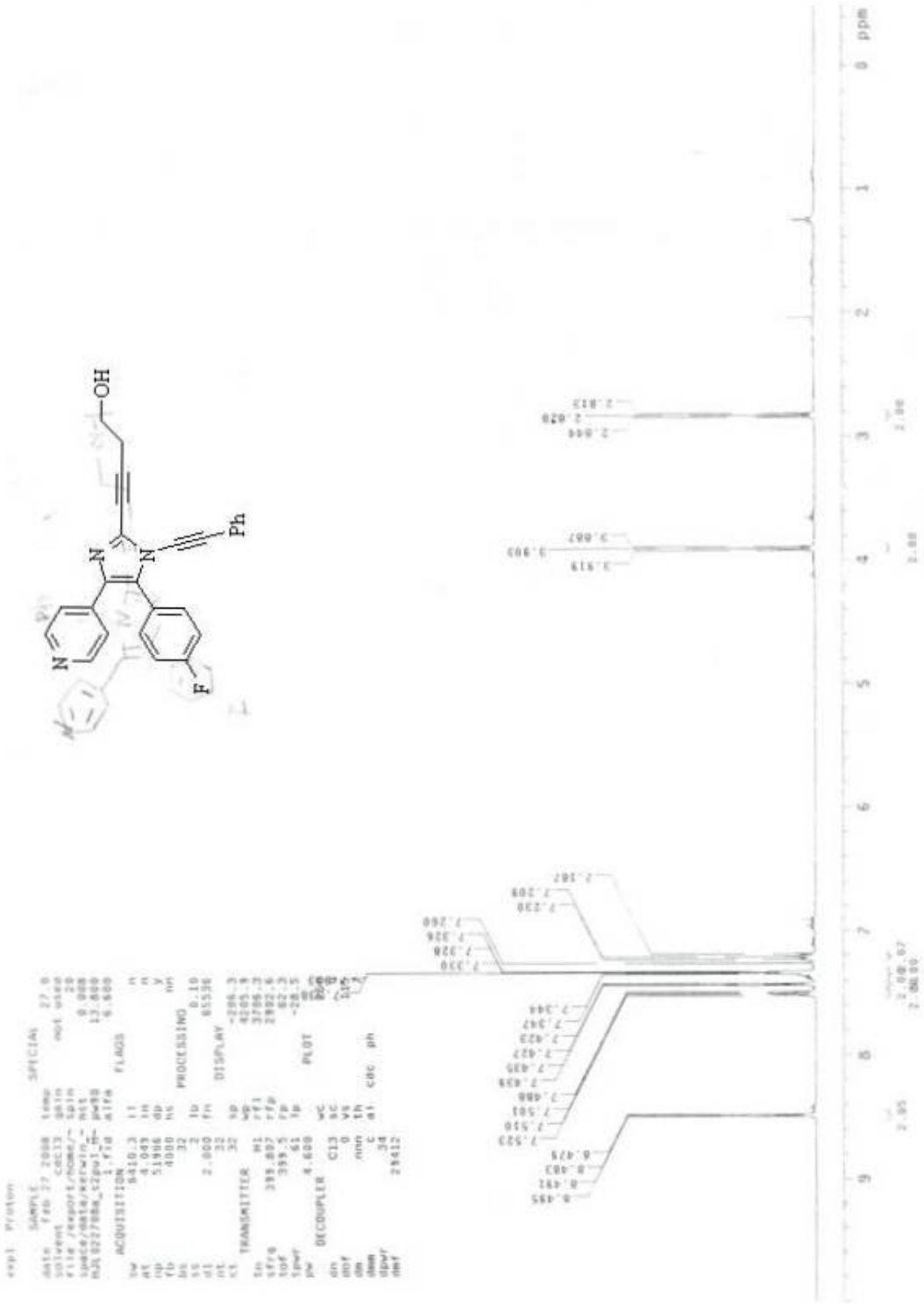

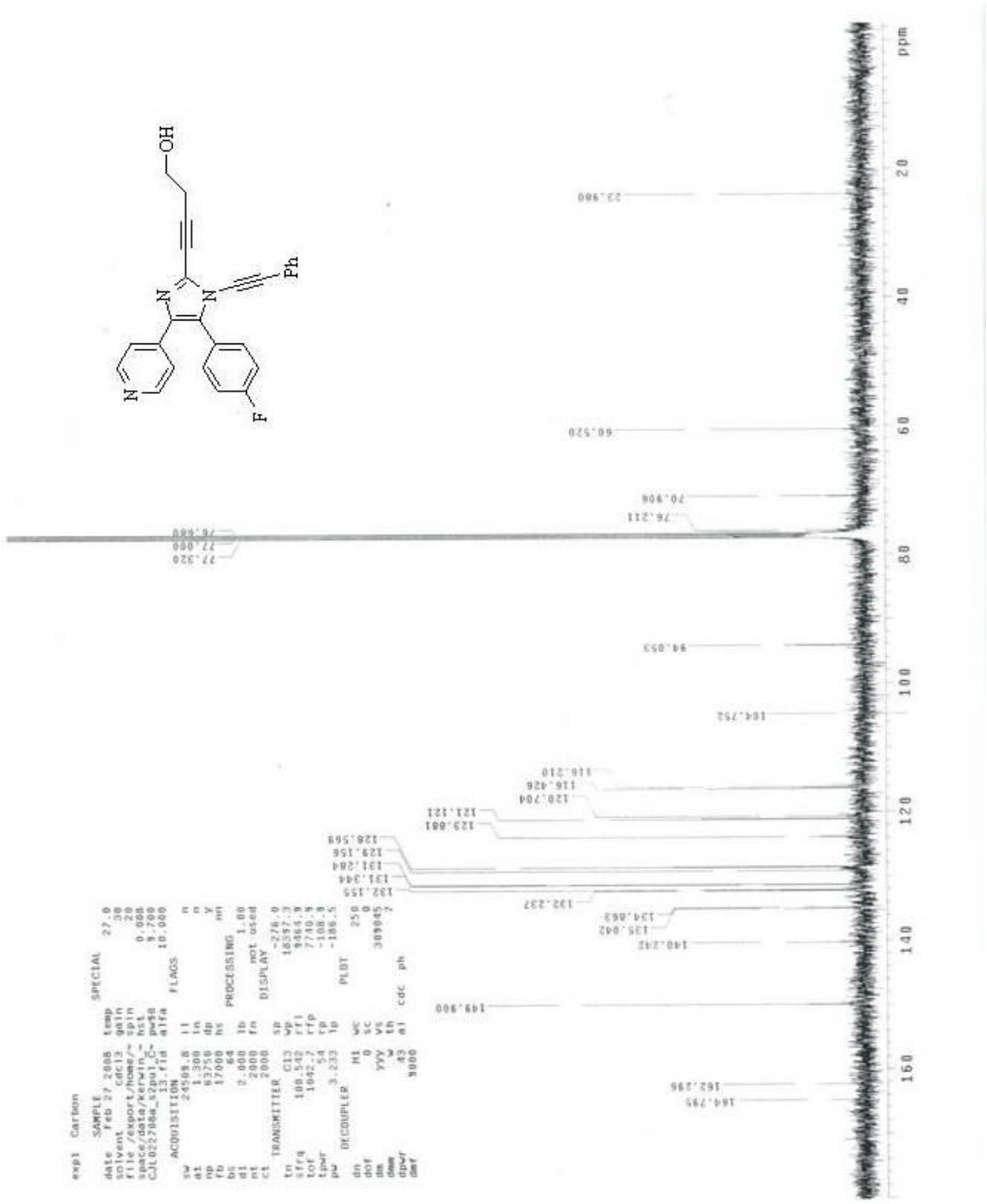
OH
Ph
N
N
N
F
ppm
20
40
60
80
100
120
140
160
22.900
60.520
70.906
76.211
77.320
77.000
76.680
94.053
104.752
116.210
116.426
120.704
121.121
123.081
126.569
129.156
131.264
131.344
132.155
132.237
134.063
135.042
140.242
149.900
162.296
164.795

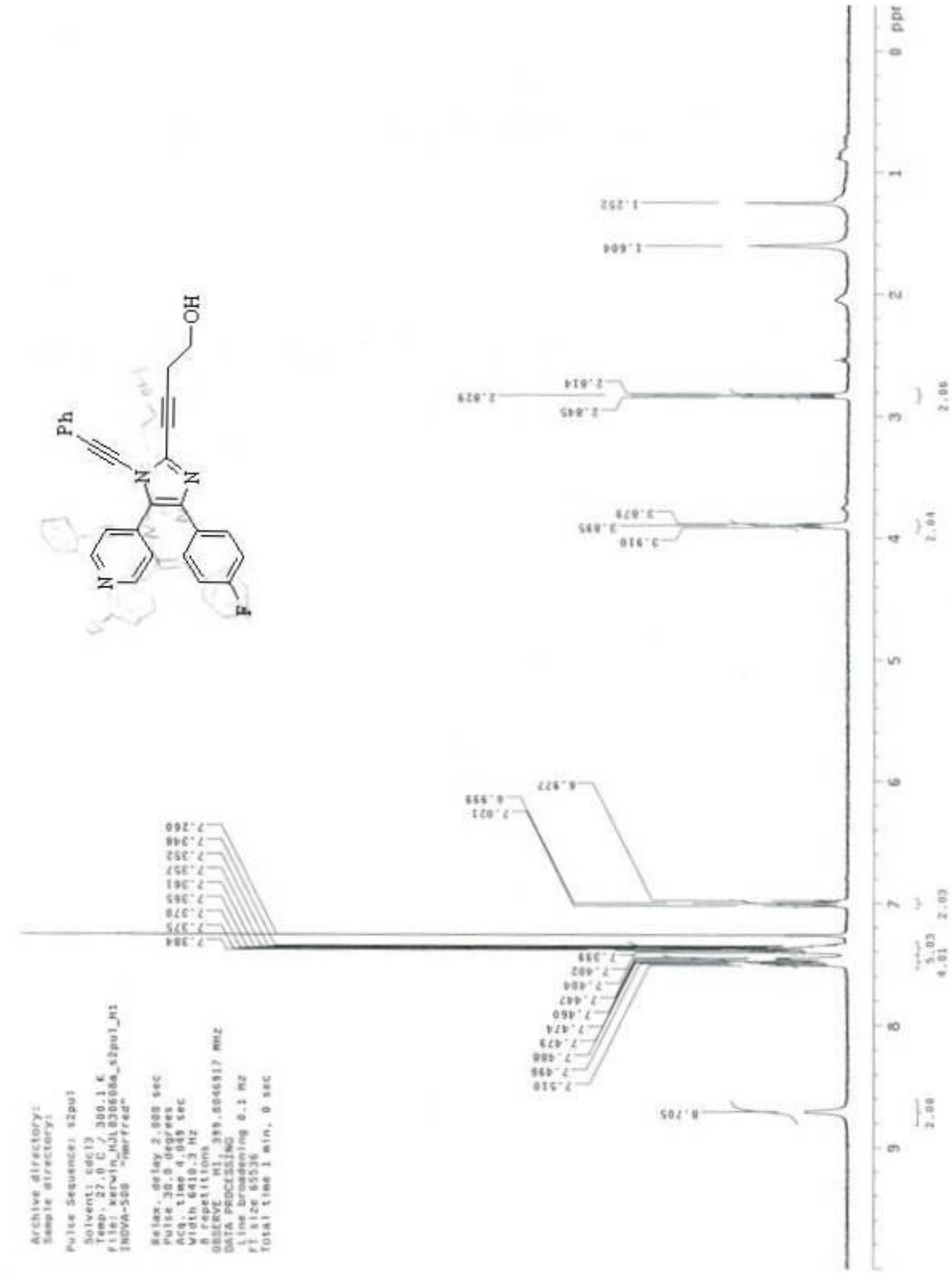
Ph
N
N
N
OH
F
Archive directory:
Sample directory:
Pulse Sequence: s2pul
Solvent: cdcl3
Temp. 27.0 C / 300.1 K
File: kerwin_HJL030608a_s2pul_H1
INOVA-500 "marfred"
Relax. delay 2.000 sec
Pulse 30.0 degrees
Acq. time 4.095 sec
Width 6410.3 Hz
8 repetitions
OBSERVE H1, 399.8846917 MHz
DATA PROCESSING
Line Broadening 0.1 Hz
FT size 65536
Total time 1 min. 0 sec
ppm

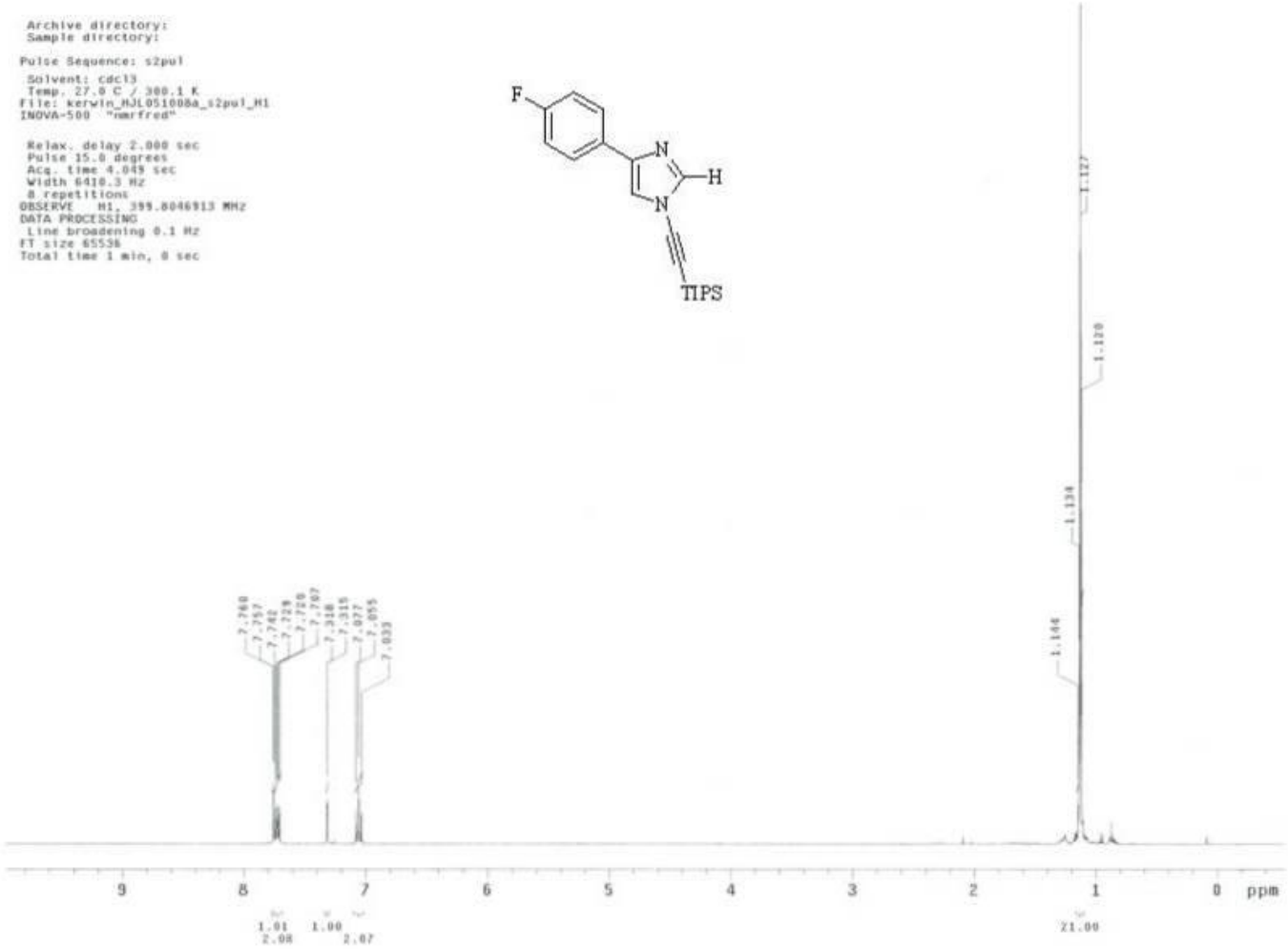
Archive directory:
Sample directory:
Pulse Sequence: s2pul
Solvent: cdcl3
Temp. 27.0 C / 300.1 K
File: kerwin_HJL051008a_s2pul_H1
INOVA-500 "nmrfred"
Relax. delay 2.000 sec
Pulse 15.0 degrees
Acq. time 4.049 sec
Width 6410.3 Hz
8 repetitions
OBSERVE H1, 399.8046913 MHz
DATA PROCESSING
Line broadening 0.1 Hz
FT size 65536
Total time 1 min, 8 sec
F
N
H
N
TIPS
7.760
7.757
7.742
7.729
7.720
7.707
7.318
7.315
7.077
7.055
7.033
1.127
1.120
1.134
1.144
9
8
7
6
5
4
3
2
1
0
ppm
1.01
2.08
1.00
2.07
21.00

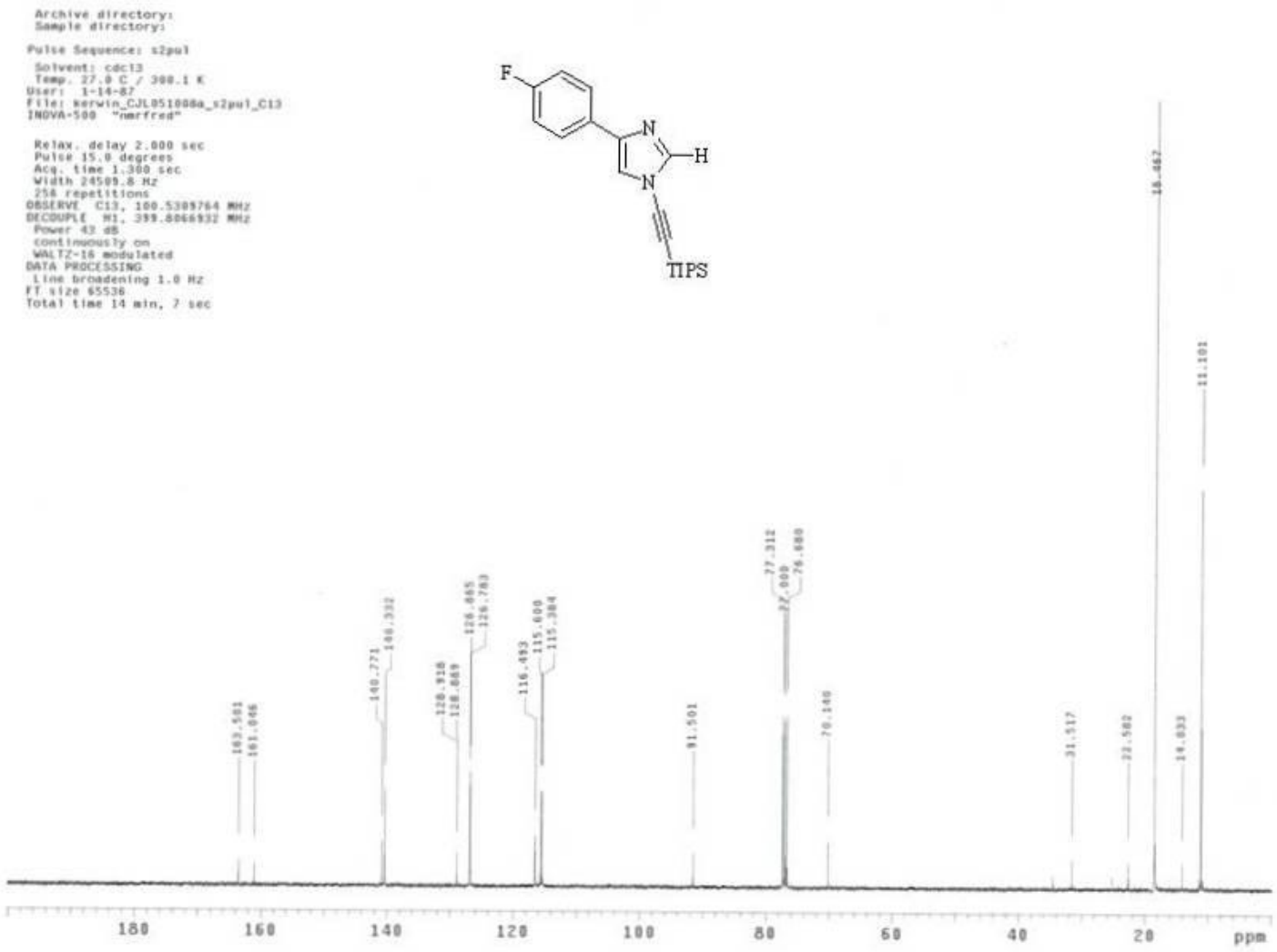
Archive directory:
Sample directory:
Pulse Sequence: s2pul
Solvent: cdcl3
Temp. 27.0 C / 300.1 K
User: 1-14-87
File: kerwin_CJL051008a_s2pul_C13
INOVA-500 "nmrfred"
Relax. delay 2.000 sec
Pulse 15.0 degrees
Acq. time 1.300 sec
Width 24509.8 Hz
256 repetitions
OBSERVE C13, 100.5389764 MHz
DECOUPLE H1, 399.8066932 MHz
Power 43 dB
continuously on
WALTZ-16 modulated
DATA PROCESSING
Line broadening 1.0 Hz
FT size 65536
Total time 14 min, 7 sec
F
N
H
N
TIPS
163.501
161.046
140.771
140.332
128.918
128.869
126.865
126.783
116.493
115.600
115.384
91.501
77.312
77.000
76.688
70.140
31.517
22.502
18.467
14.833
11.101
180
160
140
120
100
80
60
40
20
ppm

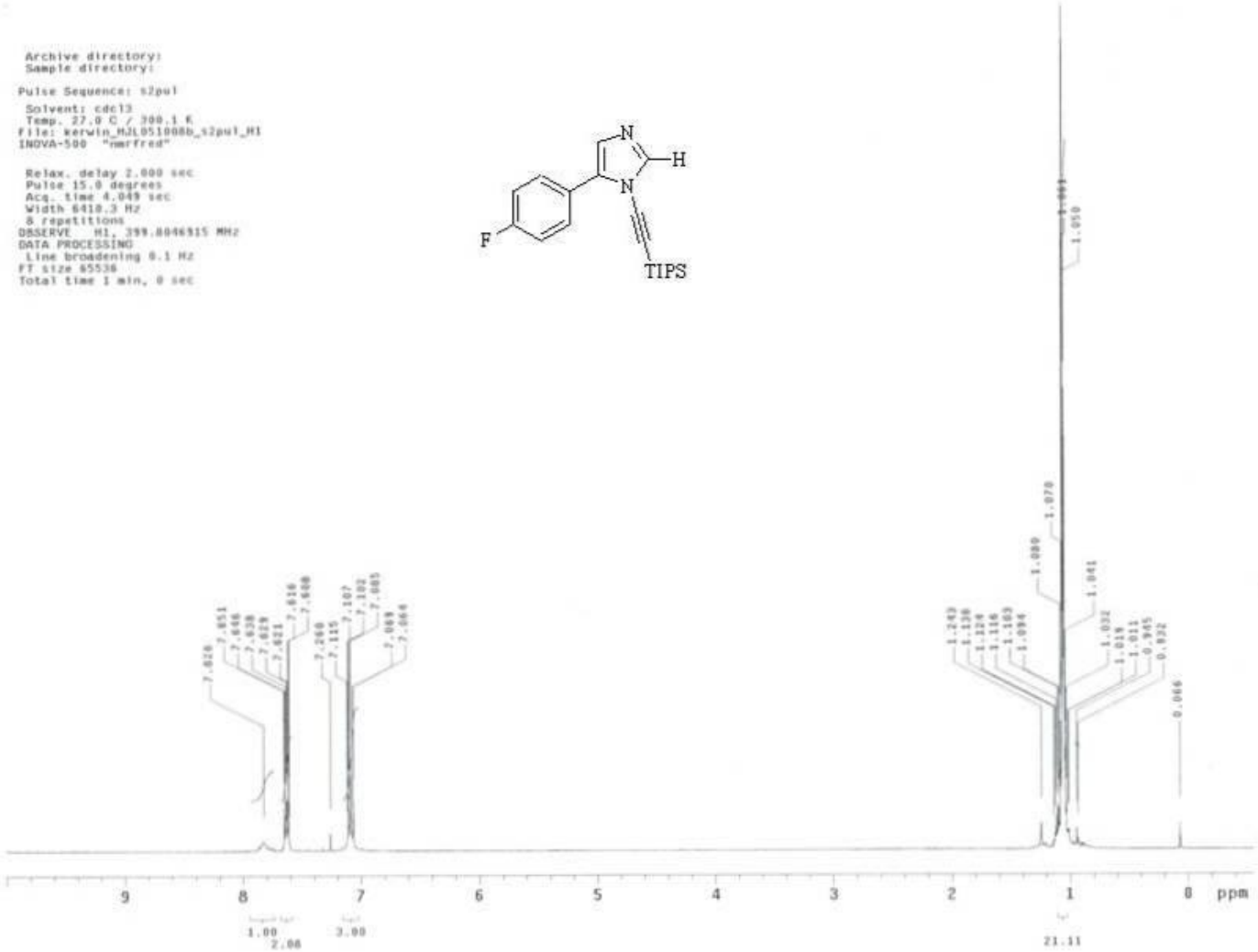
Archive directory:
Sample directory:
Pulse Sequence: s2pul
Solvent: cdcl3
Temp. 27.0 C / 300.1 K
File: kerwin_HJL0510086_s2pul_H1
INOVA-500 "nmrfred"
Relax. delay 2.000 sec
Pulse 15.0 degrees
Acq. time 4.049 sec
Width 6410.3 Hz
8 repetitions
OBSERVE H1, 399.8046515 MHz
DATA PROCESSING
Line broadening 0.1 Hz
FT size 65536
Total time 1 min, 0 sec
N
H
N
F
TIPS
7.628
7.651
7.646
7.638
7.629
7.621
7.616
7.608
7.260
7.115
7.107
7.102
7.085
7.069
7.064
1.243
1.238
1.224
1.216
1.163
1.094
1.080
1.070
1.059
1.041
1.032
1.019
1.011
0.945
0.922
0.066
9
8
7
6
5
4
3
2
1
0
ppm
1.00
2.06
3.00
21.11

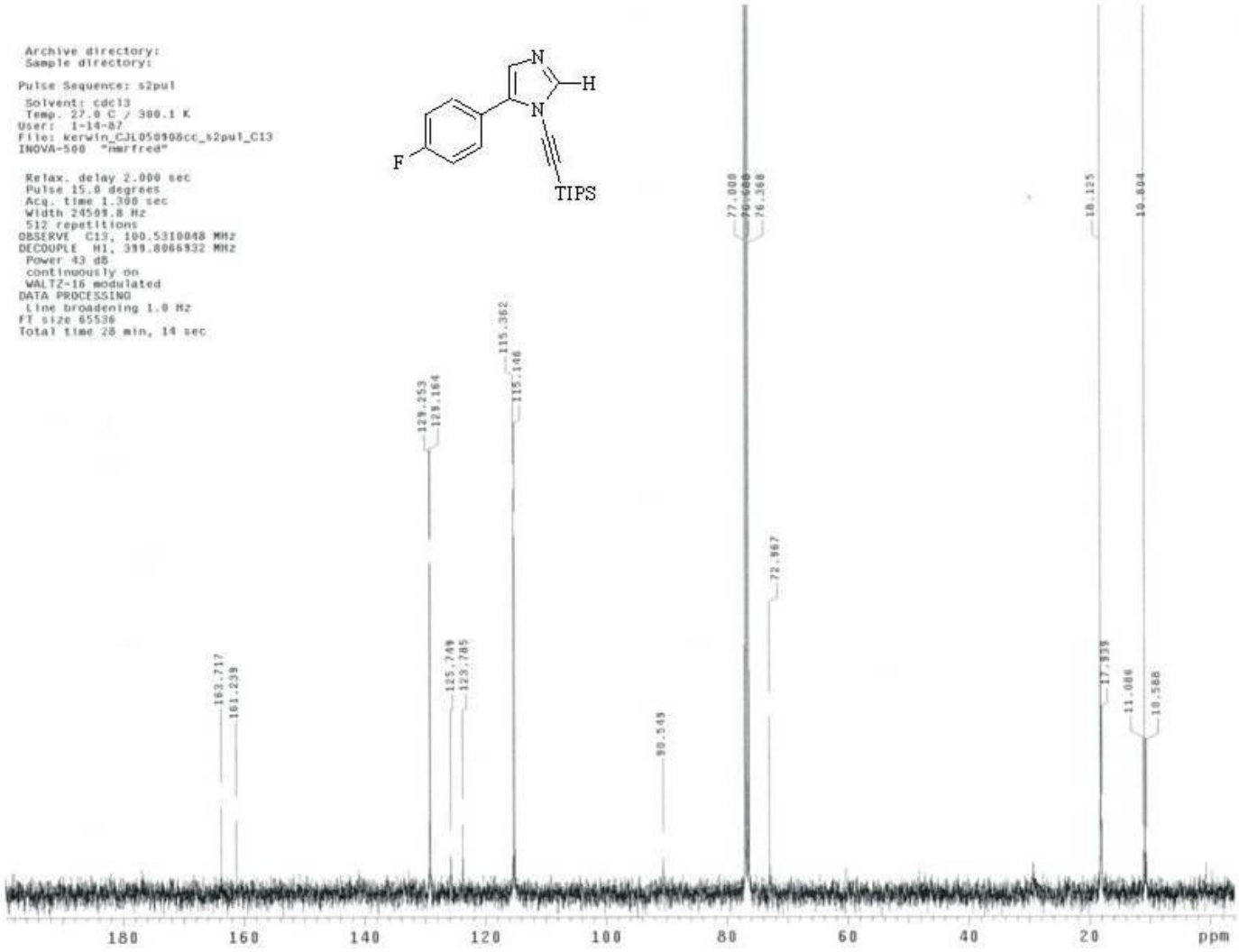
Archive directory:
Sample directory:
Pulse Sequence: s2pul
Solvent: cdcl3
Temp. 27.0 C / 300.1 K
User: I-14-87
File: kerwin_CJL050908cc_s2pul_C13
INOVA-500 "nmrfred"
Relax. delay 2.000 sec
Pulse 15.0 degrees
Acq. time 1.300 sec
Width 24509.8 Hz
512 repetitions
OBSERVE C13, 100.5310048 MHz
DECOUPLE H1, 399.8066932 MHz
Power 43 dB
continuously on
WALTZ-16 modulated
DATA PROCESSING
Line broadening 1.0 Hz
FT size 65536
Total time 28 min, 14 sec
N
H
N
F
TIPS
163.717
161.239
129.253
129.164
125.749
123.785
115.362
115.140
90.543
77.000
76.680
76.358
72.967
18.125
17.939
11.086
10.604
10.588
180
160
140
120
100
80
60
40
20
ppm

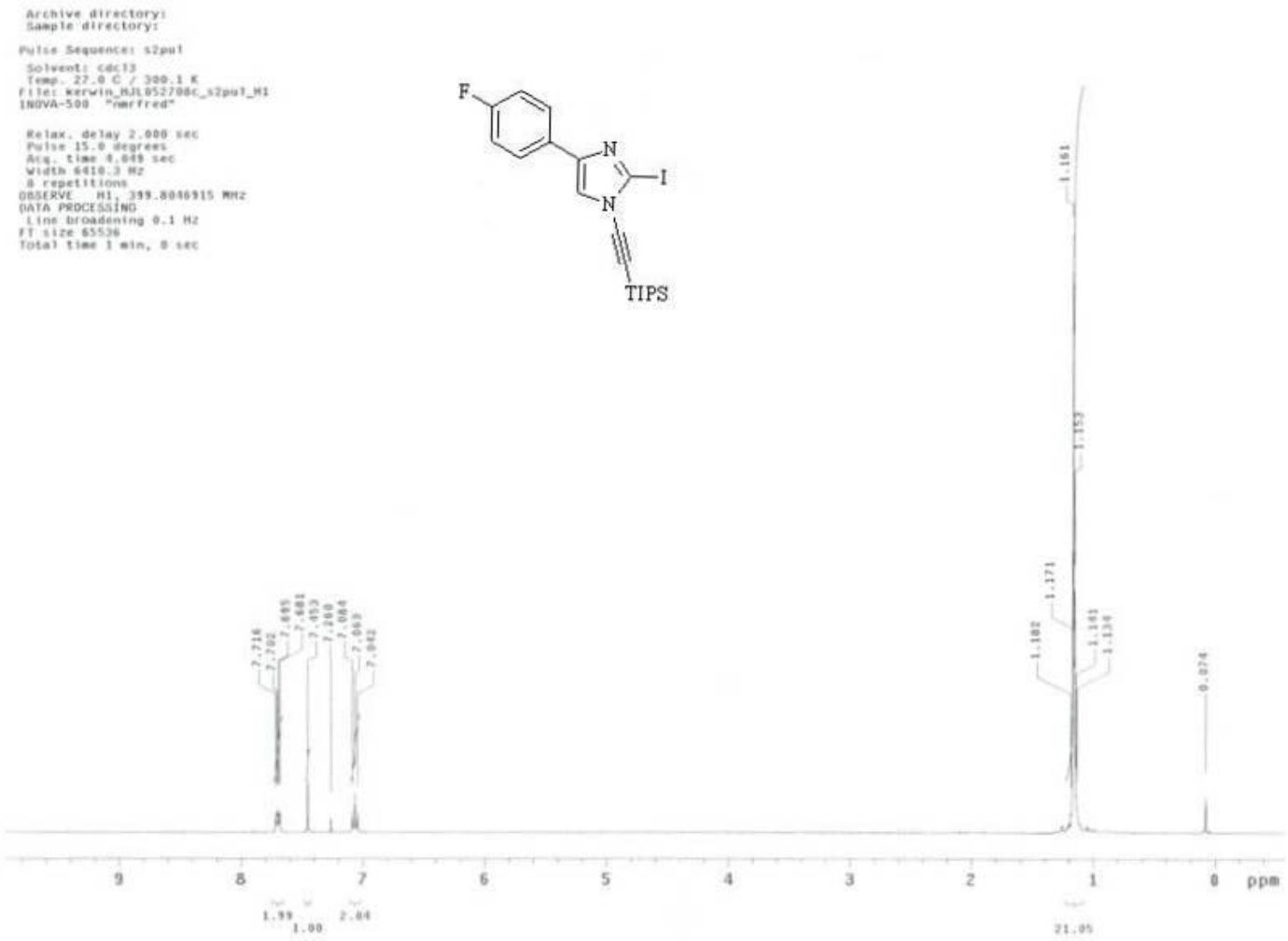
Archive directory:
Sample directory:
Pulse Sequence: s2pul
Solvent: cdcl3
Temp. 27.0 C / 300.1 K
File: kerwin_RJL052708c_s2pul_H1
INOVA-500 "nmrfred"
Relax. delay 2.000 sec
Pulse 15.0 degrees
Acq. time 4.045 sec
Width 6410.3 Hz
8 repetitions
OBSERVE H1, 399.8046915 MHz
DATA PROCESSING
Line broadening 0.1 Hz
FT size 65536
Total time 1 min, 8 sec
F
N
I
N
TIPS
7.716
7.702
7.695
7.681
7.053
7.066
7.064
7.063
7.042
1.161
1.153
1.171
1.182
1.161
1.134
0.074
9
8
7
6
5
4
3
2
1
0
ppm
1.99
1.00
2.04
21.05

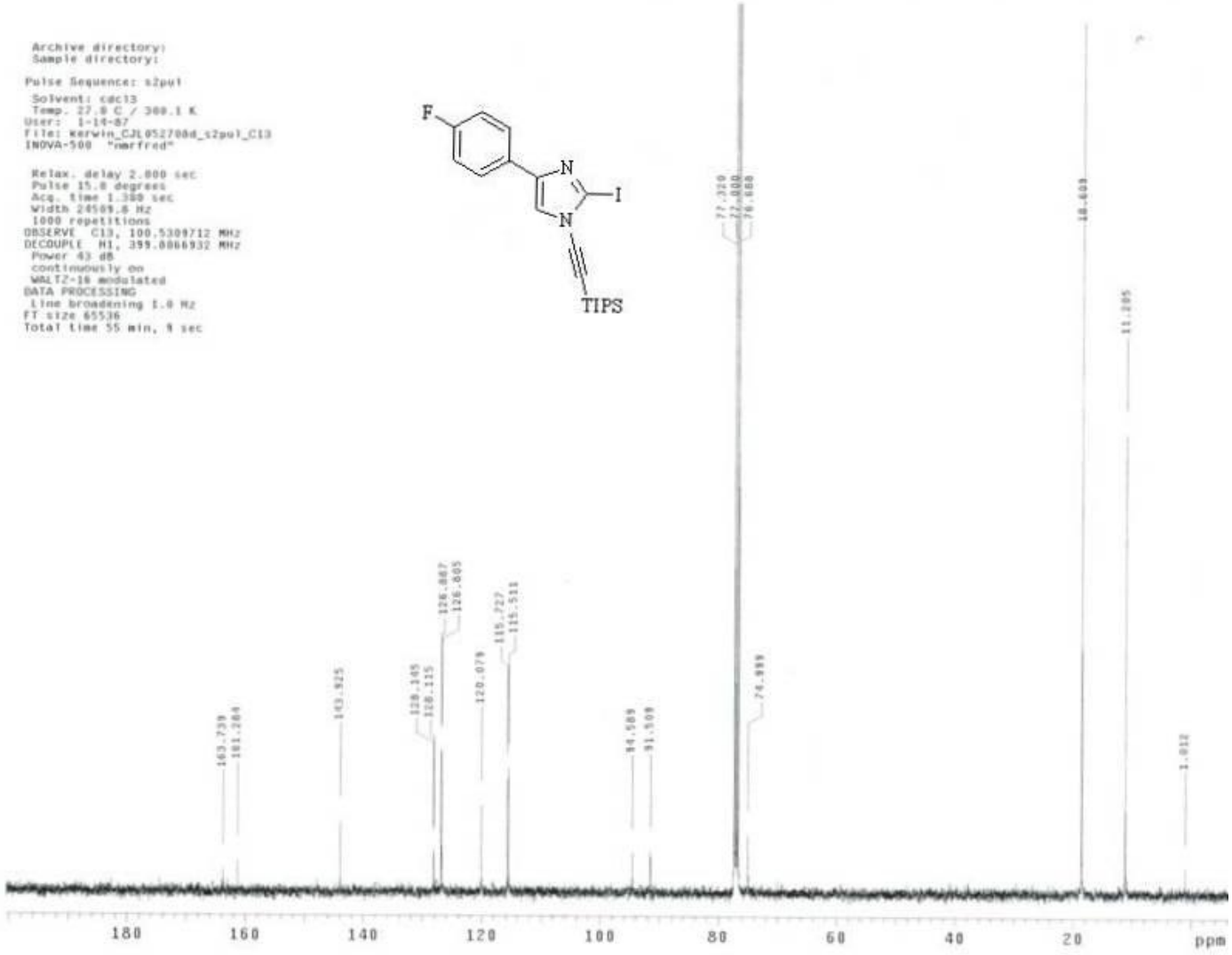
Archive directory:
Sample directory:
Pulse Sequence: s2pul
Solvent: cdcl3
Temp. 27.0 C / 300.1 K
User: I-14-87
File: kerwin_CJL052708d_s2pul_C13
INOVA-500 "nmrfred"
Relax. delay 2.000 sec
Pulse 15.0 degrees
Acq. time 1.380 sec
Width 24509.8 Hz
1000 repetitions
OBSERVE C13, 100.5309712 MHz
DECOUPLE H1, 399.8866932 MHz
Power 43 dB
continuously on
WALTZ-16 modulated
DATA PROCESSING
Line broadening 1.0 Hz
FT size 65536
Total time 55 min, 9 sec
F
N
I
N
TIPS
77.320
77.000
76.680
18.603
11.205
1.012
163.739
161.264
143.925
128.145
128.115
126.887
126.605
120.079
115.727
115.511
94.569
91.509
74.999
180
160
140
120
100
80
60
40
20
ppm

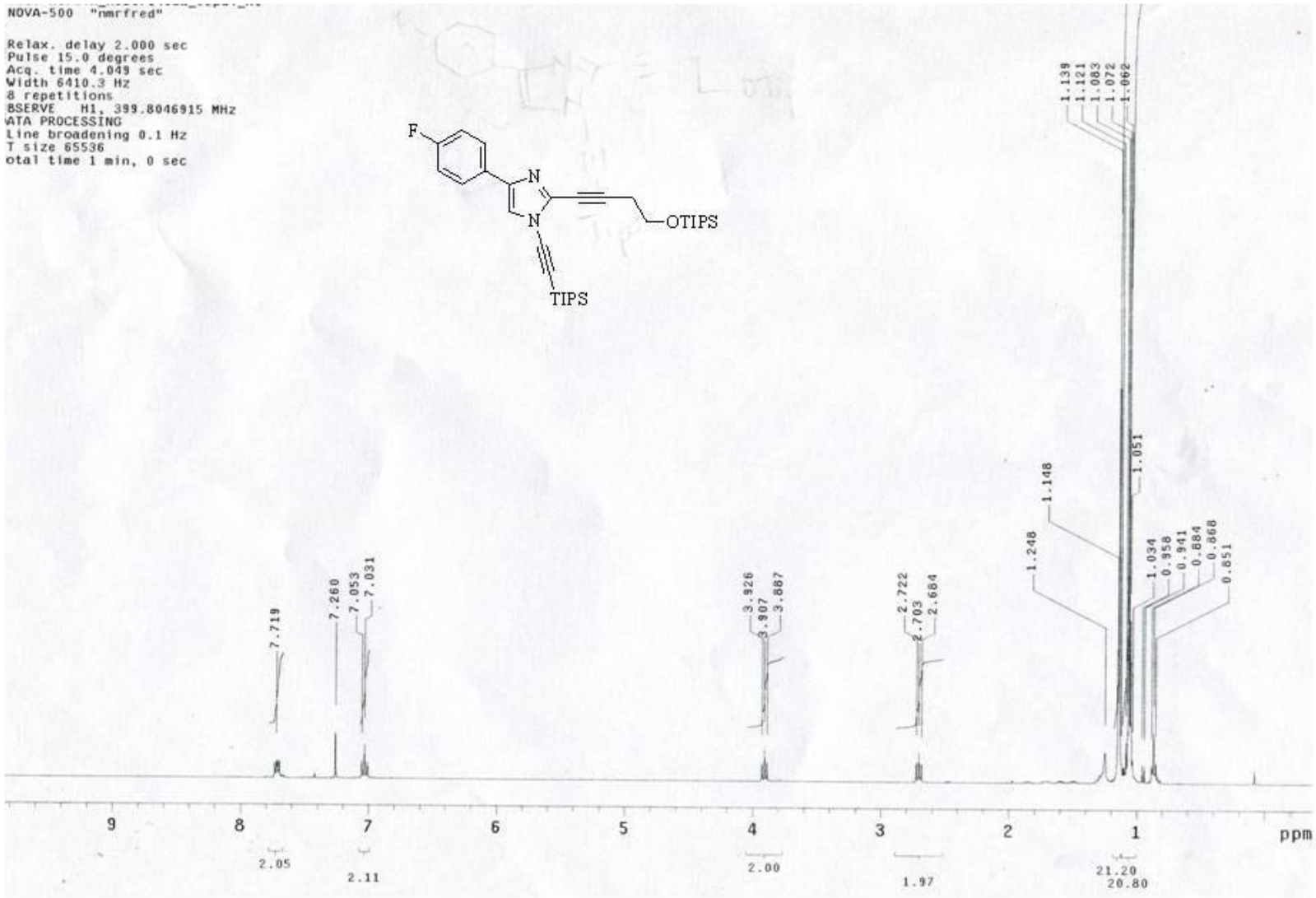
NOVA-500 "nmrfred"
Relax. delay 2.000 sec
Pulse 15.0 degrees
Acq. time 4.049 sec
Width 6410.3 Hz
8 repetitions
BSERVE H1, 399.8046915 MHz
ATA PROCESSING
Line broadening 0.1 Hz
T size 65536
otal time 1 min, 0 sec
F
N
N
OTIPS
TIPS
7.719
7.260
7.053
7.031
3.926
3.907
3.887
2.722
2.703
2.684
1.248
1.148
1.139
1.121
1.083
1.072
1.062
1.051
1.034
0.958
0.941
0.884
0.868
0.851
9
8
7
6
5
4
3
2
1
ppm
2.05
2.11
2.00
1.97
21.20
20.80

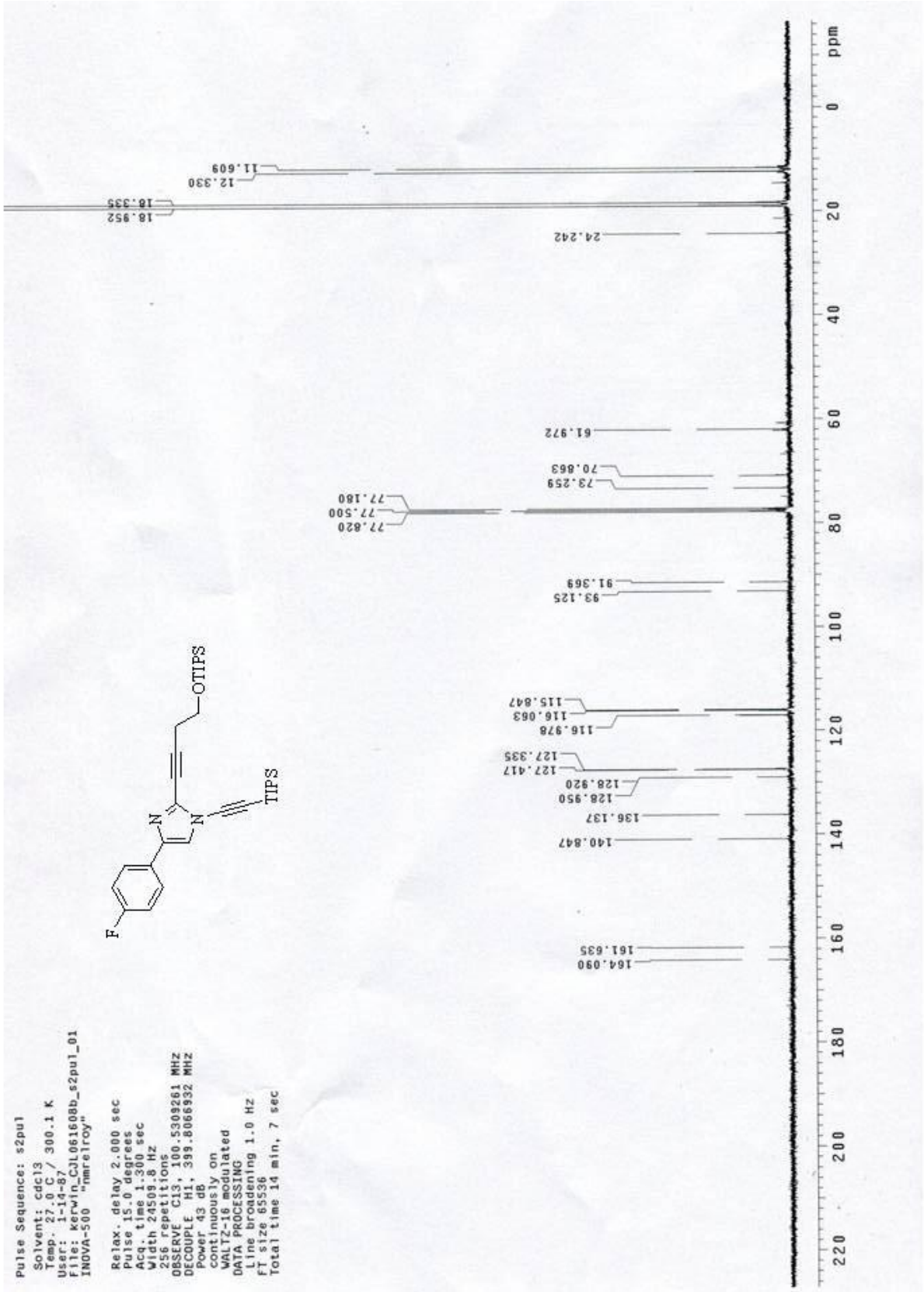
Pulse Sequence: s2pul
Solvent: cdcl3
Temp. 27.0 C / 300.1 K
User: 1-14-87
File: kerwin_CJL061608b_s2pul_01
INOVA-500 "mmelroy"
Relax. delay 2.000 sec
Pulse 15.0 degrees
Acq. time 1.300 sec
Width 24509.8 Hz
256 repetitions
OBSERVE C13, 100.5309261 MHz
DECOUPLE H1, 399.8066932 MHz
Power 43 dB
continuously on
WALTZ-16 modulated
DATA PROCESSING
Line broadening 1.0 Hz
FT size 65536
Total time 14 min, 7 sec
OTIPS
TIPS
N
N
F
ppm
0
20
40
60
80
100
120
140
160
180
200
220
11.609
12.330
18.335
18.952
24.242
61.972
70.863
73.259
77.180
77.500
77.820
91.369
93.125
115.847
116.063
116.978
127.335
127.417
128.920
128.950
136.137
140.847
161.635
164.090

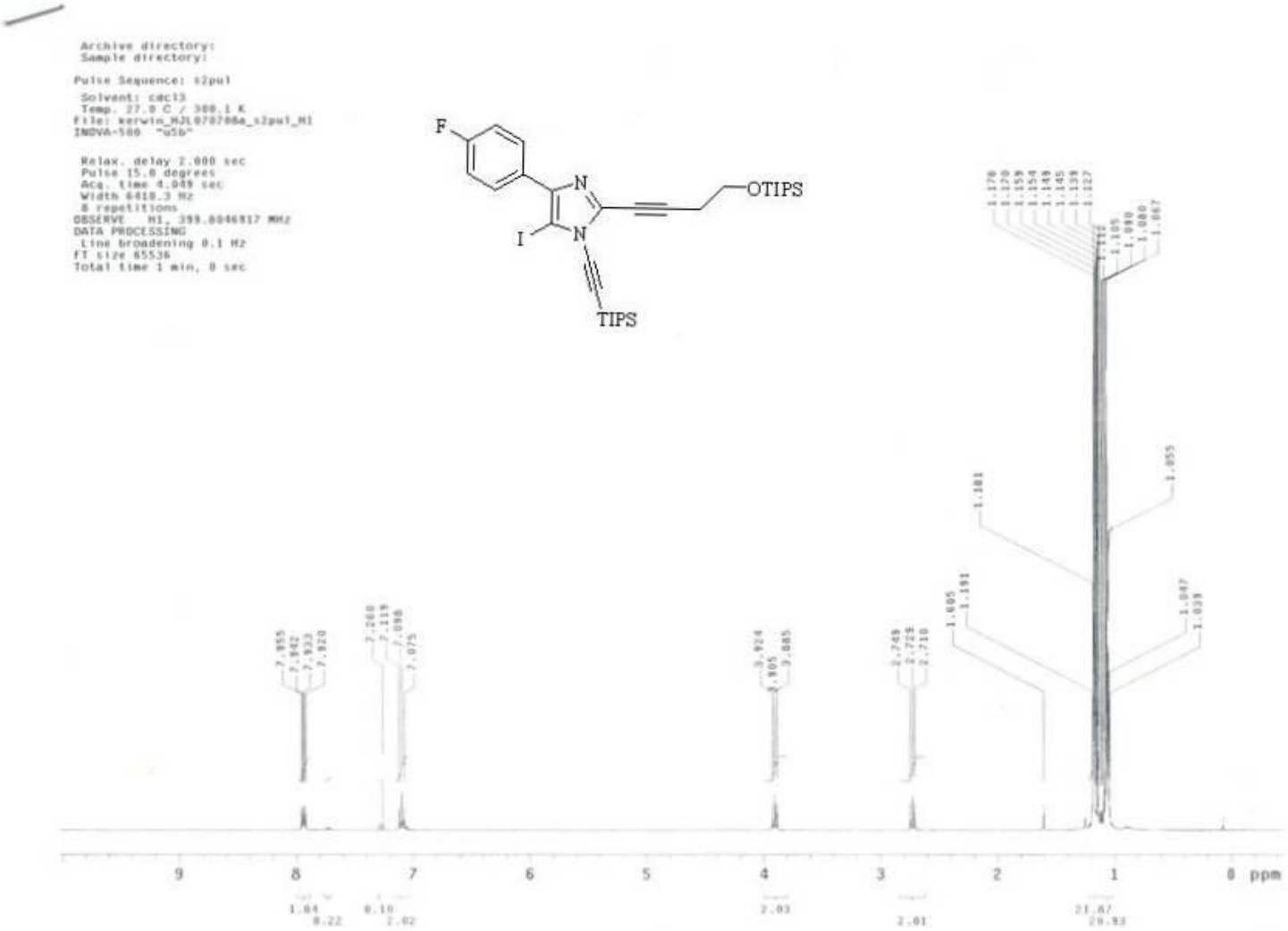
Archive directory:
Sample directory:
Pulse Sequence: s2pul
Solvent: cdcl3
Temp. 27.0 C / 300.1 K
File: kerwin_HJL070708a_s2pul_H1
INOVA-500 "g5b"
Relax. delay 2.000 sec
Pulse 15.0 degrees
Acq. time 4.049 sec
Width 6410.3 Hz
8 repetitions
OBSERVE H1, 399.8046817 MHz
DATA PROCESSING
Line broadening 0.1 Hz
FT size 65536
Total time 1 min, 8 sec
F
N
N
I
OTIPS
TIPS
9
8
7
6
5
4
3
2
1
0 ppm

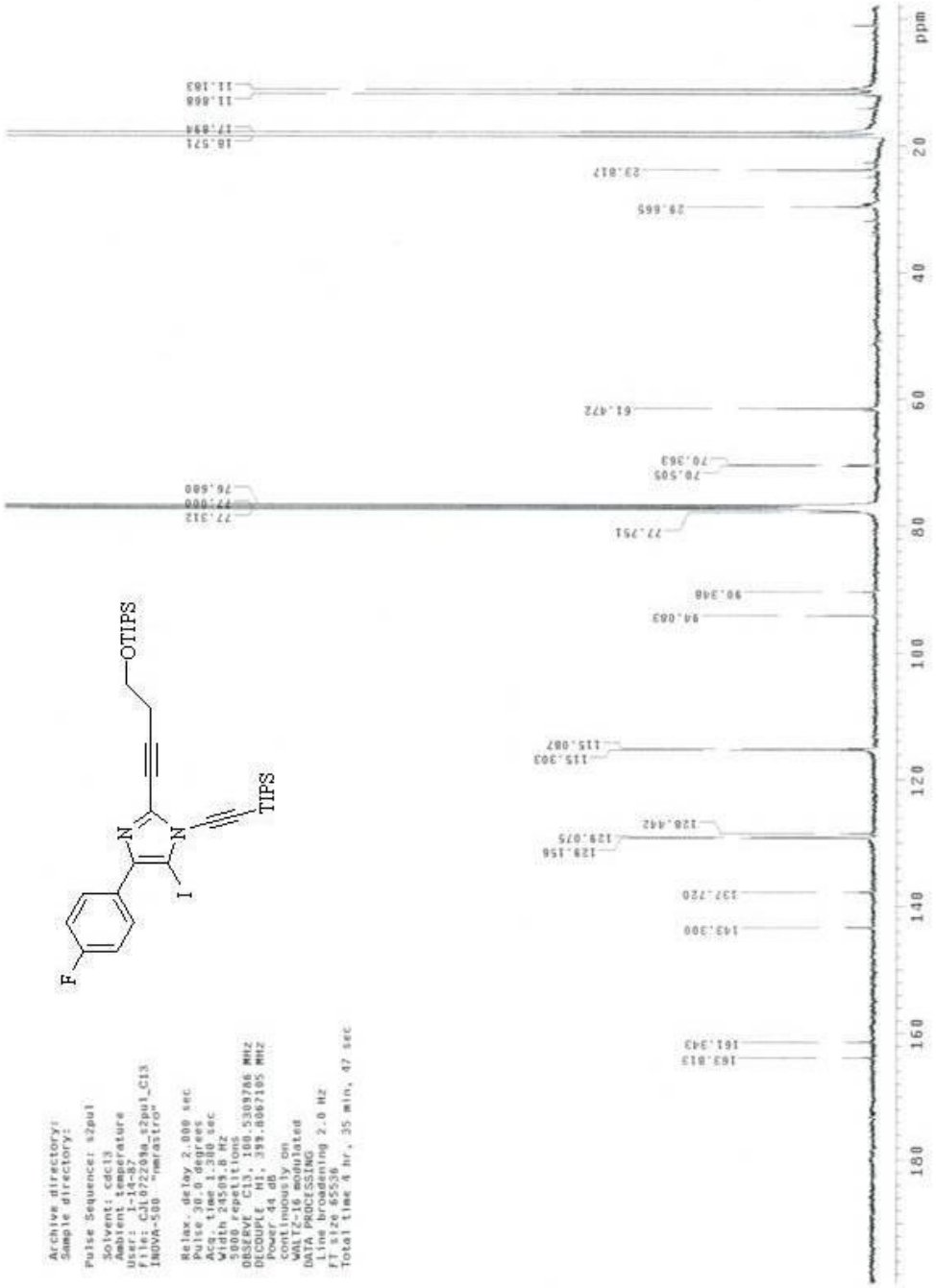
Archive directory:
Sample directory:
Pulse Sequence: s2pul
Solvent: cdcl3
Ambient temperature
User: 1 14:28:27
File: C10722ga_s2pul_C13
INOVA-500 "mafatro"
Relax. delay 2.000 sec
Pulse 90.0 degrees
Acq. time 1.200 sec
Width 24509.8 Hz
5900 repetitions
OBSERVE C13, 100.5309786 MHz
DECOUPLE H1, 399.8067185 MHz
Power 44 dB
continuously on
WALTZ-16 modulated
DATA PROCESSING
line broadening 2.0 Hz
FT size 65536
Total time 4 hr, 35 min, 47 sec
OTIPS
TIPS
N
N
I
F
ppm
20
40
60
80
100
120
140
160
180
11.163
11.868
17.894
18.571
23.817
29.665
61.472
70.363
70.505
76.600
77.000
77.312
77.751
90.348
94.063
115.087
115.303
120.442
129.075
129.156
137.720
143.300
161.343
163.813

```
expl  Proton
        SAMPLE                          SPECIAL
date   Nov  5 2008   temp        not used
solvent       cdcl3  gain        not used
file /export/home/-  spin              20
space/data/HJL1105-  hst            0.000
  08b_s2pul_H1.fid   pw90          14.800
   ACQUISITION       alfa          10.000
sw            6410.3          FLAGS
at             4.000  ii                n
np            51282   in                n
fb             4000   dp                y
bs               32   hs               nn
ss                2            PROCESSING
d1            2.000   lb             0.10
nt                8   fn            65536
ct                8            DISPLAY
   TRANSMITTER        sp              2.0
tn               H1  wp           3978.8
sfrq        399.807  rf1           3708.3
tof           399.8  rfp           2902.6
tpwr             60  rp              46.1
pw            4.933  lp               8.5
    DECOUPLER                PLOT
dn               C13  wc              250
dof                0  sc                0
dm               nnn  vs              110
dmm                c  th                4
dpwr              34  al  cdc  ph
dmf            29412
```

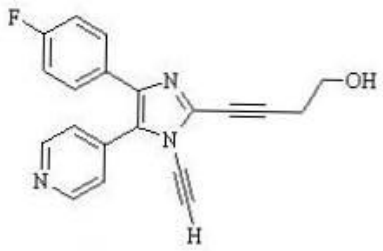

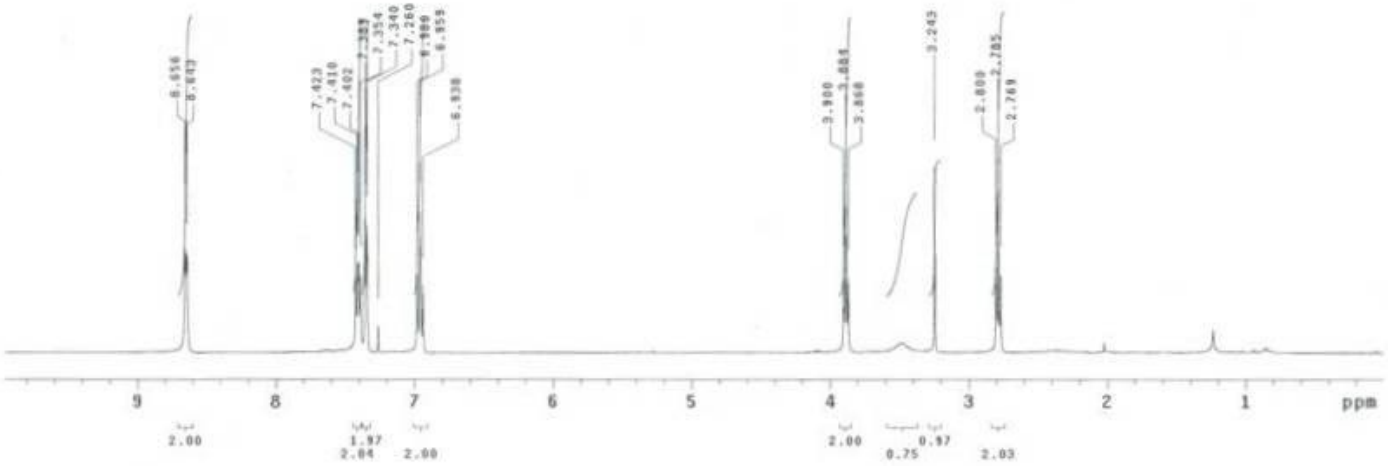

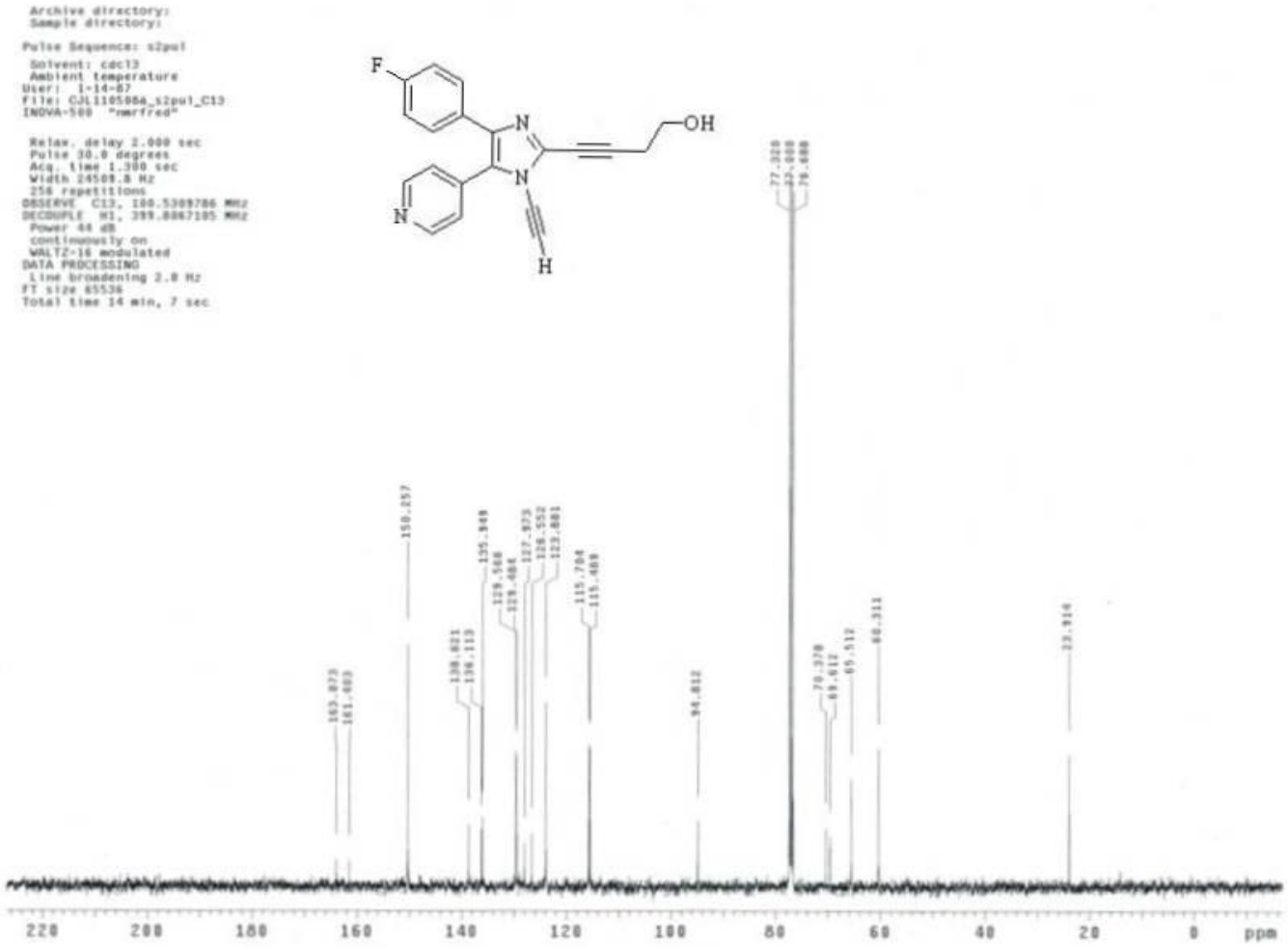
Archive directory:
Sample directory:
Pulse Sequence: s2pul
Solvent: cdcl3
Ambient temperature
User: 1-14-07
File: CJL1105086_s2pul_C13
INOVA-500 "nmrfred"
Relax. delay 2.000 sec
Pulse 30.0 degrees
Acq. time 1.300 sec
Width 24508.8 Hz
256 repetitions
OBSERVE C13, 100.5309786 MHz
DECOUPLE H1, 399.8867185 MHz
Power 44 dB
continuously on
WALTZ-16 modulated
DATA PROCESSING
Line broadening 2.0 Hz
FT size 65536
Total time 14 min, 7 sec
F
N
N
N
OH
H
163.873
161.403
150.257
140.021
136.113
135.949
129.568
129.484
127.873
126.552
123.881
115.704
115.469
94.812
77.320
77.000
76.680
70.378
69.612
65.512
60.311
23.914
220
200
180
160
140
120
100
80
60
40
20
0
ppm

Archive directory:
Sample directory:

Pulse Sequence: s2pul

Solvent: cdcl3
Ambient temperature
File: HJL082509a_01
INOVA-500 "nmrastro"

Relax. delay 2.000 sec
Pulse 30.0 degrees
Acq. time 4.000 sec
Width 6410.3 Hz
8 repetitions
OBSERVE H1, 399.8847108 MHz
DATA PROCESSING
Line broadening 0.1 Hz
FT size 65536
Total time 1 min, 8 sec

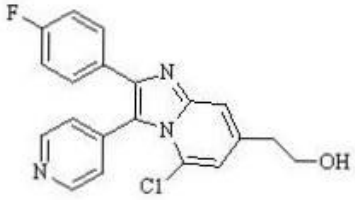

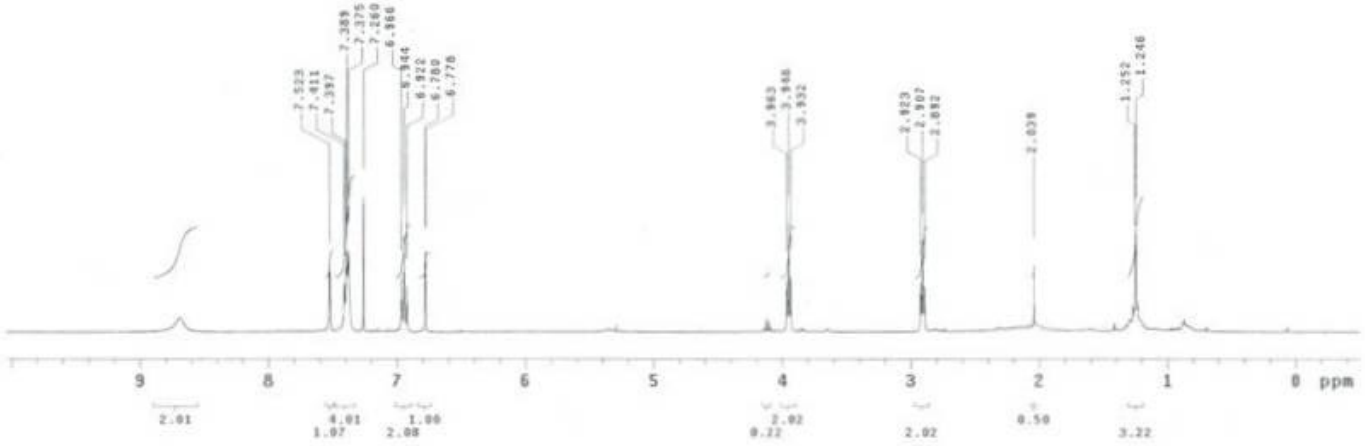

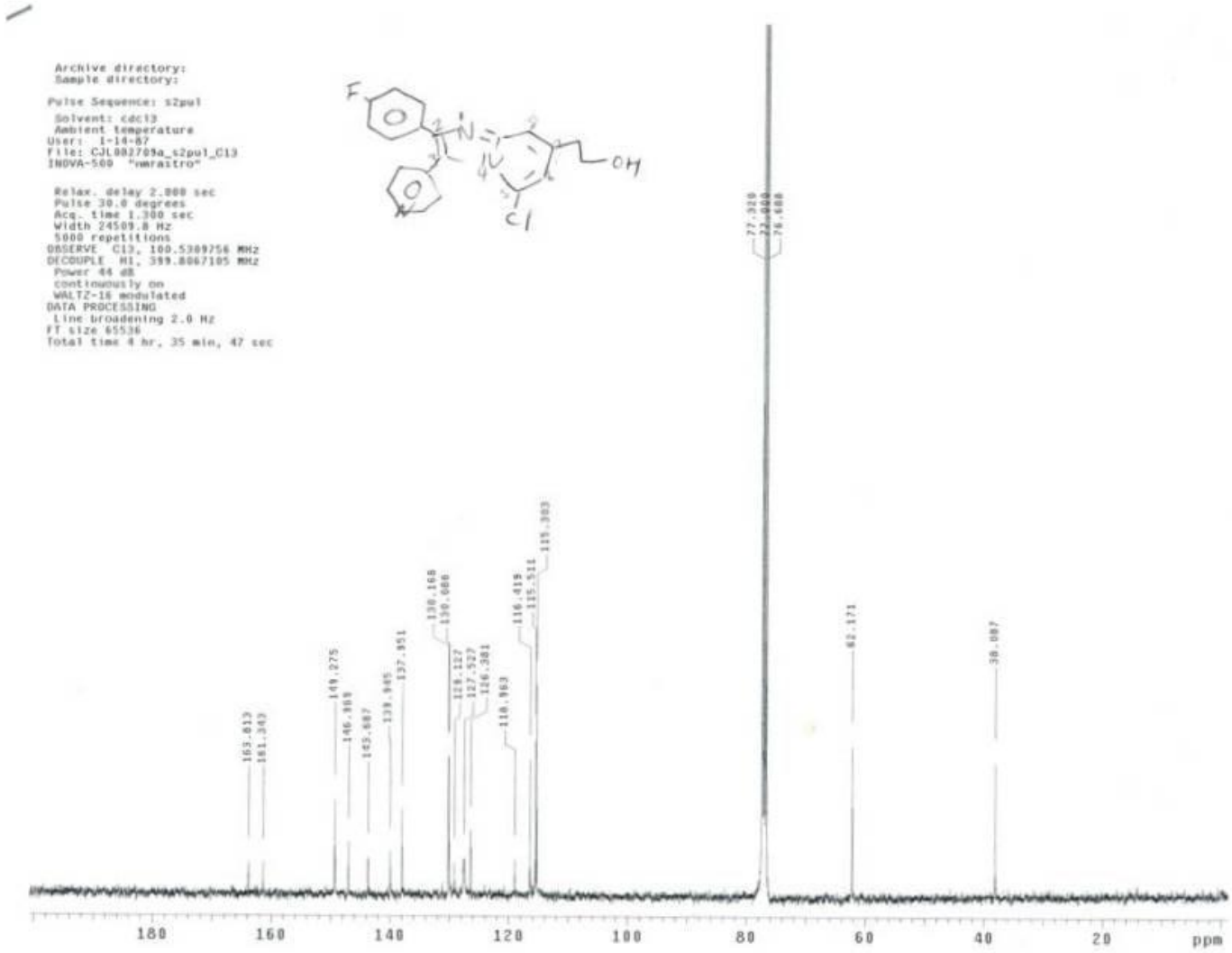
Archive directory:
Sample directory:
Pulse Sequence: s2pul
Solvent: cdcl3
Ambient temperature
User: 1-14-07
File: CJL082709a_s2pul_C13
INOVA-500 "nmrastro"
Relax. delay 2.000 sec
Pulse 30.0 degrees
Acq. time 1.300 sec
Width 24509.8 Hz
5000 repetitions
OBSERVE C13, 100.5389756 MHz
DECOUPLE H1, 399.8067105 MHz
Power 44 dB
continuously on
WALTZ-16 modulated
DATA PROCESSING
Line broadening 2.0 Hz
FT size 65536
Total time 4 hr, 35 min, 47 sec
F
OH
Cl
163.013
161.343
149.275
146.389
145.687
139.945
137.951
130.168
130.086
128.127
127.527
126.381
118.983
116.419
115.511
115.303
77.320
77.000
76.680
62.171
30.087
180
160
140
120
100
80
60
40
20
ppm

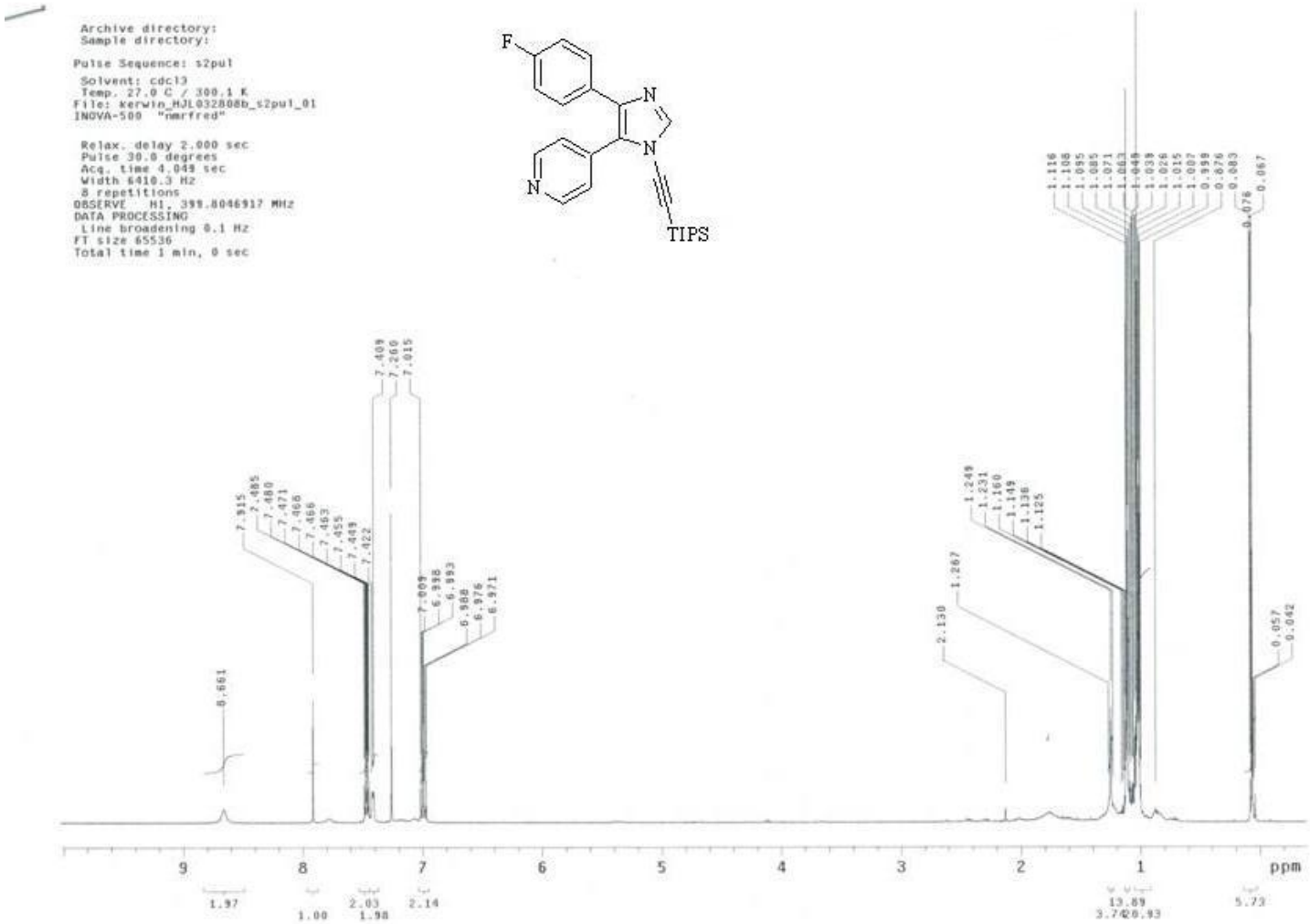
Archive directory:
Sample directory:
Pulse Sequence: s2pul
Solvent: cdcl3
Temp. 27.0 C / 300.1 K
File: kerwin_HJL032808b_s2pul_01
INOVA-500 "nmrfred"
Relax. delay 2.000 sec
Pulse 30.0 degrees
Acq. time 4.049 sec
Width 6410.3 Hz
8 repetitions
OBSERVE H1, 399.8046917 MHz
DATA PROCESSING
Line broadening 0.1 Hz
FT size 65536
Total time 1 min, 0 sec
F
N
N
N
TIPS
8.661
7.915
7.485
7.480
7.471
7.466
7.463
7.455
7.449
7.422
7.409
7.260
7.015
7.009
6.998
6.993
6.988
6.976
6.971
2.130
1.267
1.249
1.231
1.160
1.149
1.138
1.125
1.116
1.108
1.095
1.085
1.071
1.063
1.049
1.039
1.026
1.015
1.007
0.998
0.976
0.883
0.076
0.067
0.057
0.042
9
8
7
6
5
4
3
2
1
ppm
1.97
1.00
2.03
1.98
2.14
13.89
3.7@0.93
5.73

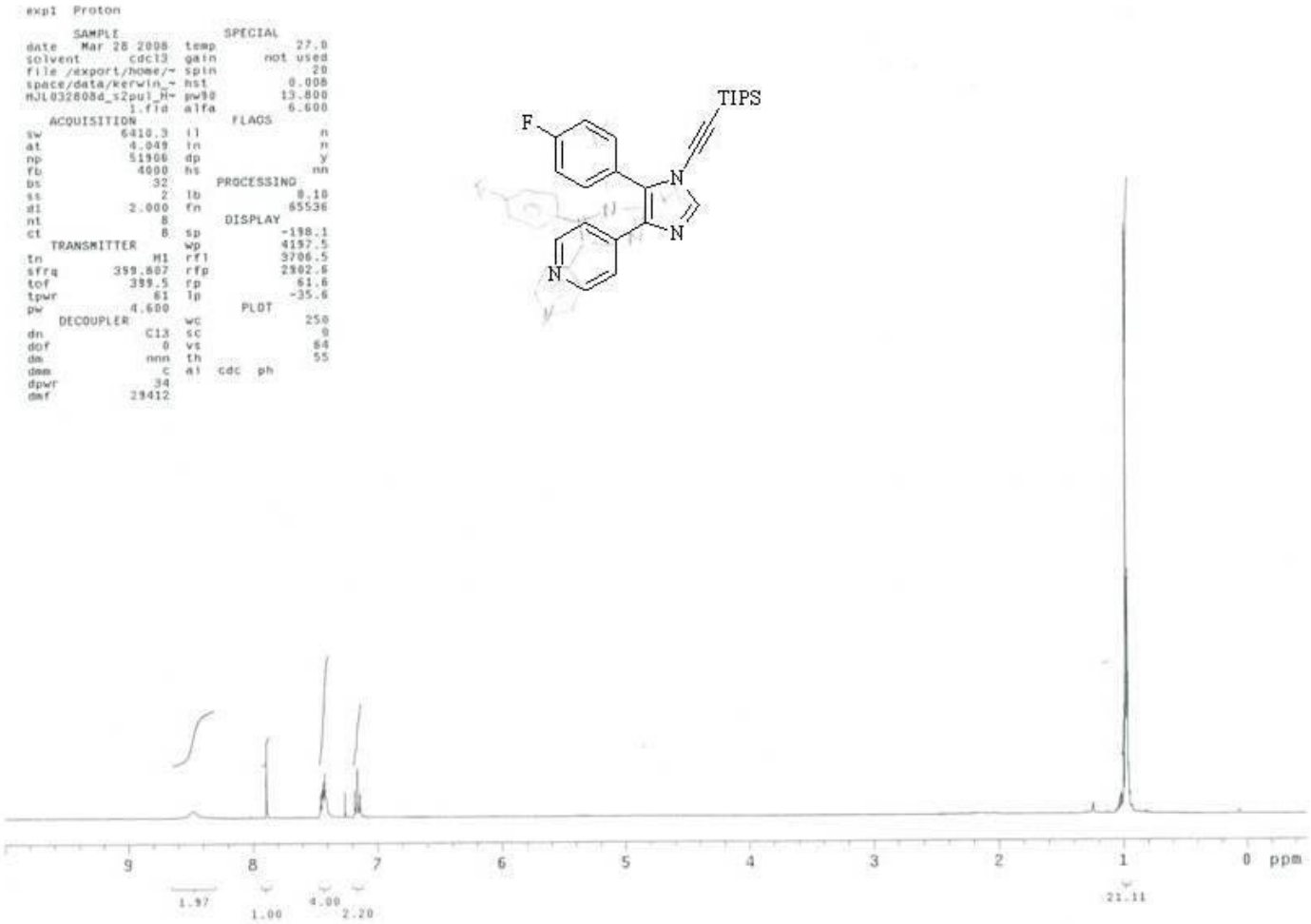
exp1 Proton
SAMPLE
date Mar 28 2008
solvent cdcl3
file /export/home/~
space/data/kerwin_~
MJL032808d_s2pul_H~
1.fid
ACQUISITION
sw 6410.3
at 4.049
np 51906
fb 4000
bs 32
ss 2
d1 2.000
nt 8
ct 8
TRANSMITTER
tn H1
sfrq 399.807
tof 399.5
tpwr 61
pw 4.600
DECOUPLER
dn C13
dof 0
dm nnn
dmm c
dpwr 34
dmf 28412
SPECIAL
temp 27.0
gain not used
spin 20
hst 0.008
pw90 13.800
alfa 6.600
FLAGS
il n
in n
dp y
hs nn
PROCESSING
lb 0.10
fn 65536
DISPLAY
sp -198.1
wp 4197.5
rf1 3706.5
rfp 2902.6
rp 61.6
lp -35.6
PLOT
wc 250
sc 0
vs 64
th 55
al cdc ph
TIPS
F
N
N
N
9
8
7
6
5
4
3
2
1
0 ppm
1.97
1.00
4.00
2.20
21.11

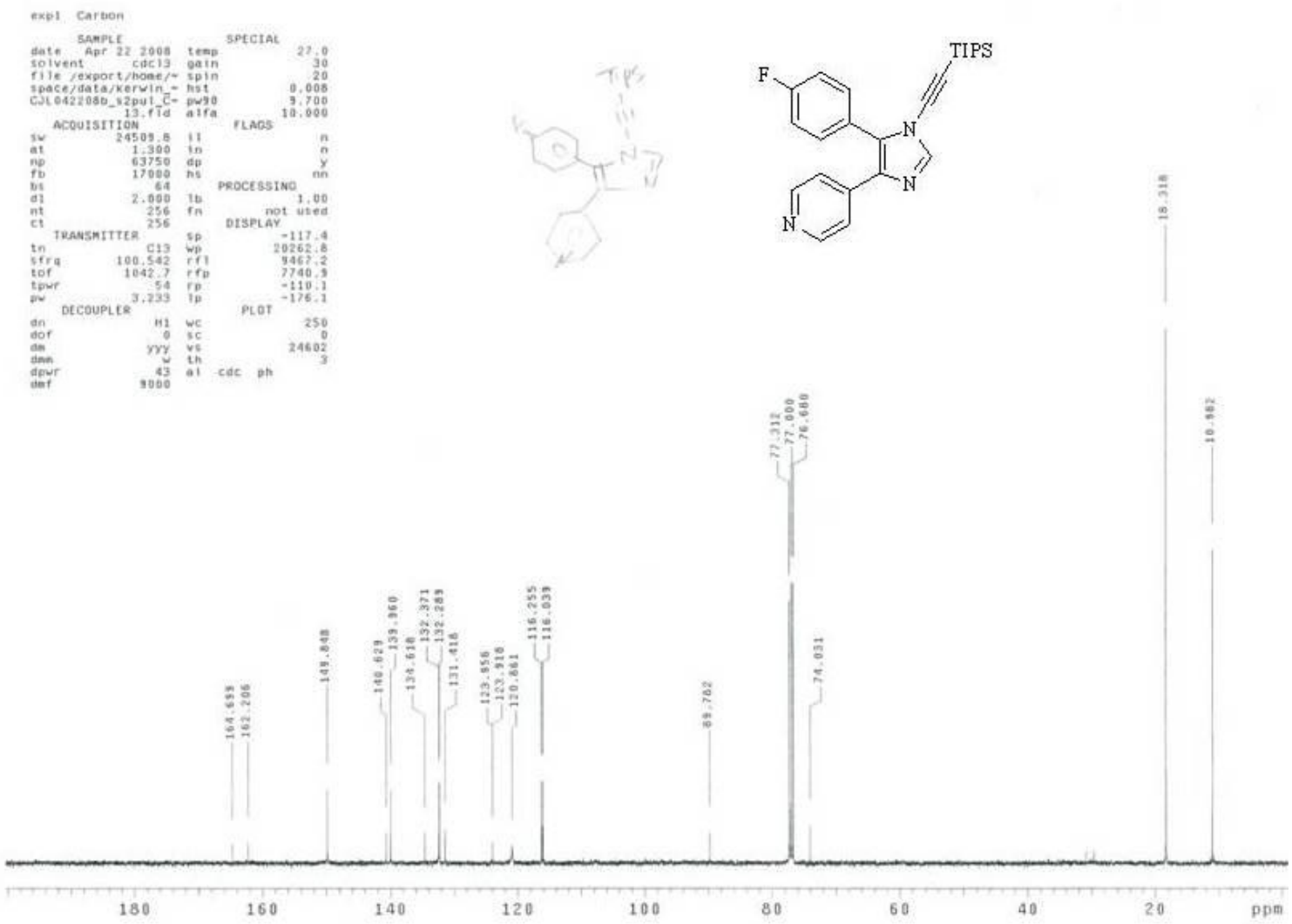
exp1 Carbon
SAMPLE
date Apr 22 2008
solvent cdcl3
file /export/home/~
space/data/kerwin_~
CJL042208b_s2pul_C-
13.fid
ACQUISITION
sw 24509.8
at 1.300
np 63750
fb 17000
bs 64
d1 2.000
nt 256
ct 256
TRANSMITTER
tn C13
sfrq 100.542
tof 1042.7
tpwr 54
pw 3.233
DECOUPLER
dn H1
dof 0
dm yyy
dmm w
dpwr 43
dmf 9000
SPECIAL
temp 27.0
gain 30
spin 20
hst 0.008
pw90 9.700
alfa 10.000
FLAGS
il n
in n
dp y
hs nn
PROCESSING
lb 1.00
fn not used
DISPLAY
sp -117.4
wp 20262.8
rf1 9467.2
rfp 7740.9
rp -110.1
lp -176.1
PLOT
wc 250
sc 0
vs 24602
th 3
al cdc ph
TIPS
F
N
N
N
164.659
162.206
149.848
140.629
139.960
134.618
132.371
132.289
131.418
125.856
123.918
120.661
116.255
116.039
89.762
77.312
77.000
76.688
74.031
18.318
10.982
180
160
140
120
100
80
60
40
20
ppm

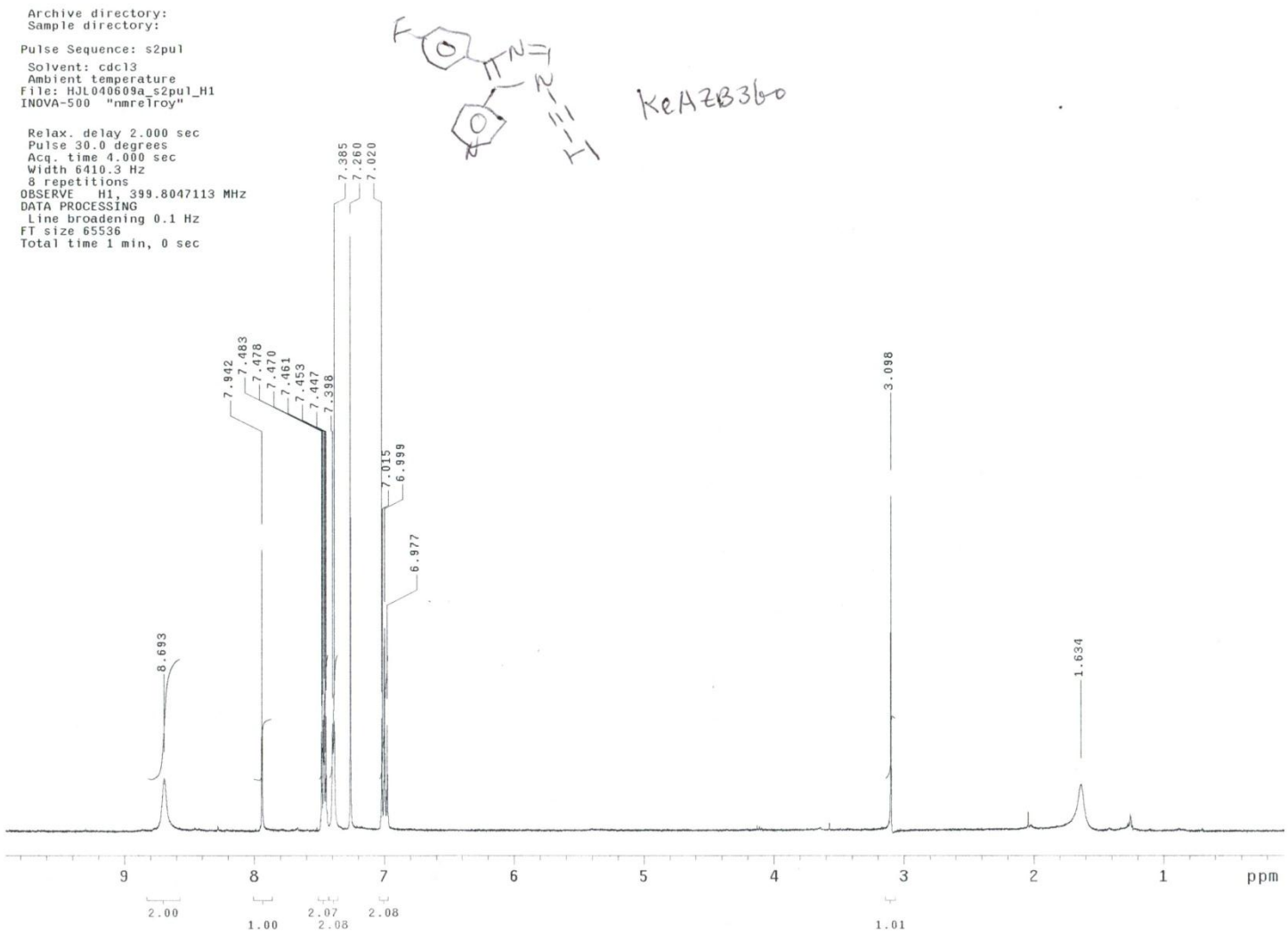
Archive directory:
Sample directory:
Pulse Sequence: s2pul
Solvent: cdcl3
Ambient temperature
File: HJL040609a_s2pul_H1
INOVA-500 "nmrelroy"
Relax. delay 2.000 sec
Pulse 30.0 degrees
Acq. time 4.000 sec
Width 6410.3 Hz
8 repetitions
OBSERVE H1, 399.8047113 MHz
DATA PROCESSING
Line broadening 0.1 Hz
FT size 65536
Total time 1 min, 0 sec
KeAZB360
8.693
7.942
7.483
7.478
7.470
7.461
7.453
7.447
7.398
7.385
7.260
7.020
7.015
6.999
6.977
3.098
1.634
9
8
7
6
5
4
3
2
1
ppm
2.00
1.00
2.07
2.08
2.08
1.01

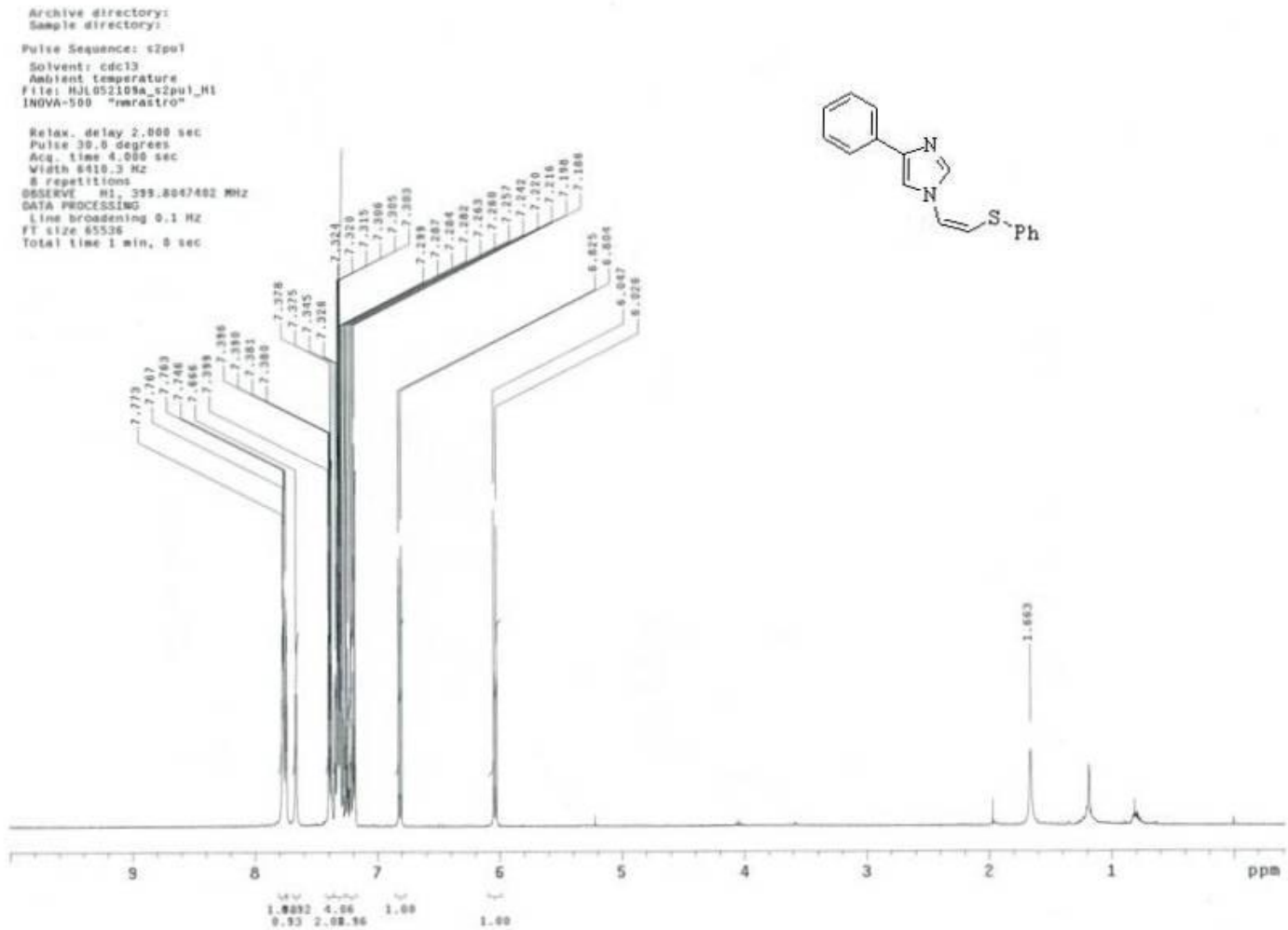
Archive directory:
Sample directory:
Pulse Sequence: s2pul
Solvent: cdcl3
Ambient temperature
File: HJL052109a_s2pul_H1
INOVA-500 "rmrastro"
Relax. delay 2.000 sec
Pulse 30.0 degrees
Acq. time 4.000 sec
Width 6410.3 Hz
8 repetitions
OBSERVE H1, 399.8047402 MHz
DATA PROCESSING
Line broadening 0.1 Hz
FT size 65536
Total time 1 min, 8 sec
N
N
S
Ph
1.663
9
8
7
6
5
4
3
2
1
ppm
1.00
1.00

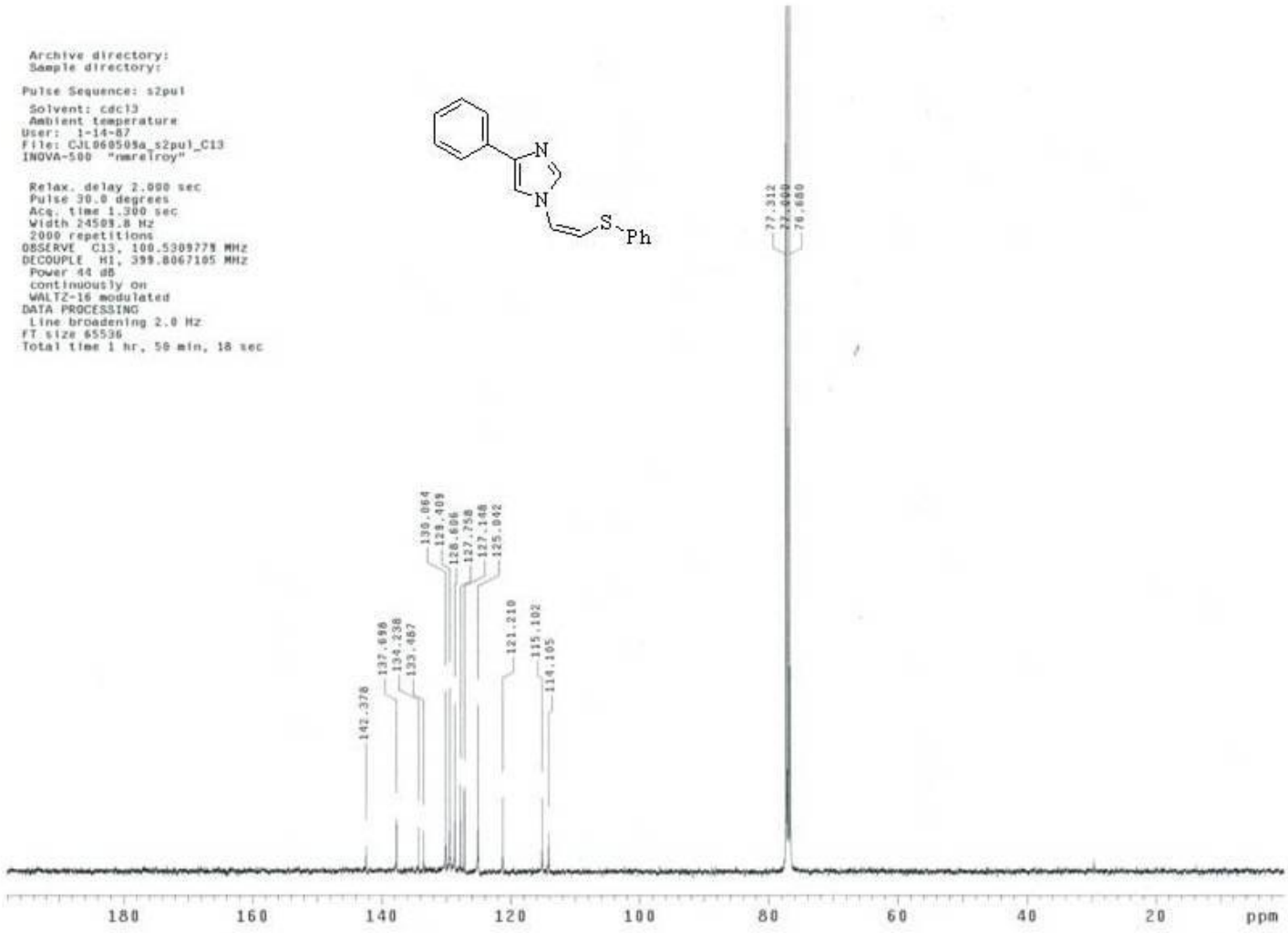
Archive directory:
Sample directory:
Pulse Sequence: s2pul
Solvent: cdcl3
Ambient temperature
User: 1-14-87
File: CJL060505a_s2pul_C13
INOVA-500 "nmrelroy"
Relax. delay 2.000 sec
Pulse 30.0 degrees
Acq. time 1.300 sec
Width 24509.8 Hz
2000 repetitions
OBSERVE C13, 100.5309779 MHz
DECOUPLE H1, 399.8067105 MHz
Power 44 dB
continuously on
WALTZ-16 modulated
DATA PROCESSING
Line broadening 2.0 Hz
FT size 65536
Total time 1 hr, 50 min, 18 sec
N
N
S
Ph
142.378
137.698
134.238
133.487
130.064
128.409
128.606
127.758
127.148
125.042
121.210
115.102
114.105
77.312
77.000
76.680
180
160
140
120
100
80
60
40
20
ppm

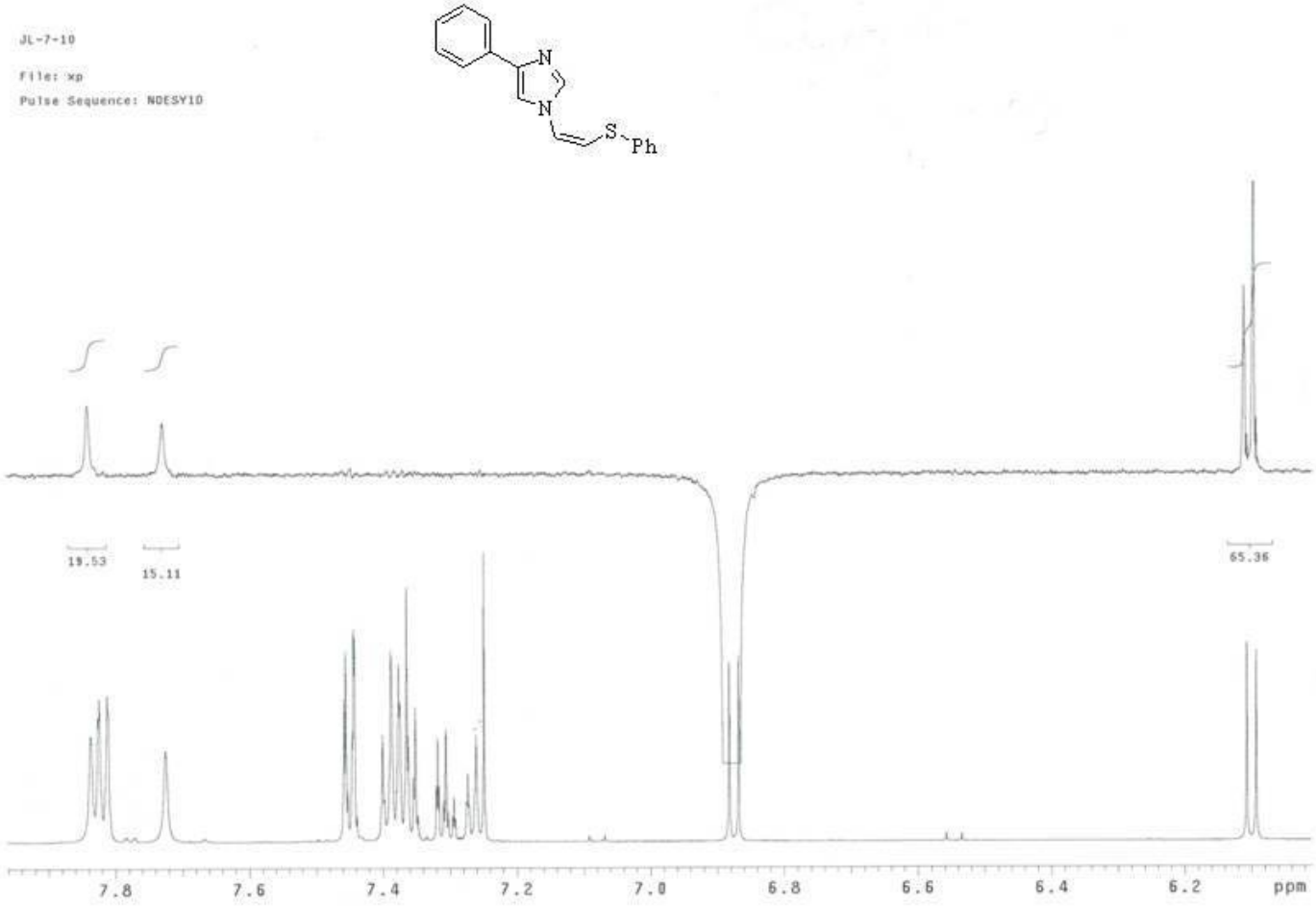
JL-7-10
File: xp
Pulse Sequence: NOESY1D
N
N
S
Ph
19.53
15.11
65.36
7.8
7.6
7.4
7.2
7.0
6.8
6.6
6.4
6.2
ppm

JL-7-10

File: xp

Pulse Sequence: NOESY1D

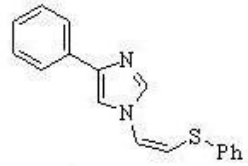

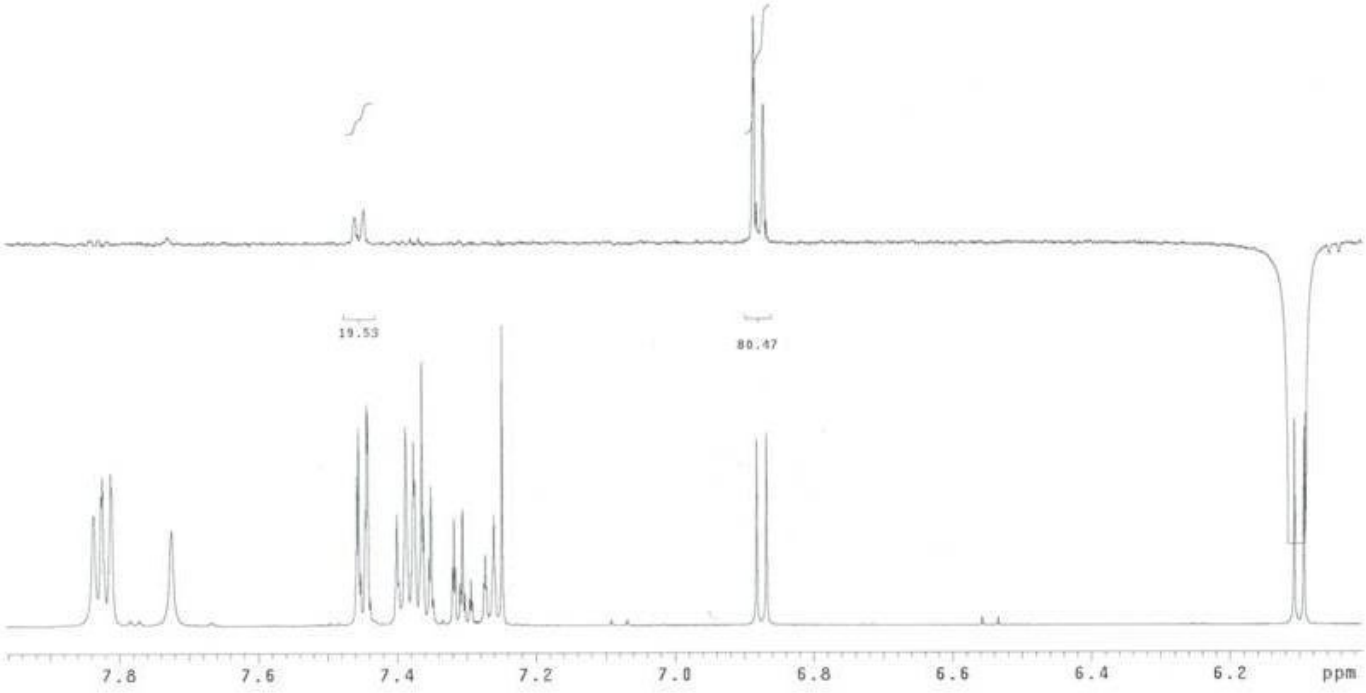

Archive directory:
Sample directory:

Pulse Sequence: s2pul

Solvent: cdcl3
Ambient temperature
File: HJL091310a_s2pul_H1
INOVA-500 "nmrastro"

Relax. delay 2.000 sec
Pulse 30.0 degrees
Acq. time 4.000 sec
Width 6410.3 Hz
8 repetitions
OBSERVE H1, 399.8047115 MHz
DATA PROCESSING
Line broadening 0.1 Hz
FT size 65536
Total time 1 min, 0 sec

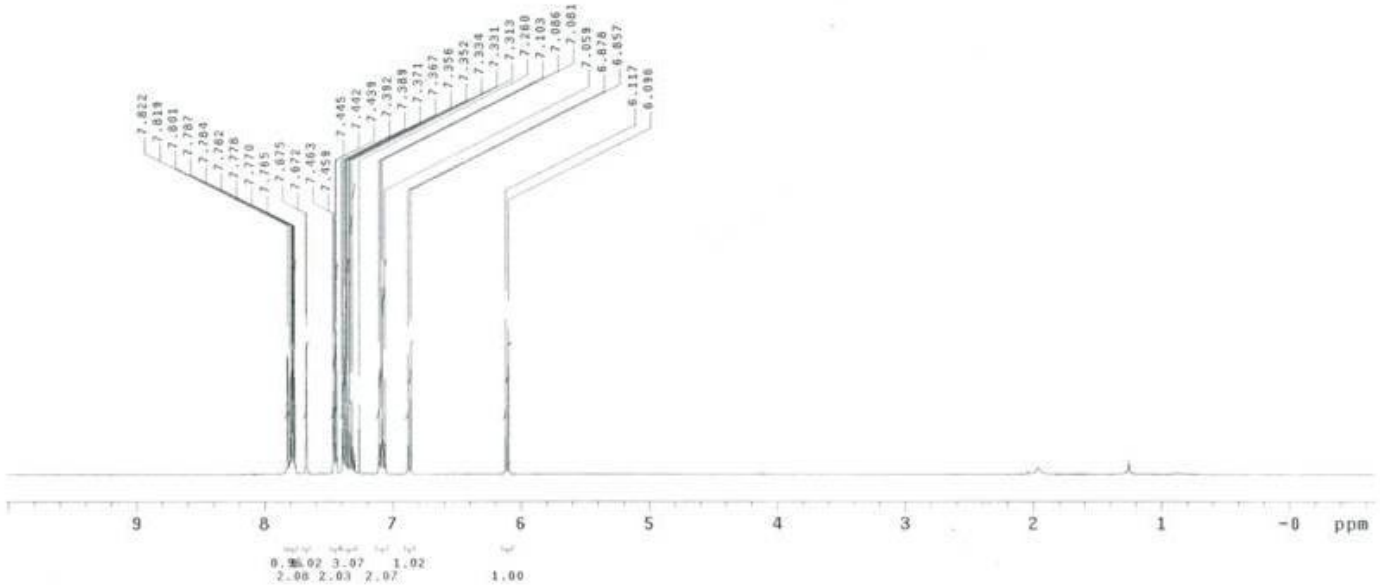

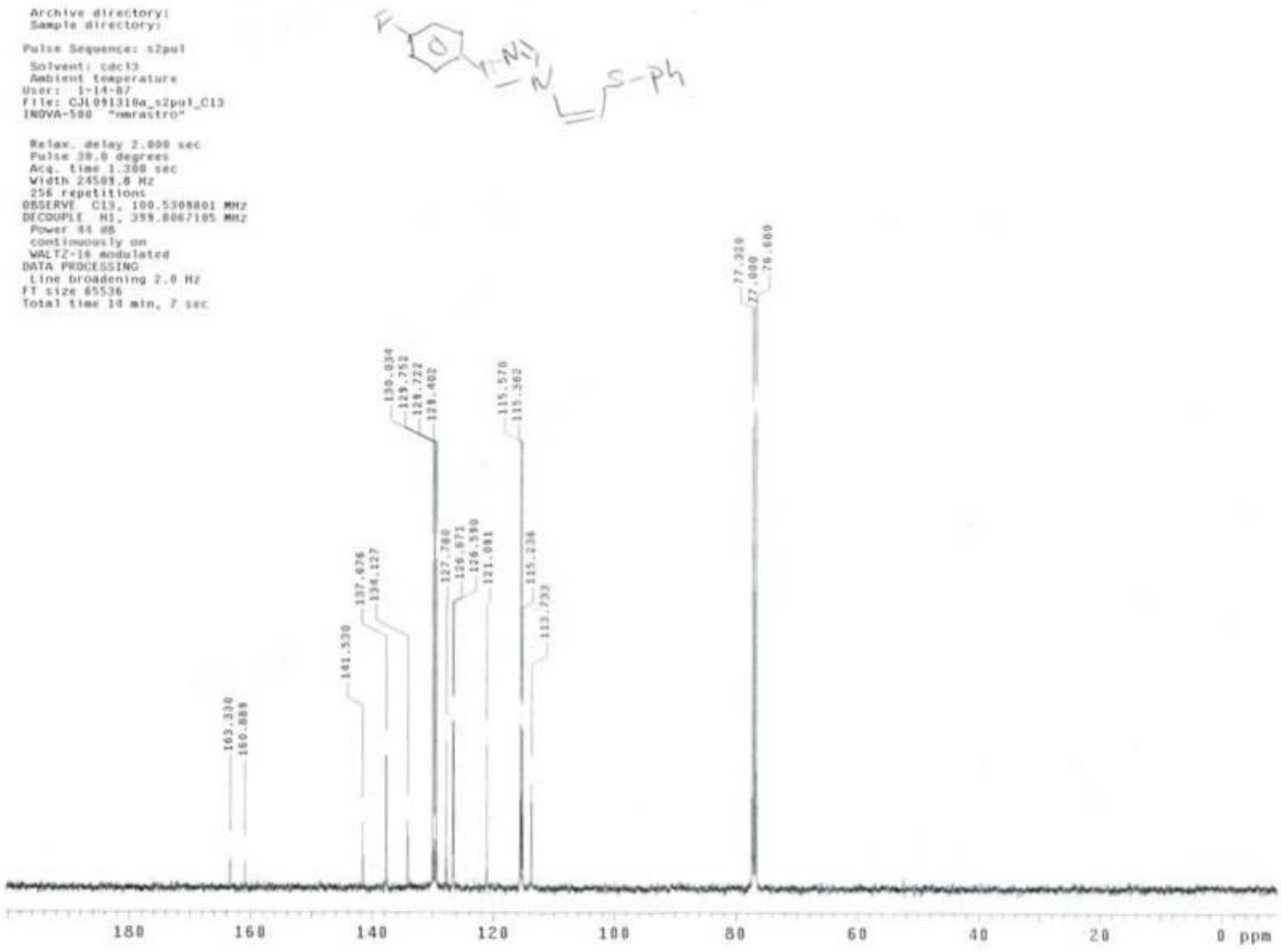
Archive directory:
Sample directory:
Pulse Sequence: s2pul
Solvent: cdcl3
Ambient temperature
User: 1-14-87
File: CJL091310a_s2pul_C13
INOVA-500 "nmrastro"
Relax. delay 2.000 sec
Pulse 30.0 degrees
Acq. time 1.300 sec
Width 24509.8 Hz
256 repetitions
OBSERVE C13, 100.5309801 MHz
DECOUPLE H1, 399.8067105 MHz
Power 44 dB
continuously on
WALTZ-16 modulated
DATA PROCESSING
Line broadening 2.0 Hz
FT size 65536
Total time 10 min, 7 sec
F
N
S-Ph
163.330
160.888
141.530
137.678
134.127
130.034
129.752
129.722
128.402
127.780
126.671
126.590
121.081
115.570
115.362
115.236
113.793
77.330
77.000
76.669
180
160
140
120
100
80
60
40
20
0 ppm

Archive directory:
Sample directory:

Pulse Sequence: s2pul

Solvent: cdcl3
Ambient temperature
File: HJL011910b_s2pul_H1
INOVA-500 "nmrelroy"

Relax. delay 2.000 sec
Pulse 30.0 degrees
Acq. time 4.000 sec
Width 6410.3 Hz
8 repetitions
OBSERVE H1, 399.8047107 MHz
DATA PROCESSING
Line broadening 0.1 Hz
FT size 65536
Total time 1 min, 0 sec

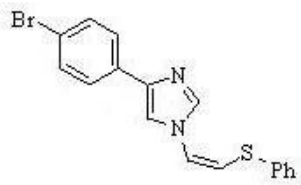

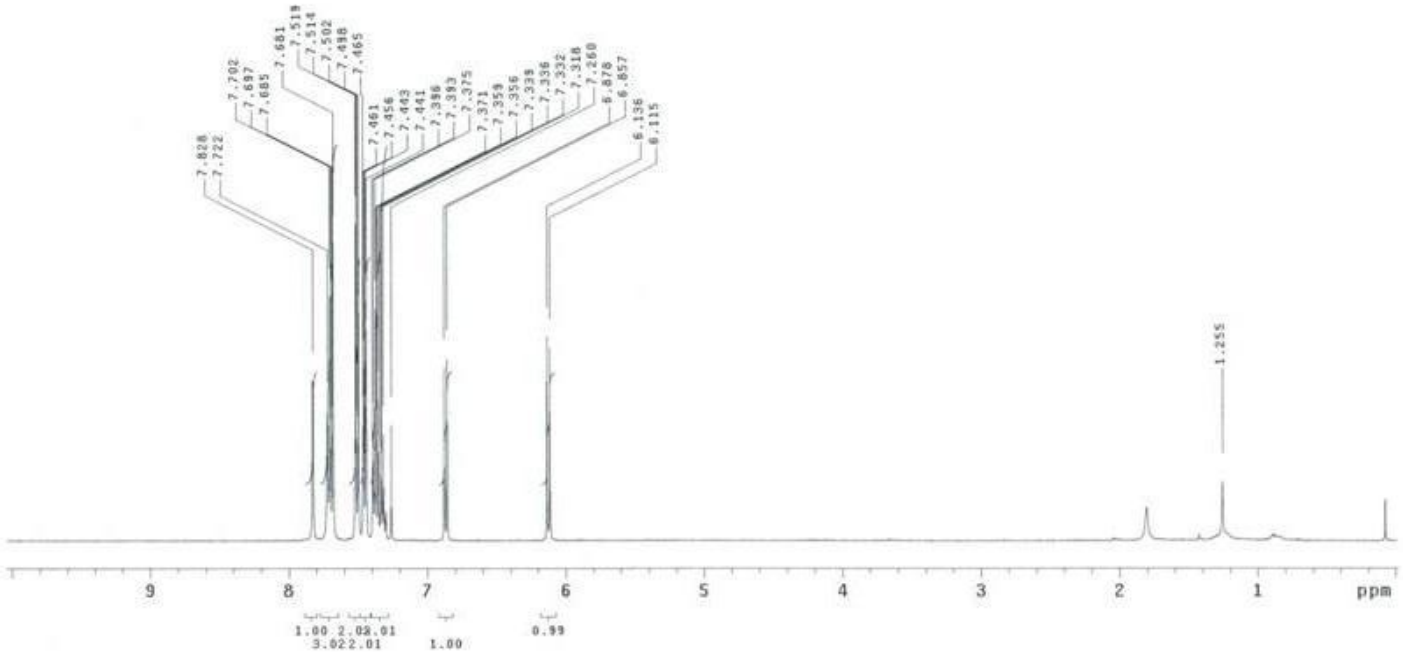

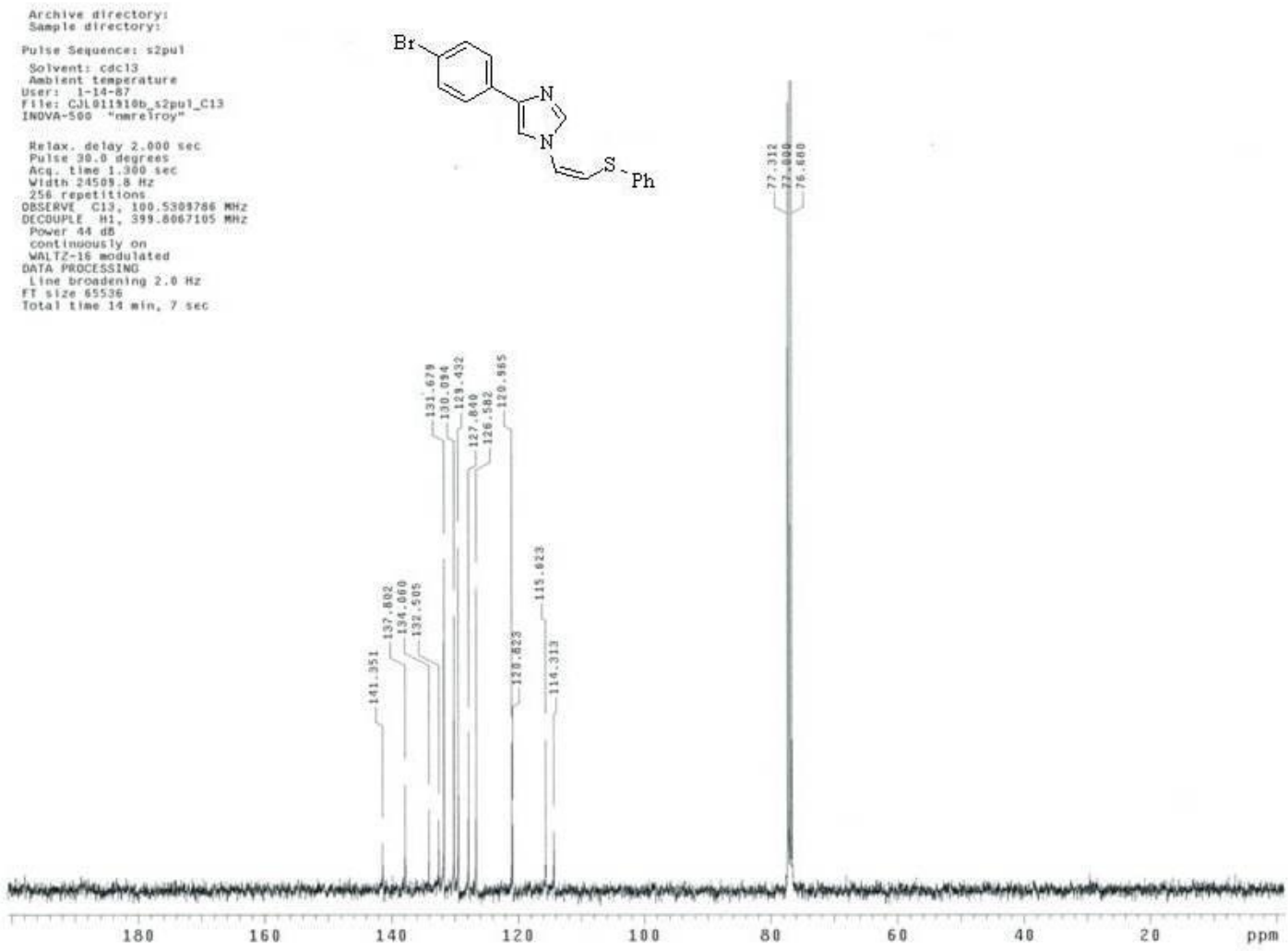
Archive directory:
Sample directory:
Pulse Sequence: s2pul
Solvent: cdcl3
Ambient temperature
User: 1-14-87
File: CJL011910b_s2pul_C13
INOVA-500 "nmrelroy"
Relax. delay 2.000 sec
Pulse 30.0 degrees
Acq. time 1.300 sec
Width 24509.8 Hz
256 repetitions
OBSERVE C13, 100.5309786 MHz
DECOUPLE H1, 399.8067105 MHz
Power 44 dB
continuously on
WALTZ-16 modulated
DATA PROCESSING
Line broadening 2.0 Hz
FT size 65536
Total time 14 min, 7 sec
Br
N
N
S
Ph
141.351
137.802
134.060
132.505
131.679
130.094
129.432
127.840
126.582
120.585
120.623
115.623
114.313
77.312
77.000
76.688
180
160
140
120
100
80
60
40
20
ppm

Archive directory:
Sample directory:

Pulse Sequence: s2pul

Solvent: cdcl3
Ambient temperature
file: HJL030B10b_s2pul_H1
INOVA-500 "nmrelroy"

Relax. delay 2.000 sec
Pulse 30.0 degrees
Acq. time 4.000 sec
Width 6410.3 Hz
8 repetitions
OBSERVE H1, 399.8047111 MHz
DATA PROCESSING
Line broadening 0.1 Hz
FT size 65536
Total time 1 min, 0 sec

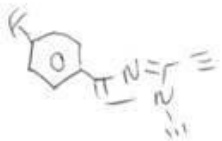

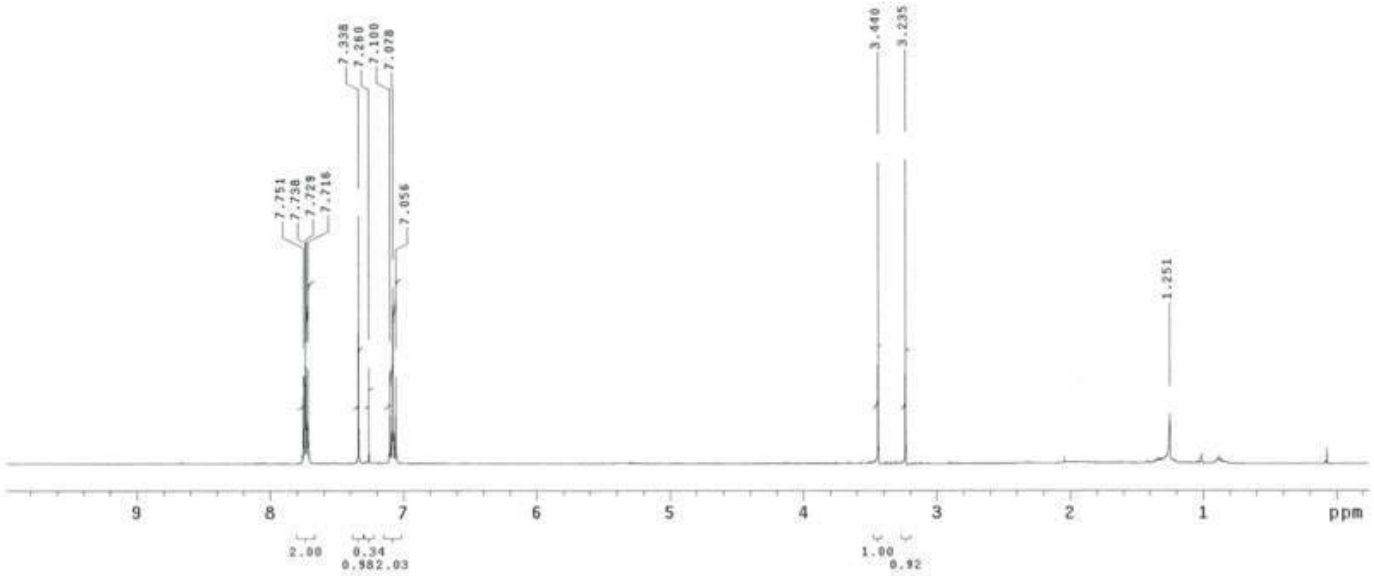

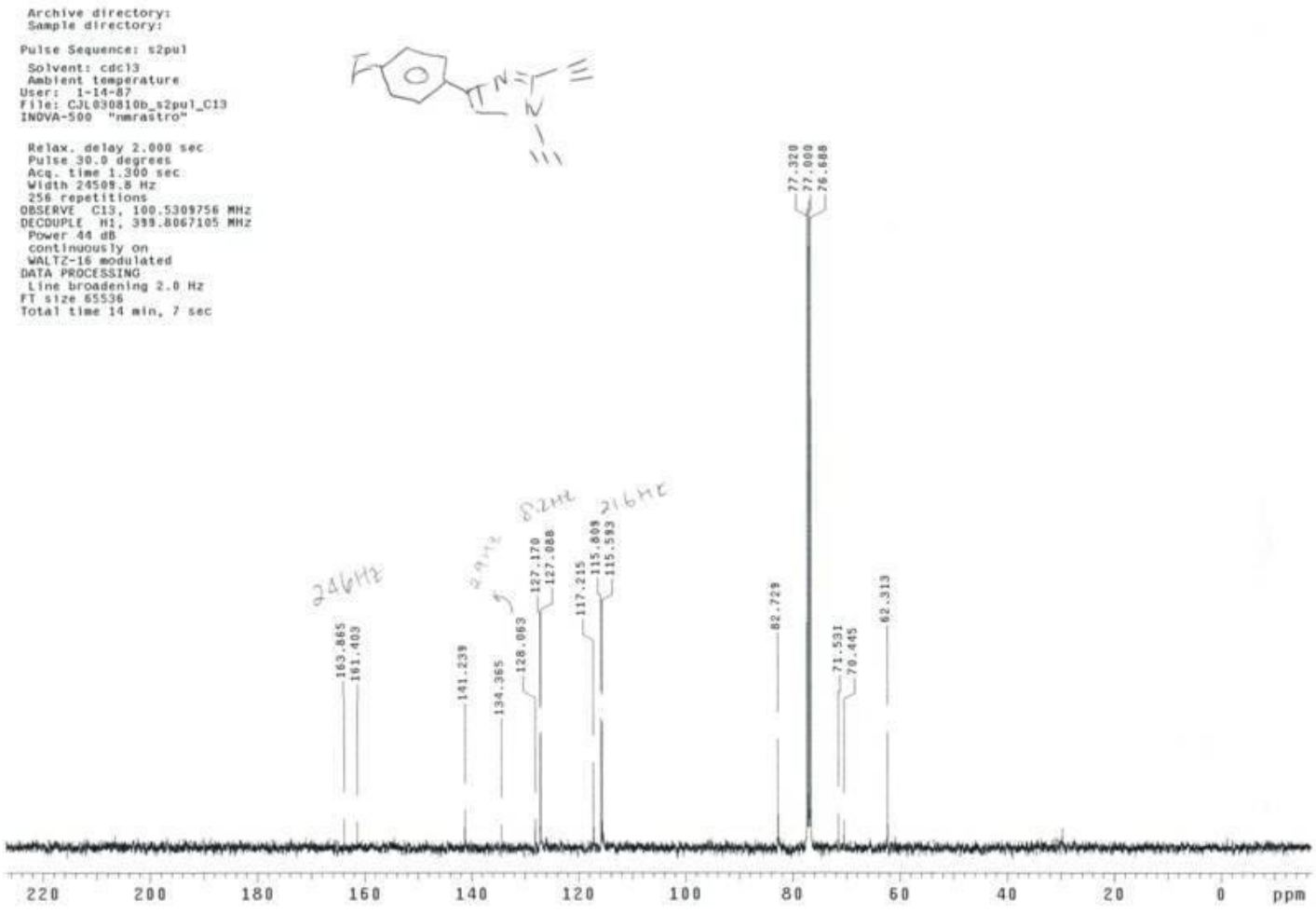
Archive directory:
Sample directory:
Pulse Sequence: s2pul
Solvent: cdcl3
Ambient temperature
User: 1-14-87
File: CJL030810b_s2pul_C13
INOVA-500 "nmrastro"
Relax. delay 2.000 sec
Pulse 30.0 degrees
Acq. time 1.300 sec
Width 24509.8 Hz
256 repetitions
OBSERVE C13, 100.5309756 MHz
DECOUPLE H1, 399.8067105 MHz
Power 44 dB
continuously on
WALTZ-16 modulated
DATA PROCESSING
Line broadening 2.0 Hz
FT size 65536
Total time 14 min, 7 sec
246Hz
29Hz
82Hz
216Hz
163.865
161.403
141.239
134.365
128.063
127.170
127.088
117.215
115.809
115.583
82.729
77.320
77.000
76.688
71.531
70.445
62.313
220
200
180
160
140
120
100
80
60
40
20
0
ppm

exp1 Proton

SAMPLE		SPECIAL	
date	Jun 27 2008	temp	27.0
solvent	cd3od	gain	not used
file	/mnt/home_dir~	spin	20
	s/space/data/kerwi~	hst	0.008
	n_HJL062708b_s2pul~	pw90	13.800
	_H1.fid	alfa	6.600
ACQUISITION		FLAGS	
sw	6410.3	il	n
at	4.049	in	n
np	51906	dp	y
fb	4000	hs	nn
bs	32	PROCESSING	
ss	2	lb	0.10
d1	2.000	fn	65536
nt	8	DISPLAY	
ct	8	sp	-200.3
TRANSMITTER		wp	4197.5
tn	H1	rf1	2125.5
sfrq	399.809	rfp	1319.4
tof	399.4	rp	155.8
tpwr	61	lp	-18.9
pw	2.300	PLOT	
DECOUPLER		wc	250
dn	C13	sc	0
dof	0	vs	29
dm	nnn	th	3
dmm	c	al cdc ph	
dpwr	34		
dmf	29412		

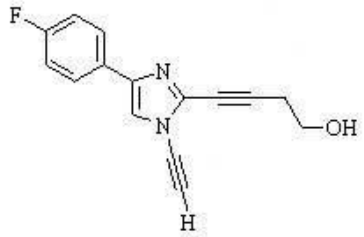

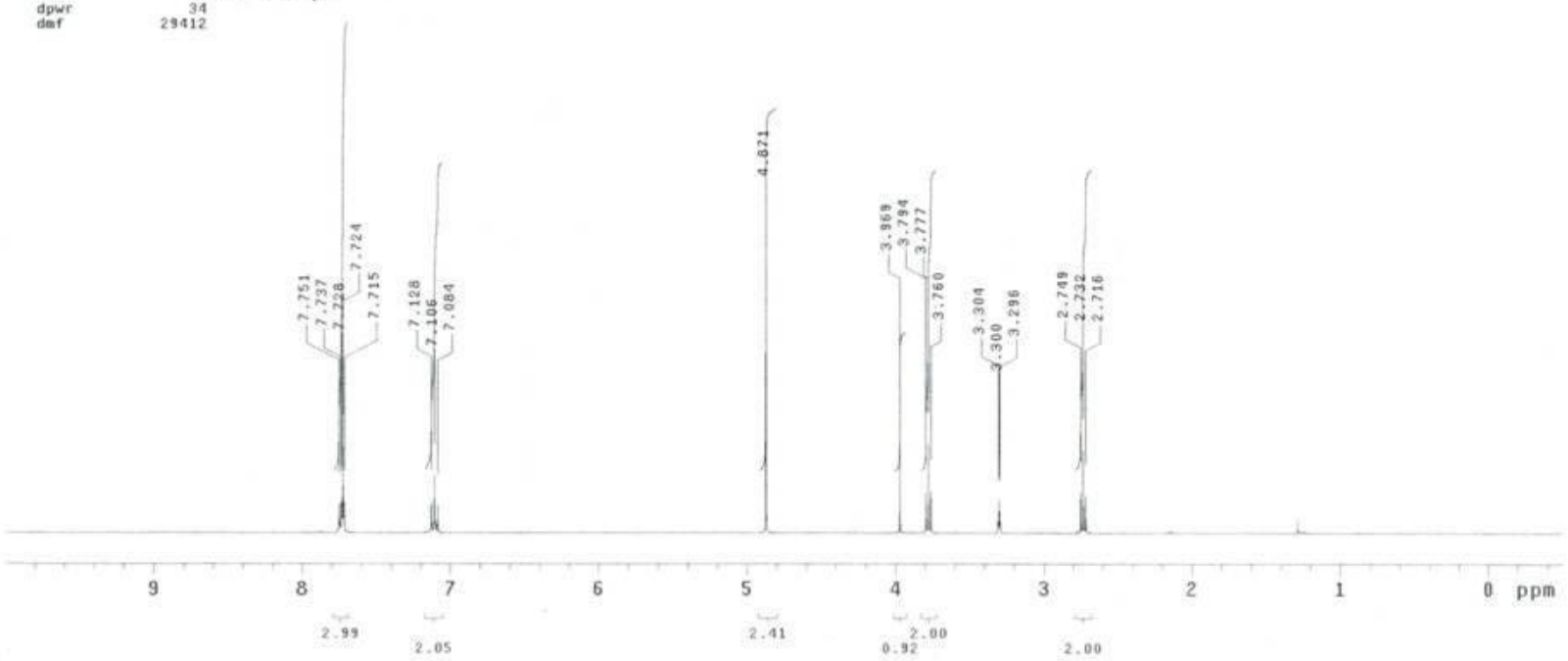

Archive directory:
Sample directory:

Pulse Sequence: s2pul

Solvent: cdcl3
Temp. 27.0 C / 300.1 K
User: 1-14-87
File: kerwin_CJL062808b_s2pul_C13
INOVA-500 "nmrfred"

Relax. delay 2.000 sec
Pulse 15.0 degrees
Acq. time 1.300 sec
Width 24509.8 Hz
2000 repetitions
OBSERVE C13, 100.5309719 MHz
DECOUPLE H1, 399.8066932 MHz
Power 43 dB
continuously on
WALTZ-16 modulated
DATA PROCESSING
Line broadening 1.0 Hz
FT size 65536
Total time 1 hr, 50 min, 18 sec

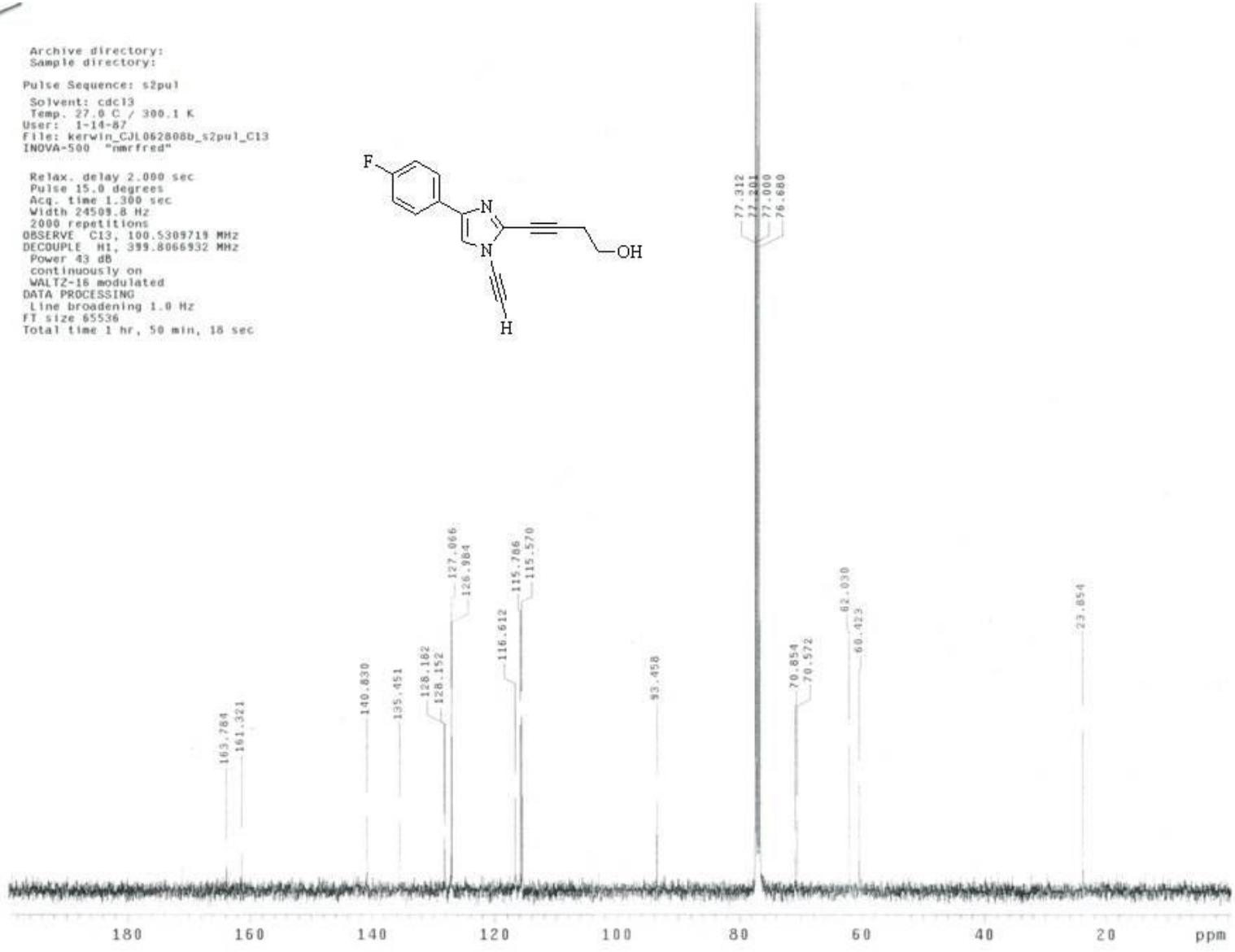

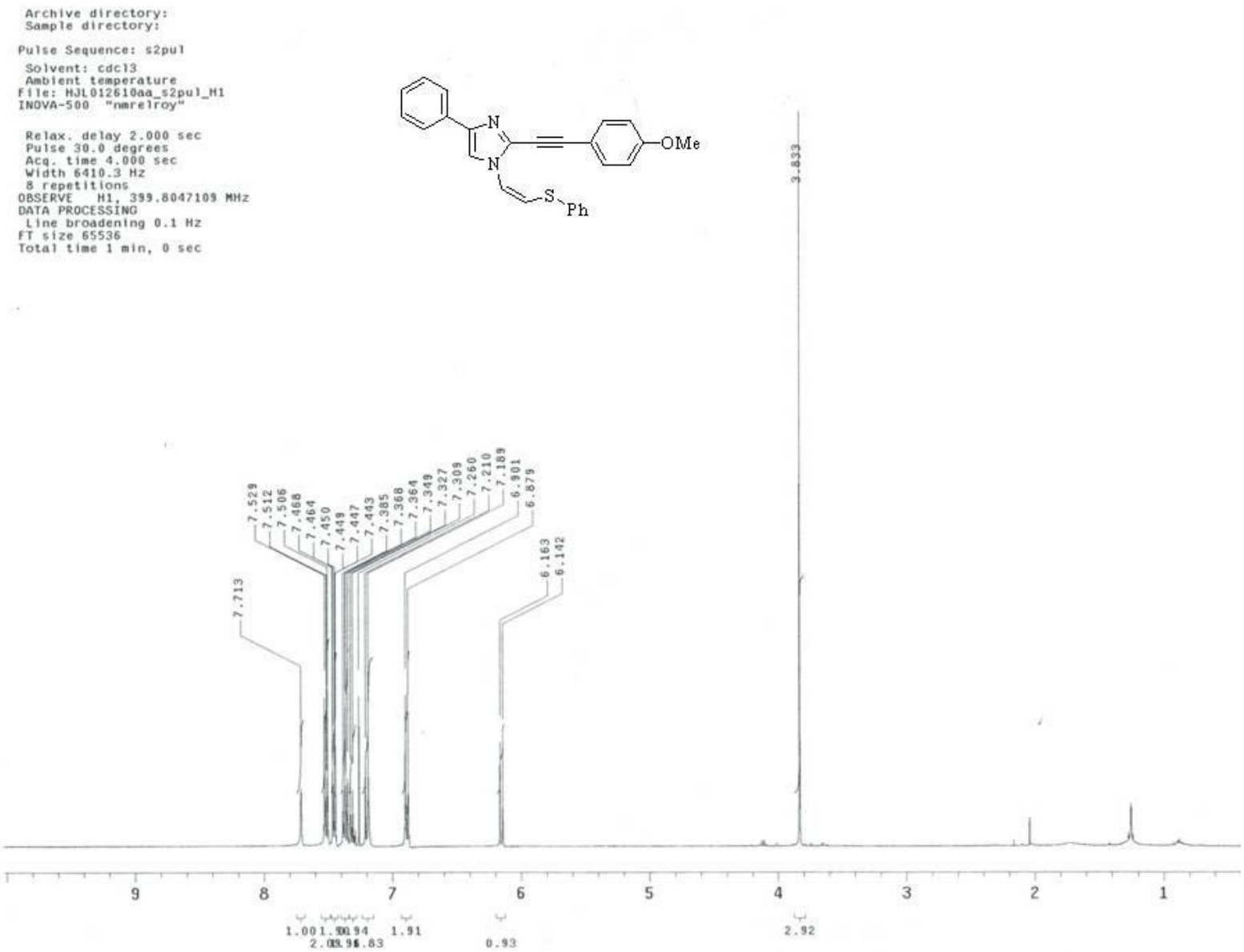
Archive directory:
Sample directory:
Pulse Sequence: s2pul
Solvent: cdcl3
Ambient temperature
File: HJL012610aa_s2pul_H1
INOVA-500 "nmrelroy"
Relax. delay 2.000 sec
Pulse 30.0 degrees
Acq. time 4.000 sec
Width 6410.3 Hz
8 repetitions
OBSERVE H1, 399.8047109 MHz
DATA PROCESSING
Line broadening 0.1 Hz
FT size 65536
Total time 1 min, 0 sec
N
N
OMe
S
Ph
7.713
7.529
7.512
7.506
7.468
7.464
7.450
7.449
7.447
7.443
7.385
7.368
7.364
7.349
7.327
7.309
7.260
7.210
7.189
6.901
6.879
6.163
6.142
3.833
9
8
7
6
5
4
3
2
1
1.00
1.91
0.93
2.92

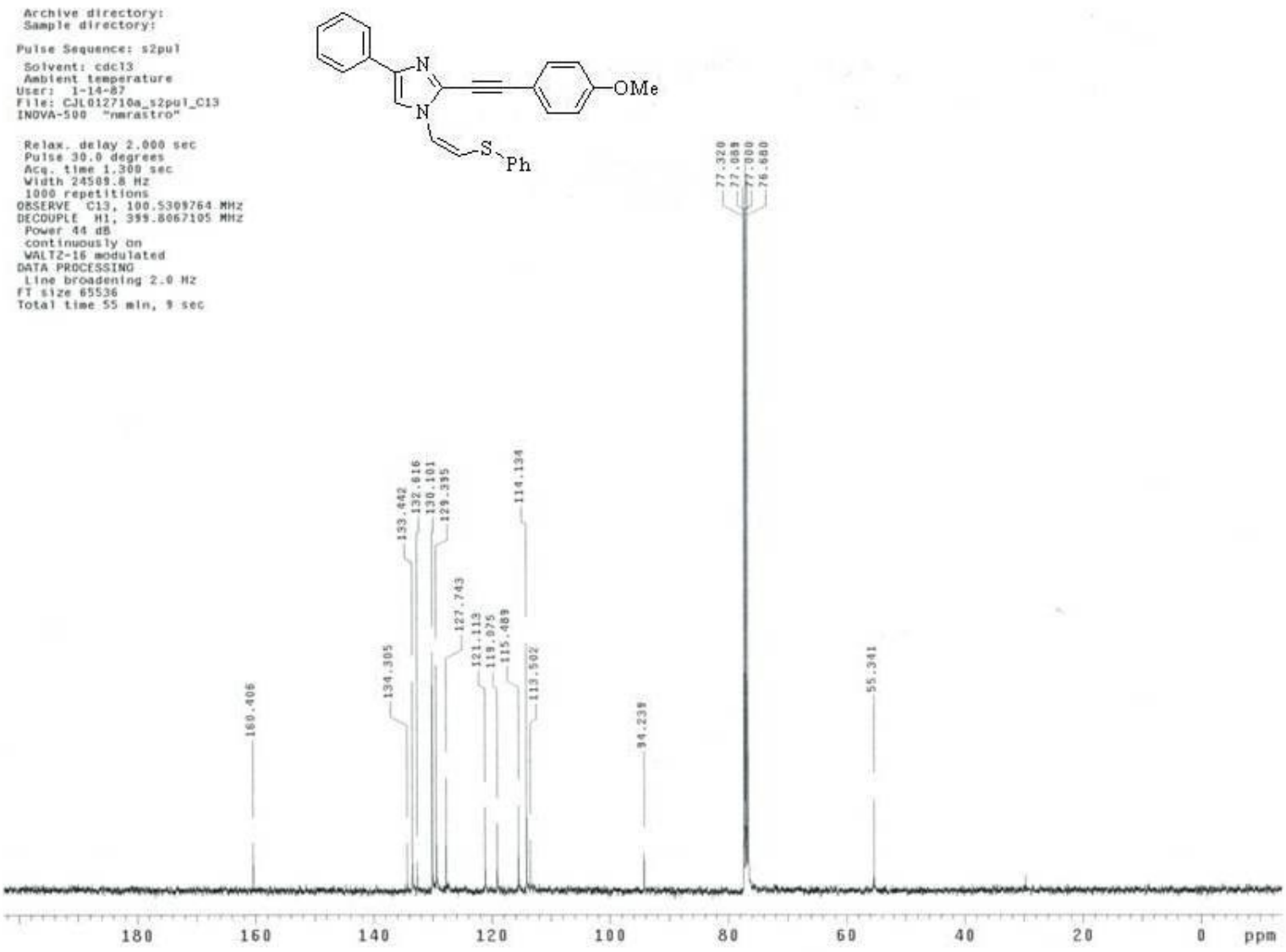
Archive directory:
Sample directory:
Pulse Sequence: s2pul
Solvent: cdcl3
Ambient temperature
User: 1-14-87
File: CJL012710a_s2pul_C13
INOVA-500 "nmrastro"
Relax. delay 2.000 sec
Pulse 30.0 degrees
Acq. time 1.300 sec
Width 24509.8 Hz
1000 repetitions
OBSERVE C13, 100.5309764 MHz
DECOUPLE H1, 399.8067105 MHz
Power 44 dB
continuously on
WALTZ-16 modulated
DATA PROCESSING
Line broadening 2.0 Hz
FT size 65536
Total time 55 min, 9 sec
N
N
OMe
S
Ph
160.406
134.305
133.442
132.616
130.101
129.395
127.743
121.113
119.875
115.489
114.134
113.502
94.239
77.320
77.089
77.000
76.680
55.341
180
160
140
120
100
80
60
40
20
0
ppm

Appendix B

X-ray Crystallography Data for Compound **7b**

(Chapter 2)

X-ray Experimental for Compound **7b**: Crystals grew as colorless plates by slow evaporation from CH_2Cl_2, MeOH and hexane. The data crystal was cut from a larger crystal and had approximate dimensions; 0.50 x 0.11 x 0.10 mm. The data were collected on a Nonius Kappa CCD diffractometer using a graphite monochromator with MoKα radiation (λ = 0.71073Å). A total of 211 frames of data were collected using ω-scans with a scan range of 2° and a counting time of 228 seconds per frame. The data were collected at 153 K using an Oxford Cryostream low temperature device. Details of crystal data, data collection and structure refinement are listed in Table 1. Data reduction were performed using DENZO-SMN.[1] The structure was solved by direct methods using SIR97[2] and refined by full-matrix least-squares on F^2 with anisotropic displacement parameters for the non-H atoms using SHELXL-97.[3] The hydrogen atoms were observed in a ΔF map and refined with isotropic displacement parameters. The function, $\Sigma w(|F_o|^2 - |F_c|^2)^2$, was minimized, where $w = 1/[(\sigma(F_o))^2 + (0.041*P)^2 + (0.319*P)]$ and $P = (|F_o|^2 + 2|F_c|^2)/3$. $R_w(F^2)$ refined to 0.105, with R(F) equal to 0.0415 and a goodness of fit, S, = 1.02. Definitions used for calculating R(F), $R_w(F^2)$ and the goodness of fit, S, are given below.[4] The data were corrected for secondary extinction effects. The correction takes the form: $F_{corr} = kF_c/[1 + (1.5(4)x10^{-5})* F_c^2 \lambda^3/(\sin 2\theta)]^{0.25}$ where k is the overall scale factor. Neutral atom scattering factors and values used to calculate the linear absorption coefficient are from the International Tables for X-ray Crystallography (1992).[5] All figures were generated using SHELXTL/PC.[7] Tables of positional and thermal parameters, bond lengths and angles, torsion angles, figures and lists of observed and calculated structure factors are located in tables 1 through 7. Crystallographic data (excluding structure factors) for compound **7b** have been deposited with the Cambridge Crystallographic Data Centre as supplementary publication number CCDC740499.

Table 1. Crystal data and structure refinement for **7b**.

Empirical formula	C25 H16 F N3 O	
Formula weight	393.41	
Temperature	153(2) K	
Wavelength	0.71070 Å	
Crystal system	Triclinic	
Space group	P-1	
Unit cell dimensions	a = 7.1511(4) Å	α= 94.044(1)°.
	b = 11.0903(6) Å	β= 103.875(1)°.
	c = 13.0643(8) Å	γ = 104.478(1)°.
Volume	964.50(10) $Å^3$	
Z	2	
Density (calculated)	1.355 Mg/m^3	
Absorption coefficient	0.091 mm^{-1}	
F(000)	408	
Crystal size	0.50 x 0.11 x 0.10 mm	
Theta range for data collection	1.91 to 27.45°.	
Index ranges	-7<=h<=9, -14<=k<=13, -16<=l<=16	
Reflections collected	6831	
Independent reflections	4362 [R(int) = 0.0160]	
Completeness to theta = 27.45°	99.0 %	
Absorption correction	None	
Refinement method	Full-matrix least-squares on F^2	
Data / restraints / parameters	4362 / 0 / 336	
Goodness-of-fit on F^2	1.024	
Final R indices [I>2sigma(I)]	R1 = 0.0415, wR2 = 0.0953	
R indices (all data)	R1 = 0.0574, wR2 = 0.1046	
Extinction coefficient	$1.5(4)x10^{-5}$	
Largest diff. peak and hole	0.186 and -0.171 $e.Å^{-3}$	

Atomic coordinates (x 10^4) and equivalent isotropic displacement parameters ($Å^2$x 10^3) for **7b**. U(eq) is defined as one third of the trace of the orthogonalized U^{ij} tensor.

	x	y	z	U(eq)
F1	3039(2)	10852(1)	3211(1)	61(1)
N2	2570(2)	6032(1)	5761(1)	24(1)
N3	2448(2)	4195(1)	4892(1)	24(1)
N4	2135(2)	3923(1)	953(1)	34(1)
O5	1188(2)	2852(1)	8863(1)	35(1)
C6	2528(2)	4780(1)	5819(1)	24(1)
C7	2553(2)	6241(1)	4722(1)	23(1)
C8	2445(2)	5089(1)	4200(1)	23(1)
C9	2624(2)	4261(1)	6789(1)	27(1)
C10	2770(2)	3832(1)	7605(1)	29(1)
C11	3015(2)	3278(2)	8600(1)	41(1)
C12	2729(2)	7496(1)	4386(1)	25(1)
C13	1357(2)	8164(1)	4494(1)	29(1)
C14	1474(2)	9306(1)	4103(1)	37(1)
C15	2961(3)	9754(1)	3619(1)	39(1)
C16	4370(3)	9138(1)	3524(1)	39(1)
C17	4254(2)	8002(1)	3917(1)	32(1)
C18	2315(2)	4712(1)	3078(1)	23(1)
C19	1818(2)	5433(1)	2274(1)	27(1)
C20	1767(2)	5008(1)	1245(1)	31(1)
C21	2563(2)	3224(1)	1726(1)	32(1)
C22	2672(2)	3577(1)	2780(1)	27(1)
C23	2600(2)	6858(1)	6595(1)	26(1)
C24	2578(2)	7465(1)	7377(1)	28(1)
C25	2537(2)	8158(1)	8339(1)	27(1)
C26	2990(2)	7682(1)	9301(1)	32(1)
C27	2900(2)	8324(2)	10231(1)	38(1)
C28	2390(2)	9444(2)	10212(1)	41(1)
C29	1946(2)	9927(1)	9267(1)	41(1)
C30	2002(2)	9286(1)	8328(1)	34(1)

Table 3. Bond lengths [Å] and angles [°] for **7b**.

F1-C15	1.3577(16)	C16-C17	1.384(2)
N2-C23	1.3656(16)	C16-H16	0.965(19)
N2-C6	1.3886(16)	C17-H17	0.988(17)
N2-C7	1.3901(16)	C18-C22	1.3928(18)
N3-C6	1.3153(16)	C18-C19	1.3960(18)
N3-C8	1.3878(16)	C19-C20	1.3827(19)
N4-C21	1.3394(19)	C19-H19	0.968(16)
N4-C20	1.3431(19)	C20-H20	1.007(16)
O5-C11	1.4068(19)	C21-C22	1.3835(19)
O5-H5	0.92(2)	C21-H21	0.997(17)
C6-C9	1.4218(18)	C22-H22	0.979(15)
C7-C8	1.3806(17)	C23-C24	1.1898(18)
C7-C12	1.4729(18)	C24-C25	1.4357(18)
C8-C18	1.4703(17)	C25-C26	1.395(2)
C9-C10	1.1903(18)	C25-C30	1.396(2)
C10-C11	1.4682(19)	C26-C27	1.388(2)
C11-H11A	0.99(2)	C26-H26	1.007(16)
C11-H11B	1.04(2)	C27-C28	1.380(2)
C12-C17	1.3939(19)	C27-H27	1.012(19)
C12-C13	1.3954(19)	C28-C29	1.380(2)
C13-C14	1.389(2)	C28-H28	0.978(18)
C13-H13	0.969(16)	C29-C30	1.389(2)
C14-C15	1.371(2)	C29-H29	0.953(19)
C14-H14	0.978(18)	C30-H30	0.969(17)
C15-C16	1.374(2)		

C23-N2-C6	124.14(11)	N3-C6-N2	111.24(11)
C23-N2-C7	128.61(11)	N3-C6-C9	126.62(12)
C6-N2-C7	107.24(10)	N2-C6-C9	122.11(11)
C6-N3-C8	105.76(10)	C8-C7-N2	104.85(11)
C21-N4-C20	116.44(12)	C8-C7-C12	132.76(11)
C11-O5-H5	105.3(13)	N2-C7-C12	122.32(11)

C7-C8-N3	110.87(11)	C20-C19-C18	118.85(12)
C7-C8-C18	130.16(11)	C20-C19-H19	117.8(9)
N3-C8-C18	118.97(11)	C18-C19-H19	123.3(9)
C10-C9-C6	177.87(14)	N4-C20-C19	124.22(13)
C9-C10-C11	177.54(15)	N4-C20-H20	117.2(9)
O5-C11-C10	112.17(12)	C19-C20-H20	118.6(9)
O5-C11-H11A	111.5(11)	N4-C21-C22	123.52(13)
C10-C11-H11A	108.3(11)	N4-C21-H21	117.1(9)
O5-C11-H11B	109.7(11)	C22-C21-H21	119.4(9)
C10-C11-H11B	107.7(11)	C21-C22-C18	119.65(13)
H11A-C11-H11B	107.3(16)	C21-C22-H22	119.4(8)
C17-C12-C13	119.53(12)	C18-C22-H22	121.0(8)
C17-C12-C7	119.22(12)	C24-C23-N2	172.81(14)
C13-C12-C7	121.22(12)	C23-C24-C25	177.95(15)
C14-C13-C12	120.03(14)	C26-C25-C30	119.13(13)
C14-C13-H13	119.4(9)	C26-C25-C24	119.55(12)
C12-C13-H13	120.5(9)	C30-C25-C24	121.30(13)
C15-C14-C13	118.59(14)	C27-C26-C25	120.16(14)
C15-C14-H14	119.7(10)	C27-C26-H26	119.9(9)
C13-C14-H14	121.7(11)	C25-C26-H26	119.9(9)
F1-C15-C14	118.46(14)	C28-C27-C26	120.21(15)
F1-C15-C16	118.58(14)	C28-C27-H27	120.2(10)
C14-C15-C16	122.96(14)	C26-C27-H27	119.6(10)
C15-C16-C17	118.36(15)	C29-C28-C27	120.21(14)
C15-C16-H16	119.3(11)	C29-C28-H28	120.9(11)
C17-C16-H16	122.3(11)	C27-C28-H28	118.9(11)
C16-C17-C12	120.48(14)	C28-C29-C30	120.18(14)
C16-C17-H17	119.9(10)	C28-C29-H29	121.4(11)
C12-C17-H17	119.7(9)	C30-C29-H29	118.4(11)
C22-C18-C19	117.29(12)	C29-C30-C25	120.11(14)
C22-C18-C8	119.55(12)	C29-C30-H30	121.7(10)
C19-C18-C8	123.15(11)	C25-C30-H30	118.2(10)

Table 4. Anisotropic displacement parameters ($Å^2 x 10^3$) for **7b**. The anisotropic displacement factor exponent takes the form: $-2\pi^2[h^2 a^{*2} U^{11} + ... + 2 h k a^* b^* U^{12}]$

	U^{11}	U^{22}	U^{33}	U^{23}	U^{13}	U^{12}
F1	85(1)	34(1)	73(1)	28(1)	27(1)	19(1)
N2	26(1)	27(1)	19(1)	4(1)	7(1)	7(1)
N3	25(1)	28(1)	22(1)	6(1)	7(1)	8(1)
N4	36(1)	38(1)	25(1)	0(1)	11(1)	7(1)
O5	43(1)	41(1)	24(1)	8(1)	14(1)	11(1)
C6	23(1)	26(1)	24(1)	6(1)	6(1)	6(1)
C7	22(1)	29(1)	20(1)	5(1)	6(1)	7(1)
C8	21(1)	26(1)	22(1)	6(1)	6(1)	7(1)
C9	27(1)	30(1)	24(1)	5(1)	8(1)	7(1)
C10	30(1)	35(1)	26(1)	6(1)	10(1)	10(1)
C11	40(1)	61(1)	30(1)	21(1)	14(1)	21(1)
C12	29(1)	23(1)	20(1)	2(1)	5(1)	6(1)
C13	33(1)	29(1)	26(1)	2(1)	8(1)	8(1)
C14	46(1)	30(1)	37(1)	5(1)	9(1)	16(1)
C15	54(1)	23(1)	38(1)	11(1)	10(1)	8(1)
C16	45(1)	33(1)	38(1)	11(1)	18(1)	4(1)
C17	34(1)	30(1)	33(1)	6(1)	12(1)	8(1)
C18	20(1)	26(1)	22(1)	3(1)	6(1)	4(1)
C19	28(1)	29(1)	25(1)	5(1)	6(1)	9(1)
C20	33(1)	36(1)	23(1)	6(1)	6(1)	7(1)
C21	34(1)	31(1)	31(1)	-1(1)	11(1)	8(1)
C22	28(1)	26(1)	27(1)	5(1)	8(1)	7(1)
C23	27(1)	29(1)	23(1)	5(1)	7(1)	8(1)
C24	28(1)	30(1)	26(1)	5(1)	7(1)	7(1)
C25	24(1)	30(1)	26(1)	0(1)	7(1)	5(1)
C26	35(1)	35(1)	28(1)	3(1)	8(1)	13(1)
C27	38(1)	49(1)	27(1)	1(1)	9(1)	11(1)
C28	39(1)	41(1)	39(1)	-9(1)	17(1)	6(1)
C29	41(1)	29(1)	57(1)	1(1)	24(1)	10(1)
C30	35(1)	34(1)	38(1)	9(1)	15(1)	12(1)

Table 5. Hydrogen coordinates (x 10^4) and isotropic displacement parameters ($Å^2$x 10^{-3}) for **7b**.

	x	y	z	U(eq)
H22	2970(20)	3014(14)	3303(12)	28(4)
H13	290(20)	7823(14)	4815(12)	33(4)
H30	1650(20)	9589(15)	7650(13)	40(4)
H17	5250(20)	7544(15)	3861(13)	39(4)
H26	3340(20)	6859(15)	9316(12)	36(4)
H19	1450(20)	6205(15)	2395(12)	34(4)
H14	510(30)	9783(17)	4152(14)	49(5)
H20	1400(20)	5527(14)	667(12)	35(4)
H21	2810(20)	2408(16)	1515(13)	40(4)
H11A	4010(30)	3915(18)	9173(16)	60(6)
H16	5370(30)	9493(17)	3168(15)	56(5)
H28	2360(30)	9888(17)	10879(14)	50(5)
H11B	3610(30)	2532(19)	8503(16)	64(6)
H29	1570(30)	10694(18)	9236(14)	53(5)
H5	1430(30)	3196(19)	9558(17)	66(6)
H27	3190(30)	7960(17)	10922(15)	51(5)

Table 6. Torsion angles [°] for **7b**.

C8-N3-C6-N2	0.24(14)	C7-C8-C18-C19	-15.3(2)
C8-N3-C6-C9	-177.92(12)	N3-C8-C18-C19	163.99(12)
C23-N2-C6-N3	178.20(11)	C22-C18-C19-C20	-1.96(19)
C7-N2-C6-N3	-1.21(14)	C8-C18-C19-C20	178.93(12)
C23-N2-C6-C9	-3.56(19)	C21-N4-C20-C19	0.4(2)
C7-N2-C6-C9	177.04(12)	C18-C19-C20-N4	1.2(2)
C23-N2-C7-C8	-177.74(12)	C20-N4-C21-C22	-1.2(2)
C6-N2-C7-C8	1.63(13)	N4-C21-C22-C18	0.4(2)
C23-N2-C7-C12	5.0(2)	C19-C18-C22-C21	1.22(19)
C6-N2-C7-C12	-175.66(11)	C8-C18-C22-C21	-179.63(12)
N2-C7-C8-N3	-1.55(14)	C23-C24-C25-C30	-153(4)
C12-C7-C8-N3	175.33(13)	C30-C25-C26-C27	0.2(2)
N2-C7-C8-C18	177.80(12)	C24-C25-C26-C27	-178.17(13)
C12-C7-C8-C18	-5.3(2)	C25-C26-C27-C28	-0.9(2)
C6-N3-C8-C7	0.85(14)	C26-C27-C28-C29	0.6(2)
C6-N3-C8-C18	-178.59(11)	C27-C28-C29-C30	0.3(2)
C8-C7-C12-C17	-52.5(2)	C28-C29-C30-C25	-1.0(2)
N2-C7-C12-C17	123.94(14)	C26-C25-C30-C29	0.7(2)
C8-C7-C12-C13	125.25(16)	C24-C25-C30-C29	179.06(13)
N2-C7-C12-C13	-58.31(17)		
C17-C12-C13-C14	2.2(2)		
C7-C12-C13-C14	-175.52(12)		
C12-C13-C14-C15	-0.3(2)		
C13-C14-C15-F1	178.20(13)		
C13-C14-C15-C16	-1.5(2)		
F1-C15-C16-C17	-178.37(13)		
C14-C15-C16-C17	1.3(2)		
C15-C16-C17-C12	0.7(2)		
C13-C12-C17-C16	-2.4(2)		
C7-C12-C17-C16	175.39(13)		
C7-C8-C18-C22	165.58(13)		
N3-C8-C18-C22	-15.11(18)		

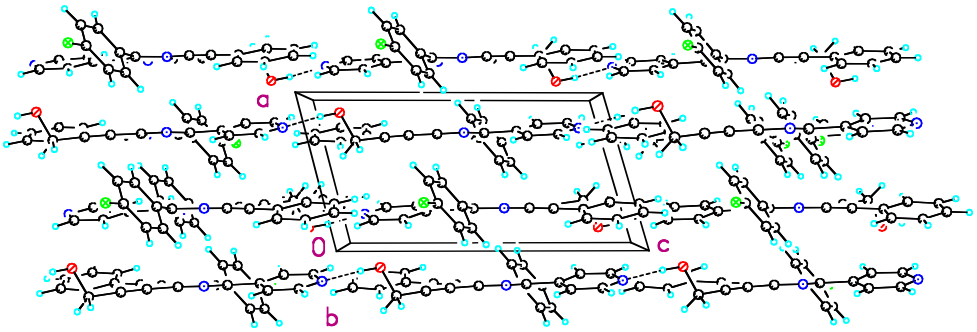

Figure 1. Unit cell packing diagram for **7b**. The view is approximately down the **b** axis.

References:

(1) DENZO-SMN. (1997). Z. Otwinowski and W. Minor, Methods in Enzymology, 276: Macromolecular Crystallography, part A, 307 – 326, C. W. Carter, Jr. and R. M. Sweets, Editors, Academic Press.

(2) SIR97. (1999). A program for crystal structure solution. Altomare A., Burla M.C., Camalli M., Cascarano G.L., Giacovazzo C., Guagliardi A., Moliterni A.G.G., Polidori G.,Spagna R. *J. Appl. Cryst. 32*, 115-119.

(3) Sheldrick, G. M. (1994). SHELXL97. Program for the Refinement of Crystal Structures. University of Gottingen, Germany.

(4) Rw(F2) = {w(|Fo|2 - |Fc|2)2/w(|Fo|)4}1/2 where w is the weight given each reflection. R(F) = (|Fo| - |Fc|)/|Fo|} for reflections with Fo > 4((Fo)).
S = [w(|Fo|2 - |Fc|2)2/(n - p)]1/2, where n is the number of reflections and p is the number of refined parameters.

(5) International Tables for X-ray Crystallography (1992). Vol. C, Tables 4.2.6.8 and 6.1.1.4, A. J. C. Wilson, editor, Boston: Kluwer Academic Press.

(6) Sheldrick, G. M. (1994). SHELXTL/PC (Version 5.03). Siemens Analytical X-ray Instruments, Inc., Madison, Wisconsin, USA.

Bibliography

Adams, J. L., Boehm, J. C., Kassis, S., Gorycki, P. D., Webb, E. F., Hall, R., Sorenson, M., Lee, J. C., Ayrton, A., Griswold, D. E., and Gallagher, T. F. (1998) Pyrimidinylimidazole inhibitors of CSBP/P37 kinase demonstrating decreased inhibition of hepatic cytochrome P450 enzymes, *Bioorgan Med Chem Lett 8*, 3111-3116.

Akella, R., Moon, T. M., and Goldsmith, E. J. (2008) Unique MAP Kinase binding sites, *Biochim Biophys Acta 1784*, 48-55.

Alessi, D. R. (1997) The protein kinase C inhibitors Ro 318220 and GF 109203X are equally potent inhibitors of MAPKAP kinase-1 beta (Rsk-2) and p70 S6 kinase, *Febs Lett 402*, 121-123.

Alley, M. C., Scudiero, D. A., Monks, A., Hursey, M. L., Czerwinski, M. J., Fine, D. L., Abbott, B. J., Mayo, J. G., Shoemaker, R. H., and Boyd, M. R. (1988) Feasibility of drug screening with panels of human tumor cell lines using a microculture tetrazolium assay, *Cancer Res 48*, 589-601.

Alonso, G., Ambrosino, C., Jones, M., and Nebreda, A. R. (2000) Differential activation of p38 mitogen-activated protein kinase isoforms depending on signal strength, *J Biol Chem 275*, 40641-40648.

Bain, J., Plater, L., Elliott, M., Shpiro, N., Hastie, C. J., McLauchlan, H., Klevernic, I., Arthur, J. S., Alessi, D. R., and Cohen, P. (2007) The selectivity of protein kinase inhibitors: a further update, *Biochem J 408*, 297-315.

Bardwell, A. J., Flatauer, L. J., Matsukuma, K., Thorner, J., and Bardwell, L. (2001) A conserved docking site in MEKs mediates high-affinity binding to MAP kinases and cooperates with a scaffold protein to enhance signal transmission, *J Biol Chem 276*, 10374-10386.

Bardwell, A. J., Frankson, E., and Bardwell, L. (2009) Selectivity of docking sites in MAPK kinases, *J Biol Chem 284*, 13165-13173.

Bardwell, L. (2006) Mechanisms of MAPK signalling specificity, *Biochemical Society Transactions 34*, 837-841.

Barluenga, S., Dakas, P. Y., Boulifa, M., Moulin, E., and Winssinger, N. (2008) Resorcylic acid lactones: A pluripotent scaffold with therapeutic potential, *Cr Chim 11*, 1306-1317.

Baroudi, A., Mauldin, J., and Alabugin, I. V. (2010) Conformationally Gated Fragmentations and Rearrangements Promoted by Interception of the Bergman Cyclization through Intramolecular H-Abstraction: A Possible Mechanism of Auto-Resistance to Natural Enediyne Antibiotics, *J Am Chem Soc 13*2, 967-979.

Basak, A., Mandal, S., and Bag, S. S. (2003) Chelation-controlled Bergman cyclization: Synthesis and reactivity of enediynyl ligands, *Chem Rev 103*, 4077-4094.

Ben-Levy, R., Hooper, S., Wilson, R., Paterson, H. F., and Marshall, C. J. (1998) Nuclear export of the stress-activated protein kinase p38 mediated by its substrate MAPKAP kinase-2, *Curr Biol 8*, 1049-1057.

Blair, J. A., Rauh, D., Kung, C., Yun, C. H., Fan, Q. W., Rode, H., Zhang, C., Eck, M. J., Weiss, W. A., and Shokat, K. M. (2007) Structure-guided development of affinity probes for tyrosine kinases using chemical genetics, *Nat Chem Biol 3*, 229-238.

Boehm, J. C., Smietana, J. M., Sorenson, M. E., Garigipati, R. S., Gallagher, T. F., Sheldrake, P. L., Bradbeer, J., Badger, A. M., Laydon, J. T., Lee, J. C., Hillegass, L. M., Griswold, D. E., Breton, J. J., Chabot-Fletcher, M. C., and Adams, J. L. (1996) 1-substituted 4-aryl-5-pyridinylimidazoles: a new class of cytokine suppressive drugs with low 5-lipoxygenase and cyclooxygenase inhibitory potency*, J Med Chem 39*, 3929-3937.

Bogoyevitch, M. A. (2005) Therapeutic promise of JNK ATP-noncompetitive inhibitors, *Trends Mol Med 11*, 232-239.

Borsello, T., Clarke, P. G., Hirt, L., Vercelli, A., Repici, M., Schorderet, D. F., Bogousslavsky, J., and Bonny, C. (2003) A peptide inhibitor of c-Jun N-terminal kinase protects against excitotoxicity and cerebral ischemia, *Nat Med 9*, 1180-1186.

Boulton, T. G., Yancopoulos, G. D., Gregory, J. S., Slaughter, C., Moomaw, C., Hsu, J., and Cobb, M. H. (1990) An insulin-stimulated protein kinase similar to yeast kinases involved in cell cycle control, *Science 249*, 64-67.

Brancho, D., Tanaka, N., Jaeschke, A., Ventura, J. J., Kelkar, N., Tanaka, Y., Kyuuma, M., Takeshita, T., Flavell, R. A., and Davis, R. J. (2003) Mechanism of p38 MAP kinase activation in vivo, *Genes Dev 17*, 1969-1978.

Brognard, J., and Hunter, T. (2011) Protein kinase signaling networks in cancer, *Curr Opin Genetics Dev 21*, 4-11.

Brzostowska, E. M., Hoffmann, R., and Parish, C. A. (2007) Tuning the bergman cyclization by introduction of metal fragments at various positions of the enediyne. Metalla-Bergman cyclizations, *J Am Chem Soc 129*, 4401-4409.

Buxade, M., Parra-Palau, J. L., and Proud, C. G. (2008) The Mnks: MAP kinase-interacting kinases (MAP kinase signal-integrating kinases), *Front Biosci 13*, 5359-5373.

Cargnello, M., and Roux, P. P. (2011) Activation and Function of the MAPKs and Their Substrates, the MAPK-Activated Protein Kinases, *Microbiol Mol Biol R 75*, 50-83.

Chang, C. I., Xu, B. E., Akella, R., Cobb, M. H., and Goldsmith, E. J. (2002) Crystal structures of MAP kinase p38 complexed to the docking sites on its nuclear substrate MEF2A and activator MKK3b*, Molecular Cell 9*, 1241-1249.

Chen, Z., Gibson, T. B., Robinson, F., Silvestro, L., Pearson, G., Xu, B., Wright, A., Vanderbilt, C., and Cobb, M. H. (2001) MAP kinases, *Chem Rev 101*, 2449-2476.

Cohen, M. S., Hadjivassiliou, H., and Taunton, J. (2007) A clickable inhibitor reveals context-dependent autoactivation of p90 RSK, *Nat Chem Biol 3*, 156-160.

Cohen, M. S., Zhang, C., Shokat, K. M., and Taunton, J. (2005) Structural bioinformatics-based design of selective, irreversible kinase inhibitors, *Science 308*, 1318-1321.

Cohen, P. (2002) Protein kinases - the major drug targets of the twenty-first century?, *Nat Rev Drug Discov 1*, 309-315.

Comess, K. M., Sun, C., Abad-Zapatero, C., Goedken, E. R., Gum, R. J., Borhani, D. W., Argiriadi, M., Groebe, D. R., Jia, Y., Clampit, J. E., Haasch, D. L., Smith, H. T., Wang, S., Song, D., Coen, M. L., Cloutier, T. E., Tang, H., Cheng, X., Quinn, C., Liu, B., Xin, Z., Liu, G., Fry, E. H., Stoll, V., Ng, T. I., Banach, D., Marcotte, D., Burns, D. J., Calderwood, D. J., and Hajduk, P. J. (2011) Discovery and characterization of non-ATP site inhibitors of the mitogen activated protein (MAP) kinases, *ACS Chem Biol 6*, 234-244.

Coulombe, P., and Meloche, S. (2007) Atypical mitogen-activated protein kinases: structure, regulation and functions, *Biochim Biophys Acta 1773*, 1376-1387.

Cramer, C. J. (1998) Bergman, aza-bergman, and protonated aza-bergman cyclizations and intermediate 2,5-arynes: Chemistry and challenge to computation, *J Am Chem Soc 120*, 6261-6269.

Cuadrado, A., and Nebreda, A. R. (2010) Mechanisms and functions of p38 MAPK signalling, *Biochem J* 429, 403-417.

Cuenda, A., and Rousseau, S. (2007) p38 MAP-kinases pathway regulation, function and role in human diseases, *Biochim Biophys Acta 1773*, 1358-1375.

Dan, I., Watanabe, N. M., and A., K. (2001) The Ste20 group kinases as regulators of MAP kinase cascades, *Trends Cell Biol 11*, 220-230.

David, W., and SM., K. (1997) Synthesis and thermal rearrangement of C,N-dialkynyl imines: A potential Aza-Bergman route to 2,5-didehydropyridine, *J Am Chem Soc 119*, 1464-1465.

Davidson, W., Frego, L., Peet, G. W., Kroe, R. R., Labadia, M. E., Lukas, S. M., Snow, R. J., Jakes, S., Grygon, C. A., Pargellis, C., and Werneburg, B. G. (2004) Discovery and characterization of a substrate selective p38alpha inhibitor, *Biochemistry 43*, 11658-11671.

Davies, J., Wang, H., Taylor, T., Warabi, K., Huang, X. H., and Andersen, R. J. (2005) Uncialamycin, a new enediyne antibiotic, *Org Lett 7*, 5233-5236.

Davies, S. P., Reddy, H., Caivano, M., and Cohen, P. (2000) Specificity and mechanism of action of some commonly used protein kinase inhibitors, *Biochem J 351*, 95-105.

Denny, W. A. (2002) Irreversible inhibitors of the erbB family of protein tyrosine kinases, *Pharmacol Ther 93*, 253-261.

Doza, Y. N., Cuenda, A., Thomas, G. M., Cohen, P., and Nebreda, A. R. (1995) Activation of the MAP kinase homologue RK requires the phosphorylation of Thr-180 and Tyr-182 and both residues are phosphorylated in chemically stressed KB cells, *Febs Lett 364*, 223-228.

Dumas, J., Sibley, R., Riedl, B., Monahan, M. K., Lee, W., Lowinger, T. B., Redman, A. M., Johnson, J. S., Kingery-Wood, J., Scott, W. J., Smith, R. A., Bobko, M., Schoenleber, R., Ranges, G. E., Housley, T. J., Bhargava, A., Wilhelm, S. M., and Shrikhande, A. (2000) Discovery of a new class of p38 kinase inhibitors, *Bioorg Med Chem Lett 10*, 2047-2050.

Eldar-Finkelman, H., and Eisenstein, M. (2009) Peptide inhibitors targeting protein kinases, *Curr Pharm Des 15*, 2463-2470.

Enslen, H., Brancho, D. M., and Davis, R. J. (2000) Molecular determinants that mediate selective activation of p38 MAP kinase isoforms, *Embo J 19*, 1301-1311.

Enslen, H., Raingeaud, J., and Davis, R. J. (1998) Selective activation of p38 mitogen-activated protein (MAP) kinase isoforms by the MAP kinase kinases MKK3 and MKK6, *J Biol Chem 273*, 1741-1748.

Erdelyi, K., Bai, P., Kovacs, I., Szabo, E., Mocsar, G., Kakuk, A., Szabo, C., Gergely, P., and Virag, L. (2009) Dual role of poly(ADP-ribose) glycohydrolase in the regulation of cell death in oxidatively stressed A549 cells, *FASEB J 23*, 3553-3563.

Fantz, D. A., Jacobs, D., Glossip, D., and Kornfeld, K. (2001) Docking sites on substrate proteins direct extracellular signal-regulated kinase to phosphorylate specific residues, *J Biol Chem 276*, 27256-27265.

Felip, E., Santarpia, M., and Rosell, R. (2007) Emerging drugs for non-small-cell lung cancer, *Expert Opin Emerg Drugs 12*, 449-460.

Feng, L., and Kerwin, S. M. (2003) *Tetrahedron Lett 44*, 3463.

Feng, L., Kumar, D., and Kerwin, S. M. (2003) An extremely facile aza-Bergman rearrangement of sterically unencumbered acyclic 3-aza-3-ene-1,5-diynes, *J Org Chem 68*, 2234-2242.

Feng, L., Zhang, A., and Kerwin, S. M. (2006) Enediynes from aza-enediynes: C,N-dialkynyl imines undergo both aza-Bergman rearrangement and conversion to enediynes and fumaronitriles, *Org Lett 8*, 1983-1986.

Fry, D. W., Bridges, A. J., Denny, W. A., Doherty, A., Greis, K. D., Hicks, J. L., Hook, K. E., Keller, P. R., Leopold, W. R., Loo, J. A., McNamara, D. J., Nelson, J. M.,

Sherwood, V., Smaill, J. B., Trumpp-Kallmeyer, S., and Dobrusin, E. M. (1998) Specific, irreversible inactivation of the epidermal growth factor receptor and erbB2, by a new class of tyrosine kinase inhibitor, *Proc Natl Acad Sci U S A 95*, 12022-12027.

Galanis, A., Yang, S. H., and Sharrocks, A. D. (2001) Selective targeting of MAPKs to the ETS domain transcription factor SAP-1, *J Biol Chem 276*, 965-973.

Gallagher, T. F., Fierthompson, S. M., Garigipati, R. S., Sorenson, M. E., Smietana, J. M., Lee, D., Bender, P. E., Lee, J. C., Laydon, J. T., Griswold, D. E., Chabotfletcher, M. C., Breton, J. J., and Adams, J. L. (1995) 2,4,5-Triarylimidazole Inhibitors of Il-1 Biosynthesis, *Bioorg Med Chem Lett 5*, 1171-1176.

Ganley, B., Chowdhury, G., Bhansali, J., Daniels, J. S., and Gates, K. S. (2001) Redox-activated, hypoxia-selective DNA cleavage by quinoxaline 1,4-di-N-oxide, *Bioorg Med Chem 9*, 2395-2401.

Garuti, L., Roberti, M., and Bottegoni, G. (2010) Non-ATP competitive protein kinase inhibitors, *Curr Med Chem 17*, 2804-2821.

Ge, B., Gram, H., Di Padova, F., Huang, B., New, L., Ulevitch, R. J., Luo, Y., and Han, J. (2002) MAPKK-independent activation of p38alpha mediated by TAB1-dependent autophosphorylation of p38alpha, *Science 295*, 1291-1294.

Giard, D. J., Aaronson, S. A., Todaro, G. J., Arnstein, P., Kersey, J. H., Dosik, H., and Parks, W. P. (1973) In vitro cultivation of human tumors: establishment of cell lines derived from a series of solid tumors, *J Natl Cancer Inst 51*, 1417-1423.

Goldstein, D. M., Alfredson, T., Bertrand, J., Browner, M. F., Clifford, K., Dalrymple, S. A., Dunn, J., Freire-Moar, J., Harris, S., Labadie, S. S., La Fargue, J., Lapierre, J. M., Larrabee, S., Li, F., Papp, E., McWeeney, D., Ramesha, C., Roberts, R., Rotstein, D., San Pablo, B., Sjogren, E. B., So, O. Y., Talamas, F. X., Tao, W., Trejo, A., Villasenor, A., Welch, M., Welch, T., Weller, P., Whiteley, P. E., Young, K., and Zipfel, S. (2006) Discovery of S-[5-amino-1-(4-fluorophenyl)-1H-pyrazol-4-yl]-[3-(2,3-dihydroxypropoxy)ph enyl]methanone (RO3201195), an orally bioavailable and highly selective inhibitor of p38 MAP kinase, *J Med Chem 49*, 1562-1575.

Goldstein, D. M., and Gabriel, T. (2005) Pathway to the clinic: inhibition of P38 MAP kinase. A review of ten chemotypes selected for development, *Curr Top Med Chem 5*, 1017-1029.

Golik, J., Dubay, G., Groenewold, G., Kawaguchi, H., Konishi, M., Krishnan, B., Ohkuma, H., Saitoh, K., and Doyle, T. W. (1987) Esperamicins, a Novel Class of Potent Antitumor Antibiotics .3. Structures of Esperamicins-A1, Esperamicin-A2, and Esperamicin-A1b, *J Am Chem Soc 109*, 3462-3464.

Guergnon, J., Dessauge, F., Dominguez , V., Viallet, J., Bonnefoy, S., Yuste, V., Mercereau-Puijalon, O., Cayla, X., Rebollo, A., and Susin, S. (2006) Use of penetrating peptides interacting with PP1/PP2A proteins as a general approach for a drug phosphatase technology, *Mol Pharmacol 69*, 1115.

Gum, R. J., and Young, P. R. (1999) Identification of two distinct regions of p38 MAPK required for substrate binding and phosphorylation, *Biochem Biophys Res Commun 266*, 284-289.

Han, J., Lee, J. D., Bibbs, L., and Ulevitch, R. J. (1994) A Map Kinase Targeted by Endotoxin and Hyperosmolarity in Mammalian-Cells, *Science 265*, 808-811.

Heymach, J. V., Nilsson, M., Blumenschein, G., Papadimitrakopoulou, V., and Herbst, R. (2006) Epidermal growth factor receptor inhibitors in development for the treatment of non-small cell lung cancer, *Clin Cancer Res 12*, 4441s-4445s.

Ho, K. K., Auld, D. S., Bohnstedt, A. C., Conti, P., Dokter, W., Erickson, S., Feng, D., Inglese, J., Kingsbury, C., Kultgen, S. G., Liu, R. Q., Masterson, C. M., Ohlmeyer, M., Rong, Y., Rooseboom, M., Roughton, A., Samama, P., Smit, M. J., Son, E., van der Louw, J., Vogel, G., Webb, M., Wijkmans, J., and You, M. (2006) Imidazolylpyrimidine based CXCR2 chemokine receptor antagonists, *Bioorg Med Chem Lett 16*, 2724-2728.

Hoffner, J., Schottelius, M. J., Feichtinger, D., and Chen, P. (1998) Chemistry of the 2,5-didehydropyridine biradical: Computational, kinetic, and trapping studies toward drug design, *J Am Chem Soc 120*, 376-385.

Hunter, T. (2007) Treatment for chronic myelogenous leukemia: the long road to imatinib, *J Clin Invest 117*, 2036-2043.

Im, J. S., and Lee, J. K. (2008) ATR-dependent activation of p38 MAP kinase is responsible for apoptotic cell death in cells depleted of Cdc7, *J Biol Chem 283*, 25171-25177.

Jacobs, D., Beitel, G. J., Clark, S. G., Horvitz, H. R., and Kornfeld, K. (1998) Gain-of-function mutations in the Caenorhabditis elegans lin-1 ETS gene identify a C-terminal regulatory domain phosphorylated by ERK MAP kinase, *Genetics 149*, 1809-1822.

Jacobs, D., Glossip, D., Xing, H., Muslin, A. J., and Kornfeld, K. (1999) Multiple docking sites on substrate proteins form a modular system that mediates recognition by ERK MAP kinase, *Genes Dev 13*, 163-175.

Johnson, G. L., and Lapadat, R. (2002) Mitogen-activated protein kinase pathways mediated by ERK, JNK, and p38 protein kinases, *Science 298*, 1911-1912.

Jones, R. R., and Bergman, R. G. (1972) Para Benzyne. Generation as an intermediate in a Thermal Isomerization Reaction and Trapping Evidence for 1,4-Benzenediyl Structure, *J Am Chem Soc 94*, 660-661.

Karcher, S. C., and Laufer, S. A. (2009) Successful structure-based design of recent p38 MAP kinase inhibitors, *Curr Top Med Chem 9*, 655-676.

Karin, M. (2006) Nuclear factor-kappaB in cancer development and progression, *Nature 441*, 431-436.

Kelemen, B. R., Hsiao, K., and Goueli, S. A. (2002) Selective in vivo inhibition of mitogen-activated protein kinase activation using cell-permeable peptides, *J Biol Chem 277*, 8741-8748.

Kerwin, S. M. in Radical and Radical Ion Reactivity in Nucleic Acid Chemistry, Greenberg, M. (Ed) Wieley: New York, 389-419.

Kerwin, S. M., and Nadipuram, A. (2004) 5H-cyclopentapyrazines from 1,2-dialkynylimidazoles, *Synlett*, 1404-1408.

Khandekar, S. S., Feng, B., Yi, T., Chen, S., Laping, N., and Bramson, N. (2005) A liquid chromatography/mass spectrometry-based method for the selection of ATP competitive kinase inhibitors, J Biomol Screen 10, 447-455.

Kirkland, L. O., and McInnes, C. (2009) Non-ATP competitive protein kinase inhibitors as anti-tumor therapeutics, *Biochem Pharmacol 77*, 1561-1571.

Klein, M., Walenzyk, T., and Konig, B. (2004) Electronic effects on the Bergman cyclisation of enediynes. A review, *Collect Czech Chem C 69*, 945-965.

Kobayashi, S., Ji, H. B., Yuza, Y., Meyerson, M., Wong, K. K., Tenen, D. G., and Halmos, B. (2005) An alternative inhibitor overcomes resistance caused by a mutation of the epidermal growth factor receptor, *Cancer Res 65*, 7096-7101.

Kolch, W. (2000) Meaningful relationships: the regulation of the Ras/Raf/MEK/ERK pathway by protein interactions, *Biochem J 351* Pt 2, 289-305.

Konishi, M., Ohkuma, H., Matsumoto, K., Tsuno, T., Kamei, H., Miyaki, T., Oki, T., Kawaguchi, H., Vanduyne, G. D., and Clardy, J. (1989) Dynemicin a, a Novel Antibiotic with the Anthraquinone and 1,5-Diyn-3-Ene Subunit, *J Antibiot 42*, 1449-1452.

Konishi, M., Ohkuma, H., Matsumoto, K., Tsuno, T., Kamei, H., Miyaki, T., Oki, T., Kawaguchi, H., Vanduyne, G. D., and Clardy, J. (1989) Dynemicin a, a Novel Antibiotic with the Anthraquinone and 1,5-Diyn-3-Ene Subunit, *J Antibiot 42*, 1449-1452.

Koser, G. F., Rebrovic, L., and Wettach, R. H. (1981) Functionalization of Alkenes and Alkynes with [Hydroxy(Tosyloxy)Iodo]Benzene - Bis(Tosyloxy)Alkanes, Vinylaryliodonium Tosylates, and Alkynylaryliodonium Tosylates, *J org chem 46*, 4324-4326.

Kraka, E., Tuttle, T., and Cremer, D. (2008) Design of a new warhead for the natural enediyne dynemicin A. An increase of biological activity, *J Phys Chem B 112*, 2661-2670.

Kufareva, I., and Abagyan, R. (2008) Type-II kinase inhibitor docking, screening, and profiling using modified structures of active kinase states, *J Med Chem 51*, 7921-7932.

Kumar, D., Jacob, M. R., Reynolds, M. B., and Kerwin, S. M. (2002) Synthesis and evaluation of anticancer benzoxazoles and benzimidazoles related to UK-1, *Bioorg Med Chem 10*, 3997-4004.

Kumar, S., Boehm, J., and Lee, J. C. (2003) p38 MAP kinases: key signalling molecules as therapeutic targets for inflammatory diseases, *Nat Rev Drug Discov 2*, 717-726.

Kwak, E. L., Sordella, R., Bell, D. W., Godin-Heymann, N., Okimoto, R. A., Brannigan, B. W., Harris, P. L., Driscoll, D. R., Fidias, P., Lynch, T. J., Rabindran, S. K., McGinnis, J. P., Wissner, A., Sharma, S. V., Isselbacher, K. J., Settleman, J., and Haber, D. A. (2005) Irreversible inhibitors of the EGF receptor may circumvent acquired resistance to gefitinib, *Proc Natl Acad Sci U S A 102*, 7665-7670.

Kyriakis, J. M., and Avruch, J. (2001) Mammalian mitogen-activated protein kinase signal transduction pathways activated by stress and inflammation, *Physiol Rev 81*, 807-869.

Laroche, C., and Kerwin, S. M. (2009) Lithiation and functionalization of 1-alkynylimidazoles at the 2-position, *Tetrahedron Lett* 50, 5194-5197.

Laroche, C., Li, J., and Kerwin, S. M. (2011) Cytotoxic 1,2-dialkynylimidazole-based aza-enediynes: aza-Bergman rearrangement rates do not predict cytotoxcitiy, *J Med Chem* 54, 5059-5069.

Laroche, C., Li, J., Freyer, M. W., and Kerwin, S. M. (2008) Coupling reactions of bromoalkynes with imidazoles mediated by copper salts: Synthesis of novel N-alkynylimidazoles, *J Org Chem 73*, 6462-6465.

Laroche, C., Li, J., Gonzales, C., David, W. M., and Kerwin, S. M. (2010) Cyclization kinetics and biological evaluation of an anticancer 1,2-dialkynylimidazole, *Org Biomol Chem 8*, 1535-1539.

Laufer, S. A., Zimmermann, W., and Ruff, K. J. (2004) Tetrasubstituted imidazole inhibitors of cytokine release: probing substituents in the N-1 position, *J Med Chem 47*, 6311-6325.

Laufer, S., Wagner, G., and Kotschenreuther, D. (2002) Ones, thiones, and N-oxides: an exercise in imidazole chemistry, *Angew Chem Int Ed Engl 41*, 2290-2293.

Lee, J. C., Laydon, J. T., McDonnell, P. C., Gallagher, T. F., Kumar, S., Green, D., McNulty, D., Blumenthal, M. J., Heys, J. R., Landvatter, S. W., and et al. (1994) A protein kinase involved in the regulation of inflammatory cytokine biosynthesis, *Nature 372*, 739-746.

Lee, M. D., Manning, J. K., Williams, D. R., Kuck, N. A., Testa, R. T., and Borders, D. B. (1989) Calicheamicins, a Novel Family of Antitumor Antibiotics .3. Isolation, Purification and Characterization of Calicheamicin-Beta-1br, Calicheamicin-Gamma-1br, Calicheamicin-Alpha-2i, Calicheamicin-Alpha-3i, Calicheamicin-Beta-1i, Calicheamicin-Gamma-1i and Calicheamicin-Delta-1i, *J Antibiot 42*, 1070-1087.

Lee, M. D., Manning, J. K., Williams, D. R., Kuck, N. A., Testa, R. T., and Borders, D. B. (1989) Calicheamicins, a Novel Family of Antitumor Antibiotics .3. Isolation, Purification and Characterization of Calicheamicin-Beta-1br, Calicheamicin-Gamma-1br,

Calicheamicin-Alpha-2i, Calicheamicin-Alpha-3i, Calicheamicin-Beta-1i, Calicheamicin-Gamma-1i and Calicheamicin-Delta-1i, *J Antibiot 42*, 1070-1087.

Lee, M. R., and Dominguez, C. (2005) MAP kinase p38 inhibitors: clinical results and an intimate look at their interactions with p38alpha protein, *Curr Med Chem 12*, 2979-2994.

Lee, T., Hoofnagle, A. N., Kabuyama, Y., Stroud, J., Min, X., Goldsmith, E. J., Chen, L., Resing, K. A., and Ahn, N. G. (2004) Docking motif interactions in MAP kinases revealed by hydrogen exchange mass spectrometry, *Mol Cell 14*, 43-55.

Lewis, T. S., Shapiro, P. S., and Ahn, G. G. (1998) Signal transduction through MAP kinase cascades, *Adv. Cancer Res 74*, 49-139.

Li, J., Kaoud, T. S., Laroche, C., Dalby, K. N., and Kerwin, S. M. (2009) Synthesis and biological evaluation of p38 alpha kinase-targeting dialkynylimidazoles, *Bioorgan Med Chem Lett 19*, 6293-6297.

Lin, C. F., Hsieh, P. C., Lu, W. D., Chiu, H. F., and Wu, M. J. (2001) A series of enediynes as novel inhibitors of topoisomerase I, *Bioorgan Med Chem 9*, 1707-1711.

Lin, M., and Wang, L. (2008) Selective labeling of proteins with chemical probes in living cells, *Physiology 23*, 131-141.

Lo, Y. H., Lin, C. C., Lin, C. F., Lin, Y. T., Duh, T. H., Hong, Y. R., Yang, S. H., Lin, S. R., Yang, S. C., Chang, L. S., and Wu, M. J. (2008) 2-(6-aryl-3(Z)-hexen-1,5-diynyl)anilines as a new class of potent antitubulin agents, *J Med Chem 51*, 2682-2688.

Lo, Y. H., Lin, I. L., Lin, C. F., Hsu, C. C., Yang, S. H., Lin, S. R., and Wu, M. J. (2007) Novel acyclic enediynes inhibit Cyclin A and Cdc25C expression and induce apoptosis phenomenon to show potent antitumor proliferation, *Bioorgan Med Chem 15*, 4528-4536.

Lynch, W.E., Kurtz, D. M., Wang, S., Scott, R. A. (1994) Strcutrual and functionalmodels for the dicopper site in hemocyanin. Dioxygen binding by copper complexes of tris(1-R-4-R'-imidazolyl-κ*N*)phosphines.

Magnus, P., Fortt, S., Pitterna, T., and Snyder, J. P. (1990) Synthetic and Mechanistic Studies on Esperamicin-A1 and Calicheamicin-Gamma-1 - Molecular Strain Rather Than Pi-Bond Proximity Determines the Cycloaromatization Rates of Bicyclo[7.3.1] Enediynes, *J Am Chem Soc 112*, 4986-4987.

McDonald, L. A., Capson, T. L., Krishnamurthy, G., Ding, W. D., Ellestad, G. A., Bernan, V. S., MAiese, W. M., Lassota, P., Discafani, C., Kramer, R. A., and Ireland, C. M. (1996) Namenamicin, a new enediyne antitumor antibiotic from the marine ascidian Polysyncraton lithostrotum, *J Am Chem Soc 118*, 10898-10899.

Michalczyk, A., Kluter, S., Rode, H. B., Simard, J. R., Grutter, C., Rabiller, M., and Rauh, D. (2008) Structural insights into how irreversible inhibitors can overcome drug resistance in EGFR, *Bioorgan Med Chem 16*, 3482-3488.

Mukherji, D., and Spicer, J. (2009) Second-generation epidermal growth factor tyrosine kinase inhibitors in non-small cell lung cancer, *Expert Opin Investig Drugs 18*, 293-301.

Murphy, L. O., Smith, S., Chen, R. H., Fingar, D. C., and Blenis, J. (2002) Molecular interpretation of ERK signal duration by immediate early gene products, *Nat Cell Biol 4*, 556-564.

Myers, A. G. (1987) *Tetrahedron Lett 28*, 4493-4496.

Myers, A. G., Cohen, S. B., and Kwon, B. (1994) *J Am Chem Soc 116*, 1670-1682.

Myers, A. G., Harrington, P. M., and Kwon, B. (1992) *J Am Chem Soc 114*, 1086-1087.

Nadipuram, A. K., and Kerwin, S. M. (2006) Intra- and intermolecular trapping of cyclopentapyrazine carbenes derived from 1,2-dialkynylimidazoles, *Tetrahedron Lett 47*, 353-356.

Nadipuram, A. K., and Kerwin, S. M. (2006) Thermal cyclization of 1,2-dialkynylimidazoles to imidazo[1,2-a]pyridines, *Tetrahedron 62*, 3798-3808.

Nadipuram, A. K., David, W. M., Kumar, D., and Kerwin, S. M. (2002) Synthesis and thermolysis of heterocyclic 3-aza-3-ene-1,5-diynes(1), Org Lett 4, 4543-4546.

Nicolaou, K. C., Dai, W. M., Tsay, S. C., Estevez, V. A., and Wrasidlo, W. (1992) Designed enediynes: a new class of DNA-cleaving molecules with potent and selective anticancer activity, *Science 256*, 1172-1178.

Noble, M. E. M., Endicott, J. A., and Johnson, L. N. (2004) Protein kinase inhibitors: Insights into drug design from structure, *Science 303*, 1800-1805.

Oku, N., Matsunaga, S., and Fusetani, N. (2003) Shishijimicins A-C, novel enediyne antitumor antibiotics from the ascidian Didemnum proliferum, *J Am Chem Soc 125*, 2044-2045.

Ono, K., and Han, J. (2000) The p38 signal transduction pathway: activation and function, *Cell Signal 12*, 1-13.

Pan, Z., Scheerens, H., Li, S. J., Schultz, B. E., Sprengeler, P. A., Burrill, L. C., Mendonca, R. V., Sweeney, M. D., Scott, K. C., Grothaus, P. G., Jeffery, D. A., Spoerke, J. M., Honigberg, L. A., Young, P. R., Dalrymple, S. A., and Palmer, J. T. (2007) Discovery of selective irreversible inhibitors for Bruton's tyrosine kinase, *ChemMedChem 2*, 58-61.

Paull, K. D., Shoemaker, R. H., Hodes, L., Monks, A., Scudiero, D. A., Rubinstein, L., Plowman, J., and Boyd, M. R. (1989) Display and analysis of patterns of differential activity of drugs against human tumor cell lines: development of mean graph and COMPARE algorithm, *J Natl Cancer Inst 81*, 1088-1092.

Pearson, G., Robinson, F., Gibson, T. B., Xu, B. E., Karandikar, M., Berman, K., and Cobb, M. H. (2001) Mitogen-activated protein (MAP) kinase pathways: Regulation and physiological functions, *Endocr Rev 22*, 153-183.

Pettus, L. H., and Wurz, R. P. (2008) Small molecule p38 MAP kinase inhibitors for the treatment of inflammatory diseases: novel structures and developments during 2006-2008, *Curr Top Med Chem 8*, 1452-1467.

Polukhtine, A., Karpov, G., and Popik, V. V. (2008) Towards photoswitchable enediyne antibiotics: single and two-photon triggering of bergman cyclization, *Curr Top Med Chem 8*, 460-469.

Rabindran, S. K., Discafani, C. M., Rosfjord, E. C., Baxter, M., Floyd, M. B., Golas, J., Hallett, W. A., Johnson, B. D., Nilakantan, R., Overbeek, E., Reich, M. F., Shen, R., Shi, X. Q., Tsou, H. R., Wang, Y. F., and Wissner, A. (2004) Antitumor activity of HKI-272, an orally active, irreversible inhibitor of the HER-2 tyrosine kinase, *Cancer Res 64*, 3958-3965.

Raingeaud, J., Gupta, S., Rogers, J. S., Dickens, M., Han, J., Ulevitch, R. J., and Davis, R. J. (1995) Pro-inflammatory cytokines and environmental stress cause p38 mitogen-activated protein kinase activation by dual phosphorylation on tyrosine and threonine, *J Biol Chem 270*, 7420-7426.

Raman, M., Chen, W., and Cobb, M. H. (2007) Differential regulation and properties of MAPKs, *Oncogene 26*, 3100-3112.

Rastelli, G., Rosenfeld, R., Reid, R., and Santi, D. V. (2008) Molecular modeling and crystal structure of ERK2-hypothemycin complexes, *J Struct Biol 164*, 18-23.

Rawat, D. S., and Zaleski, J. M. (2004) Geometric and electronic control of thermal bergman cyclization, *Synlett*, 393-421.

Regan, J., Breitfelder, S., Cirillo, P., Gilmore, T., Graham, A. G., Hickey, E., Klaus, B., Madwed, J., Moriak, M., Moss, N., Pargellis, C., Pav, S., Proto, A., Swinamer, A., Tong, L., and Torcellini, C. (2002) Pyrazole urea-based inhibitors of p38 MAP kinase: from lead compound to clinical candidate, *J Med Chem 45*, 2994-3008.

Remenyi, A., Good, M. C., and Lim, W. A. (2006) Docking interactions in protein kinase and phosphatase networks, *Curr Opin Struct Biol 16*, 676-685.

Ren, J., Agata, N., Chen, D., Li, Y., Yu, W. H., Huang, L., Raina, D., Chen, W., Kharbanda, S., and Kufe, D. (2004) Human MUC1 carcinoma-associated protein confers resistance to genotoxic anticancer agents, *Cancer Cell 5*, 163-175.

Roehrl, M. H., Kang, S., Aramburu, J., Wagner, G., Rao, A., and Hogan, P. G. (2004) Selective inhibition of calcineurin-NFAT signaling by blocking protein-protein interaction with small organic molecules, *Proc Natl Acad Sci U S A 101*, 7554-7559.

Ronkina, N., Kotlyarov, A., and Gaestel, M. (2008) MK2 and MK3--a pair of isoenzymes?, *Front Biosci 13*, 5511-5521.

Roux, P. P., and Blenis, J. (2004) ERK and p38 MAPK-activated protein kinases: a family of protein kinases with diverse biological functions, *Microbiol Mol Biol Rev 68*, 320-344.

Salituro, F. G., Germann, U. A., Wilson, K. P., Bemis, G. W., Fox, T., and Su, M. S. (1999) Inhibitors of p38 MAP kinase: therapeutic intervention in cytokine-mediated diseases, *Curr Med Chem 6*, 807-823.

Salvador, J. M., Mittelstadt, P. R., Guszczynski, T., Copeland, T. D., Yamaguchi, H., Appella, E., Fornace, A. J., Jr., and Ashwell, J. D. (2005) Alternative p38 activation pathway mediated by T cell receptor-proximal tyrosine kinases, *Nat Immunol 6*, 390-395.

Schmidtke, P., and Barril, X. (2010) Understanding and predicting druggability. A high-throughput method for detection of drug binding sites, *J Med Chem 53*, 5858-5867.

Schreiner, P. R. (1998) Monocyclic enediynes: Relationships between ring sizes, alkyne carbon distances, cyclization barriers, and hydrogen abstraction reactions. Singlet-triplet separations of methyl-substituted p-benzynes, *J Am Chem Soc 120*, 4184-4190.

Semmelhack, M. F., and Gallagher, J. C., D. . (1990) *Tetrahedron Lett 31*, 1521-1522.

Sharrocks, A. D., Yang, S. H., and Galanis, A. (2000) Docking domains and substrate-specificity determination for MAP kinases, *Trends Biochem Sci 25*, 448-453.

Sherer, E. C., Kirschner, K. N., Pickard, F. C., Rein, C., Feldgus, S., and Shields, G. C. (2008) Efficient and Accurate Characterization of the Bergman Cyclization for Several Enediynes Including an Expanded Substructure of Esperamicin A(1), *J Phys Chem B 112*, 16917-16934.

Sheridan, D. L., Kong, Y., Parker, S. A., Dalby, K. N., and Turk, B. E. (2008) Substrate discrimination among mitogen-activated protein kinases through distinct docking sequence motifs, *J Biol Chem 283*, 19511-19520.

Singh, J., Petter, R. C., and Kluge, A. F. (2010) Targeted covalent drugs of the kinase family, *Curr Opin Chem Biol 14*, 475-480.

Smith, A. J., Zhang, X., Leach, A. G., and Houk, K. N. (2009) Beyond picomolar affinities: quantitative aspects of noncovalent and covalent binding of drugs to proteins, *J Med Chem 52*, 225-233.

Smith, A. L., and Nicolaou, K. C. (1996) The enediyne antibiotics, *J Med Chem 39*, 2103-2117.

Smith, J. A., Poteet-Smith, C. E., Malarkey, K., and Sturgill, T. W. (1999) Identification of an extracellular signal-regulated kinase (ERK) docking site in ribosomal S6 kinase, a sequence critical for activation by ERK in vivo, *J Biol Chem 274*, 2893-2898.

Smith, J. A., Poteet-Smith, C. E., Malarkey, K., and Sturgill, T. W. (1999) Identification of an extracellular signal-regulated kinase (ERK) docking site in ribosomal S6 kinase, a sequence critical for activation by ERK in vivo, *J Biol Chem 274*, 2893-2898.

Snyder, J. P., and Tipsword, G. E. (1990) Proposal for blending classical and biradical mechanisms in antitumor antibiotics: dynemicin A, *J Am Chem Soc 112*, 4040-4042.

Solano, B., Junnotula, V., Marin, A., Villar, R., Burguete, A., Vicente, E., Perez-Silanes, S., Aldana, I., Monge, A., Dutta, S., Sarkar, U., and Gates, K. S. (2007) Synthesis and biological evaluation of new 2-arylcarbonyl-3-trifluoromethylquinoxaline 1,4-di-N-oxide derivatives and their reduced analogues, *J Med Chem 50*, 5485-5492.

Sugiura, Y., Arakawa, T., Uesugi, M., Shiraki, T., Ohkuma, H., and Konishi, M. (1991) Reductive and nucleophilic activation products of dynemicin A with methyl thioglycolate. A rational mechanism for DNA cleavage of the thiol-activated dynemicin A, *Biochemistry 30*, 2989-2992.

Szafranska, A. E., Luo, X. M., and Dalby, K. N. (2005) Following in vitro activation of mitogen-activated protein kinases by mass spectrometry and tryptic peptide analysis: purifying fully activated p38 mitogen-activated protein kinase alpha, Analytical *Biochemistry 336*, 1-10.

Tamaoki, T., Nomoto, H., Takahashi, I., Kato, Y., Morimoto, M., and Tomita, F. (1986) Staurosporine, a potent inhibitor of phospholipid/Ca++dependent protein kinase, *Biochem Biophys Res Commun 135*, 397-402.

Tanoue, T., Adachi, M., Moriguchi, T., and Nishida, E. (2000) A conserved docking motif in MAP kinases common to substrates, activators and regulators, *Nat Cell Biol 2*, 110-116.

Tanoue, T., and Nishida, E. (2003) Molecular recognitions in the MAP kinase cascades, *Cell Signal 15*, 455-462.

Tsou, H. R., Overbeek-Klumpers, E. G., Hallett, W. A., Reich, M. F., Floyd, M. B., Johnson, B. D., Michalak, R. S., Nilakantan, R., Discafani, C., Golas, J., Rabindran, S. K., Shen, R., Shi, X., Wang, Y. F., Upeslacis, J., and Wissner, A. (2005) Optimization of 6,7-disubstituted-4-(arylamino)quinoline-3-carbonitriles as orally active, irreversible inhibitors of human epidermal growth factor receptor-2 kinase activity, *J Med Chem 48*, 1107-1131.

Tuesuwan, B., and Kerwin, S. M. (2006) 2-Alkynyl-N-propargyl pyridinium salts: pyridinium-based heterocyclic skipped aza-enediynes that cleave DNA by deoxyribosyl hydrogen-atom abstraction and guanine oxidation, *Biochemistry 45*, 7265-7276.

Tummino, P. J., and Copeland, R. A. (2008) Residence time of receptor-ligand complexes and its effect on biological function, *Biochemistry 47*, 5481-5492.

Van Lanen, S. G., and Shen, B. (2008) Biosynthesis of enediyne antitumor antibiotics, *Curr Top Med Chem 8*, 448-459.

Wadsworth, S. A., Cavender, D. E., Beers, S. A., Lalan, P., Schafer, P. H., Malloy, E. A., Wu, W., Fahmy, B., Olini, G. C., Davis, J. E., Pellegrino-Gensey, J. L., Wachter, M. P., and Siekierka, J. J. (1999) RWJ 67657, a potent, orally active inhibitor of p38 mitogen-activated protein kinase, *J Pharmacol Exp Ther 291*, 680-687.

Wang, Z. L., Harkins, P. C., Ulevitch, R. J., Han, J. H., Cobb, M. H., and Goldsmith, E. J. (1997) The structure of mitogen-activated protein kinase p38 at 2.1-angstrom resolution, *P Natl Acad Sci USA 94*, 2327-2332.

Wissner, A., Fraser, H. L., Ingalls, C. L., Dushin, R. G., Floyd, M. B., Cheung, K., Nittoli, T., Ravi, M. R., Tan, X., and Loganzo, F. (2007) Dual irreversible kinase inhibitors: quinazoline-based inhibitors incorporating two independent reactive centers with each targeting different cysteine residues in the kinase domains of EGFR and VEGFR-2, *Bioorg Med Chem 15*, 3635-3648.

Wrobleski, S. T., and Doweyko, A. M. (2005) Structural comparison of p38 inhibitor-protein complexes: a review of recent p38 inhibitors having unique binding interactions, *Curr Top Med Chem 5*, 1005-1016.

Yang, W. Y., Breiner, B., Kovalenko, S., Ben, C., Singh, M., LeGrand, S. N., Sang, Q. X. A., Strouse, G. F., Copeland, J. A., and Alabugin, I. V. (2009) *J Am Chem Soc 131*, 11458-11470.

Zhang, J., Yang, P. L., and Gray, N. S. (2009) Targeting cancer with small molecule kinase inhibitors, *Nat Rev Cancer 9*, 28-39.

Zhou, H., Zheng, M., Chen, J., Xie, C., Kolatkar, A. R., Zarubin, T., Ye, Z., Akella, R., Lin, S., Goldsmith, E. J., and Han, J. (2006) Determinants that control the specific interactions between TAB1 and p38alpha, *Mol Cell Biol 26*, 3824-3834.

Zhou, T. J., Sun, L. G., Humphreys, J., and Goldsmith, E. J. (2006) Docking interactions induce exposure of activation loop in the MAP kinase ERK2, *Structure 14*, 1011-1019.

Zhu, H., and Gooderham, N. J. (2006) Mechanisms of induction of cell cycle arrest and cell death by cryptolepine in human lung adenocarcinoma a549 cells, *Toxicol Sci 91*, 132-139.

Vita

Jing Li was born in Shanghai, China. She obtained her bachelor degrees in Biochemistry and Chemistry from the University of Texas at Austin, and pursued her Ph.D. study in Medicinal Chemistry at the same university with Professor Sean Michael Kerwin. During her graduate study, she received Professional Development Award (2011), Cancer Prevention and Research Institute of Texas Training Grant Fellowship (2010), Jamie N. Delgado Endowed Graduate Fellowship three times (2006, 2007, 2010), University Continuing Fellowship (2010), Dr.Jerry and Joan Fineg Professional Development Endowment (2010), Johnson & Johnson Endowed Graduate Fellowship in Pharmacy (2010), Schering-Plough Research Institute Graduate Fellowship (2009), B. Berard Matthews Endowed Scholarship (2008). She is a co-author of the following publications:

1. Li, J., Kaoud, T. S., Dalby, K. N., and Kerwin, S. M. Targeting kinase docking sites: A fluorescence-based assay for p38α inhibitors targeting a substrate binding site, *Manuscript in preparation*.
2. Laroche, C., Li, J., and Kerwin, S. M. (2011) Cytotoxic 1,2-dialkynylimidazole-based aza-enediynes: aza-Bergman rearrangement rates do not predict cytotoxcitiy, *J Med Chem 54, 5059-5069*.
3. Laroche, C., Li, J., Gonzales, C., David, W. M., and Kerwin, S. M. (2010) Cyclization kinetics and biological evaluation of an anticancer 1,2-dialkynylimidazole, *Org Biomol Chem 8*, 1535-1539.
4. Li, J., Kaoud, T. S., Laroche, C., Dalby, K. N., and Kerwin, S. M. (2009) Synthesis and biological evaluation of p38 alpha kinase-targeting dialkynylimidazoles, *Bioorgan Med Chem Lett 19*, 6293-6297.

5. Laroche, C., Li, J., Freyer, M. W., and Kerwin, S. M. (2008) Coupling reactions of bromoalkynes with imidazoles mediated by copper salts: synthesis of novel N-alkynylimidazoles, *J Org Chem 73*, 6462-6465.
6. Tuesuwan, B., Kern, J. T., Thomas, P. W., Rodriguez, M., Li, J., David, W. M., and Kerwin, S. M. (2008) Simian virus 40 large T-antigen G-quadruplex DNA helicase inhibition by G-quadruplex DNA-interactive agents, *Biochemistry 47*, 1896-1909.
7. Shen, X., Mula, R. V., Li, J., Weigel, N. L., and Falzon, M. (2007) PTHrP contributes to the anti-proliferative and integrin alpha6beta4-regulating effects of 1,25-dihydroxyvitamin D(3), *Steroids 72*, 930-938.

This dissertation was typed by Jing Li.